The pancreatic -cell zinc response to chronic stimulation and extracellular zinc depletion

Lawson, Rebecca Sian

Awarding institution:
King's College London

Metal Metabolism Group

Facility of Life Sciences and Medicine

King's College London

Doctoral thesis

The pancreatic β-cell zinc response to chronic stimulation and extracellular zinc depletion

Rebecca Sian Lawson

First supervisor: Christer Hogstrand

Second supervisor: Wolfgang Maret

A thesis submitted in fulfilment of the requirements for

the degree of Doctor of Philosophy

November 2018

I. Abstract

Zinc is integral for β-cell function in glycaemic control. Intracellular zinc concentrations are regulated by buffering and membrane transportation mediated by the ZIP (14 paralogues; SLC39A) and ZnT (10 paralogues; SLC30A) families of transporters, which flux zinc into and out of the cytosol, respectively. The predominantly β-cell-specific paralogue ZnT8 (SLC30A8) uptakes zinc into granules, where it is essential for normal insulin maturation and exocytosis. Deregulation of zinc and its transporters is associated with β-cell dysfunction and Type 2 Diabetes development: the non-synonymous polymorphism rs13266684 in *SLC30A8* confers differential zinc transporting efficiencies and is linked to disease risk, and many type 2 diabetic patients and animal models of diabetes present with hypozincaemia. We hypothesised that ZIP transporters are coordinated with ZnT8 to mediate β-cell zinc content, phenotype and function in response to the hyperglycaemia and hypozincaemia present in Type 2 Diabetes. We used a systematic approach to identify *Slc39a1* in rodent, and *SLC39A6*, *SLC39A7*, *SLC39A9*, *SLC39A13* and *SLC39A14* in human and rodent as potentially biologically important for β-cell phenotype and function. We showed that both prolonged stimulation and extracellular zinc depletion, representative of hyperglycaemia and hypozincaemia *in vivo*, respectively, lower the zinc content of MIN6 β-cells and disrupt expression of multiple *Slc39a* paralogues and zinc-responsive markers for β-cell identity. Moreover, we demonstrated that ZIP6 and ZnT8 are involved in maintaining β-cell zinc content, survival and identity in response to zinc depletion, and identified potential co-regulation of ZnT8, ZIP6 and ZIP9 by the major β-cell transcription factor PDX-1. Critically, these data show that ZIP6 and ZnT8 are involved in maintaining β-cell zinc homeostasis and that stresses present in Type 2 Diabetes induce loss of β-cell zinc, which may alter cellular phenotype and reduce survival.

II. Table of contents

III. List of figures

IV. List of tables

V. List of abbreviations

ADP	Adenosine diphosphate
AMPK	AMP-activated protein kinase
ARX	Aristaless related homeobox
ATP	Adenosine triphosphate
Ca^{2+}	Calcium ion
Cas9	CRISPR-associated protein-9 nuclease
CDF	Cation diffusion facilitators
ChIP-seq	Chromatin immunoprecipitation sequencing
CREB	cAMP response element binding protein
CRISPR	Clustered Regularly Interspaced Short Palindromic Repeats
CTD	Carboxyl terminal domain
DMEM	Dulbecco's Modified Eagle's Medium
EGFR	Epidermal growth factor receptor
ER	Endoplasmic reticulum
ERK	Extracellular-signal-regulated kinase
FBS	Fetal bovine serum
FD	Fold difference
FDR	False discovery rate
FOXA1	Forkhead box A1
FOXA2	Forkhead box A2
FOXO1	Forkhead box O1
GAP	GTPase activating protein
GIP	Glucose-dependent insulinotropic polypeptide
GLP-1	Glucagon-like peptide-1
GLP-1R	GLP-1 receptor
GLUT2	Glucose transporter 2
GO	Gene ontology
GPCR	G-protein coupled receptor
GRG3	Groucho-related gene 3
GSIS	Glucose-stimulated insulin secretion
GSK-3	Glycogen synthase kinase 3

GWAS	Genome-Wide Association Studies
HSA	Human Serum Albumin
HBSS	Hanks Balanced Salt Solution
HCSS	Hepes control salt solution
HIF1	Hypoxia-inducible transcription factor 1
HNF1A	Hepatocyte nuclear factor 1A
HNF1B	Hepatocyte nuclear factor 1B
HNF4A	Hepatocyte nuclear factor 4A
ICP-MS	Inductively-coupled plasma mass spectrometry
IGFR	Insulin-like growth factor receptor
IL-6	Interleukin 6
IR	Insulin receptor
IRS-2	Insulin receptor substrate-2
JNK	c-Jun N-terminal kinase
K^+	Potassium ion
K_{ATP} channels	ATP-sensitive potassium ion channels
KCl	Potassium chloride
KRBH	Krebs-ringer bicarbonate buffer
L-VGCC	L-type voltage-gated calcium channels
MAFA	MAF BZIP transcription factor A
MAFB	MAF BZIP transcription factor B
MAPK	Mitogen-activated protein kinase
MEK	Mitogen-activated protein kinase kinase
MEM	Modified Eagle's Medium
MODY	Maternity-onset diabetes of the young
MT	Metallothionein
MTF1	Metal-response element–binding transcription factor-1
mTOR	Mammalian target of rapamycin
NEUROD1	Neuronal differentiation 1
NF-KB	Nuclear factor immunoglobulin K chain enhancer in B cells
NGN3	Neuorgenin-3
NKX2.2	NK2 homeobox 2
NKX6.1	NK2 homeobox 1

NTD	Amino terminal domain
PAL	Proline-alanine-leucine
PAX4	Paired box 4
PAX6	Paired box 6
PCA	Principal component analysis
PDGF-R	Platelet-derived growth factor receptor
PDK1	Phosphoinositide-dependent kinase-1
PDX-1	Pancreatic and duodenal homeobox 1
PI3K	phosphatidylinositol-3 kinase
PIP2	Phosphatidylinositol (4,5) P2 phosphate
PIP3	Phosphatidylinositol (3,4,5) P3 phosphate
PPAR-α	Proliferator-activated receptor α
PTP	Protein tyrosine phosphatase
ROS	Reactive oxygen species
RPMI	Roswell Park Memorial Institute medium
RPS6	Ribosomal protein S6
S6K	S6 kinase
SDS	Sodium dodecyl sulphate
SNP	Single nucleotide polymorphism
STAT	Signal transducer and activator of transcription
TBS	Tris-buffered saline
TBST	Tris-buffered saline with 0.05% (v/v) TWEEN-20
TMD	Transmembrane domains
TMM	Trimmed mean of M values
TNF	Tumour necrosis factor
TPEN	N,N,N’N’-tetrakis(-)(2-pyridylmethyl)-ethylenediamine
TRP	Transient receptor potential
UBC	Ubiquitin C
UPL	Universal Probe Library
ZIP	Zrt- and Irt-related protein
Zn^{2+}	Zinc ion
ZnT	Zinc transporter protein

VI. Acknowledgments

I would first and foremost like to thank my supervisors Christer Hogstrand and Wolfgang Maret for their guidance, advice and time throughout this project. Their supervision has been second to none and has ensured that my time at King's has been successful and, most importantly, highly enjoyable. Second, I would like to thank all the members of my lab group past and present whom have helped, supported and kept me company over the last 3 years, in particular Douglas Parsons, Elisabeth Chang, Thea Stewart, Jenny Fitzgerald, Sabine Schnell, Sandra Carvalho and Elisa Bellomo. I am further grateful to Han Lu and Sucharitha Balu (Genomics Centre, King's College London) for help with RNA-seq sample preparation and data analysis, Amazon Austin (Diabetes Research Group, King's College London) for mouse islet isolation, Andy Cakebread (London Metallomics Facility) for carrying out all ICP-MS analysis and Ben Robinson (Nikon Centre, King's College London) for help with confocal microscopy. I would additionally like to thank the leaders of my PhD programme 'MRes/PhD Biomedical and Translational Sciences' at the KBI and my funders at Guy's and St Thomas' Charity Trust, without whom this PhD would not have been possible. Last but not least, I would like to send the warmest thanks to my family and friends, in particular my husband Peter, for continued support and encouragement through all the ups and downs of the PhD.

In loving memory of Uncle Ian

xxx

1. General Introduction

1.1. Diabetes

Diabetes comprises of a heterogeneous group of metabolic disorders characterised by long-term hyperglycaemia and impairment of carbohydrate, lipid and protein metabolism [1]. In 2015, there were a total of 415 million diabetic sufferers and this is forecast to increase to affect >1 in 10 globally by 2040. Diabetes represents a leading cause of morbidity and mortality worldwide and is estimated to account for 2.5 to 15% of healthcare budgets, depending on local prevalence and treatments available [2].

1.1.1. Classification and clinical diagnosis

The majority of diabetic cases can be classified into two etiopathogenic categories, together accounting for ~99% of incidences: Type 1 diabetes (previously insulin-dependent diabetes mellitus or juvenile-onset diabetes) and Type 2 diabetes (previously non-insulin dependent diabetes mellitus or adult-onset diabetes). Type 1 Diabetes, which accounts for 5-10% cases, is an immune-mediated disorder whereby cell-mediated destruction of insulin-secreting pancreatic β-cells causes absolute insulin deficiency and requires exogenous insulin to normalise plasma glucose levels [3]. Type 2 Diabetes, which accounts for 90-95% of cases, results from inadequate β-cell insulin secretion in response to increased insulin resistance at peripheral tissues, despite β-cells remaining largely intact. Other categories of diabetes include gestational diabetes, which describes glucose intolerance arising during pregnancy, and maturity-onset diabetes of the young (MODY), which arises from monogenetic defects in pancreatic function [1]. These are listed in **Table 1.1.**

Table 1.1. Genes involved in monogenetic forms of diabetes. HNF4A, hepatocyte nuclear factor 4A; GCK, Glucokinase; HNF1A, hepatocyte nuclear factor 1A; PDX-1, pancreatic and duodenal homeobox 1; HNF1B, hepatocyte nuclear factor 1B; INS, Insulin; CEL, carboxyl ester lipase; PAX4, paired box 4. Adapted from [4].

Gene	Proportion of MODY	Function
HNF4A (MODY1)	5%	Transcription factor involved in pancreatic development and function
GCK (MODY2)	30-50%	β-cell-specific glucose sensor
HNF1A (MODY3)	30-50%	Transcription factor involved in pancreatic differentiation and function
PDX-1 (MODY4)	<1%	Transcription factor involved in pancreatic development and function
HNF1B (MODY5)	5%	Transcription factor involved in pancreatic development and function
NEUROD1 (MODY6)	<1%	Transcription factor involved in β-cell development and insulin gene transcription
INS	<1%	Insulin hormone
CEL	<1%	Digestive enzyme with role in cholesterol ester digestion
PAX4	<1%	Transcription factor involved in pancreatic differentiation and function

Clinical presentation and disease progression vary substantially between individuals suffering from all diabetic categories and classification depends on clinical presentation at diagnosis, prompted by symptoms including polydipsia, palpitation, dyspnoea, frequent urination and blurred vision [5]. Diagnostic tests are based on the haemoglobin A1c criteria, which measures glycated haemoglobin in the blood, or plasma glucose

criteria, which measures either fasting plasma glucose or plasma glucose two hours following 75g glucose oral uptake (oral glucose tolerance test) [6].

1.1.2. Type 2 Diabetes

Type 2 Diabetes is a multifactorial disorder attributed to complex pathological sequences of environmental and genetic factors. Prediabetes describes the state of impaired fasting blood glucose concentrations and/or glucose intolerance, resulting in peripheral insulin resistance, with Type 2 Diabetes developing in the subset of individuals who fail to adapt and regain glycaemic control [7]. Recent rises in type 2 diabetic incidences are attributed to population growth, aging, urbanisation, high calorie diets, increased prevalence of obesity and decreased physical activity [8]. However, genetic contributors are additionally important for disease development. Estimations for Type 2 Diabetes heritability range from 30-70% [9, 10], with concordance rates predicted to be 76% between monozygotic twins [11]. In the US, a total of 30-50% of diabetic adults do not meet individualised targets for glycaemia, blood pressure or lipid control despite structured management plans, accredited to underlying genetic factors [12]. Abnormal serum statuses of trace elements including zinc, magnesium and manganese are additionally associated with disease state and may contribute to onset and progression [13].

Type 2 Diabetes can lead to potentially disabling macro- and micro-vascular complications. These are characterised into two groups: short-term metabolic acute complications (including hyperglycaemia and ketoacidosis) and long-term chronic complications (including diabetic nephron-, neuro- and retinopathy, coronary heart disease, peripheral vascular disease and cancer), largely resulting from accumulated organ damage caused by chronic hyperglycaemia. Type 2 Diabetes therefore represents a

much larger burden for the healthcare system than simply disease treatment and to the economy as a result of lost productivity [14].

1.2. The endocrine pancreas

The endocrine pancreas consists of aggregates of cells known as the islets of Langerhans, which account for ~2% of the human adult pancreas [15]. Islets are oval in shape with diameters of 100-200μm and consist of ~1000 endocrine cells: interspaced insulin-secreting β-cells and glucagon-producing α-cells surrounded by non-β-cell mantles containing somatostatin-producing δ-cells and pancreatic polypeptide cells [16]. Together, insulin and glucagon regulate plasma glucose concentrations: insulin promotes glucose uptake at peripheral tissues and glucagon stimulates hepatic glycogenolysis and gluconeogenesis [17].

1.2.1. Pancreatic β-cells and insulin secretion

β-cells comprise ~50% of human islets [17] and have an estimated turnover of three months [18]. β-cells synthesise and secrete insulin primarily in response to extracellular glucose [glucose-stimulated insulin secretion (GSIS)], but also in response to other hormones, neuronal inputs, nutrients and the incretins glucagon-like peptide-1 (GLP-1) and glucose-dependent insulinotropic polypeptide (GIP). GLP-1 is secreted from the distal bowel and colon enteroendocrine cells, and GIP from duodenal K cells of the proximal small intestine, each in a nutrient-dependent manner to potentiate β-cell function and viability [19]. Inability of β-cells to respond appropriately leads to secretory dysfunction and systemic hyperglycaemia [20].

GSIS is initiated in a transcription-independent manner within minutes [21]. High concentrations of extracellular glucose stimulate β-cell glucose uptake via the low affinity

glucose transporter 1 in human or glucose transporter 2 (GLUT2) in rodent [22]. Cytosolic glucose is phosphorylated to glucose-6-phosphate by glucokinase [23], which is synthesised into pyruvate via the process of glycolysis. Pyruvate is metabolised by pyruvate dehydrogenase to generate acetyl-CoA. Acetyl-CoA enters the tricarboxylic acid cycle in mitochondria to create adenosine triphosphate (ATP) [24]. Elevated ATP/adenosine diphosphate (ADP) ratios hyperpolarise ATP-sensitive potassium ion (K^+) channels (K_{ATP} channels; KCNJ11), causing membrane depolarisation. Depolarisation activates L-type voltage-gated calcium channels (L-VGCC) to facilitate calcium ion (Ca^{2+}) influx, and subsequent exocytosis of insulin secretory granules [25]; approximately 60% of the β-cell surface participates in granule fusion [26]. An overview of GSIS is depicted in **Fig 1.1**. Although islet structure is not imperative for β-cell function, insulin secretion is higher in islets compared to equivalent numbers of single β-cells. Connexin36 gap junction proteins between β-cells allow stimulated cells to hyperpolarise adjacent electrically coupled cells to increase overall magnitudes of Ca^{2+} signalling and insulin secretion [27, 28].

Insulin secretion occurs as a biphasic response: an initial spike initiates after 5-6 minutes followed by a rapid decrease (first phase), proceeded by a prolonged increase over ~60 minutes (second phase) [29]. Glucose further primes time-dependent potentiation of insulin secretion whereby glucose exposure enhances secretion in response to additional stimuli in a K_{ATP} channel-independent manner [24]. The secreted insulin is first transported through the portal vein to the hepatic system to mediate storage of excess glucose as glycogen. Increases in plasma insulin in the liver activate glycogen synthesis [30] and inhibit transcription, the activities of key gluconeogenic enzymes [31] and lipolysis [32]. Deletion of hepatic insulin receptors (IR) in mouse results in glucose intolerance and insulin resistance [33]. The remaining insulin is transported through the

bloodstream to target tissues where IR binding initiates signalling cascades to stimulate glucose uptake [34].

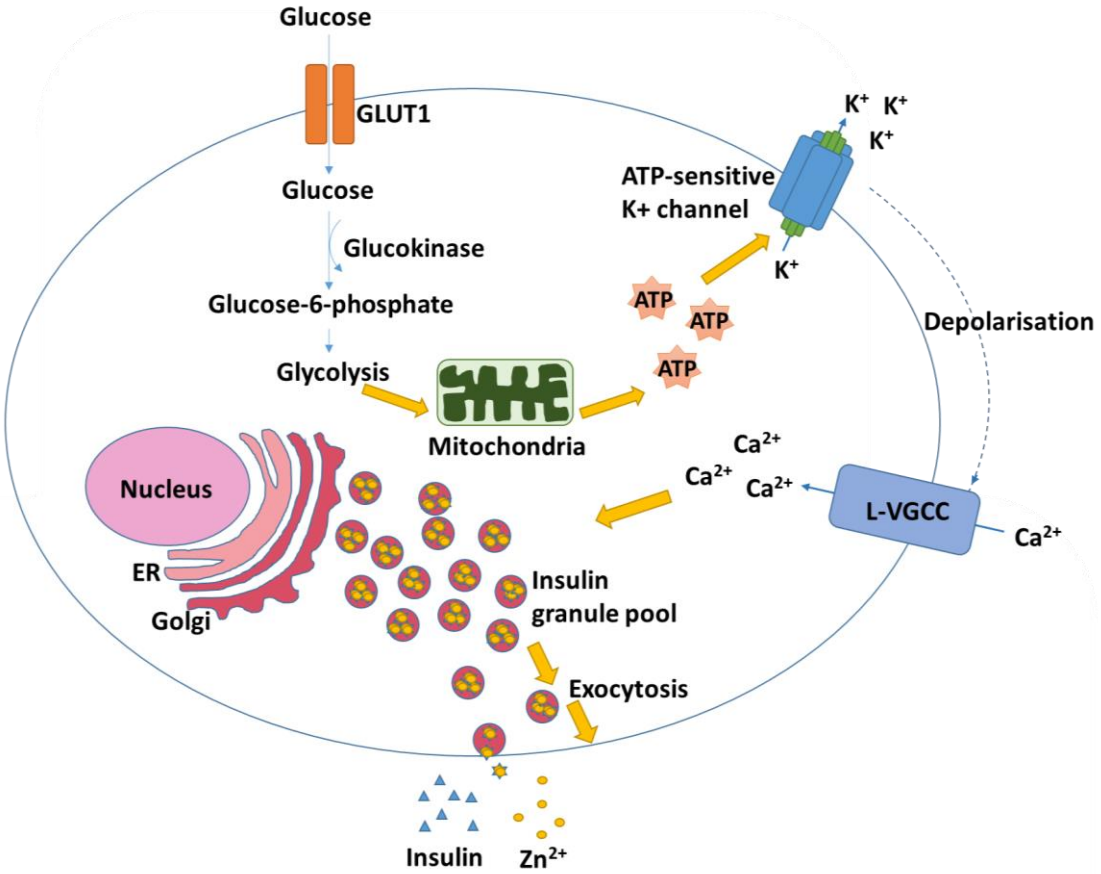

Fig 1.1. The series of events underlying GSIS in β-cells. Glucose is taken up into β-cells by GLUT1 in human or GLUT2 in rodent and is metabolised to pyruvate via the process of glycolysis. This leads to increased activity of the tricarboxylic acid cycle in mitochondria, which increases cellular ATP. Elevated ATP/ADP ratios inhibit K_{ATP} channels, resulting in cell membrane depolarisation and subsequent opening of L-VGCCs. Influx of Ca^{2+} triggers insulin granule exocytosis and insulin/Zn^{2+} co-release into circulation. Adapted from [35].

1.2.2. Pancreatic β-cell mass

Adult β-cell mass is plastic and can be adjusted in response to physiological and pathological states to maintain equity between insulin supply and demand; failure to expand appropriately results in hyperglycaemia and peripheral insulin resistance. In non-diabetic obesity, islet number and β-cell proportion increase, however these parameters decrease during diabetic onset and islets show disorganised structures [36]. A previous study showed that post-mortem islets from type 2 diabetic patients present with a 22% reduction in density and a 30% reduction in total mass compared to matched controls [37]. A progressive decline in β-cell function precedes diabetic onset, however it is unlikely the decrease in β-cell mass is entirely accountable [38].

β-cell hypertrophy and proliferation are governed by availabilities of glucose, nutrients, growth factors and incretins [19] balancing rates of proliferation, neogenesis and apoptosis; the contribution of each varies throughout postnatal life. It remains unclear which mechanism(s) primarily drive diabetes-associated decreases in β-cell mass, although age-related increases in apoptosis partially explain increased diabetes susceptibility in the elderly [39]. β-cell apoptosis is increased in both lean and obese diabetic and obese non-diabetic patients, compensated for by appropriate increases in replication, neogenesis and cell size in the latter [36]. Increases in β-cell apoptosis are driven by combinations of ER stress [40], chronic hyperglycaemia [41-43], chronic hyperlipidaemia [44, 45], oxidative stress [46, 47], cytokines [48] and deposition of amyloid fibrils [49].

Several important signalling pathways mediate β-cell survival and mass, including the insulin receptor substrate-2/ phosphatidylinositol-3 kinase/ AKT (IRS-2/PI3K/AKT) cascade, the RAS/ RAF/ mitogen-activated protein kinase kinase/ extracellular-signal-

regulated kinase (RAF/MEK/ERK) cascade, and the mammalian target of rapamycin/ S6 kinase/ ribosomal protein S6 (mTOR/S6K/RPS6) cascade [50]. These cascades can all be impacted by zinc (illustrated in **Figs 1.2-1.4** and discussed in section **1.5.2)**. The roles of these signalling cascades in β-cells are detailed below.

1.2.2.1. IRS-2/PI3K/AKT signalling

IRS-2/PI3K/AKT cascades mediate β-cell mass in response to growth factors, insulin, incretins and glucose [51]. IRS-2, an intracellular tyrosine kinase downstream of IRs and insulin-like growth factor receptors (IGFR), is especially potent at promoting β-cell survival; decreased IRS-2 signalling increases apoptosis and mutations are linked to Type 2 Diabetes development [36]. IRS-2 phosphorylation activates PI3K, which converts the phosphatidylinositol (4,5) P2 phosphate (PIP2) into phosphatidylinositol (3,4,5) P3 phosphate (PIP3). PIP3 recruits AKT and phosphoinositide-dependent kinase-1 (PDK1) to the plasma membrane [52] where PDK1 phosphorylates and activates AKT [53]. Additional phosphorylation of AKT by mTOR complex 2 (mTORC2; mTOR/Rictor/GβL) is required for full activation [54]. In β-cells, AKT plays important roles in the adaptive response to increased insulin demand [51] through regulating insulin-mediated glucose transport, protein and glycogen synthesis, proliferation, cell growth, differentiation and survival; an 80% reduction in AKT signalling causes defective insulin secretion without affecting β-cell mass [55]. Moreover, mice overexpressing constitutively active AKT ($caAKT^{Tg}$) exhibit increased β-cell mass, proliferation and neogenesis [56, 57] An overview of IRS-2/PI3K/AKT signalling is depicted in **Fig 1.2**.

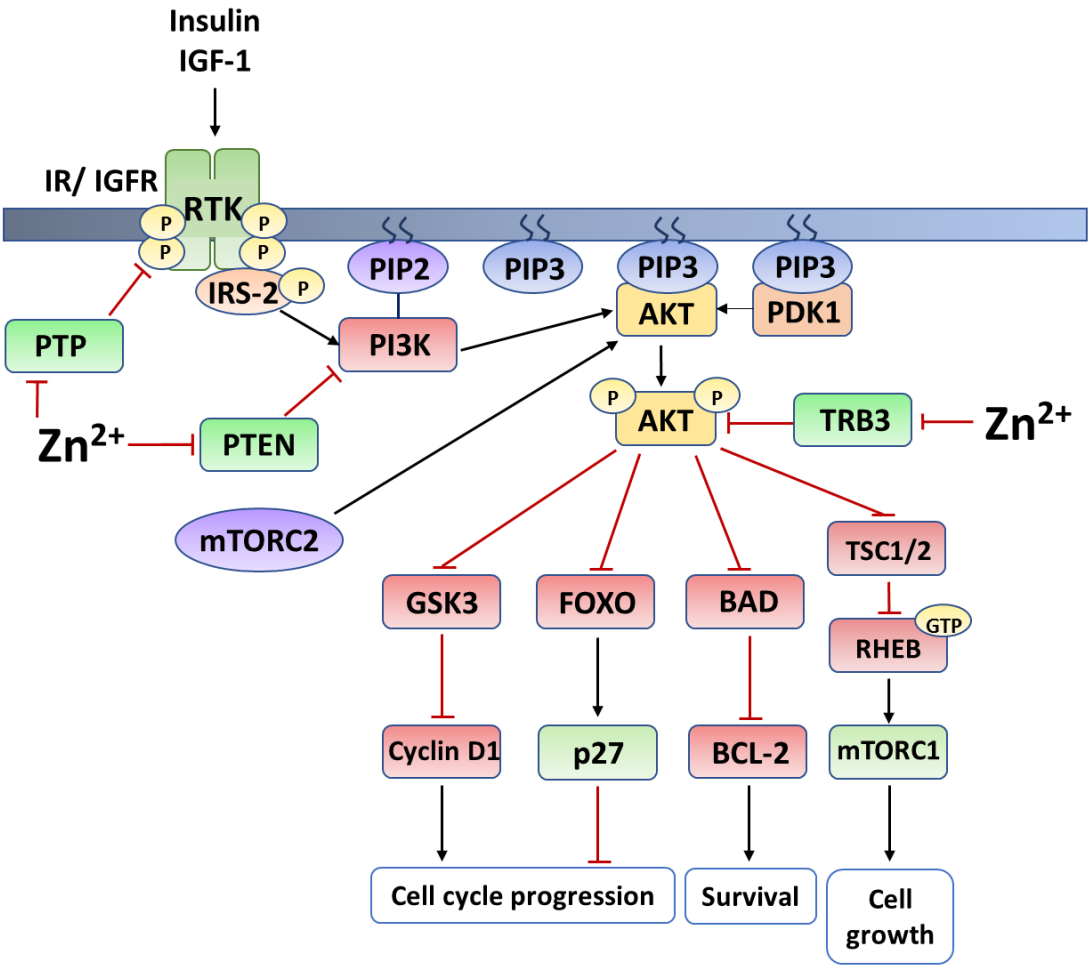

Fig 1.2. IRS-2/PI3K/AKT signalling pathways. Activated IR or IGFR tyrosine kinase receptors phosphorylate and activate IRS-2, which binds the regulatory subunit (p85) of PI3K via SRC homology 2 domains. PI3K activation is inhibited by PTEN. Activated PI3K phosphorylates and activates PIP2 to form PIP3, which recruits AKT and PDK1 to the plasma membrane where PDK1 activates AKT. The mTORC2 complex additionally phosphorylates AKT for full activation. AKT is inactivated by TRB3. AKT inhibits downstream proteins regulating cellular survival. AKT signals via glycogen synthase kinase 3 (GSK-3)/Cyclin D1 and FOXO/p27 to mediate cell cycle progression; BAD/BCL-2 to mediate apoptosis and TSC1/2/RHEB/mTORC1 to mediate cellular growth. IR/IGFR are inactivated through dephosphorylation by protein tyrosine

phosphatases (PTPs). Zinc activates IR/IGFR signalling through inhibiting PTPs, PTEN and TRB3. Black arrows: A activates B. Red lines: A inhibits B. Adapted from [58, 59].

1.2.2.2. mTOR/S6K/RPS6 signalling

mTOR cascades regulate mRNA translation to promote β-cell growth and proliferation in response to nutrients and growth factors [51]. An overview is depicted in **Fig 1.3**. mTOR is negatively regulated by TSC1/2 and the small G protein RHEB and is activated by AKT and ERK. AKT and ERK phosphorylate TSC2, disrupting the GTPase activating function (GAP activity) of TSC1-TSC2 to favour RHEB-GTP, which dissociates from and activates mTOR [60]. AKT further maintains AMP/ATP ratios in response to insulin and serum; elevated AMP activates the ATP sensor 5' AMP-activated protein kinase (AMPK) to inhibit induction of mTOR activity by growth factors and to phosphorylate and activate TSC2 [61]

mTOR forms two distinct complexes: mTORC1 (mTOR/Raptor/GβL) and mTORC2. mTORC1 phosphorylates and activates the eukaryotic initiation factor 4 binding protein 4E-BP1/2 and S6K1/2 [62]. S6K1/2 activation initiates multiple steps in protein synthesis including translation via RPS6, a component of the 40S ribosome. Both S6K1- and S6K2-mediated phosphorylation is required for full RPS6 activity. Mice harbouring knock-in mutations at all RPS6 phosphorylatable serine residues present with impaired glucose tolerance, lowered pancreatic insulin levels and increased insulin sensitivity, but do not exhibit differences in β-cell mass [63].

mTORC1 signalling is critical for regulating β-cell mass. Inhibition of mTOR by rapamycin reduces AKT-induced β-cell proliferation by destabilising cyclin D2, a critical

cell cycle regulator [64], and enhanced signalling increases β-cell mass to promote hyperinsulinemia [65]. Mice with conditional TSC2 knockout in β-cells present with hypoglycaemia, improved glucose metabolism and increased β-cell proliferation [66]. However, chronic S6K activation negatively regulates IRS, dampening PI3K/AKT cascades [67].

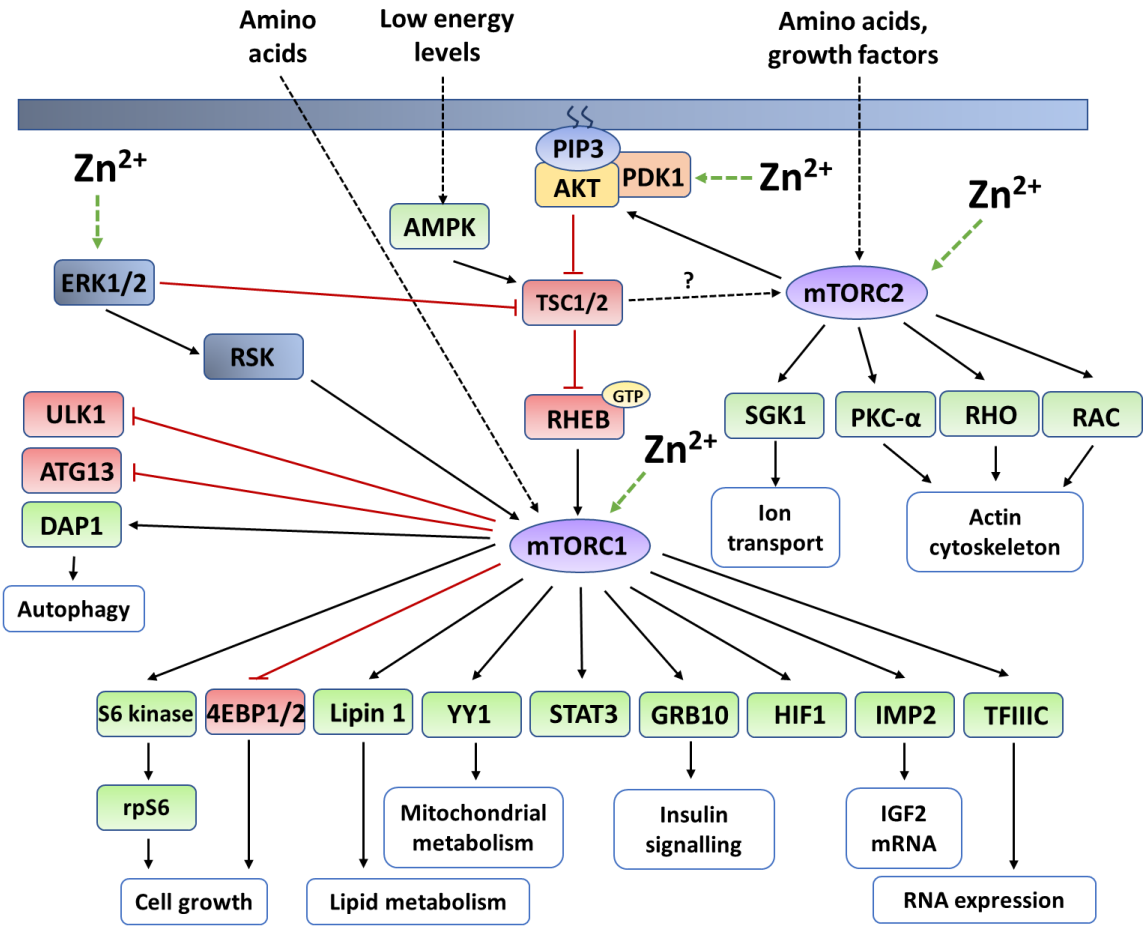

Fig 1.3. mTOR signalling pathways. Activated AKT phosphorylates and inhibits TSC1/2. Low energy conditions increase AMP/ATP ratios, which activate AMPK to phosphorylate and activate TSC1/2. TSC1/2 inhibits the GTPase RHEB, which positively regulates mTORC1 activity. mTORC1 is further activated by signalling via ERK1/2/RSK

cascades. mTORC1 signals to regulate autophagy, cell growth, lipid metabolism, mitochondrial metabolism, insulin signalling, IGF2 mRNA and RNA expression. mTORC2 is predominantly regulated by unknown pathways in response to amino acids and growth factors. Activated mTORC2 is needed for full AKT activation. mTORC2 regulates ion transport and the actin cytoskeleton. Black arrows: A activates B. Red lines: A inhibits B. Green dotted line: activation by zinc (intermediates may be present). Adapted from: [68].

1.2.2.3. RAS/RAF/MEK/ERK signalling

Growth factors and mitogens signal via RAS/RAF/MEK/ERK mitogen-activated protein kinases (MAPK) cascades to mediate gene expression, proliferation and apoptosis [69]. An overview is depicted in **Fig 1.4**. The GTP-binding protein RAS is activated by SRC/GRB2/SOS coupling complexes downstream of cytokine, growth factor and mitogen receptors. RAS-GTP recruits the protein kinase RAF, of which three isoforms exist, to the plasma membrane. RAF is regulated by RAS and other kinases and scaffolding proteins [69], including the zinc transporter ZnT1 [70], to activate MEK, the downstream target of which is predominantly ERK [71]. ERK1/2 phosphorylates and activates $p90^{RSK}$ (RSK), leading to cAMP response element binding protein (CREB) activation [72], and targets additional substrate via downstream scaffolds and/or nuclear translocation. ERK induces expression of proteins involved in cell cycle progression, and prolonged activation leads to cellular growth and subsequent cell cycle arrest. ERK further mediates proteins involved in apoptosis including BAD, BIM, MCL-1, caspase 9 and BCL-2 [73, 74] and promotes activation of nuclear factor immunoglobulin κ chain enhancer in B cells (NF-κB) by activating inhibitor κB kinase [75].

RAS/RAF/MEK/ERK cascades are induced by reactive oxygen species (ROS) that influence the activities of growth factor receptors, such as epidermal growth factor receptor (EGFR) and platelet-derived growth factor receptor (PDGF-R), in a ligand-independent manner [76]. ROS further inhibit Cys-dependent PTPs to prevent dephosphorylation of EGFRs and PDGF-Rs and promote signalling [77, 78], possibly via inducing increased cytosolic zinc, which inhibits the activities of PTPs [79]. ROS additionally target both RAS and c-SRC to induce ERK1/2 signalling independent of RAS [80].

In human islets, mouse islets and MIN6 cells, RAS/RAF/MEK/ERK signalling primarily occurs via RAS-1 and activates ERK-dependent pathways involving Ca^{2+}-dependent phosphorylation events [81]. ERK1/2 activation in β-cells is required for maximum glucose-induced insulin transcription [82] and stimulates $p70^{RSK}$ to trigger mitogenesis [50]. The β-cell transcription factor hepatocyte nuclear factor 4A (HNF4A) is required for RAS/RAF/MEK/ERK-mediated expansion of β-cell mass [83] and stimulates mitochondrial energy production to compensate for expenditure linked to GSIS [84]. In β-cells, sustained ERK1/2 activation in response to GLP-1 is dependent on continued L-VGCC-induced Ca^{2+} signalling [85], which promotes cAMP-initiated activation of protein kinase A, RAF-1 phosphorylation and ERK1/2 activation [86].

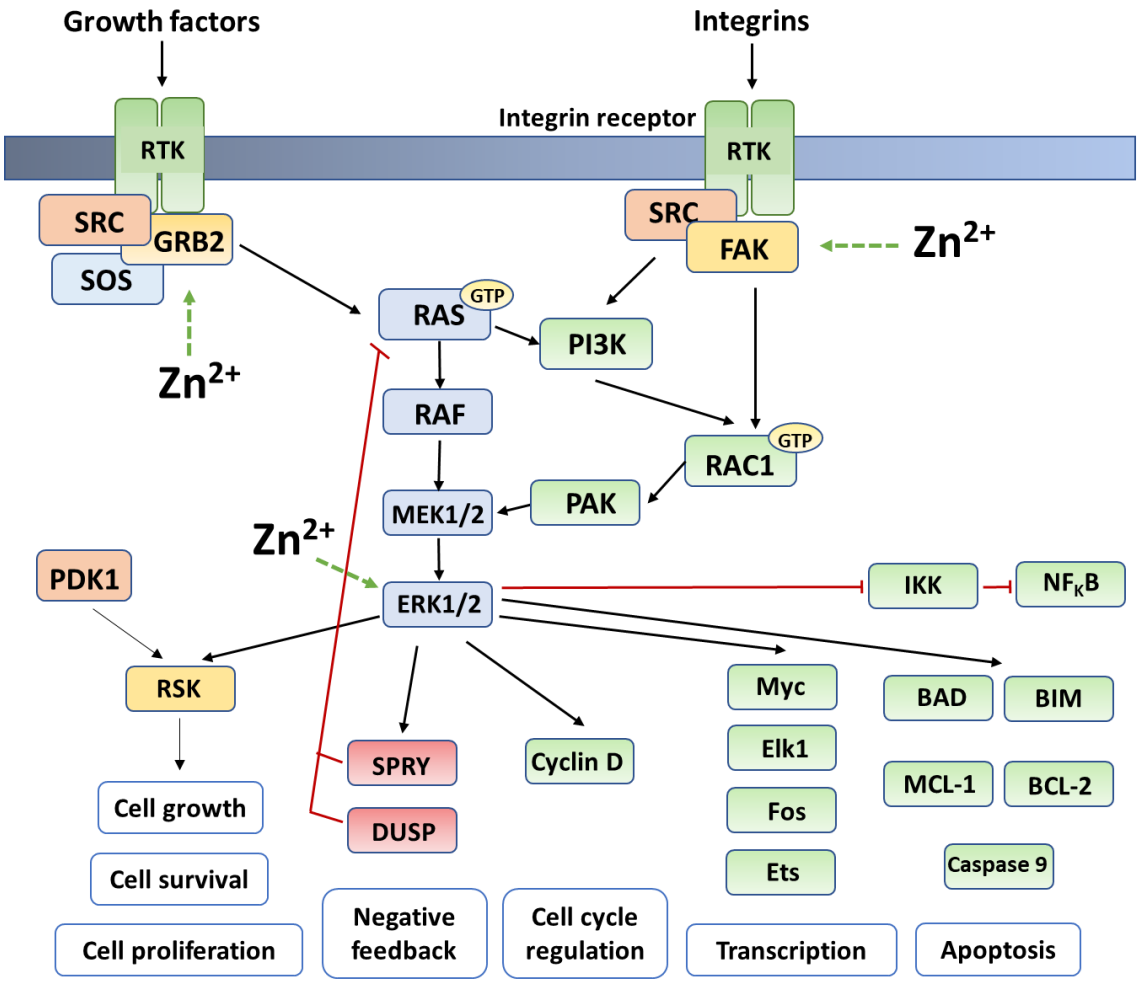

Fig 1.4. RAS/RAF/MEK/ERK signalling pathways. RAS/RAF/MEK/ERK pathways are activated by growth factor and integrin binding to receptor tyrosine kinases (RTK). SRC/SOS/GRB2 RTK coupling complexes recruit RAS, which is activated by GTP-binding. RAS-GTP recruits and activates RAF, which subsequently activates MEK1/2 to phosphorylate and activate ERK1/2. Multiple pathways converge to mediate ERK1/2 activity including signalling via the integrin receptor coupling complex SRC/FAK, which activates MEK1/2 via RAC1 and PAK, and via PI3K activation. Activated ERK1/2 regulates numerous downstream pathways including RSK, to mediate cellular growth, survival and proliferation; Cyclin D to mediate cell cycle regulation; apoptotic regulatory proteins; and a vast array of transcription factors. ERK1/2 exhibits autoregulation through activation of SPRY and DUSP, which inhibit RAS-GTP. Zinc mediates ERK1/2 activity

through targeting upstream proteins. Black arrows: A activates B. Red lines: A inhibits B. Green dotted line: activation by zinc (intermediates may be present). Adapted from: [87, 88].

1.2.3. Regulation of β-cell phenotype

Complex interplay between multiple transcription factors is required for β-cell differentiation and maintenance of phenotype. Differentiation occurs primarily during embryogenesis, controlled by temporal expression of transcription factors including pancreatic and duodenal homeobox 1 (PDX-1), NKX homeobox 1 (NKX6.1), neuorgenin-3 (NGN3) and neuronal differentiation 1 (NEUROD1) [89] (**Fig 1.5)**. The mature β-cell phenotype is majorly regulated by PDX-1, MAF BZIP transcription factor A (MAFA) and NKX6.1 in combination with forkhead box A1 (FOXA1), forkhead box A2 (FOXA2), forkhead box O1 (FOXO1), hepatocyte nuclear factor 1A (HNF1A), hepatocyte nuclear factor 1B (HNF1B), HNF4A, MAF BZIP transcription factor B (MAFB; only primates), NEUROD1, NK2 homeobox 2 (NKX2.2), paired box 4 (PAX4) and paired box 6 (PAX6) [90]. The key roles of PDX-1, MAFA and NKX6.1 are summarised below.

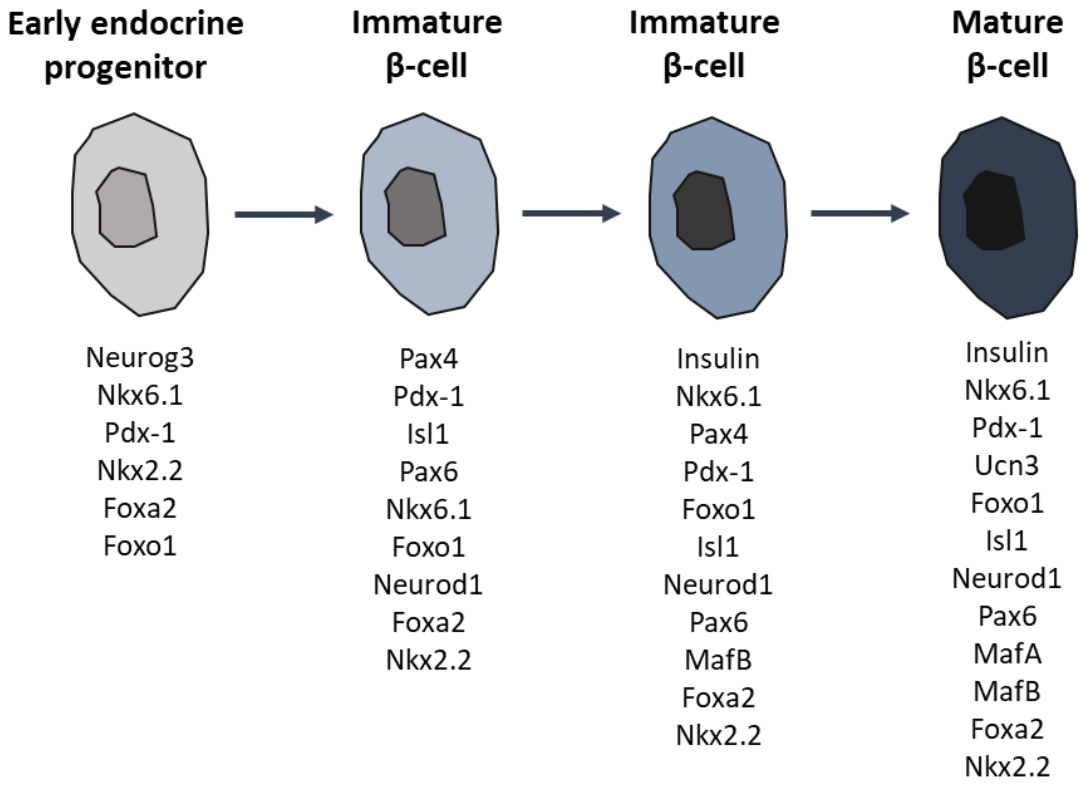

Fig 1.5. Transcription factors governing differentiation of β-cells from foregut endoderm progenitors. Adapted from [90].

1.2.3.1. PDX-1

The homeodomain protein PDX-1 is the major transcription factor in β-cells and represents a key marker for the endocrine pancreas [91]. PDX-1 is essential for differentiation of all endocrine cells, however high expression is confined to β-cells in mature islets [92, 93]. PDX-1 knockout is embryonically lethal [94] and hypomorphic variants containing regulatory sequence deletions prevent development of the endocrine pancreas [95]. Heterozygous PDX-$1^{+/-}$ mice present with abnormal islet architecture, impaired insulin secretion, increased β-cell apoptosis and downregulation of GLUT2 [96, 97]. PDX-1 interacts with specific co-factors to tightly regulate β-cell gene expression,

including NEUROD1 to mediate insulin [98, 99] and hepatocyte nuclear factor 6 to mediate NGN3 [100]. PDX-1 further regulates β-cell proliferation, in part through targeting FOXO1 downstream of IRs and IGFRs [101].

1.2.3.2. MAFA

MAFA is highly expressed in mature β-cells [102] where it is critical for maintaining cellular phenotype; loss of MAFA promotes β-cell dedifferentiation [103]. Decreased MAFA expression and/or DNA-binding ability induces abnormal islet morphology [103] and is characteristic of most compromised β-cells in human type 2 diabetic islets [104]. $MAFA^{-/-}$ mice are glucose intolerant and develop age-dependent diabetes [105]. MAFA acts as a potent activator of insulin transcription through binding at the conserved C1/RIPE3b element in the promoter, interacting directly with PDX-1 and NEUROD1 [106], and mediates expression of other important β-cell genes including GLUT2, the GLP-1 receptor (GLP-1R) and prohormone convertase 1/3 [107]. *MAFA* mRNA expression is regulated by FOXO1 in response to glucose and oxidative stress [108] and, specifically in β-cells, by PDX-1, FOXA2 and NKX2.2 at an upstream cis-regulatory region [109]. *MAFA* mRNA stability is further mediated post-transcriptionally in response to oxidative stress [107]. However, MAFA is not involved in specification of endocrine cells during development or initial differentiation [110, 111].

1.2.3.3. NKX6.1

NKX6.1 is a homeodomain transcription factor restricted to β-cells within the mature pancreas [112]. In both human and rodent, decreased NKX6.1 expression [113, 114] and variants identified through Genome-Wide Association Studies (GWAS) [115] result in loss of β-cell identify and diabetes development. NKX6.1 is necessary to confer β-cell identity to differentiating progenitors [116] and stimulates islet proliferation independent

to PDX-1 [92]. NKX6.1 expression is controlled at the transcriptional level by PDX-1 and NKX2.2, and at either the post-transcriptional or post-translational level since NKX6.1 mRNA but not protein can be detected within mature α-cell lines [117].

1.2.4. Loss of β-cell identity

Loss of β-cell phenotype, function and mass are early indicators of β-cell failure. Differentiated endocrine cells are not terminally differentiated and can, under certain conditions, transdifferentiate into other hormone-expressing cell types. In human, pancreatic α- to β-cell ratios increase following Type 2 Diabetes onset [118], the major factor promoting loss of β-cell identity being glucotoxicity [119].

Loss of markers involved in maintaining β-cell specification alter cellular function and identity. NKX6.1-deficient β-cells transdifferentiate to acquire molecular characteristics of δ-cells [120] and FOXO1-deficient cells dedifferentiate to represent a distinctive pre-β-cell differentiation stage [114]. MAFA null mice exhibit reduced β- to α-cell ratios, and β-cells contain 'empty' secretory granules due to reduced insulin synthesis [103]. Heterozygous mutations in PAX6 impair glucose tolerance and β-cell-specific inactivation in adult mice repress key β-cell genes including *Ins2*, *Slc30a8* and *MafA*, upregulate genes usually 'disallowed' in mature β-cells such as *Slc16a1,* and promote progressive hyperglycaemia [121]. Liver kinase B1 and AMPK maintain β-cell identity through surpassing pathways linked to other cell types (including neuronal and hepatic) and loss of function induces expression of 'disallowed' genes [122]. Moreover, deletion of the von Hippel-Lindau genes, which encode an E3 ubiquitin ligase involved in oxygen sensing, disrupt effectors downstream of Notch, Wnt and Hedgehog signalling cascades and upregulate SOX9, which is normally repressed in adult β-cells [123]. Furthermore, knockdown of the repressor Groucho-related gene 3 (GRG3), which interacts with

NKX6.1 to supress glucagon activation and maintain monohormonal β-cell identity, in INS1-E cells promotes β- to α-cell transition [124]. Whereas in α-cells, expression of GRG3 represses glucagon and aristaless related homeobox (ARX) and, with addition to PDX-1, promotes GLUT2 expression and induces GSIS [125].

1.3. Zinc metabolism

Zinc is an essential micronutrient that exists as a non-redox-active divalent cation (Zn^{2+}) under physiological conditions. Intracellular zinc consists of zinc(II) bound to proteins and free Zn^{2+}, which describes the labile cation freely available to bind proteins [126]. Zinc is fundamental for a multitude of biological processes as a structural, catalytic, and inter- and intracellular signalling component [127, 128]. The human genome encodes ~3000 zinc(II)-binding metalloproteins [129] that affect diverse arrays of cellular processes ranging from DNA repair, replication and translation [130] to differentiation and protection against oxidative stress [131-133]. Zinc most commonly binds proteins at zinc-finger domains, which include classical C2H2-type domains in addition to RING-type, PHD-type and LIM-type domains. A large number of transcription factors contain C2H2 ZNFs, to which zinc binding is essential for protein-DNA interactions [134]. An imbalance in intracellular zinc is linked to an array of disorders including Alzheimer's disease [135], Acrodermatitis Enteropathica [136], cancer [137, 138] and diabetes [139-141]. Zinc is implicated in almost all levels of glycaemic control from β-cell insulin release to insulin uptake and action at target tissues [142, 143].

Alike all essential metal ions, intracellular zinc concentrations are tightly regulated, allowing for zinc-specific reactions whilst avoiding cross-metal interference. Cytosolic free Zn^{2+} is maintained within the pM range, with much higher concentrations in zinc-storing intracellular compartments and vesicles [127]. Cells maintain zinc at specific

concentrations through buffering and muffling (time-dependent zinc redistribution through intracellular compartmentalisation) dynamics, which vary dependent on cellular state [144]. Buffering is mediated by metallothionein (MT1-4) zinc(II)-binding proteins and muffling by families of membrane transporters, namely the Zrt- and Irt-related protein (ZIP; SLC39A) and zinc transporter (ZnT; SLC30A) families, which flux zinc into and out of the cytosol, respectively [145]. Co-ordinated regulation allows environmental-induced zinc fluctuations to mediate signalling pathways and physiological targets, thought to initiate from outside the cell and from intracellular organelles such as the endoplasmic reticulum (ER), Golgi apparatus and mitochondria, which contain high concentrations of zinc [146]. Responses are dependent on signal duration and amplitude, with both early and late zinc signalling described, associated with transcription-independent and -dependent responses, respectively [147]. An overview of regulation of zinc homeostasis in mammalian cells is depicted in **Fig 1.6**.

1.3.1. MTF1

Zinc-dependent changes in gene expression are primarily regulated by the metal-response element–binding transcription factor 1 (MTF1) [148]. MTF1 comprises of six Cys_2His_2 zinc fingers with the lowest Zn^{2+} affinities of any known zinc fingers (nM to sub-µM range) [149, 150]. MTF1 translocates to the nucleus in response to cytosolic free Zn^{2+}, where it binds metal response elements (core sequence TGCRCNC) in the promoters of zinc-regulated genes; *mtf1* knockdown in zebrafish ZF4 cells alters the transcriptional response to cytosolic zinc fluctuations for over 1000 genes [151]. MTF1 recruits the histone acetyltransferase p300/CBP and the transcription factor SP1 to form a multiprotein complex to potentiate its activity [152]. The zinc-finger transcription factors KLF4 [153] and ZNF658 [154] additionally mediate Zn^{2+}-responsive gene expression.

Intracellular zinc homeostasis is further maintained through zinc-dependent marking of proteins for degradation by the ubiquitination pathway [155].

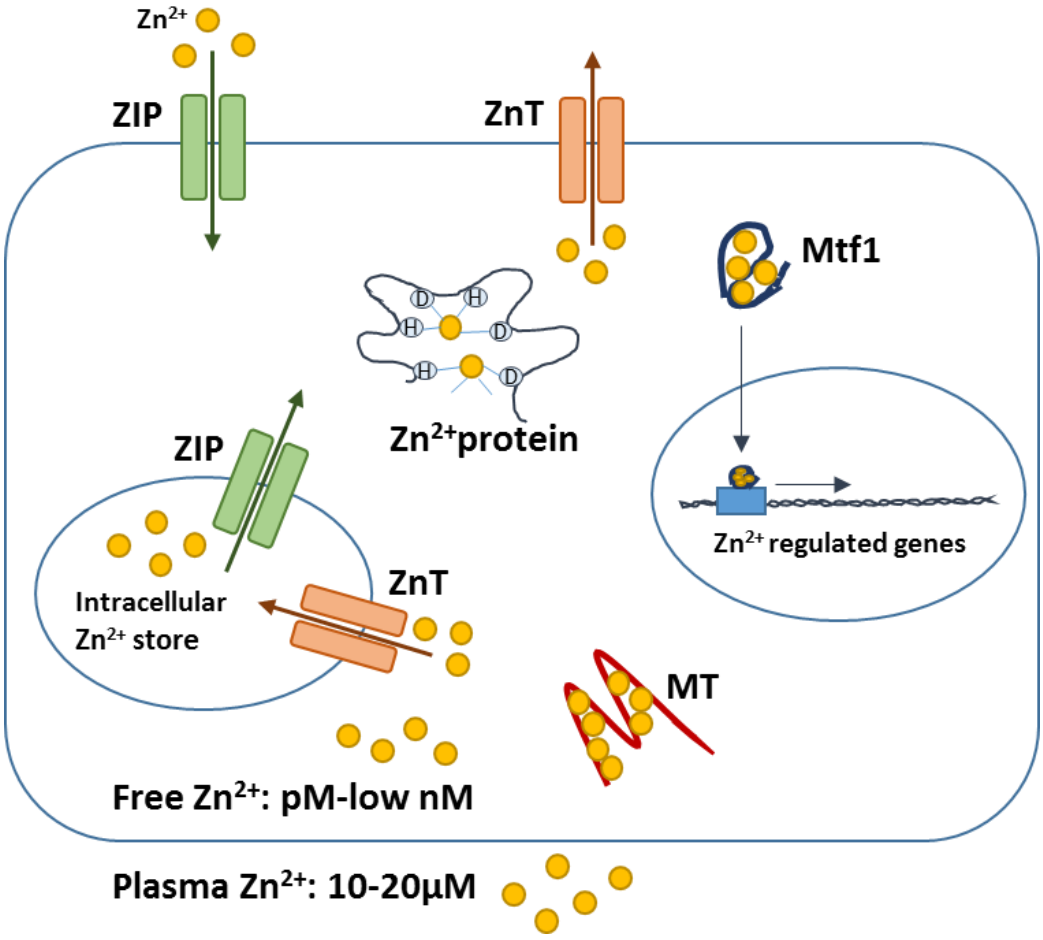

Fig 1.6. Regulation of zinc homeostasis in mammalian cells. Mobilisation of zinc into and out of cells is mediated by the ZIP and ZnT families of transporters, respectively. MT proteins bind and buffer cytosolic free Zn^{2+}. MTF1 binds zinc to regulate expression of zinc-regulated genes. Cytosolic free Zn^{2+} concentrations are maintained in the pM-low nM range. Adapted from [145].

1.3.2. MT proteins

MTs are low molecular weight (6-7kDa, 61-68 amino acid) cysteine-rich proteins, fundamental and ubiquitous in eukaryotes. MTs maintain cytosolic zinc concentrations by Zn^{2+} donation, sequestration and/or redox control [156]. The metal-free apo-protein binds zinc to activate zinc-inhibited enzymes, act as a buffer to provide zinc to target proteins in low zinc conditions, and act as a chaperone to remove zinc from zinc finger transcription factors such as TFIIIA and SP1, eliminating their DNA-binding abilities [157, 158]. MT C-terminal α-domains have high affinities for up to three Zn^{2+}, and the N-terminal β-domains can coordinate four others, but at lower affinities. In total, MTs occupy 5-15% of the cellular zinc pool. MT buffering capacities depend on pZn, which describes the physiological Zn^{2+} potential, determined by the K_d of the buffering ligand(s) ($pZn = -\log[Zn^{2+}]$). Strongly buffered zinc is associated with low free Zn^{2+} and rapid returns to resting levels after stimulation, whereas weakly buffered zinc is associated with reaching a new steady-state following elevation [159].

In human, eleven functional MT isoforms exist (MT1A, B, E, F, G, H, M and X, MT2A, MT3 and MT4), whereas one copy of each MT1-4 are harboured in mice [160]. MT1 and MT2 are expressed in almost all mammalian tissues and are responsible for zinc buffering within β-cells. MT3 and MT4 are generally tissue specific, primarily in the brain and certain epithelial tissues, respectively. MTs bind and release zinc dependent on changes to the oxidation environment: oxidation induces MT zinc release whereas reduction increases their zinc-binding capacities [161]. MTF1 is the main transactivator of MT1 and MT2 expression [162, 163]. Although MT1 and MT2 abundances have been attributed to several conditions including oxidative stress and inflammation, it is fairly convincing that the MTF1 regulatory response is dominant and that other factors, such as hypoxia-inducible transcription factor 1 (HIF1), glucocorticoids and interleukin 6 (IL-6)

mediate this response [164-167]. Expression of MT1 and MT2 are further regulated by epigenetic mechanisms including cell-specific promoter methylation [168, 169].

1.3.3. Zinc transporters

The ZIP and ZnT transporters have multiplied through evolution through gene duplication events to exhibit tissue-, cellular- and subcellular-specific expression [170]. Mammalian paralogues show differing Zn^{2+}-affinities, transporting efficiencies, regulatory mechanisms, metal-specificities (ZIP8 and ZIP14 transport non-transferrin bound iron and cadmium ions, amongst others, in addition to zinc [171-173]) and some functional redundancies [128, 174]. The transporters are regulated at epigenetic, transcriptional, post-transcriptional (microRNA [175, 176]), translational and protein (proteolysis, phosphorylation, ubiquitination and heterodimer formation) levels in response to stimuli and nutrients including zinc [177, 178]. Expression of many β-cell zinc transporters are dependent on sufficient concentrations of extracellular glucose [179].

1.3.4. ZnT transporters

ZnT transporters are members of the cation diffusion facilitators (CDFs) superfamily which, with the exception of ZnT5 [180], consist of six transmembrane domains (TMD) and cytoplasmic amino and carboxyl terminal domains (NTD and CTD, respectively) [62]. ZnT5 contains a nine TMD N-terminus fused to the conserved 6 TMD region at the C-terminus [180]. Zinc binding and transport is predicted to occur between TMDs IV and V [174]. ZnT paralogues can be grouped into four subgroups based on phylogenetic analysis and sequence similarities: (A) ZnT1 and ZnT10; (B) ZnT2, ZnT3, ZnT4 and ZnT8; (C) ZnT5 and ZnT7 and (D) ZnT6 [181]. All mammalian ZnT paralogues, with the exception of ZnT6, form homodimers [181, 182]; ZIP6 forms heterodimers with ZIP5 in the early secretory pathway [183]. Many other ZnTs can additionally form

heterodimers, including ZnT1:ZnT2, ZnT1:ZnT3, ZnT1:ZnT4 and ZnT3:ZnT4, which often exhibit altered subcellular localisations from respective homodimers [184]. Details of predicted tissue distributions, subcellular localisations and disease associations of human ZnT paralogues are provided in **Table 1.2**.

Most ZnT transporters are expressed in β-cells, with similar expression profiles predicted between human and mouse [185]. ZnT1 and ZnT2 are detected at the plasma membrane [185], suggesting key roles in β-cell zinc export, and supplementation of human islets with zinc increases expression of ZnT1 [186]. Although not described specifically for β-cells, ZnT2 additionally localises to the secretory granules in specialised secretory tissues [187]. ZnT3, which is known to localise to neuronal synaptic vesicles [188], is implicated in insulin production in rat INS-1E cells, where it presumably localises to endosomes, and streptozotocin-treated ZnT3 null mice present with decreased insulin expression and secretion, and hyperglycaemia [189]. However, independent studies report ZnT3 at high levels in human but not mouse islets [185, 190]. ZnT4, ZnT5 and ZnT6 are abundantly expressed at the TGN and vesicular compartments in β-cells, and ZnT5 additionally localises to the secretory granules [185, 191-194]. An additional ZnT5 variant localises to the plasma membrane [193], however plasma membrane expression has not yet been described for β-cells. ZnT7 concentrates at the Golgi apparatus in β-cells [195] and ZnT7 null mice show increased susceptibility to diet-induced glucose intolerance and insulin resistance, in part due to decreased insulin secretion [196]. ZnT9 and ZnT10 exhibit perinuclear and vesicular localisations and ZnT10 additionally localises to the plasma membrane in islets, but not cultured β-cells [185], possibly due to zinc-dependent translocation [197].

Table 1.2. Overview of human ZnT (SLC30A) paralogues. Tissue distributions, subcellular localisations and associated diseases are listed. Adapted from [147, 187, 193].

Paralogue	Tissue distribution	Subcellular localisation	Disease associations
ZnT1 (SLC30A1)	Ubiquitous	Plasma membrane	Alzheimer's disease, Pancreatic cancer
ZnT2 (SLC30A2)	Pancreas, kidney, epithelial cells, small intestine, mammary glands, prostate, pancreas	Variant A: Vesicles, lysosomes Variant B: plasma membrane	Transient neonatal zinc deficiency
ZnT3 (SLC30A3)	Brain, testis	Synaptic vesicles	Alzheimer's disease
ZnT4 (SLC30A4)	Mammary gland, brain, small intestine, placenta, blood, epithelial cells	Intracellular compartments	Alzheimer's disease
ZnT5 (SLC30A5)	Ubiquitous	Variant A: Secretory granules, Golgi apparatus Variant B: ER, plasma membrane	Osteopenia
ZnT6 (SLC30A6)	Small intestine, liver, brain, adipose tissue	Secretory granules, Golgi apparatus, ER	Alzheimer's disease
ZnT7 (SLC30A7)	Retina, small intestine, liver, blood, epithelial cells, spleen	Golgi apparatus, ER, secretory granules	Prostate cancer
ZnT8 (SLC30A8)	Pancreatic α- and β-cells	Secretory granules	Type I and Type II diabetes
ZnT9 (SLC30A9)	Ubiquitous	Cytoplasm, nucleus	Unknown
ZnT10 (SLC30A10)	Liver, brain	Plasma membrane, early endosomes, Golgi apparatus	Syndrome of hepatic cirrhosis, dystonia, polycythemia, and hypermanesemia, Parkinson's disease

The most abundantly expressed ZnT paralogue in β-cells is ZnT8, which shows almost exclusive expression in pancreatic α- and β-cells. ZnT8 exists as a ~70kDa homodimer

that functions to flux zinc into β-cell insulin secretory granules [198, 199]. The role of ZnT8 in β-cells has been extensively explored and is discussed in section **1.4**. ZnT8 expression is regulated by multiple transcription factors including PDX-1 at two enhancers [200] and is mediated post-transcriptionally, since high mRNA levels recorded for both α- and β-cells are only reflected at the protein level in the latter [201, 202].

1.3.5. ZIP transporters

The ZIP transporter superfamily contains over 100 SLC39A sequences [178, 203], of which 14 mammalian paralogues exist. The 14 human and mouse SLC39A paralogues are grouped into 4 subcategories based on structural homology: Subfamily I (ZIP9), Subfamily II (ZIP1, ZIP2 and ZIP3), the LIV-1 subfamily (ZIP4-8, ZIP10 and ZIP12-14) and the GufA subfamily (ZIP11) [203]. Details of predicted tissue distributions, subcellular localisations and associated diseases are provided in **Table 1.3**. Some ZIP transporters show different subcellular localisations dependent on post-translational modifications and in response to stimuli. For example, ZIP6 is initially expressed at the ER but following cleavage of the NTD localises to the plasma membrane [204], and the N-terminal ectodomain of ZIP4 is cleaved in response to prolonged zinc deficiency to promote increased ZIP4 accumulation at the plasma membrane in the intestine and visceral endoderm [205]. There is some evidence for ZIP heterodimerisation, such as ZIP6:ZIP10, which heterodimerize to induce proliferation, protect against anoikis and promote cellular migration [206]. Many ZIP transporters exhibit roles in cells in addition to zinc transport and can be considered membrane-bound chaperones. Multiple kinases binding sites have been identified on ZIP cytoplasmic domains, such as binding sites for GSK-3 on histidine-rich cytoplasmic loops of ZIP6:ZIP10 heteromers [207].

Table 1.3. Overview of human ZIP (SLC39A) paralogues. Tissue distributions, subcellular localisations and associated diseases are listed. Adapted from [147, 208, 209].

Paralogue	Subfamily	Tissue distribution	Subcellular localisation	Disease associations
ZIP1 (SLC39A1)	Subfamily II	Prostate, small intestine, kidney, liver, pancreatic α-cells	Plasma membrane, ER	Prostate cancer, Parkinson disease, Huntington disease, schizophrenia, ADAH
ZIP2 (SLC39A2)	Subfamily II	Prostate, uterine, epithelial cells, ovary liver, skin, mammary gland	Plasma membrane	Carotid artery disease, bladder cancer
ZIP3 (SLC39A3)	Subfamily II	Mammary gland, prostate, testes, pancreatic cells	Plasma membrane, intracellular compartments	Bipolar disorder
ZIP4 (SLC39A4)	LIV-1	Small intestine, stomach, colon, kidney, brain, pancreas, cecum	Plasma membrane	Pancreatic cancer, Acrodermatitis enteropathica
ZIP5 (SLC39A5)	LIV-1	Pancreas, kidney, liver, spleen, colon, stomach,	Plasma membrane	High myopia
ZIP6 (SLC39A6)	LIV-1	Ubiquitous	Plasma membrane	Breast cancer, oesophageal squamous-cell carcinoma
ZIP7 (SLC39A7)	LIV-1	Ubiquitous	ER, Golgi apparatus	Breast cancer
ZIP8 (SLC39A8)	LIV-1	Ubiquitous	Vesicles, plasma membrane	Hypertension, chronic stress, schizophrenia, circulating high-density lipoprotein cholesterol, metabolic syndrome, metabolic syndrome
ZIP9 (SLC39A9)	Subfamily I	Ubiquitous	Plasma membrane, Golgi, Trans-Golgi network	Unknown
ZIP10 (SLC39A10)	LIV-1	Ubiquitous	Plasma membrane	Breast cancer
ZIP11 (SLC39A11)	GufA	Mammary gland, testis, stomach, ileum and cecum	Golgi, plasma membrane	Autism, sporadic amyotrophoc lateral sclerosis
ZIP12 (SLC39A12)	LIV-1	Retina, brain, testis, lung, smooth muscle and interstitial cells	Plasma membrane	Schizophenia, high blood pressure, bipolar disorder
ZIP13 (SLC39A13)	LIV-1	Ubiquitous	Golgi apparatus, ER	Spondylocheirodysplastic Ehlers-Danlos syndrome (SCD-EDS)
ZIP14 (SLC39A14)	LIV-1	Ubiquitous	Plasma membrane, mitochondria, endosome, lysosome	Asthma

ZIPs comprise of a predicted 8 TMD topology with extracellular or intra-compartmental CTDs and NTDs. Highly conserved histidine, serine and glycine residues reside in TMDIV to facilitate zinc translocation and a histidine-rich sequence (HXHXH, where H is histidine and X is any amino acid) is present on the long intracellular loop between TMDIII and IV, critical for zinc binding [210]. LIV-1 subfamily members contain large extracellular domains that are important for optimal zinc transport activity. Crystal structures of the ZIP4 extracellular domain show that it exists as two structurally distinct subdomains with a conserved proline-alanine-leucine (PAL) motif at the dimerization interface, connected by a flexible bridging domain. The helix-rich NTD and bridging domain interact with core TMD components to facilitate zinc transport. ZIP4 forms homodimers via its extracellular domain, a mechanism predicted to be shared by additional LIV-1 members containing PAL motifs (ZIP5, ZIP6, ZIP8, ZIP10, ZIP12 and ZIP14) [211]. Crystal structures for prokaryotic ZIP homologs demonstrate that ZIPs encompass a 3+2+3 TMD architecture containing a binuclear metal centre. This fold is predicted to be different from other known substrate carriers, whereby an inward open confirmation occludes the extracellular side and symmetrically related substrate-binding TMDs (TMD4 and TMD5) are sandwiched by 3-TMD repeats [212]. However, ZIP transport mechanism(s) remain unresolved, partly due to conflicting transporter properties. ZIP1 and ZIP2 are homologous to Zrt1 and Zrt2 zinc transporters in the model fungus *Saccharomyces cerevisiae*; Zrt1 and Zrt2 [213, 214] but not human ZIP1 or ZIP2 [215, 216] show ATP-dependent zinc transport. Moreover, ZIP8 and ZIP14 facilitate transport of $Zn^{2+}[HCO_3^-]^2$ electroneutral complexes when overexpressed in *Xenopus oocytes* [217].

Limited information is known about the ZIP transporters in β-cells [218]. Data from quantitative PCR (qPCR) studies [192, 218] suggest that ZIP6 and ZIP7 are highly

expressed and cooperate with ZnT paralogues to regulate zinc transport from the ER and plasma membrane (ZIP6), and the Golgi apparatus (ZIP7). However, the additional ZIPs chiefly responsible for β-cell zinc homeostasis remain less clear. ZIP4 overexpression in MIN6 cells increases cytosolic free Zn^{2+}, resulting in increases in granule zinc and GSIS independent of the mitochondrial membrane potential, and ZIP4 deletion in mouse islets upregulates ZnT8 and marginally improves glucose homeostasis without inducing changes to insulin secretion [219], possibly an adaptive response to prevent granule zinc depletion [220]. However, ZIP4 shows low relative expression in mouse MIN6 cells [218]. Additional studies highlight high mRNA expression in β-cells for ZIP1 [221] and ZIP14 [218] in human, and for ZIP3 [218], ZIP8 [192, 218, 222] and ZIP13 [218] in mouse, indicative of a potential biological importance.

1.3.6. Zinc transporting membrane channels

Zinc additionally enters cells through certain membrane ion channels. β-cell L-VGCC show highly specific Zn^{2+}, in addition to Ca^{2+}, influx; surprisingly, a similar mechanism is not observed for α-cells, despite abundance of similar channels [223]. Multiple transient receptor potential (TRP) channels, of which six families exist, many exhibiting roles in insulin secretion, can specifically channel zinc into β-cells [224]. TRPV1 and TRPA1 are expressed in rat INS-1 and RINm5F cells, and the TRPM3 splice variant TRPM3a2 mediates spontaneous β-cell zinc uptake with a high specificity [224]. β-cell TRPs are activated by GLP-1R stimulation, membrane depolarisation and extracellular zinc. Moreover, TRPA1 is activated by free Zn^{2+} concentrations within the low nM range in neurons [225] and TRPM7 can facilitate zinc uptake into neurons in total extracellular zinc concentrations of 30μM [226].

1.4. *SLC30A8* – A diabetes susceptibility gene

ZnT8 abundance and genotype have repeatedly been associated with β-cell function and Type 2 Diabetes development. ZnT8 downregulation is associated with stresses linked to β-cell dysfunction, including hypoxia [227], lipotoxicity [186], hypozincaemia [186] and cytokines [179], and is observed during the early stages of diabetes in both db/db and Akita mice [228]. Addition of the zinc chelator N,N,N'N'-tetrakis(-)(2-pyridylmethyl)-ethylenediamine (TPEN) to human islets downregulates ZnT8, decreases GSIS through enhancing ATP production and increases apoptosis, whilst ZnT8 overexpression protects against decreases in GSIS induced by palmitate and TPEN [186]. ZnT8 overexpression in rat INS-1E cells increases cytosolic free Zn^{2+} and is protective against TPEN-induced apoptosis [191], indicating beneficial roles for ZnT8 against zinc depletion-induced β-cell dysfunction. However, a recent study found that ZnT8 is upregulated in islets of diabetic and insulin-resistant patients, and that ZnT8 knockdown in MIN6 cells increases proliferation and protects against inflammation-induced cell death [229].

A shorter ZnT8 isoform has been recently described which lacks the N-terminal extension of the full-length protein (320 compared to 369 amino acids) but exhibits a comparable zinc-transporting capacity [230]. RNA-seq analysis suggests that the longer ZnT8 form accounts for 71.3% of *SLC30A8* mRNA transcripts in human islets [231], however current understanding cannot confirm if both proteins are expressed *in vivo*. When overexpressed in HEK293 cells, a relatively small amount of full-length ZnT8 resides at the plasma membrane, whereas the shorter form is mainly intracellular, suggestive of additional roles for ZnT8 aside from granule zinc uptake [191, 230]. It currently remains unknown if plasma membrane ZnT8 exhibits roles in cellular zinc efflux; other human ZnT paralogues (ZnT2 and ZnT5) exist as different isoforms that localise to either the

plasma membrane or the membranes of intracellular organelles [230]. ZnT8 is additionally a major $CD8^+$ T-cell recognised autoantigen in Type 1 Diabetes [232].

1.4.1. The rs13266684 polymorphism

Over 100 genetic loci are linked to Type 2 Diabetes predisposition [233]. In 2007, ZnT8 was first identified as a Type 2 Diabetes risk loci in a GWAS French cohort [234]. The identified non-synonymous C>T single nucleotide polymorphism (SNP) at rs13266684 resides in exon 9 of the *SLC30A8* coding region, in a 33-kb linkage disequilibrium block on chromosome 8 containing the 3' end of the gene. The SNP results in an Arginine (R) to Tryptophan (W) substitution at amino acid position 325 in the unstructured CTD [235] (denoted ZnT8-R and ZnT8-W, respectively), substituting a hydrophobic polar amino acid in place of a basic amino acid [201]. Multiple GWAS have since replicated the finding and significant associations have been described in cohorts from European and Eastern Asian [21, 236-249], but not African [250, 251], Indian [252], Moroccan or Ashkenazi [253] populations. rs13266634 variants are additionally not associated with gestational diabetes in Euro-Brazilian populations [254], despite women exhibiting higher risks of Type 2 Diabetes following pregnancy [255]. The polymorphism therefore probably confers risk in the context of specific genetic backgrounds. HapMap data (build 35) suggests that the ZnT8-R risk variant has an estimated prevalence of 55%, 75% and 95% in Asian, European and African populations, respectively [243]. Independent meta-analyses report an overall odds ratio for predisposition of 1.14-1.15, with a ~16.5% increase in relative risk per risk allele [243, 256-259].

ZnT8-R carriers present with increased proinsulin:insulin ratios [260], lowered β-cell function (assessed through Homeostatic model assessment B) [261] and impaired insulin secretion during intravenous glucose tolerance tests [262, 263]. The mutation is thought

to alter the kinetics of zinc uptake into β-cell secretory granules, however the molecular details remain unclear. Alignment of ZnT8 sequences from several species shows that the amino acid at position 325 and its properties (such as hydrophobicity and ability to form H-bonds) are poorly conserved, leaving investigations challenging [230]. Zinc uptake assays using ^{65}Zn and isolated β-cell vesicles or fluorescence probes and rodent cell lines [201, 264] suggest that ZnT8-R is less active than ZnT8-W and promotes decreased granule zinc uptake. However, when variants were overexpressed in *Xenopus laevis* oocytes, which do not normally exhibit net zinc flux, ^{65}Zn transport assays did not reveal any differences in zinc flux between the two variants [230]. Whereas when variants were reconstituted in proteoliposomes, the ZnT8-R variant was found to be more active than ZnT8-W [265]. This study noted that the lipid environment affects loading of zinc into insulin granules during biogenesis. Consistent with the latter, higher islet zinc is associated with ZnT8-R risk variant carriers, potentially due to increased granule zinc influx [266]. Increased granule zinc may subsequently deplete cytosolic zinc and adversely affect β-cell function.

There is currently no crystal structure for any eukaryotic CDF protein. All ZnT8 data-structural relationships are based on the *Escherichia coli* homolog YiiP, which displays 51.8% sequence homology to the mammalian protein [267]. YiiP dimers binds eight zinc ions: two in the primary TMD transport site; two between the domains, exhibiting an unknown function, and four at the CTD interface. The CTD is believed to be involved in metal sensing to induce conformational changes to the transporter and facilitate Zn^{2+}/proton antiport [268]. In human, 3D homology models suggest that R/W325 is not directly involved in CTD Zn^{2+}-binding and that both isoforms are predicted to adopt αββαβ structures, comparable to YiiP. However, mammalian zinc transporters must function differently than bacterial orthologues: bacterial zinc exporters only function in

high levels of cytosolic Zn^{2+} whereas loading of zinc into insulin secretory granules occurs under normal concentrations of cytosolic Zn^{2+}. The human ZnT8-R/W genotype likely impacts zinc transport through altering transporter dimer formation and stability: the CTD of ZnT8-R (ZnT8-cR) exhibits a higher thermostability but a lower dimerization affinity than ZnT8-cW [269]. ZnT8-R/W polymorphisms may further alter protein-protein interactions [270], however few biding partners have yet been identified.

1.4.2. *SLC30A8* truncating polymorphisms

Twelve rare (<0.1% of the population) ZnT8 nonsense (truncating) or missense loss-of-function variants are protective against Type 2 Diabetes, which collectively represent a 65% decrease in disease risk [271]. These polymorphisms group into structurally distinct variants from ancestrally distinct cohorts, of which the two most common sequences fail to express stable proteins. Explanations for relative diabetic risk include a bimodal (bell-shaped) impact of ZnT8 activity for β-cell zinc release and action on target tissues. A modest decrease in ZnT8 activity and zinc secretion may primarily enhance hepatic insulin clearance [272] (described in **1.5.5**), whereas loss-of-function mutant proteins may increase pancreatic insulin release, outweighing the impact on insulin clearance.

1.4.3. Animal studies

Multiple groups have produced global and β-cell-specific ZnT8 knockout animals to help elucidate the role of ZnT8 in glucose homeostasis [201, 202, 227, 273]. Results from these studies are summarised in **Table 1.4.** Variations in the phenotypic traits observed are majorly attributed to differences in genetic background, environment and deletion strategy. For example, disrupted glucose tolerances were reported for mice from mixed [201, 202] but not C57BL6 [274] backgrounds, and several β-cell-specific *Cre* deleter

strains (notably PDX-1 and RIP2Cre) are complicated by off-target deletion in additional tissues such as in neuronal cells [275].

In general, β-cells from ZnT8 null mice show large changes in granule morphologies. Granules lacking dense cores and granules containing 'rod-like' structures have been described that accompany ~12% larger fractions of the cells due to sparser packaging, possibly due to lack of insulin crystallisation in low zinc [202]. Concurrently, islets from ZnT8 null mice exhibit lowered total zinc contents [201, 273, 276], however no differences in insulin processing [201, 202], frequencies or amplitudes of Ca^{2+} oscillations, nor full or partial granule fusion events during exocytosis [201] have been described. Although GSIS from ZnT8 null islets remains unchanged or slightly elevated, consistent with insulin crystallisation having no effect on insulin diffusion into circulation, circulating insulin is generally lowered in ZnT8 null animals, similar to human ZnT8-R carriers [277]. Female mice transgenic for hZnT8-W (with native levels of mZnT8) are characterised by improved glucose tolerances without a change to insulin sensitivity, and islets secrete less insulin but more zinc in response to glucose compared to mZnT8 controls [278]. However, male mice transgenic for hZnT8-W (with native levels of mZnT8) exhibit lowered amounts of zinc and proinsulin in the pancreas, but higher rates of insulin secretion and increased glucose tolerances when fed on high fat diets compared to hZnT8-R transgenic mice [279]. Moreover, a recent study investigated the effects of one of the most abundant loss-of-function variants R138X, which encodes a premature stop codon, in mouse. Mice containing knock-in R138X mutations at *Slc30a8* exhibited loss of ZnT8 function, however islets secreted elevated amount of insulin in response to IR inhibition-induced hyperglycaemia [280].

Table 1.4. Overview of ZnT8 knockout mouse studies using male mice. N.R. = not relevant. GSIS = glucose stimulated insulin secretion. Adapted from [198].

Deletion location	Deletion domain	Genetic background	Body mass	Islet insulin content	Islet zinc content	Islet number	Islet EM	GSIS *In Situ*	Fasting glucose	Fasting insulin	REF
Global	Exon 3 2 Transmembrane	Mixed	No change	No change	Down	No change	N.R.	Down	No change	Down	[273]
Global	Exon 3 2 Transmembrane	C57BL /6J	No change	No change	Down	N.R.	No change	No change	No change	No change	[274]
Global	Exon 1 Initiation codon	Mixed	No change	No change	Down	No change	Altered	No change	No change	N.R.	[201]
Global	Exon 1 Initiation codon	Mixed	No change	N.R.	Down	No change	Altered	Up	Up	N.R.	[201]
Global	Exon 1 Initiation codon	Mixed	No change	No change	Down	N.R.	Altered	No change	No change	N.R.	[202]
β-cell	Exon 1 Initiation codon	Mixed	No change	N.R.	Down	No change	Altered	Down	No change	No change	[276]
β-cell	Exon 5 Zinc binding	C57BL /6J	No change	No change	Down	No change	Altered	Up	No change	No change	[272]

1.5. Zinc in β-cell function

Pancreatic β-cells maintain one of the highest zinc contents of any known cell type. Total zinc concentrations reach 150-200μM, of which 70% is contained in insulin secretory granules [281]. β-cells exhibit an exceptionally high turnover of zinc [266]; high glucose stimulation doubles cytosolic free Zn^{2+} and up-regulates Zn^{2+}-regulated genes [192]. Links between zinc and diabetes were established as early as 1938, when a 75% reduced pancreatic zinc content was described for diabetic compared to non-diabetic cadavers [282], and diabetes has since been associated with systemic hypozincaemia [140, 283, 284]. A study of 82,000 women in the US reported that a low zinc intake increases the relative risk of diabetes by 17% compared to those taking sufficient amounts of zinc [285], and negative associations between plasma zinc and diabetes onset have been described in Chinese [286] and Japanese [287] populations. However, a further longitudinal study exploring zinc in toenails as a marker of long-term zinc exposure in American young adults [288] and a systematic review including 334,387 type 2 diabetic patients [289] did not find any associations between serum zinc and diabetes. Excessive oral zinc uptake can lead to cytotoxicity through inhibiting copper uptake [290] and altering lipid metabolism [291]. A tightly regulated zinc content is therefore fundamental for normal β-cell function and the endocrine pancreas encompasses specialist mechanisms to compensate for subclinical deficiency [292]. These functions are detailed below.

1.5.1. Anti-oxidant properties

Oxidative stress plays a major role in loss of β-cell mass and function through DNA, lipid and protein damage [293]. β-cells are particularly vulnerable to oxidative stress since ROS are produced during proinsulin disulphide bond formation in the ER [294] and as

by-products during glucose metabolism [295]. Moreover, chronic hyperglycaemia and hyperlipidaemia present in Type 2 Diabetes induce excess ROS production through increased mitochondrial oxidation [296] and β-cells produce low levels of ROS-scavenging enzymes [297]. Unsurprisingly therefore diabetic animals exhibit significant redox imbalances compared to controls [298].

Oxidative stress can stimulate increases in cytosolic free Zn^{2+} to over 2nM within minutes, such as through oxidation or nitrosylation of zinc(II)-thiolate bonds [299]. Increases in cytosolic free Zn^{2+} mediate expression of antioxidant genes. For example, MTF-1 induces expression of selenoprotein 1, which encodes an antioxidant glutathione-binding protein to scavenge free radicals [300]. Furthermore, zinc is an essential cofactor of superoxide dismutase, which detoxifies ROS [301], and interferes with mitochondrial antioxidant production by inhibiting α-ketoglutarate-dependent respiration to help prevent oxidative stress-induced dysfunction [302]. Zinc additionally binds sulfhydryl groups, protecting molecules from oxidation [293], and reduces and neutralises intracellular free radicals to prevent oxidation-induced damage [303]. Concurrently, zinc depletion is associated with increased sensitivity to oxidative stress-induced apoptosis [304].

1.5.2. Intracellular signalling pathways

Zn^{2+} is a potent signalling molecule in β-cells, implicated in glucose signal recognition, second messenger metabolism, protein kinase activity and transcription factor regulation [301]. Zinc inhibits PTP1B, a prominent β-cell phosphatase with an apparent K_i of 5.6 nM for Zn^{2+} [79]. PTP1B inhibition ameliorates high-fat-diet and obesity-induced insulin resistance in mice [305], and genome-wide and tissue-specific PTP1B ablation increases insulin sensitivity and protects against obesity and diabetes [306, 307]. PTP1B inhibition

allows zinc to mimic the actions of hormones and growth factors to activate important signalling cascades involved in β-cell function, survival and mass, including insulin secretion [308]. Loss of PTP1B activity increases net IRS-1/2 phosphorylation to promote IR and IGF-1R signalling and proliferation [309], activation of the MAPKs ERK1/2, c-Jun N-terminal kinase (JNK) and p38 [310], and glycogen synthesis by inhibiting GSK-2 [311]. Zinc additionally stimulates signalling via the G-protein coupled receptor (GPCR) GPR39 by activating $G\alpha_q$, $G\alpha_{12/13}$ and $G\alpha_s$ proteins, important for the normal insulin secretory response; GPR39 is considered an important transducer of autocrine and paracrine zinc signals in β-cells [312]. Zinc influences gene expression by mediating activation of mTORC1 [313] and ERK1/2 [314], and signals to regulate pathways influencing the activity of NF-κB. Moreover, zinc plays significant roles in lipoprotein and glucose metabolism through altering expression of proliferator-activated receptor α (PPAR-α), which additionally suppress NF-κB activity [315]. Zinc further influences signal transducer and activator of transcription (STAT) signalling cascades, which regulate proliferation, differentiation, survival and apoptosis. STAT3 induces transcription of ZIP6 and ZIP10 [207, 316] and zinc deficiency reduces STAT1 and STAT3 phosphorylation in foetal rat brains [317].

Multiple zinc transporters are implicated in regulating intracellular signalling cascades. ZIP7 is a gated zinc transporter localised to the ER and Golgi apparatus and is activated by CK2 tyrosine kinase phosphorylation at multiple MAPK-binding motifs to initiate temporal zinc release and pathway activation [318]. ZIP6:ZIP10 heterodimers interact with GLP-1Rs to facilitate incretin signalling [218] and promote insulin gene expression and biosynthesis, GSIS, suppression of apoptosis, and restoration of glucose competence in glucose-resistant β-cells [319]. ZIP6:ZIP10 heteromers additionally regulate the potent

kinases GSK-3α and GSK-3β [206, 311] and downstream ERK1/2-SNAIL-SLUG pathways [320, 321] to mediate proliferation and epithelial-mesenchymal transition. Furthermore, ZnT1 interacts with RAF-1 via its CTD to activate ERK1/2 cascades [322], ZnT3 promotes ERK1/2 signalling from post-synaptic vesicles in the brain [323], and ZIP13 influences BMP/TGF-β cascades involved in cellular differentiation, growth and survival [324]. Moreover, ZIP14 is involved in GPCR cAMP signalling and knockout in mouse represses phosphodiesterase activity, leading to enhanced systemic growth [325].

1.5.3. Transcription factor regulation

Several transcription factors involved in islet development and endocrine function are Zn^{2+}-responsive in zebrafish, including *neurod1*, *hnf1ß*, *hnf4α*, *foxa1*, *nkx2.2*, and *pax6* [151, 326-328]; of these, at least *neurod1* and *foxa1* are predicted to be directly regulated by *mtf1* [151]. A recent study using human insulin-secreting β-cell like stem cells showed that zinc supplementation induces up-regulation of the β-cell markers PDX-1 and PAX4 [329]. There might therefore be a link between β-cell zinc deregulation and loss of β-cell phenotype and function. The functions of these transcription factors and associations with Type 2 Diabetes are detailed below.

1.5.3.1. NEUROD1

NEUROD1 is a basic helix-loop-helix transcription factor that mediates transcription through binding E-box containing promoter core sequences. NEUROD1 is critical for pancreatic development from progenitors and the function of mature β-cells by mediating a multitude of genes including insulin. NEUROD1 null mice develop severe diabetes at a young age and fail to develop properly differentiated islets [330], whilst β-cell-specific knockout mice present with mild hyperglycaemia and severe glucose intolerances [331].

Heterozygous loss-of-function mutations result in MODY6 [332] and homozygous truncating mutations are associated with monogenic permanent neonatal diabetes [333].

1.5.3.2. HNF1B

HNF1B is a homeodomain-containing transcription factor which exists as either a homodimer or as a heterodimer with HNF1A. HNF1B exhibits critical roles in β-cell differentiation and regulates signalling cascades involved in glucose homeostasis [93]. HNF1B abundance is suppressed by palmitate, which further downregulates expression of HNF1A [334]. Heterozygous HNF1B mutations result in multi-system disorders including MODY5, and HNF1B SNPs have been shown to predispose to Type 2 Diabetes in Finnish, Swedish, Canadian and Chinese populations [335-338].

1.5.3.3. HNF4A

HNF4A is an essential transcriptional regulator of β-cell phenotype, acting as a dimer to mediate expression of genes involved in glucose transport and glycolysis. HNF4A is required for maximal insulin production [339] and heterozygous mutations cause MODY1 [340, 341]. HNF4A null mice exhibit normal β-cell architecture but defective GSIS, and present with hyperinsulinemia and glucose intolerance [342]. However, an association study on a Japanese cohort did not find any variants in the *HNF4A* chromosomal loci associated with Type 2 Diabetes risk [343].

1.5.3.4. FOXA1

The FOXA1 transcription factor exhibits critical roles in differentiation and development of the endocrine pancreas. FOXA1 induces chromatin remodeling independent of ATP-dependent remodeling complexes, acting as a pioneer factor to establish chromosomal binding of steroid receptors including the estrogen receptor and androgen receptor [344-

346]. FOXA1 is further implicated in oxidative phosphorylation since FOXA1 knockout islets exhibit increased expression of mitochondrial protein uncoupling protein 2 and lowered intracellular ATP [347]. FOXA1 additionally mediates CREB, a master regulator of carbohydrate metabolism [348] and, along with the related protein FOXA2, interacts with PDX-1 enhancers during β-cell development [348]. FOXA1 knockout in the fetal pancreas induces hyperglycaemia as a consequence of defective insulin secretion and FOXA1 null mice present with hyperinsulinaemic hypoglycaemia and retarded growth [349].

1.5.3.5. NKX2.2

The transcription factor NKX2.2 is involved in the final differentiation of β-cells and in maintaining mature β-cell phenotype and function [350, 351]. NKX2.2 interacts with ARX to regulate development of endocrine hormone expressing cells and NKX2.2 mutations are linked to neonatal diabetes [351]. In NKX2.2 null mice, endocrine progenitors remain incompletely differentiated with a complete absence of insulin-secreting β-cells, and mice present with severe hyperglycaemia [352]. Loss of NKX2.2 function in the β-cells of NKX2.2-repressor transgenic mice further disrupts islet architecture [350].

1.5.3.6. PAX6

The transcription factor PAX6 is essential for β-cell development, morphology and insulin expression through repressing alternative islet cell programs. In PAX6 null mice, production of both β- and α-cells are severely reduced [353]. PAX6 deletion in mature islets causes hyperglycaemia [354] and in adult mice causes lethal hyperglycaemia due to loss of β-cells coupled with increases in α-cells [353]. Both human and mouse heterozygous for active PAX6 exhibit a perturbed glucose homeostasis [355], in part

through downregulating GLP-1 [356], and a common PAX6 variant reduces insulin secretion [357]. PAX6 is further downregulated in the β-cells of two diabetic mouse models: db/db mice and wildtype mice treated with an IR agonist [353].

1.5.4. The response to cytokines

β-cells are extremely sensitive to cytokines. Interleukin 1β alone or in combination with interferon γ and tumour necrosis factor (TNF) α induces β-cell dysfunction and death [179, 200]. Cytokine sensitivity is dependent on the β-cell's metabolic state, primarily mediated by inducing transcriptional changes such as insulin gene suppression. Multiple ZIP and ZnT paralogues show cytokine-responsive expression [179]. ZIP8 and ZIP14 are transcriptionally regulated by TNF and IL-6 in mouse, the response differing by time and between different tissues [358]. In independent studies, cytokine stimulation suppressed ZnT5 and ZnT8 in β-cells [179, 359] and ZnT8 knockdown in rat INS-1E cells increased sensitivity to IL-1β-induced apoptosis [179].

1.5.5. Insulin biosynthesis and crystallisation

The role of zinc in insulin biosynthesis and crystallisation has been extensively described and is illustrated in **Fig 1.7**. Insulin gene transcription is initiated by the transcription factors MAFA, PDX-1 and NEUROD1 to express a 110 amino precursor, preproinsulin [360]. Preproinsulin enters the rough ER through peptide-conducting channels, where it is cleaved by signal peptidase to form proinsulin, a heterodimer containing a 21 amino acid A chain linked to a 30 amino acid B chain via two disulphide bonds and an intervening C-peptide, and is folded by chaperones [361]. Proinsulin is transported into the Golgi apparatus where it is packaged into immature secretory vesicles. Here, prohormone convertase 1/3 and prohormone convertase 2 cleave proinsulin and the CTD basic residues are removed by the exopeptidase carboxypeptidase E to yield mature

insulin and C-peptide [21]. C-peptide is able to bind cell membranes and activate specific GPCRs [362], and can be taken up into cellular endosomes to provide a platform for intracellular signalling [363], such as through inducing cytosolic Ca^{2+} signalling [364]. Intracellular C-peptide may additionally localise to nucleoli and promote transcription of genes encoding ribosomal RNA [365].

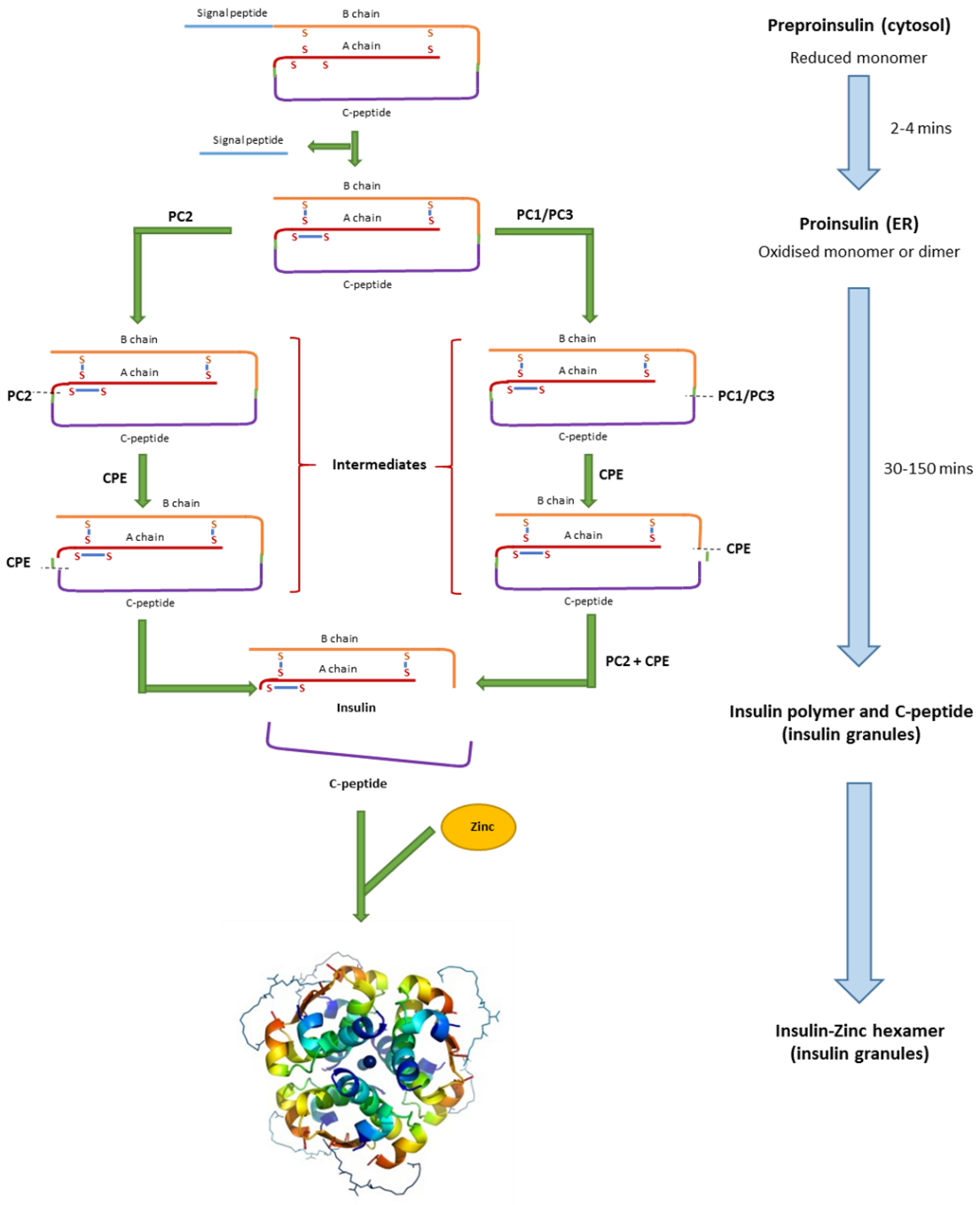

Fig 1.7. Insulin biosynthesis and crystallisation in β-cell insulin granules. The cytosolic insulin precursor preproinsulin is delivered to the ER via its N-terminal signal peptide, which is subsequently cleaved to form proinsulin. In the ER, proinsulin is oxidised to form three disulphide bridges, allowing the protein to fold and dimerise. Proinsulin travels through the Golgi apparatus into secretory granules, where it is processed by PC1/2, PC2 and CPE to create insulin and C-peptide. Insulin dimers form hexamers with increasing concentrations of Zn^{2+} in secretory granules. Adapted from [366, 367].

Zinc is transported into insulin granules via ZnT8, where local zinc concentrations reach 20mM [281, 368]. Insulin monomers dimerise at increasing insulin concentrations, aggregating to form hexamers consisting of three dimers with near perfect 2-fold symmetry in the presence of high zinc, coordinating Zn^{2+} at His10 and Glu13 on the B-peptide [369]. High granule zinc in addition to an acidic pH (pH <6) is required to maintain insulin hexamers and granule osmotic stability [370] and to protect against proteolytic degradation [371]. Insulin biosynthesis occurs within the region of 120 minutes and mature insulin is stored for 4-8 days [26].

1.5.6. Zinc secreted from pancreatic β-cells

Two Zn^{2+} crystallise with each insulin hexamer, however core Zn^{2+}/insulin hexamer ratios are predicted at 2:1-to-4:1, indicative of a further importance for granule zinc [272]. Zinc is co-released with insulin into the portal vein at a rate of 1.73 ± 0.74pmol/islet upon stimulation [202]. Secreted zinc suppresses insulin [132, 370] and IAPP [372] fibrillation at the site of release and in circulation under a physiological pH, avoiding formation of toxic amyloid deposits. Zinc shows autocrine effects on β-cells to reduce further insulin secretion through targeting K_{ATP} and L-VGCC channels [373] and suppresses cellular death [374]. A paracrine role of zinc on α-cells has been suggested whereby zinc binds α-cell K_{ATP} channels to inhibit membrane depolarisation and glycogen secretion [375, 376], however this remains in dispute [377].

A role for β-cell zinc in peripheral insulin regulation has further been described [272]. Prior to systemic circulation, the portal vein transports insulin and zinc from the pancreas to the hepatic system, where around 50% of secreted insulin binds IRs and is internalised and proteolytically degraded by insulin-degrading enzymes to prevent hypoglycaemia [378]. During the postprandial state, hepatic clearance is reduced by approximately 20%

[379], potentially regulated by dose-dependent zinc inhibition of clathrin-mediated IR endocytosis [272, 380].

1.6. Targeting zinc homeostasis

Multiple groups have investigated the consequences of zinc deficiency for rodent physiology [381-386]. Zinc deficient rats show impaired glucose tolerances compared to pair-fed controls following administration of glucose by both intravenous and intraperitoneal routes [381, 382]. Moreover, various zinc chelators induce diabetes in mammals (including hamsters, mice and rabbits) through β-cell destruction [387, 388] and zinc deficiency increases the risk of diabetes development in diabetic-prone animals. Diabetic mice are less able to maintain whole-body zinc levels following introduction of a low-zinc diet compared to non-diabetic controls, elevating this effect [389].

Zinc supplementation has been proposed as a potential therapy for Type 2 Diabetes [390]. Dietary zinc supplementation improves glycaemic control, promotes healthy lipid parameters [385], enhances antioxidant status [383, 384], and restores normal plasma zinc [386] in zinc deficient rodents. Zinc supplementation further attenuates hyperglycaemia and hyperinsulinemia in obese ob/ob [391], db/db mice [392] and high fat-fed mice [393], improves polydipsia and high density lipoprotein cholesterol levels in streptozotocin-induced diabetic mice [394] and improves blood glucose and serum lipid profiles in type 2 diabetic rats [298]. Moreover, zinc supplementation reduces the diabetic phenotype of human diabetic patients by improving glycaemic control and promoting healthy lipid parameters [142, 385, 395]; however, individual studies show considerable heterogenicity, with some concluding no benefit for zinc [142, 385]. Zinc administration may further induce unwanted side effects: high dietary zinc can alter lipid metabolism

[291], inhibit copper absorption [396] and can outcompete copper for substrate binding, such as to the Cu/Zn-superoxide dismutase [397]. Novel mechanisms to target disrupted zinc homeostasis specifically in β-cells may be needed before zinc supplementation therapies can meaningfully be implemented into clinical practice.

1.7. Hypothesis and aims

Maintaining adequate zinc is essential for normal β-cell function in glycaemic control. Systemic hypozincaemia is present in many type 2 diabetic patients [140, 283, 284] and polymorphisms in the predominantly β-cell-specific zinc transporter ZnT8 are associated with Type 2 Diabetes risk [234]. However, aside from its role in insulin granules, the importance of zinc for β-cell phenotype and survival remains largely unexplored. Since many zinc transporters carry out other very specific roles in addition to zinc transport and may be regarded as membrane-bound zinc chaperones, such as ZIP6:ZIP10 heteromers which stimulate proliferation through promoting phosphorylation and inhibition of GSK-3 [207], altered zinc trafficking may induce β-cell dysfunction aside from disrupting the cellular zinc content; these mechanisms could be important to understand for development of novel therapeutics for type 2 diabetic patients. In this project we postulated that zinc uptake into insulin granules is coordinated with ZIP-facilitated cytosolic zinc influx and that different ZnT8 abundances and genotypes associated with Type 2 Diabetes interfere with ZIP-regulated zinc trafficking. We further hypothesized that alterations to the abundances/functions of these ZIP transporters impact β-cell phenotype and function. During this PhD project we therefore sought to address the following aims:

I. To identify ZIP transporters that functionally coordinate with ZnT8 to maintain normal zinc trafficking in β-cells and explore whether these transporters are regulated differently based on ZnT8 activity.

II. To explore the consequences of the hyperglycaemia and hypozincaemia associated with Type 2 Diabetes for β-cell ZIP transporter expression, zinc content and cellular phenotype.

III. To explore the roles of highlighted ZIP transporters for the β-cell response to hypozincaemia.

2. General methods

2.1. Cell line and culture

The adherent insulinoma β-cell–like clonal cell line MIN6 (Mus musculus) was maintained in Dulbecco's Modified Eagle's Medium containing 25mM glucose (DMEM, Thermo Fisher), supplemented with 15% fetal bovine serum (FBS, Thermo Fisher), 4mM L-glutamine, 50μM β-mercaptoethanol, 100μg/ml streptomycin and 100 units/ml penicillin (all Sigma Aldrich), at 37^{o}C in a humidified atmosphere of 95% air and 5% CO_2. Cells were used from passages 24-38. Cells were passaged through trypsinisation [0.25% trypsin-EDTA (Thermo Fisher) in PBS (5 mins, 37^{o}C)] with passage intervals of 3-4 days.

2.1.1. Freezing cells

Cells were suspended in 50% (v/v) cell culture medium, 40% (v/v) FBS and 10% (v/v) Dimethyl sulfoxide (Sigma Aldrich) in 1ml cryovials. Cells were immediately frozen at 20^{o}C (1 h) before transfer to -80^{o}C.

2.2. Stimulation of cells with zinc

FBS was depleted of heavy metal ions through incubation with 5% (w/v) Chelex-100 (Sigma Aldrich) for 1 h, and sterile filtered through a 0.22μm syringe. Chelex-100 treated FBS was diluted 1:100 in 0.5% nitric acid (Sigma Aldrich) and heavy metal analysis carried out through inductively-coupled plasma mass spectrometry (ICP-MS) [4] by the London Metallomics Facility funded by the Wellcome trust (grant reference 202902/Z/16/Z). Chelex-100 treated FBS was supplemented with Ca^{2+} ($CaCl_2$), K^{+} (KCl) and Mg^{2+} ($MgSO_4$) (all Sigma Aldrich) to original concentrations. *Mouse islets* (detailed

in chapter 5, section **5.3.5.3**): growth media were replaced with 25mM glucose Roswell Park Memorial Institute (RPMI; Thermo Fisher) containing 10% Chelex-100 treated-FBS, 4mM L-glutamine, 50μM β-mercaptoethanol, 100μg/ml streptomycin and 100 units/ml penicillin, supplemented with $ZnCl_2$ (Sigma Aldrich) to total concentrations of 1μM or 8μM (control) Zn^{2+} for 48 h. *MIN6 cells:* growth media were replaced with 25mM glucose DMEM containing 15% Chelex-100 treated-FBS, 4mM L-glutamine, 50μM β-mercaptoethanol, 100μg/ml streptomycin and 100 units/ml penicillin, supplemented with $ZnCl_2$ to total concentrations of 1μM, 8μM (control) or 42μM Zn^{2+} for 24 h, 48 h or 96 h. The metal ion concentrations for all media used are provided in **Appendix 5**.

2.3. Determination of cellular zinc content

Cells were lysed in hot 0.2% sodium dodecyl sulphate (SDS; Sigma Aldrich). Samples were diluted 1:100 with trace element grade 0.5% nitric acid (Sigma Aldrich) and the zinc concentrations determined through ICP-MS [4], carried out by the London Metallomics Facility funded by the Wellcome trust (grant reference 202902/Z/16/Z). The total zinc content was normalised to protein content, determined through Bradford assays (Bio-Rad; **2.7.2**) [5].

2.4. Cell transfection

2.4.1. Transfection with siRNA

Cells were transfected with siRNA using Lipofectamine RNAiMAX transfection reagent (Thermo Fisher) 24 h after seeding, following manufacturer's instructions. Per well of 6-well plate: 30pmol siRNA, 7.5ul Lipofectamine RNAiMAX reagent and 250μl Opti-MEM medium (Thermo Fisher) was added.

2.4.2. Transfection with plasmid DNA

Cells were transfected with plasmid DNA using Lipofectamine 3000 transfection reagent (Thermo Fisher) 24 h after seeding, following manufacturer's instructions. Per well of 6-well plate: 7.5μL Lipofectamine 3000 reagent, 5μL P3000 transfection reagent, 2.5μg plasmid DNA and 250μL Opti-MEM medium was added.

2.5. CRISPR/Cas9 gene knockout

CRISPR (Clustered Regularly Interspaced Short Palindromic Repeats) is a genome editing technique based upon the Type II CRISPR-associated protein-9 nuclease (Cas9) system in *Streptococcus pyrogenes*. CRISPR/Cas9 technology utilises an RNA-guided nuclease system containing a guide RNA sequence in the form [5'20nt-NGG] to facilitate targeted double-stranded DNA cleavage. Cleavage promotes error-prone non-homologous end joining repair and results in insertion, deletion and/or frameshift mutations, which disrupt the protein-coding capability [398]. Alternatively, CRISPR/Cas9 can replace target sequences with novel sequences of DNA. CRISPR/Cas9 nickase technology decreases off-target mutation frequencies through requiring DNA binding and cleavage at the target loci by two mutated versions of Cas9 on opposite DNA strands [399]. CRISPR/Cas9 technology is an important tool for replacing point-mutations in recessive disorders, studying complex diseases and vaccine development [400].

2.5.1. Cell transfection

Cells were transfected with the SLC30A8 Double Nickase Plasmid (m) (sc-433687-NIC), SLC39A6 Double Nickase Plasmid (m) (sc-430685-NIC) or control CRISPR/Cas9

plasmids (sc-418922) [all Santa Cruz Biotechnologies (**Fig 2.2.**)] as described in section **2.4.2.**

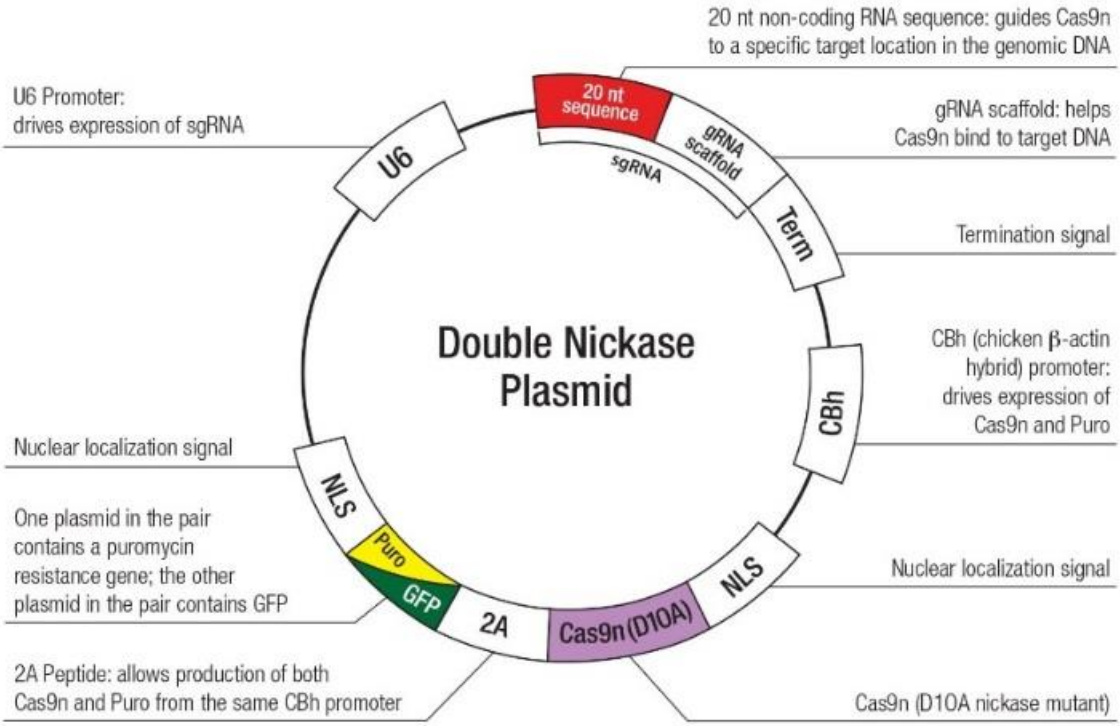

Fig 2.1. The CRISPR/Cas9 double nickase plasmids. Plasmids encode single guide RNA targeting *Slc39a6, Slc30a8* or scramble DNA, and either GFP or a puromycin dihydrochloride resistance gene for selection. Diagram courtesy of Santa Cruz Biotechnology (https://www.scbt.com/scbt/product/znt-8-crispr-knockout-and-activation-products-m).

2.5.2. Generation of clonal populations

At 72 h following transfection, cells were selected using 1.25ng/µl puromycin dihydrochloride (Santa Cruz Biotechnologies) for 6 days and imaged for GFP fluorescence. Cells were transferred into a 96-well plate through serial dilution. Clonal cell populations were amplified through passaging cells into wells of increasing size.

2.5.3. Verification of genome editing

DNA was extracted using the DNeasy Blood and Tissue Kit (Qiagen). DNA targeted by the CRISPR/Cas9 constructs were PCR amplified in reactions containing: 1X Taq reaction buffer, 200µM dNTP mix, 20µg DNA template, 1.25units/50µl PCR Taq Polymerase (all Thermo Fisher) and 0.2µM forward and reverse primers (Sigma Aldrich; sequences provided in relevant chapters), and subjected to the cycling conditions in **Table 2.1**. Amplicons were separated on 2% agarose gels supplemented with 0.1% (v/v) gel red (Biotum) at 40V. Amplicons showing bands shifted from those from control cells were purified using the QIAquick Gel Extraction Kit (Qiagen). Amplicons were subjected to a second PCR amplification, treated with ExoSAP-IT PCR Product Clean-up Reagent [37^{o}C, 15 mins, followed by 80^{o}C, 15 mins (Affymetrix)] and Sanger sequenced (Eurofins Genomics).

Table 2.1. Cycling conditions used for PCR assays.

Stage	Temperature (^{O}C)	Duration (seconds)	Cycles
Initial denaturation	95	30	1
Denaturation	95	30	30
Annealing	58	30	30
Elongation	68	1	30
Final elongation	72	5	1

2.5.4. *In silico* sequence analysis

To explore predicted translation of mutated proteins, we uploaded edited mRNA sequences into ExPASy bioinformatics software [401] and aligned amino acid sequences to native sequences using the Clustal Omega multiple sequence alignment tool [402]. We depicted the protein domains for the edited proteins by using topology descriptions on UniProt [403].

2.6. Gene expression analysis

2.6.1. RNA extraction and reverse transcription

Total RNA was extracted using TRIzol Reagent (Invitrogen) and was assessed for purity and quantity using a Nanodrop 1000 spectrophotometer. RNA was reverse transcribed to cDNA using the high capacity RNA-to-cDNA kit (Thermo Fisher) and diluted ≥1:10 prior to experimentation.

2.6.2. qPCR

qPCR assays were designed using the online Universal Probe Library (UPL) assay design tool (Roche). Assay designs are provided in **Tables 2.2.-2.3.** Primer Blast [6] was used to predict the binding of primers to mouse and human *SLC39A* isoforms. The mouse primers bind all respective ZIP transporter isoforms. The human primers bind all isoforms for ZIP2, ZIP4, ZIP5, ZIP6, ZIP8, ZIP10, ZIP11, ZIP12 and ZIP13. Primers for ZIP1, ZIP3, ZIP7, ZIP9 and ZIP14 covered either all the isoforms expressed within human islets, or those predominantly expressed (**Fig 3.1 and Appendices 6-7**). PCR plates were loaded using the Biomek FX liquid handling robot (Beckman Coulter) and reactions [20-40ng cDNA, 0.1µM UPL probe, 0.2µM forward primer, 0.2µM reverse primer and 1X TaqMan Fast Advanced Mastermix (Applied Biosystems)] amplified using the

Prism7900HT sequence detection system (Applied Biosystems) and analysed using sequence detection systems v2.4 software. All gene expression values were normalised to the housekeeping gene ubiquitin C (UBC). Validation of *Ubc* as an appropriate housekeeping gene is presented in **Fig 2.2**. Differential and relative expression were calculated using the ΔΔCT method as follows:

Differential expression:

$$\log_2 \mathrm{FC} = \log_2(2^{-\Delta\Delta\mathrm{CT}})$$

$$\text{Where: } \Delta\Delta\mathrm{CT} = \Delta\mathrm{Ct}(\text{Target sample}) - \Delta\mathrm{Ct}(\text{Calibrator sample})$$

$$\text{And: } \Delta\mathrm{CT} = \mathrm{Ct}(\text{Target gene}) - \mathrm{Ct}(\text{Housekeeping gene})$$

Relative expression:

$$\%\ \text{relative expression} = 100 * (2^{-\Delta\Delta\mathrm{CT}})$$

$$\text{Where: } \Delta\Delta\mathrm{CT} = \Delta\mathrm{Ct}(\text{Target sample}) - \Delta\mathrm{Ct}(\text{Calibrator sample})$$

$$\text{And: } \Delta\mathrm{CT} = \mathrm{Ct}(\text{Target gene}) - \mathrm{Ct}(\text{Housekeeping gene})$$

Assay efficiencies were validated through standard curves created from serial dilution of mRNA pooled from multiple samples (**Fig 2.3**). The efficiencies for primers targeting genes with appreciable expression ranged from 79.31 to 119.61% for mouse and 75.49 to 106.68% for human (**Tables 2.2-2.3**).

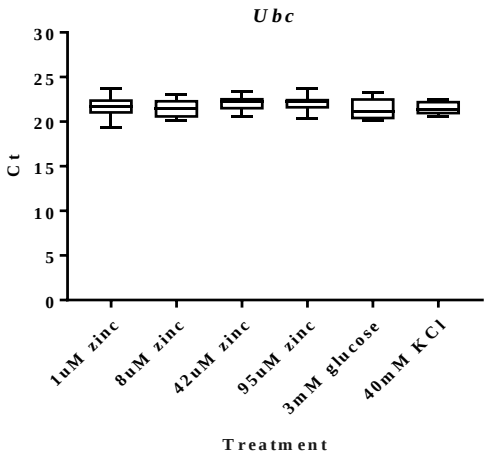

Fig 2.2. Validation of *Ubc* as an appropriate housekeeping gene. Box plot showing qPCR Ct values for *Ubc* mRNA expression following culture of MIN6 cells in 6 experimental conditions [1µM, 8µM, 42µM and 95µM zinc, 3mM glucose and 40mM potassium chloride (KCl)]. RNA (1.5µg) was reverse transcribed to cDNA and diluted 1:20 for use in qPCR. The 'whiskers' show range. N=6.

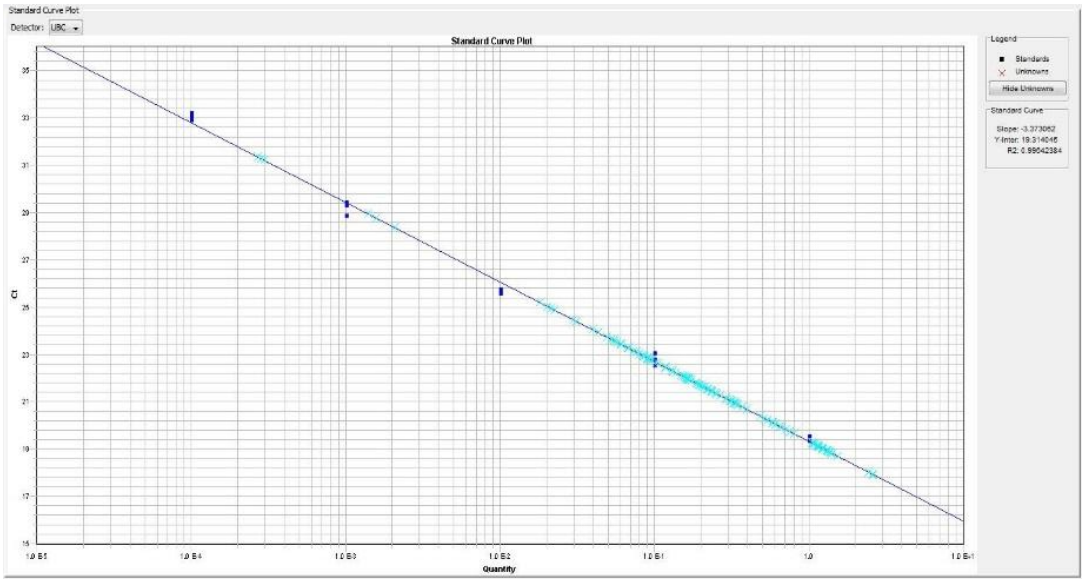

Fig 2.3. Example standard curve plot for validation of primer efficiencies. Graph shows data for mouse primers targeting *Ubc* and is an average of three biological repeats. Slope: -3.373, R^2: 0.990. Generated using sequence detection systems v2.4 software.

Table 2.2. qPCR assay designs for mouse genes undertaken in this study. * = Assay efficiency could not be determined due to low expression.

Gene	RefSeq ID	Forward primer (5' – 3')	Reverse primer (5' – 3')	Amplicon	UPL Probe	CAT. Nº	Assay efficiency
Slc39a1	NM_013901.2	CGACAGCAATGGAGTGAGAC	TCCGATGCGACTGCTTCT	119	#81	4689046001	89.24%
Slc39a2	NM_001039676.2	CCTGCTTGCTCTTCTGGTTC	ACCCTGTGGTGATGACCTG	99	#26	4687574001	100.12%
Slc39a3	NM_134135.1	CGTATTCCTGGCTACATGCTT	CGGGTAGTCGGTGCTGAT	97	#27	4687582001	92.17%
Slc39a4	NM_028064.2	CAGCTACTGCAGAAGATTGAGG	TCCAGCAGTTGGGGAAGAT	83	#07	4685059001	103.40%
Slc39a5	NM_028051.3	GGCTGACCATCTGAATGAGG	AGGGCTCAGTCCAAAATTGA	67	#33	4687663001	*
Slc39a6	NM_139143.3	CCAGTCCCTTCGGACCTC	CTGTGGCCATTGCACCTT	89	#70	4688937001	88.57%
Slc39a6 (2)	NM_139143.3	GTCGCTCTGGTTGACATGG	CCGAGAAGTATCCCAGCATT	107	#4	4685016001	93.92%
Slc39a7	NM_008202.2	GGATTTTGCCATCCTGGTC	TTGCAGTCACGAGTTGCAG	71	#71	4688945001	101.18%
Slc39a8	NM_026228.4	TCAGCGTTGTATCCCTCCA	GTTTGGGCCCCTTCAGAC	69	#21	4686942001	102.43%
Slc39a9	NM_026244.2	CGTGGCAATAATGCTACACAA	CATGCATCAGGAAGGAAACC	62	#67	4688660001	110.68%
Slc39a10	NM_172653.2	TTTCAGATCATAAGTTAAACAGCACA	CCGAGTCATCCGTTCCAG	78	#89	4689143001	87.92%
Slc39a11	NM_027216.5	GAGGATTGCTTTGCTCATCC	AATCCTACGCCAACAGCAAG	72	#09	4685075001	99.96%
Slc39a12	NM_001012305.2	TGGACACAAGGAGACTGCAA	TTCCCCCAGCTGTGAGTAAC	64	#38	4687965001	*
Slc39a13	NM_026721.2	AGATGTTCCTCAACAGCAAGG	GCAGCAGTGGGGTCTTTG	61	#20	4686934001	96.92%
Slc39a14	NM_001135151.1	GCTCTCTAACGCCCTTTTCC	ATTGTCCTGAGGGTTGAAGC	61	#110	4692306001	97.39%
Ubc	NM_019639.4	GACCAGCAGCAGGCTGATCTT	CCTCTGAGGCGAAGGACTAA	110	#11	4685105001	98.03%
Gadph	NM_008084.2	TGTCCGTCGTGGATCTGC	CCTGCTTCACCACCTTCTTG	75	#80	4689038001	96.18%
Slc30a1	NM_009579.3	AACACCAGCAATTCCAACG	TCCACTGGGTCATCACTTCTC	74	#13	4685121001	101.31%
Slc30a2	NM_001039677.2	TGCAGACTATGGACAAGCAGA	TTCCACAGAGATCCTAAGAAGGAC	73	#67	4688660001	100.33%

Slc30a3	NM_011773.3	CTGCACACCTGGCTATTGAC	GGGAATAGAGCCGGGATG	75	#41	4688007001	103.00%
Slc30a4	NM_011774.2	TGCCATCATACTCACTCTGCTT	ATCATGGCCGACAAAACCT	102	#05	4685024001	94.47%
Slc30a5	NM_022885.2	CATTGTCGTAATCTCTCTGCTCA	AAAGCAGCCCCTCTTGTCTT	78	#25	4686993001	87.34%
Slc30a6	NM_144798.5	GCTTCCTGCTCATGTGGTG	AAGATGGTGAGGTAAGTATAGGCAGT	70	#22	4686969001	98.23%
Slc30a7	NM_023214.7	ATGGAGGTCACGGACATTCT	GCACCATTAAAGAGGGAATGA	64	#21	4686942001	84.36%
Slc30a8	NM_172816.3	GCTGCTTCAGCAATATGCTTC	CAGACTCCCAGCAACGTGT	69	#53	4688503001	104.76%
Slc30a9	NM_178651.3	GCTTTGAGTTCTGCGCCTAT	GCTTTGAGTTCTGCGCCTAT	105	#100	4692187001	100.97%
Slc30a10	NM_001033286.2	GGGCACAGCAGTGACTCTC	TTCTCGGTGTTCAGGGAATC	102	#18	4686918001	*
Mtf1	NM_008636.4	CCAAGAGACTAGTTGGCAGCA	GGTGGGACCAAGATCACCT	65	#10	4685091001	102.61%
Mt1	NM_013602.3	CAAGTGCACCTCCTGCAA	TTCGTCACATCAGGCACAG	124	#18	4686918001	93.73%
Mt2	NM_008630.2	CATGGACCCCAACTGCTC	AGCAGGAGCAGCAGCTTT	110	#04	4685016001	95.64%
Ins1	NM_008386.3	CGGGGACCTTCAGACCTT	GTGCAGCACTGATCCACAAT	69	#10	4685091001	99.50%
Ins2	NM_008387.5	GAAGTGGAGGACCCACAAGT	CAGTGCCAAGGTCTGAAGGT	78	#32	4687655001	100.37%
Foxa1	NM_008259.3	GAACAGCTACTACGCGGACA	CGGAGTTCATGTTGCTGACA	65	#82	4689054001	96.03%
Foxa2	NM_001291065.1	AAGTAGCCACCACACTTCAGG	TGTGGCCCATCTATTTAGGG	71	#32	4687655001	94.39%
Foxo1	NM_019739.3	GTGGGGCAACCTGTCGTA	TTCTCGGCTGAGCTCTCG	60	#9	4685075001	93.99%
Hnf1b	NM_009330.2	AATCCCCAGCAATCTCAGAA	GGCTTGGGAGGTGTTGAG	84	#109	4692284001	80.83%
Hnf4a	NM_008261.2	CAGCAATGGACAGATGTGTGA	TGGTGATGGCTGTGGAGTC	76	#27	4687582001	119.61%
MafA	NM_194350.1	CTCCAGAGCCAGGTGGAG	GTACAGGTCCCGCTCCTTG	66	#10	4685091001	98.11%
Mnx1	NM_019944.2	GATGCCGGACTTCAGCTC	AGCTGCTGGCTGGTGAAG	84	#60	4688589001	90.25%
Neurod1	NM_010894.2	CGCAGAAGGCAAGGTGTC	TTTGGTCATGTTTCCACTTCC	90	#01	4684974001	93.07%
Nkx2.2	NM_010919.2	GCAGCGACAACCCCTACA	ATTTGGAGCTCGAGTCTTGG	105	#20	4686934001	95.76%
Nkx6.1	NM_144955.2	CCCGGAGTGATGCAGAGT	GAACGTGGGTCTGGTGTGTT	114	#103	4692217001	99.17%

Pax4	NM_011038.2	AAGACCAGACCACCAGCAA	AAGTTTCTCTTTGGGACTGGTTC	107	#01	4684974001	79.31%
Pax6	NM_001244198.1	CACCAGACTCACCTGACACC	ACCGCCCTTGGTTAAAGTC	62	#96	4692136001	96.37%
Pdx-1	NM_008814.3	GAAATCCACCAAAGCTCACG	CGGGTTCCGCTGTGTAAG	65	#51	4688481001	98.23%
Arx	NM_001305940.1	ACTTGTTACCGCTTGTCCTGA	CCTCTGCTCCTCTCTCCTCA	64	#55	4688520001	117.14%
Stat3	NM_213659.3	GTTCCTGGCACCTTGGATT	CAACGTGGCATGTGACTCTT	70	#71	4688945001	104.61%

Table 2.3. qPCR assay designs for human genes undertaken in this study. * = Assay efficiency could not be determined due to low expression.

Gene	RefSeq ID	Forward primer (5' – 3')	Reverse primer (5' – 3')	Amplicon	UPL Probe	CAT. Nº	Assay efficiency
SLC39A1	NM_014437.3	GGAGAAAGCTCCGGGAAA	GAGTGACGTCAGTTAGGAGCAA	91	#71	4688945001	106.38%
SLC39A2	NM_014579.3	GAACAGATCAGCAAGTGAGAGAAA	AGCTCTCCATAGGGATACTCCA	75	#09	4685075001	*
SLC39A3	NM_144564.4	GTTTCTGGCCACGTGCTT	AGGCTCAGGACCTTCTGGA	69	#74	4688970001	96.14%
SLC39A4	NM_017767.2	GCTCCAGTGTGTGGGACA	GCCTGTTCCGACAGTCCA	73	#46	4688066001	97.35%
SLC39A5	NM_173596.2	CCTCTTCCTGCTCTTTGTGC	TCGAGATTCCTTCGTTTTCG	96	#45	4688058001	93.22%
SLC39A6	NM_012319.3	ACTGGCCGTTGGGACTTT	ATGGTGGTGACTTGCATGAG	73	#09	4685075001	97.59%
SLC39A7	NM_006979.2	CGAAGGTGGAACGGAACTT	AGGCCTGGAAAGGATGGTAG	134	#55	4688520001	86.17%
SLC39A8	NM_022154.5	TTTTGGTGGGCAACAATTTC	CAGCATATCATTCATCTCTGGAA	107	#67	4688660001	92.53%
SLC39A9	NM_018375.4	GGTCTGGTTGTCCATGCTG	AACTGGACACTGGTCTGTGAAGT	77	#32	4687655001	75.49%
SLC39A10	NM_001127257.1	TGTAGCCTTGGTGGATATGCT	CCACAGGACAAAAGCCATGT	77	#09	4685075001	101.61%
SLC39A11	NM_139177.3	GGGCTGATGGAAGTGCAG	CCTTGGAGCATGCTGGATAC	63	#19	4686926001	*
SLC39A12	NM_152725.3	TGAAATACTCTCCAGGATTTAAAAGG	GGGGTAAACTTGTAACCAAAGGA	96	#50	4688112001	*
SLC39A13	NM_001128225.2	GGCCAACACCATCGATAACT	TTGTCAGGAGCCCGATCTT	83	#05	4685024001	95.72%
SLC39A14	NM_015359.4	TCTCTGCCAACTGGATTTTTG	CCTCATTCATCTCAGGGAACA	84	#78	4689011001	93.07%
SLC30A8	NM_173851.2	AGTAATTCTCTCAGCTCATGTTGC	GCAATTTCTCTCCGAACCAC	69	#66	4688651001	94.43%
UBC	M26880.1/M26880.EMI	CAGAGGTTGATCTTTGCTGGA	GCAGGGTGGACTCTTTCTGA	82	#11	4685105001	99.05%
GADPH	NM_002046.3	AGCCACATCGCTCAGACAC	GCCCAATACGACCAAATCC	66	#60	4688589001	106.38%

2.7. Protein expression analysis

2.7.1. Protein extraction

Cells were harvested by trypsinization (0.25% trypsin-EDTA (Thermo Fisher) in PBS) and lysed in ice-cold radioimmunoprecipitation buffer (50mM Tris (pH 8), 150mM NaCl, 1% Triton X-100, 0.5% sodium deoxycholate, 0.1% SDS) supplemented with 1X Protease Inhibitor Cocktail and 1X Phosphatase Inhibitor Cocktail (both Sigma Aldrich). Lysates were incubated with agitation (40 mins, 4^{o}C), the nucleic acids pelleted by centrifugation (12,000rpm, 20 mins, 4^{o}C) and the protein lysate aspirated.

2.7.2. Bradford assays

Protein concentrations were calculated through Bradford assays. Samples were diluted 1:100 with Bradford Reagent (Bio-Rad) in a microtiter plate in triplicate. Absorbance was measured at wavelength 595nm (reference: 450nm) using a microplate reader and standardised to dilutions of BSA (0.5, 1, 2, 5, 10, 20 and 30µg/ml; Sigma Aldrich) in PBS.

2.7.3. Immunoblotting

Protein lysates were prepared in 2x loading dye (Thermo Fisher) and boiled (10 mins, 72^{o}C). Lysates (20µg) were separated on 12% acrylamide SDS-PAGE gels (Thermo Fisher) using SDS-PAGE buffer (Thermo Fisher) supplemented with 0.1% SDS (200V, 40 mins). Proteins were transferred onto nitrocellulose membranes [GE Healthcare Life Sciences (1 h, 100V)] using transfer buffer (25mM Tris, 192mM glycine, 10% methanol), and membranes blocked through incubation in 5% (w/v) BSA/Tris-buffered saline [TBS (50mM Tris-Cl pH 7.5, 150mM NaCl)] and 0.05% (v/v) TWEEN-20 [TBST (1 h, RT)]. Membranes were incubated with primary antibodies diluted in 1% BSA/TBST (16 h,

4ºC), followed by HRP-linked secondary antibodies diluted in 1% BSA/TBST (1 h, RT). Details of the antibodies used are provided in the appropriate chapters. Cells were washed three times with TBST between each step. Membranes were treated with ECL Western Blotting Detection Reagent (GE Healthcare Life Sciences) and visualised on X-ray film (GE Healthcare Life Sciences) using a film imager.

2.7.4. Membrane stripping

Immunoblots were washed with TBST, incubated in stripping buffer [Thermo Fisher (15 mins, RT)] and further washed with TBST (10 mins, RT). Membranes were blocked with 5% (v/v) BSA/TBST (1 h, RT) before additional antibody incubation, as described in section **2.7.3**.

2.8. ^{65}Zinc uptake assays

Cells were washed in serum- and antibiotic-free DMEM (5 mins, RT) and incubated in Hepes control salt solution (HCSS; 145mM NaCl, 5.4mM KCl, 1.8mM $CaCl_2$, 0.8mM $MgCl_2$, 20mM HEPES, 5.5mM Glucose, pH to 7.4 with NaOH) containing 0-30µM ^{65}ZnCl [75MBq/mg, 25.8mM Zn^{2+} (15 mins, 37ºC); Diagnostic Imaging]. To terminate the reaction, cells were immediately placed on ice, washed 3 times in ice-cold quench buffer (HCSS, 10mM $CaCl_2$, 200µM $ZnCl_2$, 5mM CaEDTA), and further incubated on ice (5 mins). Cells were lysed in hot 0.2% SDS solution and the radioactivity (cpm) of aspirated HCSS and the total cells counted using an automated gamma counter (1282 compugamma; LKB Wallac). Zn^{2+} influx (*J*in) was calculated as follows:

$$Jin = \frac{cpm}{SA \times protein \times t}$$

Where cpm is the counts in the cells (cts min^{-1}), SA is the average specific activity of Zn^{2+} transport throughout the assay (cts min^{-1} $nmol^{-1}$), protein is the total amount of protein in

the assay, as calculated through Bradford assays of parallel (Bio-rad; section **2.7.2**), non-radioactive samples, and *t* is the time over which flux occurred (mins).

2.9. Proliferation assays

The rate of cellular proliferation was determined using the Cell Proliferation ELISA, BrdU (colorimetric) assay (Roche), following manufacturer's instructions. A 2 h incubation period with BrdU labelling solution was used. The absorbance was measured using a microplate reader at wavelength 450nm (reference: 690nm).

2.10. Apoptosis assays

The rate of cellular apoptosis was determined through Caspase-Glo® 3/7 assays (Thermo Fisher), following manufacturer's instructions, using 50µl reagent per 100µl sample. The luminescence was measured using a microplate reader.

2.11. Assessment of oxidative stress

Oxidative stress was assayed using dihydrofluorescin diacetate (Sigma Aldrich). Cells were washed once with warm Hanks Balanced Salt Solution (HBSS; Thermo Fisher) and incubated in HBSS containing 1µM dihydrofluorescin diacetate (30 mins, 37^{o}C). Cells were placed on ice, washed with ice-cold HBSS and the fluorescence measured using a microplate reader (excitation/emission: 485/528).

2.12. Insulin secretion assays

Cells were starved in DMEM containing 3mM glucose (24 h, 37^{o}C). Cells were washed with PBS, incubated in Krebs-ringer bicarbonate buffer [KRBH, 10mM Hepes, 2mM $NaHCO_3$, 70mM NaCl, 3.6mM KCl, 0.5mM NaH_2PO_4, 0.5mM $MgSO_4$, 1.5mM $CaCl_2$.

10mM NaCl, 0.1% BSA, adjusted to pH 7.4 with NaOH (30 mins, 37^{o}C)] supplemented with 3mM glucose (30 mins, 37^{o}C), followed by KRBH supplemented with 3mM glucose or 3mM glucose and 40mM KCl (30 mins, 37^{o}C). The supernatant containing secreted insulin was aspirated and diluted 1:20. The amounts of secreted insulin were determined using the colorimetric Rat/Mouse Insulin ELISA assay kit (EZRMI-13K, Merck Millipore), following manufacturer's instructions, and normalised to total protein, determined through Bradford assays (Bio-Rad; section **2.7.2**).

2.13. Statistical analysis

Unless otherwise stated, all statistical analysis was carried out through unpaired t-tests or 2-way ANOVA followed by either Tukey's or Sidak's multiple comparison tests, as appropriate. Data were considered statistically significant when $p < 0.05$ and presented as mean ± SEM.

3. Expression of the ZIP/*SLC39A* transporters in β-cells: a systematic review and integration of multiple datasets

3.1. Candidate contributions to chapter 3

The work in this chapter has been published in BMC Genomics (published online September 2017; DOI: 10.1186/s12864-017-4119-2 [404]). I carried out all data collection and analysis and constructed all the tables and figures. I additionally produced the original draft and all further revisions of the manuscript, under the supervision of my supervisors.

3.2. Context of chapter 3 in this thesis

The work in this chapter goes towards addressing the first aim of this project: *To identify ZIP transporters that functionally coordinate with ZnT8 to maintain normal zinc trafficking in β-cells and explore whether these transporters are regulated differently based on ZnT8 activity.* I encompass a systematic approach to reveal ZIP transporters potentially important for β-cell function and complement these findings with experimental data to support a biological relevance of these results. The data presented in this publication dictated which ZIP transporters I focused on for experimentation during chapters 4-7.

Lawson et al. BMC Genomics (2017) 18:719
DOI 10.1186/s12864-017-4119-2

BMC Genomics

RESEARCH ARTICLE Open Access

Expression of the ZIP/*SLC39A* transporters in β-cells: a systematic review and integration of multiple datasets

Rebecca Lawson, Wolfgang Maret and Christer Hogstrand*

Abstract

Background: Pancreatic β-cells require a constant supply of zinc to maintain normal insulin secretory function. Following co-exocytosis with insulin, zinc is replenished via the Zrt- and Irt-like (ZIP; *SLC39A*) family of transporters. However the ZIP paralogues of particular importance for zinc uptake, and associations with β-cell function and Type 2 Diabetes remain largely unexplored. We retrieved and statistically analysed publically available microarray and RNA-seq datasets to perform a systematic review on the expression of β-cell *SLC39A* paralogues. We complemented results with experimental data on expression profiling of human islets and mouse β-cell derived MIN6 cells, and compared transcriptomic and proteomic sequence conservation between human, mouse and rat.

Results: The 14 ZIP paralogues have 73–98% amino sequence conservation between human and rodents. We identified 18 datasets for β-cell *SLC39A* analysis, which compared relative expression to non-β-cells, and expression in response to PDX-1 activity, cytokines, glucose and type 2 diabetic status. Published expression data demonstrate enrichment of transcripts for ZIP7 and ZIP9 transporters within rodent β-cells and of ZIP6, ZIP7 and ZIP14 within human β-cells, with ZIP1 most differentially expressed in response to cytokines and PDX-1 within rodent, and ZIP6 in response to diabetic status in human and glucose in rat. Our qPCR expression profiling data indicate that *SLC39A6, −9, −13, and − 14* are the highest expressed paralogues in human β-cells and *Slc39a6* and *−7* in MIN6 cells.

Conclusions: Our systematic review, expression profiling and sequence alignment reveal similarities and potentially important differences in ZIP complements between human and rodent β-cells. We identify ZIP6, ZIP7, ZIP9, ZIP13 and ZIP14 in human and rodent and ZIP1 in rodent as potentially biologically important for β-cell zinc trafficking. We propose ZIP6 and ZIP7 are key functional orthologues in human and rodent β-cells and highlight these zinc importers as important targets for exploring associations between zinc status and normal physiology of β-cells and their decline in Type 2 Diabetes.

Keywords: Type 2 diabetes, Zinc, ZIP, *SLC39A*, Systematic review, Expression data, Microarray, RNA-seq

Background

Pancreatic β-cells require a constant supply of zinc for normal function in maintaining glycaemic control [1, 2]. Zinc acts at multiple stages within the insulin secretory pathway [3, 4]. Zinc ions (Zn^{2+}) are loaded into insulin granules via the predominantly β-cell specific zinc transporter 8 (ZnT8) [5], where two ions co-crystallise with insulin hexamers [6], important for proper insulin processing, protection of insulin from proteolytic degradation [7] and for maintaining granule osmotic stability [8]. Zinc is subsequently co-released with mature insulin upon exocytosis where it is proposed to fulfil additional roles in glycaemic control [9–11].

Significant amounts of Zn^{2+} are lost from β-cells during insulin secretion and coordinated replenishment is required. The Zrt- and Irt-like (ZIP; *SLC39A*) family of zinc importer proteins, of which 14 paralogues are present within both humans and rodents [12, 13], tightly control cellular Zn^{2+} influx into the cytosol and are thought responsible for restoring β-cell zinc content [14]. ZIP paralogues exhibit differing Zn^{2+} affinities ($K_{0.5}$) and transporting efficiencies, and show cell- and

* Correspondence: christer.hogstrand@kcl.ac.uk
King's College London, Faculty of Life Sciences and Medicine, Diabetes and Nutritional Sciences, Metal Metabolism Group, 150 Stamford St, London SE1 9NH, UK

condition-dependent expression [12, 15], thus it is expected that the β-cell ZIP profile closely reflects the unique cellular demand for Zn^{2+} and ability to adapt to stresses such as hyperglycaemia and inflammatory cytokines. Since both hyperzincemic and hypozincemic Zn^{2+}statuses are observed in diabetic patients [16–18] and animal models of diabetes [19, 20], one can hypothesize that altered ZIP expression profiles are associated with disease state. However exploration of the β-cell *SLC39A* transcriptome, and therefore the liable transporters, has been limited to a few studies [4, 14, 21–23], where an importance of ZIP4 [23], ZIP6 [21, 22], ZIP7 [14, 21, 22], ZIP8 [22], and ZIP14 [14, 24] has been suggested.

Type 2 Diabetes is rapidly evolving into a major public health crisis. The disease pathogenesis generally results from an increasingly inadequate insulin response due to enhanced insulin resistance and a compensatory demand on insulin production that eventually leads to β-cell failure. Multiple studies have associated diabetes with hypozincemia, likely caused by hyperzincuria, and a negative correlation between the glycated haemoglobin percentage and plasma zinc [16–18]. Accordingly, there is a positive effect of adequate plasma zinc levels on glycemic control [18], suggesting a compromised zinc status in diabetes [25].

Since zinc plays an integral role within β-cells, understanding its regulation may prove central for targeting loss of secretory function during Type 2 Diabetes. Much of our understanding of β-cell physiology has derived from studies on rodents due to very limited accessibility of human islets [26]. However, differences in physiology between humans and rodents remain often unacknowledged when interpreting rodent studies. We hypothesised that the ZIP transporters most important to β-cells should be robustly expressed and show enrichment relative to other cell types [27], with changes in expression influenced by cellular stresses associated with compromised insulin secretion. We thereby aimed to identify and evaluate the complement of ZIP transporters most important within human and rodent (mouse and rat) β-cells for regulating zinc influx and accumulation.

Here we show through systematic review of microarray and RNA-seq studies [28, 29] that transcripts for multiple ZIP paralogues are enriched in β-cells and/or show transcriptional regulation in response to cytokines, hyperglycaemia, Type 2 Diabetes status, and pancreatic and duodenal homeobox 1 (PDX-1) activity, the major transcription factor for β-cells. We used quantitative PCR (qPCR) to verify the relative expression of these paralogues within human islets and/or murine MIN6 β-cells. Furthermore, we computationally aligned human, mouse and rat SLC39A mRNA and protein sequences to demonstrate high cross-species conservation of the paralogues identified as key for β-cell zinc homeostasis within our systematic review. We highlight ZIP6, ZIP7, ZIP9, ZIP13 and ZIP14 in human and rodent, and ZIP1 in rodent as biologically important candidates for mediating β-cell Zn^{2+} influx and zinc-signalling processes, such as cell proliferation. In addition to normal physiology, we suggest ZIP6, ZIP7 and ZIP14 downregulation is associated with diabetic status; however the relationship to zinc content in the β-cells/pancreas remains unknown. Critically, our review highlights potentially important differences between human islets and rodent cells in their complements of zinc importers, again demonstrating the limitations of rodent models for human diabetes.

Methods

Systematic review

Identification of eligible expression datasets

This systematic review was conducted in accordance with the guidelines provided in the PRISMA statement. Microarray and RNA-seq expression profiling studies were identified through searching the NCBI PubMed database and the Gene Expression Omnibus (GEO) database [30] to April 2016, using combinations of the following key terms: "β-cell, islet" and "diabetes, gene expression, microarray, RNA-seq", and compiled studies screened for duplicates. Eligibility was independently assessed through first screening by title and abstract, and then by the full text, based on the following inclusion criteria: original research article published in English, RNA-seq or microarray platform, expression profiling of mature β-cells, islets and/or β-cell line, and human or rodent genome. The eligibility was finally confirmed through verifying the presence of accessible expression data for ZIP transporter transcripts (*SLC39A/Slc39a*). Included datasets explored: (a) expression within β-cells compared to non-β-cells, (b) expression in response to extracellular cytokines, (c) expression in response to PDX-1 activity, (d) expression in response to extracellular glucose, and (e) expression within human diabetic islets. From each identified dataset, the accession number (if appropriate), platform, species, sample types and sizes, and gene expression data were extracted. This pipeline is depicted in Fig. 1.

Data pre-processing

The heterogeneity of different platforms, gene nomenclature and control samples can cause difficulties when comparing datasets from different sources. Normalisation is therefore critical to reduce the chance of skewing the results and enhances credibility of individual expression changes. To minimise inconsistency, a standardised normalisation method was performed within datasets [31] using Qlucore Omics Explorer (version 3.2; Qlucore

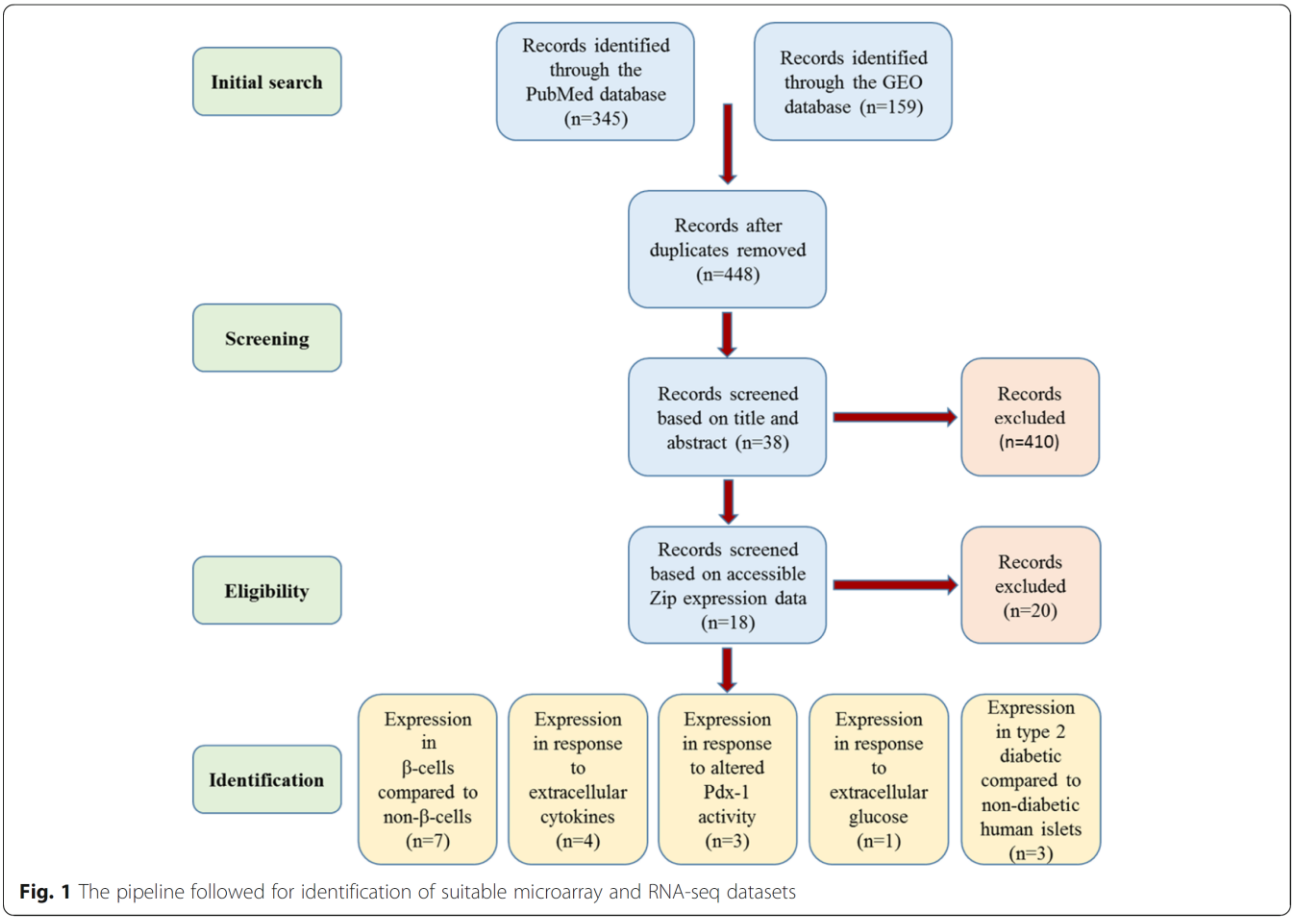

Fig. 1 The pipeline followed for identification of suitable microarray and RNA-seq datasets

AB, Lund, Sweden). Raw data was log (base = 2; $\log_2$) transformed and normalised through applying a standard score (Z-score) transformation, which calculates normalised expression intensities (y_i) of each probe as follows:

$$y_i = \frac{x_i - m}{\delta}$$

Where x_i represents raw intensity values (x_i, i = 0…N-1) for each gene, m represents average gene intensity for the experiment, and δ represents the standard deviation of all measured intensities.

Statistical analysis

Statistical analysis was undertaken using the Qlucore Omics Explorer (version 3.2; Qlucore AB, Lund, Sweden) bioinformatics software. Fold differences (FD) in expression between relevant conditions were derived, and significance calculated on the global transcriptomic data set through unpaired t-tests, adjusted using the Benjamini-Hochberg False Discovery Rate (FDR) procedure [32]. Genes were considered differentially expressed in comparisons at an FDR of 15%. Arbitrary FD cut offs of ≥1.5-fold on significantly regulated genes were chosen to indicate biologically relevant differential expression. Full results from analysis are provided in Additional file 1.

Datasets with inaccessible raw data

Where the full raw datasets were not available for download, normalised data were extracted from supplementary data tables and $\log_2$ transformed FD (Log_2FD) values and significance extracted/calculated using Excel as appropriate. Data analysed in this way are annotated.

Experimental analysis

Human islet cDNA

Human islet cDNA originating from healthy cadaver donors was obtained via the Human Islet Isolation Unit at King's College Hospital.

Cell line and RNA extraction

The adherent insulinoma β-cell line MIN6 (*Mus musculus*) was maintained within Dulbecco's Modified Eagle's Medium supplemented with 15% fetal bovine serum, 4 mM L-glutamine, 50 μM β-mercaptoethanol, 100 μg/ml streptomycin and 100 units/ml penicillin (both Sigma-Aldrich), at 37 °C in a humidified atmosphere of 95% air

and 5% CO_2. Total RNA was extracted using TRIzol Reagent (ThermoFisher), reverse transcribed to cDNA using the high capacity RNA-to-cDNA kit (ThermoFisher), and diluted ≥1:10 prior to experimentation.

Quantitative PCR

Quantitative PCR (qPCR) assays were designed using the online Universal Probe Library (UPL) assay design tool (Roche). Assay designs are provided within Additional files 2 and 3: Tables S1 and S2. Primer Blast [33] was used to predict the binding of our primers to mouse and human RNA. The mouse primers bind all respective ZIP transporter isoforms. The human primers bind all isoforms for ZIP2, ZIP4, ZIP5, ZIP6, ZIP8, ZIP10, ZIP11, ZIP12 and ZIP13. Primers for ZIP1, ZIP3, ZIP7, ZIP9 and ZIP14 covered either all the isoforms expressed within human islets, or those predominantly expressed (Additional files 2 and 3: Tables S1 and S2, Additional file 4). PCR plates were loaded using the Biomek FX liquid handling robot (Beckman Coulter) and reactions [20-40 μg cDNA, 0.1 μM UPL probe, 0.2 μM forward primer, 0.2 μM reverse primer and 1X TaqMan Fast Advanced Mastermix (Applied Biosystems)] amplified using the Prism7900HT sequence detection system, Applied Biosystems, and analysed with SDS (sequence detection systems) 2.4 software. All gene expression values were normalised to the housekeeping gene ubiquitin C (*UBC*), and relative expression calculated using the ΔΔCT method. The efficiencies for primers targeting genes with appreciable expression (mouse: ZIP1, ZIP2, ZIP3, ZIP4, ZIP6, ZIP7, ZIP8, ZIP9, ZIP10, ZIP11, ZIP13, ZIP14, UBC, GADPH; human: ZIP1, ZIP3, ZIP4, ZIP5, ZIP6, ZIP7, ZIP8, ZIP9, ZIP10, ZIP13, ZIP14, UBC, GADPH) ranged from 88 to 111% for mouse and 75–106% for human. Data show an average of two biological repeats for human islets and three biological repeats for MIN6 cells.

Exploration of zinc transporter heterogeneity

Human and mouse ZIP orthologues were aligned to assess transcriptomic and proteomic similarities using MUSCLE (3.8) [34, 35] and percent similarity values recorded.

Results

Overview of included datasets

A systematic review allows integrated analysis of multiple high throughput gene expression datasets. Following the pre-defined criteria, 18 appropriate β-cell/islet expression profiling studies were identified. These studies are summarised in Table 1. Seven studies compared expression within β-cells to non-β-cells, four investigated expression in response to extracellular cytokines, three studied expression in response to PDX-1 activity, one explored expression in response to extracellular glucose, and three measured expression within human diabetic islets.

Specificity of ZIP transporter expression within β-cells

Multiple microarray and RNA-seq studies have sought to assess β-cell gene expression relative to other pancreatic cells and additional tissues. Since ZIP paralogues exhibit cell-specific profiles reflecting function [12, 15], β-cell enrichment may indicate important cell-specific roles. Analysis of human islet cell transcriptomics datasets uncovered *SLC39A13* and *SLC39A14* as enriched within β-cells compared to α-cells [2- to 3-fold], and *SLC39A1, SLC39A10* and *SLC39A11* as ≥1.5-fold depleted [36, 37]. However, when β-cell expression was compared to sorted pancreatic exocrine cell populations (human duct and acinar cells), enrichment of *SLC39A7* and *SLC39A9* was observed (1.7- and 1.6-fold respectively) alongside relative depletion of *SLC39A5* (11-fold), *SLC39A8* (4.3-fold), *SLC39A10* (1.8-fold) and *SLC39A11* (1.5-fold) (data calculated from supplementary tables). Similarly RNA-seq data from Nica et al. uncovered depletion of *SLC39A5* and *SLC39A10* within sorted human β-cells over both total islets (2- and 6.8-fold, respectively) and non-β-cells [islet cell populations considered depleted of β-cells (2.8- and 4-fold, respectively)], accompanied by depletion of *SLC39A2* (2-fold over total islets and 4-fold over non-β-cells) and *SLC39A3* (1.7-fold over both total islets and non-β-cells), with enrichment of *SLC39A1* (2.4-fold over total islets and 2.1-fold over non-β-cells), and of *SLC39A14* (1.9-fold, only over non-β-cell preparations) [38].

Analysis of microarray datasets of human β-cell-enriched pancreatic samples and 15 other tissues [β-cell-enriched pancreas, pancreatic duct cells, cerebrum, colon, foetal brain, kidney, liver, lung, myocardial, skeletal muscle, prostate, small intestine, spleen, stomach, testis and thymus (dataset GSE30803)] revealed ≥1.5-fold enrichment of *SLC39A1*, *SLC39A6*, *SLC39A7* and *SLC39A14*, however without statistical significance [39]. Further investigation of probe-specific expression revealed that relative enrichment was biased by elevated expression of specific paralogues within other tissues (ZIP6 within the brain [40] and prostate [41], ZIP7 within the colon [42] and ZIP14 within the liver [43]). Omitting these tissues indicated ≥3-fold enrichment of *SLC39A6* ($q < 0.1$) and *SLC39A14* ($q < 0.15$), and 1.6-fold *SLC39A7* ($q < 0.05$) enrichment within β-cells compared to the remaining tissues analysed (Fig. 2a).

Analysis of a mouse RNA-seq dataset [44] suggested *Slc39a4*, *Slc39a5* and *Slc39a8* are ≥4-fold depleted within sorted β-cells over islets (Fig. 2b). Further investigation of non-β-cell depleted paralogues compared to total islets and six other cell types [brain, liver, lung fibroblasts, neural progenitor cells (NPC), skeletal muscle,

Table 1 Overview of the datasets identified for analysis

Dataset ID	Platform	Species	Sample	Number of samples	Reference
E-MTAB-463 and E-MTAB-465	Agilent-014850 Whole Human Genome Microarray 4x44K G4112F	*Homo sapiens*	β-cells and α-cells	β-cells: 4 α-cells: 4	Dorrell et al., 2014
–	RNA-seq	*Homo sapiens*	Sorted β-cells, α-cells and exocrine cells (duct and acinar)	β-cells: 3 α-cells: 3 Exocrine cells: 2	Bramswig et al., 2013
EGAS00001000442	RNA-seq	*Homo sapiens*	Sorted β-cells, α-cells and non-β-cells	7 DNA libraries, pooled	Nica et al., 2013
GSE30803	[HG-U133A] Affymetrix Human Genome U133A Array	*Homo sapiens*	Islets (and 16 other primary cell types)	Islets: 3	Martens et al., 2011
–	RNA-seq	*Mus musculus*	β-cells and islets	Unknown. Data for 5 additional cell types downloaded from NCBI	Ku et al., 2012
GSE13381	[Rat230_2] Affymetrix Rat Genome 230 2.0 Array	*Rattus norvegicus*	β-cells and α-cells	β-cells: 2 Non-β-cells: 2	Kutlu et al., 2009
GSE10785	Rosetta/Merck Mouse 44 k 1.0 microarray	*Mus musculus*	Islets (and 5 other primary cell types)	Islets: 40	Keller et al., 2008
GSE35296	RNA-seq	*Homo sapiens*	Islets	Control: 5 IL-1β and IFN-γ: 5	Eizirik et al., 2012
–	[HG-U133A] Affymetrix Human Genome U133A Array	*Homo sapiens*	Islets	Control: 3 IL-1β and IFN-γ: 3	Ylipaasto et al., 2005
–	[Rat230_2] Affymetrix Rat Genome 230 2.0 Array	*Rattus norvegicus*	FACS purified β-cells	For control and cytokine stimulation at each time point: 3	Ortis et al., 2010
–	[Rat230_2] Affymetrix Rat Genome 230 2.0 Array	*Rattus norvegicus*	INS-1E rat insulinoma cell line	For control and cytokine stimulation at each time point: 3	Moore et al., 2011
GSE40642	[Rat230_2] Affymetrix Rat Genome 230 2.0 Array	*Rattus norvegicus*	INS-1ab rat insulinoma cell line	Control: 8 IL-1β: 20 PDX-1 overexpression: 8 PDX-1 overexpression and IL-1β: 20	Hansen et al., 2012
GSE49786	[Rat230_2] Affymetrix Rat Genome 230 2.0 Array	*Rattus norvegicus*	Islets	Untreated: 5 Pdx-1 overexpression: 5	Hayes et al., 2013
E-MTAB-127	A-CBIL-10-UPenn Mouse PancChip 6.1	*Mus musculus*	Islets and MIN6 murine insulinoma cell line	Islets Pdx-1$^{+/-}$: 3 Islets Pdx-1$^{+/+}$: 3 MIN6 treated: 4 MIN6 control: 4	Sachdeva et al., 2009
GSE12817	[Rat230_2] Affymetrix Rat Genome 230 2.0 Array	*Rattus norvegicus*	Islets	2 mM Glucose: 4 5 mM Glucose: 4 10 mM Glucose: 4 30 mM Glucose: 4	Bensellam et al., 2009
GSE25724	[HG-U133A] Affymetrix Human Genome U133A Array	*Homo sapiens*	Islets	Non-diabetic: 7 Diabetic: 6	Dominguez et al., 2011
GSE20966	[U133_X3P] Affymetrix Human X3P Array	*Homo sapiens*	β-cell-enriched pancreatic tissue	Non-diabetic: 10 Diabetic: 10	Marselli et al., 2010
GSE38642	[HuGene-1_0-st] Affymetrix Human Gene 1.0 ST Array [transcript (gene) version]	*Homo sapiens*	Islets	Non-diabetic: 54 Diabetic: 9	Taneera et al., 2012

total islet (Fig. 2c)] revealed *Slc39a7* and *Slc39a9* as the most β-cell enriched Zip paralogues in mouse with 2.3- and 3-fold elevated expression, respectively. Analysis of a further rat dataset comparing expression of β-cells over α-cells (dataset GSE13381) displayed ≥1.5-fold enrichment of *Slc39a3* and *Slc39a6*, and ≥2-fold enrichment of

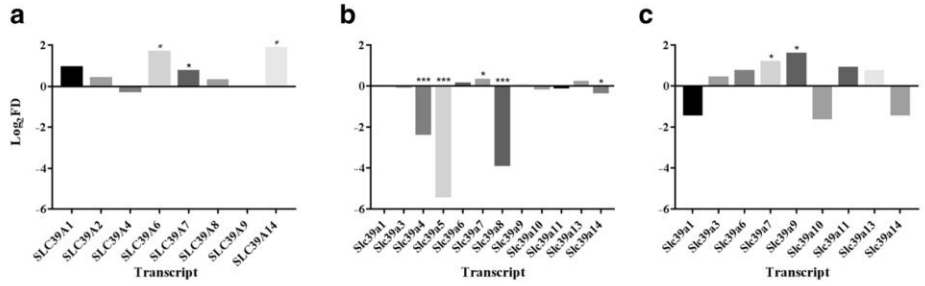

Fig. 2 Enrichment of *SLC39A* paralogues within human and murine β-cells. **a** Expression within human β-cell-enriched pancreatic samples compared to 11 other tissues (pancreatic duct cells, cerebrum, kidney, lung, myocardial, skeletal muscle, small intestine, spleen, stomach, testis and thymus). **b** Expression within sorted mouse β-cells compared to mouse islets. **c** Expression within sorted mouse β-cells compared to six other cell types (brain, liver, lung fibroblasts, NPC, skeletal muscle, islets), after exclusion of β-cell depleted paralogues. Data for (**a**) analysed from dataset GSE30803 and (**b**-**c**) analysed from supplementary tables within [44]. $^{\#}P < 0.15$, $^{*}P < 0.05$, $^{***}P < 0.001$. NPC = neural progenitor cells

Slc39a7 and *Slc39a14*, but without statistical significance. However, there was no differential *Slc39a* expression between murine islets and five other tissues (adipose, gastrocnemius muscle, hypothalamus, liver, and soleus muscle) from 10-week old lean and obese C57BL/6 and BTBR mice (dataset GSE10785).

Cytokine stimulation and ZIP transporter expression

Pro-inflammatory cytokines profoundly affect cellular metabolism and utilisation of nutrients such as metal ions [45]. Chronic exposure of islets to the inflammatory cytokines interleukin-1 beta (IL-1β), tumor necrosis factor-alpha (TNF-α) and interferon-gamma (IFN-γ) is associated with β-cell destruction and decreased secretory parameters in both Type 1 and Type 2 Diabetes [46]. Cytokine-dependent expression may indicate ZIP paralogues important for maintaining normal β-cell parameters when adapting to extracellular cytokine stress. RNA-seq dataset analysis of human islets exposed to IL-1β and IFN-γ for two days (dataset GSE35296) revealed 1.4- and 2.0-fold upregulation of *SLC39A8* and *SLC39A14* transcripts, respectively, and 2-fold downregulation of *SLC39A10* [47]. However an additional microarray study using human islets [48] did not show any ZIP transporter transcripts differentially expressed following 48 h incubation with IL-1β and IFN-γ.

Within independent studies, both fluorescence assisted cell sorting (FACS) purified rat β-cells [49] and the rat INS-1E β-cell line [50] were cultured with IL-1β and IFN-γ before microarray analysis (data from both studies calculated from supplementary data). Within rat β-cells [49] differential regulation of *Slc39a1* (2.5-fold) was observed at 2 h, and of *Slc39a1* and *Slc39a10* at both 12 h (2.0- and −3.5-fold, respectively) and 24 h (1.5-fold and −1.6-fold, respectively). Similarly, INS-1E cells [50] displayed upregulation of *Slc39a1* at both 6 and 24 h (2.6- and 2.1-fold, respectively) and of *Slc39a6* at 24 h (1.7-fold), alongside downregulation of *Slc39a13* at 6 h (−1.5-fold). INS-1E cells were additionally analysed after 6 and 24 h incubation with IFN-γ and TNF-α to show *Slc39a1* upregulation (2.8- and 2.4-fold, respectively) and *Slc39a14* downregulation (2.8- and 2.4-fold, respectively).

PDX-1 and ZIP transporter expression

PDX-1 is the key transcription factor mediating β-cell-specific gene expression within developing and mature β-cells [51]. Changes in ZIP expression as a consequence of PDX-1 activity may indicate roles of respective transporters in maintaining normal β-cell parameters. Critically, constitutive overexpression of PDX-1 sensitises β-cells to cytokine-induced apoptosis [52, 53]. Overexpression of PDX-1 within rat INS-1ab cells (dataset GSE40642) resulted in downregulation of *Slc39a6* and *Slc39a14* (Fig. 3). Stimulation of PDX-1 overexpressing cells with cytokine IL-1β further exacerbated these effects and also upregulated *Slc39a1* ≥ 2.5-fold [54] (Fig. 3). Whereas within rat islets (dataset GSE49786), PDX-1 overexpression upregulated *Slc39a8* (2.1-fold, $P < 0.01$) [55]; however *Slc39a5* and *Slc39a8* were up- and downregulated 1.5- and −2.6-fold, respectively, in mouse MIN6 cells (dataset E-MTAB-127) [56]. Data analysis from E-MTAB-127 additionally showed 2.8-fold downregulation of *Slc39a5* in $PDX^{+/-}$ mouse islets compared to $PDX^{+/+}$ control mouse islets.

Expression in response to glucose stimulation

Hyperglycaemia is universal within all prediabetic and diabetic cases, and glucose-responsive expression may indicate genes and pathways important for adapting to an enhanced demand for insulin secretion. Examination of microarray datasets of isolated rat islets cultured with 2 mM, 5 mM, 10 mM and 30 mM glucose (dataset GSE12817) uncovered ≥1.5-fold upregulation of *Slc39a2*, *Slc39a4* and *Slc39a6* and ≥1.5-fold downregulation of *Slc39a3* and *Slc39a5* when glucose increases [57].

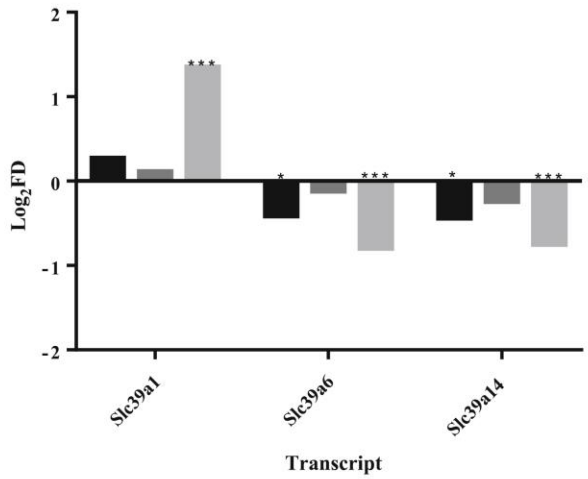

Fig. 3 *Slc39a* transcripts differentially expressed in rat INS-1ab cells following PDX-1 overexpression and IL-1β stimulation. Black bars: PDX-1 overexpression; dark grey bars: IL-1β stimulation; light grey bars: PDX-1 overexpression and IL-1β stimulation. Data analysed from dataset GSE40642. *$P < 0.05$, ***$P < 0.001$

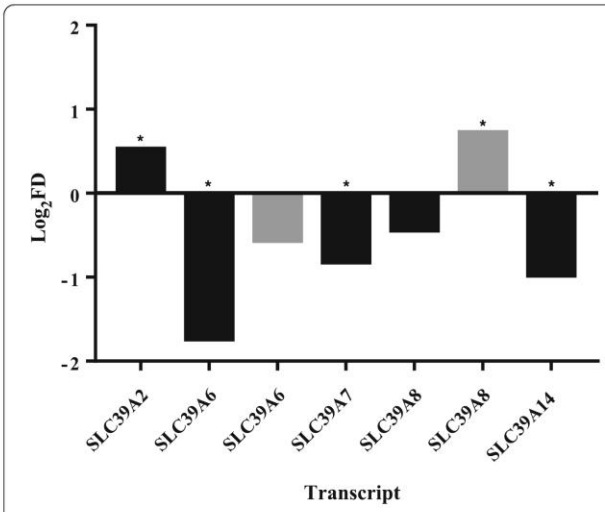

Fig. 4 *SLC39A* transcripts differentially expressed in human type 2 diabetic islets compared to non-diabetic islets. Probes targeting the same transcript(s) are averaged for each assay. Black bars: data analysed from dataset GSE25724; grey bars: data analysed from dataset GSE20966. *$P < 0.05$

Expression within islets from type 2 diabetic patients

Transcriptomic datasets of islets derived from normoglycaemic and Type 2 diabetic patients were next analysed to explore relevance to the human disease. Three paralogues (*SLC39A2*, *SLC39A5* and *SLC39A8*) showed ≥1.5-fold upregulation and four paralogues (*SLC39A6*, *SLC39A7*, *SLC39A8* and *SLC39A14*) ≥1.5-fold downregulation in diabetic compared to non-diabetic individuals [results combined from studies GSE25724 [58] and GSE20966 [59], Fig. 4]. However in a cohort of Nordic patients (dataset GSE38642), no ZIP paralogues were found differentially (≥1.5-fold) expressed between diabetic and non-diabetic islets [60].

SLC39A Paralogues identified within our systematic review are experimentally verified to show high β-cell/islet expression and sequence conservation

Enhanced relative expression may suggest a biological relevance of respective putative ZIP orthologues in maintaining intracellular Zn^{2+} homeostasis in β-cells/islets. To verify the biological relevance of the ZIP orthologues we identified in our systematic review in terms of β-cell function, we performed qPCR expression profiling of human and mouse *SLC39A* mRNA transcripts. There was notably a wider range of mRNA for ZIP transporters expressed in human islets, compared with murine MIN6 cells. We observed highest expression of *SLC39A6, SLC39A9, SLC39A13* and *SLC39A14* in human islets and of *Slc39a6* and *Slc39a7* in mouse MIN6 cells (Fig. 5).

We next assessed cross-species homologies between human and putative rodent ZIP orthologues. Enhanced similarity increases the likelihood of inferring molecular function [61], and increases confidence when applying results encompassing data derived from multiple species. We calculated the transcriptomic and proteomic homologies between human and mouse ZIP orthologues, and between mouse and rat ZIP orthologues through bioinformatics. We showed all respective orthologues have high similarities, with lowest protein homology between human and mouse observed for ZIP4 (73%) and highest for ZIP1 (94%). All rat and mouse orthologues showed protein similarities of ≥90% aside from ZIP4 (89.8%) and ZIP14 (89.5%) (Table 2). The high sequence similarities observed indicate that all ZIP paralogues identified as important in our systematic review have the potential to substitute functionally in human, mouse and rat β-cells.

Discussion

Associations between Zn^{2+} status and β-cell function have been extensively described in independent studies [1, 2, 62]. ZnT8 expression is positively correlated with granule Zn^{2+} release and glucose tolerance in mice [63], and high glucose stimulation increases free Zn^{2+} content within mouse islets [22] and hamster HIT-T15 cells [64]. Intracellular Zn^{2+} exhibits roles in protection against oxidative stress-induced apoptosis [65] whereas chronic elevation contributes to β-cell dysfunction [22]. The ZIP importer paralogues responsible for maintaining β-cell Zn^{2+} homeostasis remain largely unexplored and are important to investigate for understanding β-cell function in health and diabetic disease.

A systematic review allows integrated analysis of relative consistencies in differential expression from high throughput gene expression techniques, despite heterogeneities between studies involving experimental design

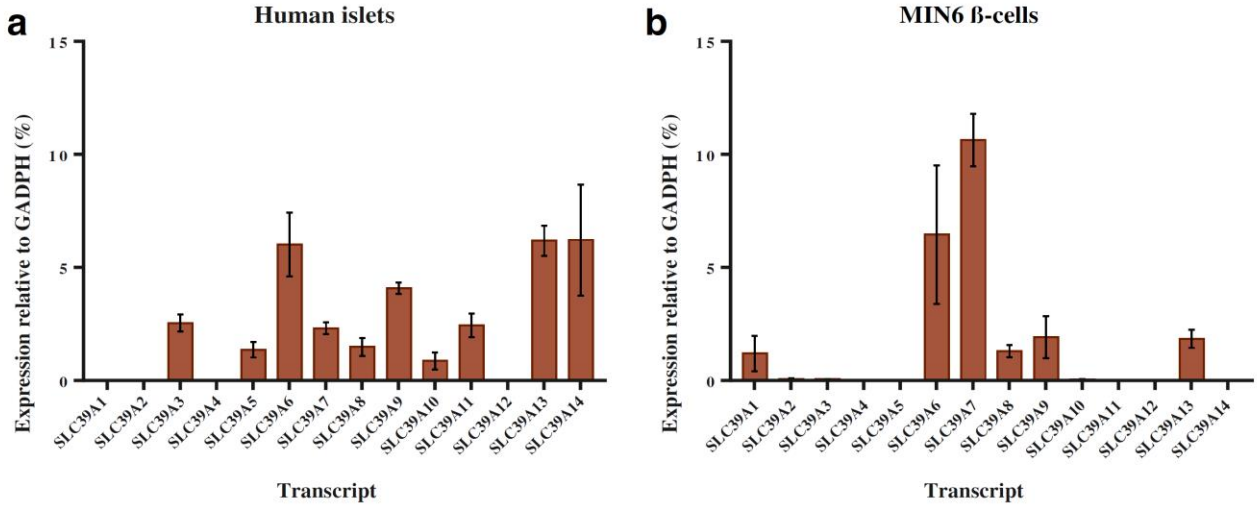

Fig. 5 Expression profiles of *SLC39A* mRNA transcripts in human islets and murine MIN6 cells. **a** The human *SLC39A* transcriptome. *N* = 2 and error bars show ± range. **b** The MIN6 β-cell *Slc39a* transcriptome. *N* = 3 and error bars show ±SEM

and platform used. It has the capacity to identify consistent but modest variations, important for genes involved in processes where small expression changes can have amplified effects. Through this systematic review we re-analysed raw microarray and RNA-seq data in parallel with unannotated high-throughput datasets to compare and contrast β-cell ZIP complemets in human, mouse and rat β-cells/islets. We show enrichment of mRNA for ZIP7 and ZIP9 within rodent and ZIP6, ZIP7 and ZIP14 within human, with mRNA for ZIP1, ZIP6 and ZIP14 differentially expressed in response to cytokines and PDX-1 within rodent, and ZIP6 in response to diabetic status in human and glucose in rat. To query the biological relevance of our data, we carried out experimental expression profiling of human islet and MIN6 β-cell cDNA, and computationally aligned human, mouse and rat mRNA and protein sequences. Highest expression was observed for mRNA corresponding to ZIP6, ZIP9, ZIP13 and ZIP14 in human islets and ZIP6 and ZIP7 in mouse MIN6 cells, which is in agreement with previous observations [21]. The mRNA profile for ZIPs generated through our qPCR analyses also corresponds well to expression data on specific isoforms in human islets as produced by RNA-seq (Additional file 4). All ZIP

Table 2 Percentage similarity between human, mouse and rat ZIP/*SLC39A* protein and mRNA sequences

Gene	Refseq transcript ID			Entrez protein ID			Percentage similarities (human:mouse)		Percentage similarities (mouse:rat)	
	Human	Mouse	Rat	Human	Mouse	Rat	Transcript	Protein	Transcript	Protein
SLC39A1	NM_014437.4	NM_013901.2	NM_001134577.1	Q9NY26	Q9QZ03	B5DEF5	80.77	93.83	91.60	98.46
SLC39A2	NM_014579.3	NM_001039676.2	NM_001107260.1	Q9NP94	Q2HIZ9	D3ZIN1	78.51	77.99	91.87	94.82
SLC39A3	NM_144564.4	NM_134135.1	NM_001008356.1	Q9BRY0	Q99K24	Q5U1X7	80.99	84.04	91.23	97.16
SLC39A4	NM_017767.2	NM_028064.2	NM_001077669.1	Q6P5W5	Q78IQ7	A0JPN2	74.55	73.17	91.98	89.79
SLC39A5	NM_173596.2	NM_028051.3	NM_001108728.1	Q6ZMH5	Q9D856	D3ZSF7	83.42	84.30	92.24	94.00
SLC39A6	NM_012319.3	NM_139143.3	NM_001024745.1	Q13433	Q8C145	Q4V887	80.04	88.20	92.01	95.28
SLC39A7	NM_006979.2	NM_008202.2	NM_001164744.1	Q92504	Q31125	Q6MGB4	81.72	85.90	90.62	93.72
SLC39A8	NM_022154.5	NM_001135150.1	NM_001011952.1	Q9C0K1	Q91W10	Q5FVQ0	76.15	89.35	90.74	96.10
SLC39A9	NM_018375.4	NM_026244.2	NM_001034929.1	Q9NUM3	Q8BFU1	Q3KR82	78.04	93.49	93.35	92.33
SLC39A10	NM_001127257.1	NM_172653.2	NM_001108796.2	Q9ULF5	Q6P5F6	D4A517	84.50	87.36	92.25	96.16
SLC39A11	NM_001159770.1	NM_001166503.1	NM_001013042.1	Q8N1S5	Q8BWY7	Q6P6S2	77.62	90.32	91.32	95.22
SLC39A12	NM_001145195.1	NM_001012305.2	XM_006254285.3	Q504Y0	Q5FWH7	D4A8R5	78.31	78.17	91.15	90.41
SLC39A13	NM_001128225.2	NM_001290765.1	NM_001039196.1	Q96H72	Q8BZH0	Q2M1K6	81.54	90.58	93.42	93.84
SLC39A14	NM_001128431.2	NM_001135151.1	NM_001107275.1	Q15043	Q75N73	D3ZZM0	75.84	86.91	90.11	89.53

Comparisons were generated using Clustal multiple sequence alignment by MUSCLE (3.8) [34, 35]

orthologues displayed high sequence conservation between species. Surprisingly ZIP4, which is essential for intestinal zinc uptake in both mouse and human [27, 66], shows the lowest homology (73%) between these two species and it also does not appear to play a major role in β-cells. Based on their expression levels, relative enrichment in β-cells/islets (compared with other cells/tissues), and regulation in response to conditions relevant to diabetes, we propose that ZIP6, ZIP7 and ZIP14 in human, and ZIP6 and ZIP7 in rodent may be of particular importance for β-cell Zn^{2+} uptake and/or homeostasis. This conclusion is similar to that of Liu et al. [21], who highlighted the roles of ZIP6 and ZIP7 in β-cell zinc transport and viability. Our study also indentifies ZIP1, ZIP9 and ZIP13 as being of potential additional significance for β-cell function.

The abundance of ZIP transporters varies substantially between tissues and cells, allowing those with differing Zn^{2+} affinities, cellular localisations and regulatory mechanisms to tightly maintain the homeostatic balance [67]. We found significant differences in ZIP mRNA abundance between β-cells and non-pancreatic tissues; specifically, enrichment of ZIP7 and ZIP9 within mouse β-cells, and ZIP6, ZIP7 and ZIP14 within human islets. With the exception for ZIP7, which is found in the endoplasmic reticulum (ER) and in some cells in the Golgi apparatus, these zinc channels are operating at the plasma membrane [13, 68]. ZIP6 and ZIP7 enrichment is consistent with a report [21], suggesting that ZIP6 and ZIP7 mediate influx of zinc into the β-cell cytosol in tandem from the plasma membrane and the ER. In addition to their roles in transporting zinc, ZIP6, ZIP7 and ZIP14 strongly stimulate cell proliferation, drastically increasing the number of cells in G_2/M phase, and their expression changes in cancers [27, 69–73]. Also of potential importance is that ZIP14 mediates import of both zinc and non-heme iron [74, 75] and that ZIP9 has been identified as a plasma membrane androgen receptor [76]. Interestingly, transcripts of ZIP9 and ZIP14, which were both found expressed at comparable abundances to ZIP6 and ZIP7 within human islets by ourselves and others [21], were additionally enriched within β-cells. ZIP9 and ZIP14 both show predicted localisation at the plasma membrane (with localisation of ZIP9 at the Golgi and trans-Golgi network additionally described) [77, 78], and currently remain unexplored in this context. Our expression profiling further identified ZIP13 as highly expressed in both human islets and MIN6 cells. ZIP13 is phylogenically grouped with ZIP7 [79] and studies have suggested ZIP13 localises at the ER, Golgi [80, 81] and intracellular vesicles [82]. However, to our knowledge ZIP13 has not been studied in β-cells. ZIP9, ZIP13 and ZIP14 may represent novel targets for understanding β-cell zinc uptake and homeostasis.

PDX-1 is the major transcriptional regulator in mature β-cells and mediates expression of key β-cell genes, with homozygous mutations linked to Type 2 Diabetes development [83]. Furthermore, PDX-1 drives β-cell (re)generation from neurogenin-3 positive endocrine precursors and pancreatic α-cells [84, 85], and β-cell-specific recovery of activity within $Ins2^{Akita}$ mice (βPdx1; $Ins2^{Akita}$ mice) promotes significantly improved glucose tolerance compared to control littermates [86]. Of interest, PDX-1 binds enhancers (cis elements) of the ZnT8 gene *SLC30A8* [87], indicating a role of PDX-1 in β-cell zinc homeostasis parallel to its role in insulin gene regulation [88]. Our analysis suggests PDX-1 activity sensitizes the β-cell zinc response to cytokines through ZIP6 and ZIP14 downregulation and ZIP1 upregulation within rat INS-1ab cells. We additionally established ZIP1 to be consistently upregulated following stimulation with IL-1β and IFN-γ, and IFN-γ and TNF-α within rat β-cells [49] and INS-1E cells [50], highlighting ZIP1 as potentially important in the adaptive response to cytokines. Interestingly, ZIP1 and ZIP6 abundances have been negatively correlated with the obesity-associated inflammatory state [89]. In contrast to the data in rodents, our review further identified ZIP8 and ZIP14 upregulation in response to the inflammatory cytokines IL-1β and IFN-γ in human islets [47]. Inflammatory mediators such as lipopolysaccharides (LPS) and TNF-α upregulate *SLC39A8* within human lung epithelia [90] and *Slc39a14* is upregulated in response to LPS-initiated inflammation within the mouse pancreas and liver [43] and shows an acute-phase gene response to IL-6 [91].

Hyperglycaemia is well recognised as a universal driver in the pathogenesis of Type 2 Diabetes [92]. Our analysis showed high glucose stimulation of rat islets significantly enhanced ZIP6 mRNA expression, consistent with glucose-dependent increases of additional ZIP7 and ZIP8 upregulation [22]. Similarly, analysis of islets from human type 2 diabetic donors displayed ZIP6, ZIP7, ZIP8 and ZIP14 mRNA downregulation compared to normoglycaemic controls [58, 59]. Decreased transcript expression supports a disease relevance of these paralogues for mediating β-cell zinc accumulation, indicating abnormally low zinc uptake may occur within diabetic β-cells as a result of disrupted ZIP6, ZIP7, ZIP8 and/or ZIP14 expression.

At a proteomic level no significant differences in protein abundances were observed for any ZIP paralogue within human islets incubated with high or low glucose [93–95]. Though in one of these studies non-significant trends for enrichment of ZIP6 (2.6-fold) and ZIP14 (1.6-fold) in human islets were observed following culture in high compared to low glucose [95]. However, these proteomic studies likely bias towards proteins with higher abundances [96], and accurately evaluating less

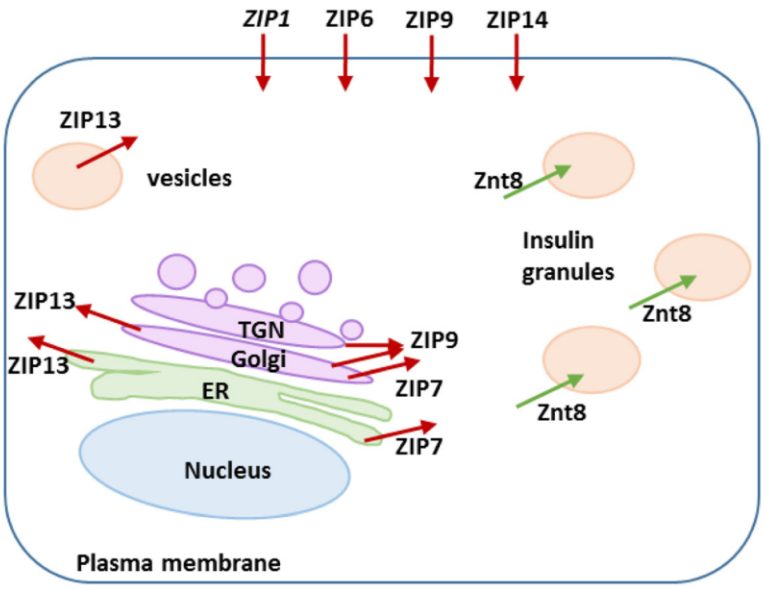

Fig. 6 Predicted subcellular localisation of the identified ZIP transporters within human and rodent β-cells. Based on the data analysed in the present study ZIP6, ZIP7, ZIP9, ZIP13 and ZIP14 in human, and the same transporters in addition to ZIP1 in rodent appear to be of particular importance for β-cell biology and pathology. Zinc Transporter 8 (ZnT8) which transports zinc into the insulin granules is also shown. ER = endoplasmic reticulum; TGN = trans-Golgi network

abundant species away from central pathways and those in complexes remains challenging, with membrane proteins imposing further challenges [97]. Although it is acknowledged that mRNA abundances often poorly correlate with protein abundances and functional activity [98], transcriptomic analysis remains important for pinpointing expression control and pathways of disruption during disease states.

This systematic review provides an overview of ZIP transcript expression in the context of β-cell specificity, cytokine stimulation, PDX-1 activity, glucose status and Type 2 Diabetes. It has allowed us to collectively analyse ZIP expression within multiple high throughput datasets, complemented by experimental work, providing evidence for differential regulation as a consequence of β-cell stresses associated with decreased insulin secretion. The study's limitations should nevertheless be acknowledged. Firstly, although all raw datasets (if appropriate) were subjected to the same normalisation process to minimise inconsistencies, the platform and genomic heterogeneities and differing probe hybridization efficiencies could skew global interpretation, and the analysis used may not have been equally suited to all datasets. Secondly, RNA-seq offers unbiased analysis of sequences present however microarray datasets are limited by hybridization efficiencies and the probes present [99], such that in multiple studies probes did not target all ZIP paralogues. Multiple datasets analysed and our qPCR expression data utilised islets incorporating non-β-cells. Relative *SLC39A* abundances may be impacted by additional cell populations, such as *SLC39A14* enrichment in α-cells [100]. Furthermore, although we have shown high conservation of ZIP mRNA and protein sequences between human and mouse, results may not be entirely translatable across species. Finally, several microarray studies identified within the systematic review search criteria were excluded during the final screening due to the absence of available experimental data for download and analysis. Despite these limitations, our systematic review distinguishes specific *SLC39A* paralogues as important within each human and rodent β-cells. The results are strongly supported by our experimental expression profiling of human islet and MIN6 β-cell cDNA through confirming relative enrichment and a biological relevance.

Conclusions

We have used a systematic approach to identify key ZIP complements in human, mouse and rat β-cells. We have verified a biological importance of these paralogues through proving high relative expression in human islets and/or murine MIN6 β-cells, and have demonstrated their potential to serve as functional orthologues in human and rodent through verifying high sequence similarities. Importantly, our results highlight similarities and potentially biologically relevant differences in zinc regulation between human and rodent ZIP orthologues which may prove critical when evaluating rodent β-cell models of disease. We propose ZIP6 and ZIP7 serve as key functional rodent-human orthologues in β-cells. We further identify ZIP9, ZIP13 and ZIP14 in human and

rodent, and ZIP1 in rodent as potentially biologically important for β-cell function (Fig. 6). These paralogues represent interesting targets for future investigation into zinc regulation and homeostasis in β-cell failure and Type 2 Diabetes.

Additional files

Additional file 1: Analysed datasets. (XLSX 61 kb)

Additional file 2: Table S1. Designs for human qPCR assays undertaken. (DOCX 12 kb)

Additional file 3: Table S2. Designs for mouse qPCR assays undertaken. (DOCX 12 kb)

Additional file 4: ZIP isoforms in human islets. (DOCX 56 kb)

Abbreviations

ER: Endoplasmic reticulum; FACS: Fluorescence assisted cell sorting; FD: Fold difference; FDR: False Discovery Rate; GEO: Gene Expression Omnibus; IFN-γ: Interferon-gamma; IL-1β: Interleukin-1 beta; Log_2FD: Log_2 transformed FD; LPS: Lipopolysaccharides; NPC: Neural progenitor cells; PDX-1: Pancreatic and duodenal homeobox 1; qPCR: quantitative PCR; TNF-α: Tumor necrosis factor-alpha; UPL: Universal Probe Library; ZIP: Zrt- and Irt-like protein; Zn^{2+}: Zinc ions; ZnT8: Zinc transporter 8

Acknowledgments

Human islet material was obtained from Dr. Pratik Choudhary and Dr. Guo-Cai Wang of the Human Islet Isolation Unit at King's College Hospital. We thank Dr. Matthew Arno (King's College London Genomics Centre) for technical support and Dr. Christine Baldwin (King's College London) for advice on presenting the systematic review methodology. The authors wish to thank Dr. Theodora Stewart for proofreading the final manuscript.

Funding

RL was supported by the King's Bioscience Institute and the Guy's and St Thomas' Charity Prize PhD Programme in Biomedical and Translational Science. The funding body was not involved in the design of the study, collection, analysis or interpretation of data, or in writing the manuscript.

Availability of data and materials

Datasets analysed during the current study are available in either the GEO repository [https://www.ncbi.nlm.nih.gov/geo/] or the ArrayExpress repository [https://www.ebi.ac.uk/arrayexpress/]. Respective dataset ID's are provided in Table 1.

Authors' contributions

RL performed the systematic review, all experiments, analysis and drafted the manuscript. CH and WM supervised the study. All the authors reviewed, approved and contributed to the final version of this manuscript.

Ethics approval and consent to participate

The King's College Hospital Research Ethics Committee has approved human islet isolation and use for research (Protocol number 01–082, Human Islet Isolation and Research), and an assent form is completed by a relative of the cadaver pancreas donor for all islets used for research. The MIN6 cell line was a kind gift from Dr. Jun-ichi Miyazaki [101], distributed to WM under the appropriate materials transfer agreement.

Consent for publication

Not applicable

Competing interests

The authors declare that they have no competing interests.

Publisher's Note

Received: 22 May 2017 Accepted: 5 September 2017
Published online: 11 September 2017

References

1. Li YV. Zinc and insulin in pancreatic beta-cells. Endocrine. 2014;45(2):178–89.
2. Chabosseau P, Rutter GA. Zinc and diabetes. Arch Biochem Biophys. 2016; 611:79-85.
3. Maret W. Zinc in pancreatic islet biology, insulin sensitivity, and diabetes. Prev Nutr Food Sci. 2017;22(1):1–8.
4. Huang L. Zinc and its transporters, pancreatic β-cells, and insulin metabolism. Vitam Horm. 2014;95:365–90.
5. Chimienti F, Devergnas S, Favier A, Seve M. Identification and cloning of a beta-cell-specific zinc transporter, ZnT-8, localized into insulin secretory granules. Diabetes. 2004;53(9):2330–7.
6. Chan SJ, Seino S, Gruppuso PA, Schwartz R, Steiner DF. A mutation in the B chain coding region is associated with impaired proinsulin conversion in a family with hyperproinsulinemia. Proc Natl Acad Sci U S A. 1987;84(8):2194–7.
7. Liu FY, Kildsig DO, Mitra AK. Insulin aggregation in aqueous media and its effect on alpha-chymotrypsin-mediated proteolytic degradation. Pharm Res. 1991;8(7):925–9.
8. Noormägi A, Gavrilova J, Smirnova J, Tõugu V, Palumaa P. Zn(II) ions co-secreted with insulin suppress inherent amyloidogenic properties of monomeric insulin. Biochem J. 2010;430(3):511–8.
9. Tamaki M, Fujitani Y, Hara A, Uchida T, Tamura Y, Takeno K, et al. The diabetes-susceptible gene SLC30A8/ZnT8 regulates hepatic insulin clearance. J Clin Invest. 2013;123(10):4513–24.
10. Kim BJ, Kim YH, Kim S, Kim JW, Koh JY, Oh SH, et al. Zinc as a paracrine effector in pancreatic islet cell death. Diabetes. 2000;49(3):367–72.
11. Ferrer R, Soria B, Dawson CM, Atwater I, Rojas E. Effects of Zn2+ on glucose-induced electrical activity and insulin release from mouse pancreatic islets. Am J Phys. 1984;246(5 Pt 1):C520–7.
12. Gaither LA, Eide DJ. Eukaryotic zinc transporters and their regulation. Biometals. 2001;14(3–4):251–70.
13. Taylor KM, Nicholson RI. The LZT proteins; the LIV-1 subfamily of zinc transporters. Biochim Biophys Acta. 2003;1611(1–2):16–30.
14. Bosco MD, Mohanasundaram DM, Drogemuller CJ, Lang CJ, Zalewski PD, Coates PT. Zinc and zinc transporter regulation in pancreatic islets and the potential role of zinc in islet transplantation. Rev Diabet Stud. 2010;7(4):263–74.
15. Fukada T, Kambe T. Molecular and genetic features of zinc transporters in physiology and pathogenesis. Metallomics. 2011;3(7):662–74.
16. Pidduck HG, Wren PJ, Evans DA. Hyperzincuria of diabetes mellitus and possible genetical implications of this observation. Diabetes. 1970;19(4):240–7.
17. Garg VK, Gupta R, Goyal RK. Hypozincemia in diabetes mellitus. J Assoc Physicians India. 1994;42(9):720–1.
18. de Carvalho GB, Brandão-Lima PN, Maia CS, Barbosa KB, Pires LV. Zinc's role in the glycemic control of patients with type 2 diabetes: a systematic review. Biometals. 2017;30(2):151–62.
19. Simon SF, Taylor CG. Dietary zinc supplementation attenuates hyperglycemia in db/db mice. Exp Biol Med (Maywood). 2001;226(1):43–51.
20. Begin-Heick N, Dalpe-Scott M, Rowe J, Heick HM. Zinc supplementation attenuates insulin secretory activity in pancreatic islets of the ob/ob mouse. Diabetes. 1985;34(2):179–84.
21. Liu Y, Batchuluun B, Ho L, Zhu D, Prentice KJ, Bhattacharjee A, et al. Characterization of Zinc Influx Transporters (ZIPs) in Pancreatic Beta Cells: roles in regulating cytosolic zinc homeostasis and insulin secretion. J Biol Chem. 2015.
22. Bellomo EA, Meur G, Rutter GA. Glucose regulates free cytosolic Zn^{2+} concentration, Slc39 (ZiP), and metallothionein gene expression in primary pancreatic islet β-cells. J Biol Chem. 2011;286(29):25778–89.
23. Hardy AB, Prentice KJ, Froese S, Liu Y, Andrews GK, Wheeler MB. Zip4 Mediated zinc influx stimulates insulin secretion in pancreatic beta cells. PLoS One. 2015;10(3):e0119136.
24. Mohanasundaram D, Drogemuller C, Brealey J, Jessup CF, Milner C, Murgia C, et al. Ultrastructural analysis, zinc transporters, glucose transporters and hormones expression in new world primate (Callithrix Jacchus) and human pancreatic islets. Gen Comp Endocrinol. 2011;174(2):71–9.

25. Praveena S, Pasula S, Sameera K. Trace elements in diabetes mellitus. J Clin Diagn Res. 2013;7(9):1863–5.
26. Kulkarni RN, Stewart AF. Summary of the Keystone islet workshop (April 2014): the increasing demand for human islet availability in diabetes research. Diabetes. 2014;63(12):3979–81.
27. Hogstrand C, Maret W. Genetics of Human Zinc Deficiencies. In: eLS. John Wiley & Sons, Ltd; 2016.
28. Rapaport F, Khanin R, Liang Y, Pirun M, Krek A, Zumbo P, et al. Erratum to: comprehensive evaluation of differential gene expression analysis methods for RNA-seq data. Genome Biol. 2015;16:261.
29. Liang M, Cowley AW, Greene AS. High throughput gene expression profiling: a molecular approach to integrative physiology. J Physiol. 2004;554(Pt 1):22–30.
30. Barrett T, Wilhite SE, Ledoux P, Evangelista C, Kim IF, Tomashevsky M, et al. NCBI GEO: archive for functional genomics data sets–update. Nucleic Acids Res. 2013;41(Database issue):D991–5.
31. Yang Z, Chen Y, Fu Y, Yang Y, Zhang Y, Li D. Meta-analysis of differentially expressed genes in osteosarcoma based on gene expression data. BMC Med Genet. 2014;15:80.
32. Benjamini Y, Hochberg Y. Controlling the false discovery rate: a practical and powerful approach to multiple testing. Journal of the Royal Statistical Society Series B. 1995;57(57):289–300.
33. Ye J, Coulouris G, Zaretskaya I, Cutcutache I, Rozen S, Madden TL. Primer-BLAST: a tool to design target-specific primers for polymerase chain reaction. BMC Bioinformatics. 2012;13:134.
34. Edgar RC. MUSCLE: a multiple sequence alignment method with reduced time and space complexity. BMC Bioinformatics. 2004;5:113.
35. Edgar RC. MUSCLE: multiple sequence alignment with high accuracy and high throughput. Nucleic Acids Res. 2004;32(5):1792–7.
36. Dorrell C, Schug J, Lin CF, Canaday PS, Fox AJ, Smirnova O, et al. Transcriptomes of the major human pancreatic cell types. Diabetologia. 2011;54(11):2832–44.
37. Bramswig NC, Everett LJ, Schug J, Dorrell C, Liu C, Luo Y, et al. Epigenomic plasticity enables human pancreatic α to β cell reprogramming. J Clin Invest. 2013;123(3):1275–84.
38. Nica AC, Ongen H, Irminger JC, Bosco D, Berney T, Antonarakis SE, et al. Cell-type, allelic, and genetic signatures in the human pancreatic beta cell transcriptome. Genome Res. 2013;23(9):1554–62.
39. Martens GA, Jiang L, Hellemans KH, Stangé G, Heimberg H, Nielsen FC, et al. Clusters of conserved beta cell marker genes for assessment of beta cell phenotype. PLoS One. 2011;6(9):e24134.
40. Chowanadisai W, Lönnerdal B, Kelleher SL. Zip6 (LIV-1) regulates zinc uptake in neuroblastoma cells under resting but not depolarizing conditions. Brain Res. 2008;1199:10–9.
41. Lue HW, Yang X, Wang R, Qian W, Xu RZ, Lyles R, et al. LIV-1 promotes prostate cancer epithelial-to-mesenchymal transition and metastasis through HB-EGF shedding and EGFR-mediated ERK signaling. PLoS One. 2011;6(11):e27720.
42. Hogstrand C, Kille P, Nicholson RI, Taylor KM. Zinc transporters and cancer: a potential role for ZIP7 as a hub for tyrosine kinase activation. Trends Mol Med. 2009;15(3):101–11.
43. Beker Aydemir T, Chang SM, Guthrie GJ, Maki AB, Ryu MS, Karabiyik A, et al. Zinc transporter ZIP14 functions in hepatic zinc, iron and glucose homeostasis during the innate immune response (endotoxemia). PLoS One. 2012;7(10):e48679.
44. Ku GM, Kim H, Vaughn IW, Hangauer MJ, Myung Oh C, German MS, et al. Research resource: RNA-Seq reveals unique features of the pancreatic β-cell transcriptome. Mol Endocrinol. 2012;26(10):1783–92.
45. Moldawer LL, Copeland EM. Proinflammatory cytokines, nutritional support, and the cachexia syndrome: interactions and therapeutic options. Cancer. 1997;79(9):1828–39.
46. Cnop M, Welsh N, Jonas JC, Jörns A, Lenzen S, Eizirik DL. Mechanisms of pancreatic beta-cell death in type 1 and type 2 diabetes: many differences, few similarities. Diabetes. 2005;54(Suppl 2):S97–107.
47. Eizirik DL, Sammeth M, Bouckenooghe T, Bottu G, Sisino G, Igoillo-Esteve M, et al. The human pancreatic islet transcriptome: expression of candidate genes for type 1 diabetes and the impact of pro-inflammatory cytokines. PLoS Genet. 2012;8(3):e1002552.
48. Ylipaasto P, Kutlu B, Rasilainen S, Rasschaert J, Salmela K, Teerijoki H, et al. Global profiling of coxsackievirus- and cytokine-induced gene expression in human pancreatic islets. Diabetologia. 2005;48(8):1510–22.
49. Ortis F, Naamane N, Flamez D, Ladrière L, Moore F, Cunha DA, et al. Cytokines interleukin-1beta and tumor necrosis factor-alpha regulate different transcriptional and alternative splicing networks in primary beta-cells. Diabetes. 2010;59(2):358–74.
50. Moore F, Naamane N, Colli ML, Bouckenooghe T, Ortis F, Gurzov EN, et al. STAT1 is a master regulator of pancreatic {beta}-cell apoptosis and islet inflammation. J Biol Chem. 2011;286(2):929–41.
51. Cerf ME, Muller CJ, Du Toit DF, Louw J, Wolfe-Coote SA. Transcription factors, pancreatic development, and beta-cell maintenance. Biochem Biophys Res Commun. 2005;326(4):699–702.
52. Nielsen K, Karlsen AE, Deckert M, Madsen OD, Serup P, Mandrup-Poulsen T, et al. Beta-cell maturation leads to in vitro sensitivity to cytotoxins. Diabetes. 1999;48(12):2324–32.
53. Nielsen K, Kruhøffer M, Orntoft T, Sparre T, Wang H, Wollheim C, et al. Gene expression profiles during beta cell maturation and after IL-1beta exposure reveal important roles of Pdx-1 and Nkx6.1 For IL-1beta sensitivity. Diabetologia. 2004;47(12):2185–99.
54. Hansen JB, Tonnesen MF, Madsen AN, Hagedorn PH, Friberg J, Grunnet LG, et al. Divalent metal transporter 1 regulates iron-mediated ROS and pancreatic β cell fate in response to cytokines. Cell Metab. 2012;16(4):449–61.
55. Hayes HL, Moss LG, Schisler JC, Haldeman JM, Zhang Z, Rosenberg PB, et al. Pdx-1 activates islet α- and β-cell proliferation via a mechanism regulated by transient receptor potential cation channels 3 and 6 and extracellular signal-regulated kinases 1 and 2. Mol Cell Biol. 2013;33(20):4017–29.
56. Sachdeva MM, Claiborn KC, Khoo C, Yang J, Groff DN, Mirmira RG, et al. Pdx1 (MODY4) Regulates pancreatic beta cell susceptibility to ER stress. Proc Natl Acad Sci U S A. 2009;106(45):19090–5.
57. Bensellam M, Van Lommel L, Overbergh L, Schuit FC, Jonas JC. Cluster analysis of rat pancreatic islet gene mRNA levels after culture in low-, intermediate- and high-glucose concentrations. Diabetologia. 2009;52(3):463–76.
58. Dominguez V, Raimondi C, Somanath S, Bugliani M, Loder MK, Edling CE, et al. Class II phosphoinositide 3-kinase regulates exocytosis of insulin granules in pancreatic beta cells. J Biol Chem. 2011;286(6):4216–25.
59. Marselli L, Thorne J, Dahiya S, Sgroi DC, Sharma A, Bonner-Weir S, et al. Gene expression profiles of Beta-cell enriched tissue obtained by laser capture microdissection from subjects with type 2 diabetes. PLoS One. 2010;5(7):e11499.
60. Taneera J, Lang S, Sharma A, Fadista J, Zhou Y, Ahlqvist E, et al. A systems genetics approach identifies genes and pathways for type 2 diabetes in human islets. Cell Metab. 2012;16(1):122–34.
61. Sokolov A, Funk C, Graim K, Verspoor K, Ben-Hur A. Combining heterogeneous data sources for accurate functional annotation of proteins. BMC Bioinformatics. 2013;14(Suppl 3):S10.
62. Rutter GA, Chabosseau P, Bellomo EA, Maret W, Mitchell RK, Hodson DJ, et al. Intracellular zinc in insulin secretion and action: a determinant of diabetes risk? Proc Nutr Soc. 2016;75(1):61–72.
63. Mitchell RK, Hu M, Chabosseau PL, Cane MC, Meur G, Bellomo EA, et al. Molecular genetic regulation of Slc30a8/ZnT8 reveals a positive association with glucose tolerance. Mol Endocrinol. 2016;30(1):77–91.
64. Slepchenko KG, Li YV. Rising intracellular zinc by membrane depolarization and glucose in insulin-secreting clonal HIT-T15 beta cells. Exp Diabetes Res. 2012;2012:190309.
65. Baynes JW. Role of oxidative stress in development of complications in diabetes. Diabetes. 1991;40(4):405–12.
66. Kasana S, Din J, Maret W. Genetic causes and gene–nutrient interactions in mammalian zinc deficiencies: acrodermatitis enteropathica and transient neonatal zinc deficiency as examples. J Trace Elem Med Biol. 2015;29:47–62.
67. Lichten LA, Cousins RJ. Mammalian zinc transporters: nutritional and physiologic regulation. Annu Rev Nutr. 2009;29:153–76.
68. Huang L, Kirschke CP, Zhang Y, Yu YY. The ZIP7 gene (Slc39a7) encodes a zinc transporter involved in zinc homeostasis of the Golgi apparatus. J Biol Chem. 2005;280(15):15456–63.
69. Thorsen K, Mansilla F, Schepeler T, Oster B, Rasmussen MH, Dyrskjot L, et al. Alternative Splicing of SLC39A14 in Colorectal Cancer is Regulated by the Wnt Pathway. Molecular & Cellular Proteomics. 2011;10(1)M110.002998.
70. Aydemir TB, Sitren HS, Cousins RJ. The Zinc Transporter Zip14 Influences c-Met Phosphorylation and Hepatocyte Proliferation During Liver Regeneration in Mice. Gastroenterology. 2012;142(7):1536–1546.e1535.
71. Taylor KM, Muraina IA, Brethour D, Schmitt-Ulms G, Nimmanon T, Ziliotto S, et al. Zinc transporter ZIP10 forms a heteromer with ZIP6 which regulates embryonic development and cell migration. Biochem J. 2016;473:2531–44.

72. Hogstrand C, Kille P, Ackland ML, Hiscox S, Taylor KM. A mechanism for epithelial-mesenchymal transition and anoikis resistance in breast cancer triggered by zinc channel ZIP6 and STAT3 (signal transducer and activator of transcription 3). Biochem J. 2013;455:229–37.
73. Taylor KM, Hiscox S, Nicholson RI, Hogstrand C, Kille P. Protein Kinase CK2 Triggers Cytosolic Zinc Signaling Pathways by Phosphorylation of Zinc Channel ZIP7. Sci Signal. 2012;5(210):ra11.
74. Liuzzi JP, Lichten LA, Lanata T, Cousins RJ. Zip14 Protein is induced in mouse liver by endotoxin injection and functions as a zinc transporter. FASEB J 2005;19(5):A974-A974.
75. Liuzzi JP, Aydemir F, Nam H, Knutson MD, Cousins RJ. Zip14 (Slc39a14) Mediates non-transferrin-bound iron uptake into cells. Proc Natl Acad Sci U S A. 2006;103(37):13612–7.
76. Thomas P, Pang Y, Dong J. Membrane androgen receptor characteristics of human ZIP9 (SLC39A) zinc transporter in prostate cancer cells: androgen-specific activation and involvement of an inhibitory G protein in zinc and MAP kinase signaling. Mol Cell Endocrinol. 2017;447:23-34.
77. Matsuura W, Yamazaki T, Yamaguchi-Iwai Y, Masuda S, Nagao M, Andrews GK, et al. SLC39A9 (ZIP9) Regulates zinc homeostasis in the secretory pathway: characterization of the ZIP subfamily I protein in vertebrate cells. Biosci Biotechnol Biochem. 2009;73(5):1142–8.
78. Jenkitkasemwong S, Wang CY, Mackenzie B, Knutson MD. Physiologic implications of metal-ion transport by ZIP14 and ZIP8. Biometals. 2012;25(4):643–55.
79. Taylor KM, Morgan HE, Smart K, Zahari NM, Pumford S, Ellis IO, et al. The emerging role of the LIV-1 subfamily of zinc transporters in breast cancer. Mol Med. 2007;13(7–8):396–406.
80. Giunta C, Elçioglu NH, Albrecht B, Eich G, Chambaz C, Janecke AR, et al. Spondylocheiro dysplastic form of the Ehlers-Danlos syndrome–an autosomal-recessive entity caused by mutations in the zinc transporter gene SLC39A13. Am J Hum Genet. 2008;82(6):1290–305.
81. Fukada T, Civic N, Furuichi T, Shimoda S, Mishima K, Higashiyama H, et al. The zinc transporter SLC39A13/ZIP13 is required for connective tissue development; its involvement in BMP/TGF-beta signaling pathways. PLoS One. 2008;3(11):e3642.
82. Jeong J, Walker JM, Wang F, Park JG, Palmer AE, Giunta C, et al. Promotion of vesicular zinc efflux by ZIP13 and its implications for spondylocheiro dysplastic Ehlers-Danlos syndrome. Proc Natl Acad Sci U S A. 2012;109(51):E3530–8.
83. Clocquet AR, Egan JM, Stoffers DA, Muller DC, Wideman L, Chin GA, et al. Impaired insulin secretion and increased insulin sensitivity in familial maturity-onset diabetes of the young 4 (insulin promoter factor 1 gene). Diabetes. 2000;49(11):1856–64.
84. Matsuoka TA, Kawashima S, Miyatsuka T, Sasaki S, Shimo N, Katakami N, et al. Mafa enables Pdx1 to effectively convert pancreatic islet progenitors and committed islet α-cells into β-cells in vivo. Diabetes. 2017;66(5)1293-1300.
85. Cheng CW, Villani V, Buono R, Wei M, Kumar S, Yilmaz OH et al. Fasting-Mimicking Diet Promotes Ngn3-Driven β-Cell Regeneration to Reverse Diabetes. Cell. 2017;168(5):775–788.e12.
86. Yamamoto Y, Miyatsuka T, Sasaki S, Miyashita K, Kubo F, Shimo N, et al. Preserving expression of Pdx1 improves β-cell failure in diabetic mice. Biochem Biophys Res Commun. 2017;483(1):418–24.
87. Pound LD, Hang Y, Sarkar SA, Wang Y, Milam LA, Oeser JK, et al. The pancreatic islet β-cell-enriched transcription factor Pdx-1 regulates Slc30a8 gene transcription through an intronic enhancer. Biochem J. 2011;433(1):95–105.
88. Ohlsson H, Karlsson K, Edlund T. IPF1, a homeodomain-containing transactivator of the insulin gene. EMBO J. 1993;12(11):4251–9.
89. Noh H, Paik HY, Kim J, Chung J. The alteration of zinc transporter gene expression is associated with inflammatory markers in obese women. Biol Trace Elem Res. 2014;158(1):1–8.
90. Besecker B, Bao S, Bohacova B, Papp A, Sadee W, Knoell DL. The human zinc transporter SLC39A8 (Zip8) is critical in zinc-mediated cytoprotection in lung epithelia. Am J Physiol Lung Cell Mol Physiol. 2008;294(6):L1127–36.
91. Liuzzi JP, Lichten LA, Rivera S, Blanchard RK, Aydemir TB, Knutson MD, et al. Interleukin-6 regulates the zinc transporter Zip14 in liver and contributes to the hypozincemia of the acute-phase response. Proc Natl Acad Sci U S A. 2005;102(19):6843–8.
92. Aronson D. Hyperglycemia and the pathobiology of diabetic complications. Adv Cardiol. 2008;45:1–16.
93. Waanders LF, Chwalek K, Monetti M, Kumar C, Lammert E, Mann M. Quantitative proteomic analysis of single pancreatic islets. Proc Natl Acad Sci U S A. 2009;106(45):18902–7.
94. Maris M, Ferreira GB, D'Hertog W, Cnop M, Waelkens E, Overbergh L, et al. High glucose induces dysfunction in insulin secretory cells by different pathways: a proteomic approach. J Proteome Res. 2010;9(12):6274–87.
95. Schrimpe-Rutledge AC, Fontès G, Gritsenko MA, Norbeck AD, Anderson DJ, Waters KM, et al. Discovery of novel glucose-regulated proteins in isolated human pancreatic islets using LC-MS/MS-based proteomics. J Proteome Res. 2012;11(7):3520–32.
96. Brackeva B, Kramer G, Vissers JP, Martens GA. Quantitative proteomics of rat and human pancreatic beta cells. Data Brief. 2015;3:234–9.
97. Chandramouli K, Qian PY. Proteomics: challenges, techniques and possibilities to overcome biological sample complexity. Hum Genomics Proteomics. 2009;2009:239204.
98. Maier T, Güell M, Serrano L. Correlation of mRNA and protein in complex biological samples. FEBS Lett. 2009;583(24):3966–73.
99. Steger D, Berry D, Haider S, Horn M, Wagner M, Stocker R, et al. Systematic spatial bias in DNA microarray hybridization is caused by probe spot position-dependent variability in lateral diffusion. PLoS One. 2011;6(8):e23727.
100. Gyulkhandanyan AV, Lu H, Lee SC, Bhattacharjee A, Wijesekara N, Fox JE, et al. Investigation of transport mechanisms and regulation of intracellular Zn2 + in pancreatic alpha-cells. J Biol Chem. 2008;283(15):10184–97.
101. Miyazaki J, Araki K, Yamato E, Ikegami H, Asano T, Shibasaki Y, et al. Establishment of a pancreatic beta cell line that retains glucose-inducible insulin secretion: special reference to expression of glucose transporter isoforms. Endocrinology. 1990;127(1):126–32.

3.3. Additional files in publication

Additional file 1. Dataset analysis results (excel file available online; DOI: 10.1186/s12864-017-4119-2).

Table 3.1. Additional table 1: Designs for human qPCR assays undertaken.

Gene	RefSeq ID	Forward primer (5' – 3')	Reverse primer (5' – 3')	Amplicon	UPL Probe
SLC39A1	NM_014437.3	GGAGAAAGCTCCGGGAAA	GAGTGACGTCAGTTAGGAGCAA	91	#71
SLC39A2	NM_014579.3	GAACAGATCAGCAAGTGAGAGAAA	AGCTCTCCATAGGGATACTCCA	75	#09
SLC39A3	NM_144564.4	GTTTCTGGCCACGTGCTT	AGGCTCAGGACCTTCTGGA	69	#74
SLC39A4	NM_017767.2	GCTCCAGTGTGTGGGACA	GCCTGTTCCGACAGTCCA	73	#46
SLC39A5	NM_173596.2	CCTCTTCCTGCTCTTTGTGC	TCGAGATTCCTTCGTTTTCG	96	#45
SLC39A6	NM_012319.3	ACTGGCCGTTGGGACTTT	ATGGTGGTGACTTGCATGAG	73	#09
SLC39A7	NM_006979.2	CGAAGGTGGAACGGAACTT	AGGCCTGGAAAGGATGGTAG	134	#55
SLC39A8	NM_022154.5	TTTTGGTGGGCAACAATTTC	CAGCATATCATTCATCTCTGGAA	107	#67
SLC39A9	NM_018375.4	GGTCTGGTTGTCCATGCTG	AACTGGACACTGGTCTGTGAAGT	77	#32
SLC39A10	NM_001127257.1	TGTAGCCTTGGTGGATATGCT	CCACAGGACAAAAGCCATGT	77	#09
SLC39A11	NM_139177.3	GGGCTGATGGAAGTGCAG	CCTTGGAGCATGCTGGATAC	63	#19
SLC39A12	NM_152725.3	TGAAATACTCTCCAGGATTTAAAAGG	GGGGTAAACTTGTAACCAAAGGA	96	#50
SLC39A13	NM_001128225.2	GGCCAACACCATCGATAACT	TTGTCAGGAGCCCGATCTT	83	#05
SLC39A14	NM_015359.4	TCTCTGCCAACTGGATTTTTG	CCTCATTCATCTCAGGGAACA	84	#78
UBC	M26880.1/M26880.EMI	CAGAGGTTGATCTTTGCTGGA	GCAGGGTGGACTCTTTCTGA	82	#11
GAPDH	NM_002046.3	AGCCACATCGCTCAGACAC	GCCCAATACGACCAAATCC	66	#60

Table 3.2. Additional table 2: Designs for mouse qPCR assays undertaken.

Gene	RefSeq ID	Forward primer (5' – 3')	Reverse primer (5' – 3')	Amplicon	UPL Probe
Slc39a1	NM_013901.2	CGACAGCAATGGAGTGAGAC	TCCGATGCGACTGCTTCT	119	#81
Slc39a2	NM_001039676.2	CCTGCTTGCTCTTCTGGTTC	ACCCTGTGGTGATGACCTG	99	#26
Slc39a3	NM_134135.1	CGTATTCCTGGCTACATGCTT	CGGGTAGTCGGTGCTGAT	97	#27
Slc39a4	NM_028064.2	CAGCTACTGCAGAAGATTGAGG	TCCAGCAGTTGGGGAAGAT	83	#07
Slc39a5	NM_028051.3	GGCTGACCATCTGAATGAGG	AGGGCTCAGTCCAAAATTGA	67	#33
Slc39a6	NM_139143.3	CCAGTCCCTTCGGACCTC	CTGTGGCCATTGCACCTT	89	#70
Slc39a7	NM_008202.2	GGATTTTGCCATCCTGGTC	TTGCAGTCACGAGTTGCAG	71	#71
Slc39a8	NM_026228.4	TCAGCGTTGTATCCCTCCA	GTTTGGGCCCCTTCAGAC	69	#21
Slc39a9	NM_026244.2	CGTGGCAATAATGCTACACAA	CATGCATCAGGAAGGAAACC	62	#67
Slc39a10	NM_172653.2	TTTCAGATCATAAGTTAAACAGCACA	CCGAGTCATCCGTTCCAG	78	#89
Slc39a11	NM_027216.5	GAGGATTGCTTTGCTCATCC	AATCCTACGCCAACAGCAAG	72	#09
Slc39a12	NM_001012305.2	TGGACACAAGGAGACTGCAA	TTCCCCCAGCTGTGAGTAAC	64	#38
Slc39a13	NM_026721.2	AGATGTTCCTCAACAGCAAGG	GCAGCAGTGGGGTCTTTG	61	#20
Slc39a14	NM_001135151.1	GCTCTCTAACGCCCTTTTCC	ATTGTCCTGAGGGTTGAAGC	61	#110
Ubc	NM_019639.4	GACCAGCAGCAGGCTGATCTT	CCTCTGAGGCGAAGGACTAA	110	#11
Gapdh	NM_008084.2	TGTCCGTCGTGGATCTGC	CCTGCTTCACCACCTTCTTG	75	#80

Fig 3.1. Additional file 4: ZIP isoforms in human islets. Data produced through RNAseq from Eizirik DL et al., PLoS Genet. 2012;8(3):e1002552.

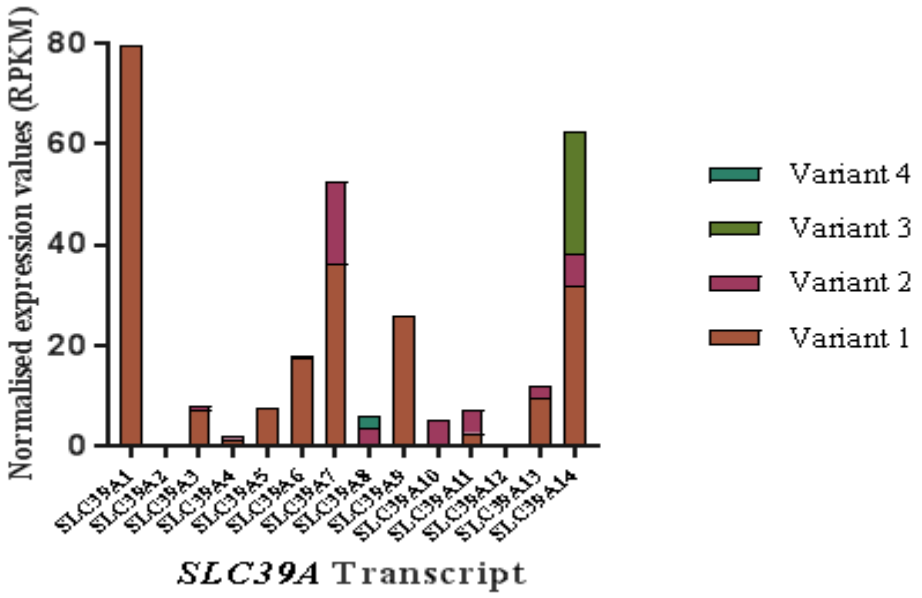

4. Prolonged stimulation of insulin-release from MIN6 cells causes zinc depletion and loss of β-cell markers

4.1. Candidate contributions to chapter 4

The work in this chapter has been published in The Journal of Trace Elements in Medicine and Biology (published online April 2018; DOI: 10.1016/j.jtemb.2018.04.020 [405]). I carried out all the data collection and analysis and constructed all the tables and figures. I additionally produced the original draft and all subsequent revisions of the manuscript, under the supervision of my supervisors.

4.2. Context of chapter 4 in this thesis

The work in this chapter goes towards addressing the second aim of this project*: To explore the consequences of the hyperglycaemia and hypozincaemia associated with Type 2 Diabetes for β-cell ZIP transporter expression, zinc content and cellular phenotype.* I examined the consequences of chronic stimulation, representative of the hyperglycaemia present in Type 2 Diabetes, for the β-cell zinc content, and explored the biological relevance of these data by assessing expression of Zn^{2+}-responsive β-cell markers. The data presented in this publication reveal a plausible link between hyperglycaemia and zinc-induced loss of β-cell phenotype. These results strengthen the basis for chapters 5-7 of this thesis by showing that decreases in cellular zinc may be detrimental for β-cell phenotype and function.

Journal of Trace Elements in Medicine and Biology 49 (2018) 51–59

Contents lists available at ScienceDirect

Journal of Trace Elements in Medicine and Biology

journal homepage: www.elsevier.com/locate/jtemb

Physiology

Prolonged stimulation of insulin release from MIN6 cells causes zinc depletion and loss of β-cell markers

Rebecca Lawson, Wolfgang Maret, Christer Hogstrand*

King's College London, Faculty of Life Sciences and Medicine, School of Life Course Sciences, Metal Metabolism Group, 150 Stamford St., London SE1 9NH, UK

ARTICLE INFO

Keywords:
Zinc
β-cells
ZIP transporters
Transcription factors
Gene expression
Dedifferentiation

ABSTRACT

Zinc is integral for the normal function of pancreatic β-cells in glycaemic control. Large amounts of zinc are secreted from β-cells following insulin exocytosis and regulated replenishment is required, which is thought to be mediated by the ZIP family of zinc importer proteins. Within Type 2 Diabetic patients, β-cells are stressed through prolonged stimulation by hyperglycaemia and this is thought to be a major factor contributing to loss of β-cell identity and mass. However, the consequences for the β-cell zinc status remain largely unexplored. We used inductively coupled plasma mass spectrometry (ICP-MS) to show that 24 h treatment of MIN6 cells with potassium chloride, mimicking hyperglycaemic stimulation, reduces the total cellular zinc content 2.8-fold, and qPCR to show an increase in mRNA expression for metallothioneins (*Mt1* and *Mt2)* following 4 and 24 h of stimulation, suggestive of an early rise in cytosolic zinc. To determine which ZIP paralogues may be responsible for zinc replenishment, we used immunocytochemistry, Western blot and qPCR to demonstrate initial ZIP1 protein upregulation proceeded by downregulation of mRNA coding for ZIP1, ZIP6, ZIP7 and ZIP14. To assign a biological significance to the decreased total cellular zinc content, we assessed expression of key β-cell markers to show downregulation of mRNA for *MafA*, *Mnx-1*, *Nkx2.2* and *Pax6*. Our data suggest hyperglycaemia-induced zinc depletion may contribute to loss of β-cell markers and promote β-cell dedifferentiation through disrupting expression of key transcription factors.

1. Introduction

Zinc is an essential micronutrient in mammalian physiology and human health. Links between zinc and diabetes were first established in 1938 [1], and a hypozincaemic status has since been described in some Type 2 Diabetic patients [2,3] and in animal models of diabetes [4,5]. Roles of both environmental and genetic contributors to Type 2 Diabetes pathogenesis and progression have been extensively documented, and estimates for heritability range from 30 to 70% [6,7].

Zinc is a structural, catalytic, and regulatory component of proteins within and outside cells [8]. Even at very low concentrations the free zinc ions (Zn^{2+}) exhibit potent effects [9,10]. Intracellular Zn^{2+} concentrations are therefore tightly regulated to mediate physiological targets whilst avoiding cross-metal interference [11]. Cells maintain intracellular Zn^{2+} concentrations through buffering and muffling (time-dependent redistribution through intracellular compartmentalisation) dynamics, which vary dependent on cellular state [12]. Buffering is mediated by metallothionein (MT1-4) zinc-binding proteins. MT mRNA levels are rapidly increased in response to a rise in cytosolic Zn^{2+}, primarily driven by activation of the Zn^{2+}-sensing transcription factor MTF1, which regulates expression of genes involved in intracellular zinc homeostasis [13]. Translocation of Zn^{2+} across biological membranes is mediated by the Zrt- and Irt-related protein (ZIP; SLC39A) and the zinc transporter protein (ZnT; SLC30A) families of zinc transporters, which move zinc into and out of the cytosol, respectively. In humans and rodents, 14 ZIP and 10 ZnT paralogues exist [14,15], varying in terms of tissue distribution, cytolocation, zinc affinities, transporting efficiencies and regulatory mechanisms to tightly and specifically deliver zinc to different cell types and organelles [14,16].

Type 2 Diabetes is a chronic metabolic disease characterised by hyperglycaemia proceeding to loss of insulin-secreting pancreatic β-cells through apoptosis and dedifferentiation to a progenitor-like state [17–19]. Critically, zinc is integral for β-cell function in glycaemic control [20,21]. β-cells maintain total zinc concentrations at 150–200 μM, of which 70% is contained within insulin secretory

Abbreviations: Zn^{2+}, zinc ions; MT, metallothionein; ZIP, Zrt- and Irt-related protein; ZnT, zinc transporter protein; GSIS, glucose-stimulated insulin secretion; K_{ATP} channels, ATP-sensitive potassium channels; L-VGCC, L-type voltage-gated calcium channels; Ca^{2+}, calcium ions; TRP, transient receptor potential; qPCR, quantitative PCR; ICP-MS, inductively-coupled plasma mass spectrometry; MODY, maternity-onset diabetes of the young; MRE, metal response element

* Corresponding author.
E-mail addresses: rebecca.tarrant@kcl.ac.uk (R. Lawson), wolfgang.maret@kcl.ac.uk (W. Maret), christer.hogstrand@kcl.ac.uk (C. Hogstrand).

https://doi.org/10.1016/j.jtemb.2018.04.020
Received 22 December 2017; Received in revised form 19 March 2018; Accepted 18 April 2018

granules at much higher concentrations [22]. Zinc is loaded into granules via the predominantly β-cell-specific zinc transporter 8 (ZnT8) [9,23], where two Zn^{2+} bind insulin hexamers, essential for proper insulin processing and granule maturation [24]. High concentrations of extracellular glucose (16.7–22.2 mM [25]) stimulate signalling cascades resulting in Zn^{2+} and insulin co-release from β-cell granules [26,27], known as glucose-stimulated insulin secretion (GSIS). The GSIS pathway involves metabolism of glucose through glycolysis to elevate the ATP/ADP ratio, which agonises ATP-sensitive potassium ion (K^+) channels (K_{ATP} channels) to promote membrane depolarisation, activation of L-type voltage-gated calcium channels (L-VGCC), resulting in calcium ion (Ca^{2+}) and Zn^{2+} influx [28], membrane fusion of granules and insulin exocytosis [29]. ZnT8 is a recognised Type 2 Diabetes risk locus at which an arginine to tryptophan substitution polymorphism confers a ~14% increase in risk per arginine risk allele [30,31]. Rare loss-of-function ZnT8 polymorphisms are protective against Type 2 Diabetes [32], highlighting the complex relationship between zinc trafficking and β-cell function. An adequate zinc status is further important for maintaining the intracellular redox balance, signalling pathways linked to β-cell mass [33], and is associated in zebrafish with expression of transcription factors (*neurod1*, *hnf1ß*, *hnf4α*, *foxa1*, *nkx2.2*, and *pax6*) required for ß-cell differentiation and endocrine function [34–37]. A recent study using human insulin-secreting β-cell like stem cells additionally showed zinc supplementation induces up-regulation of the β-cell markers PDX1 and PAX4 [38]. Thus, there might be a link between zinc dysregulation in β-cells during diabetes and loss of β-cell phenotype and associated endocrine function.

Hyperglycaemia is universal in all Type 2 Diabetic patients and contributes to loss of β-cell mass through promoting β-cell dedifferentiation [18]; prolonged stimulation of the GSIS pathway is therefore characteristic of Type 2 Diabetic pathology. β-Cells exhibit an exceptionally high turnover of zinc to maintain homeostatic control over zinc concentrations following insulin granule exocytosis, and replenishment is required to maintain intracellular homeostasis [39]. High glucose stimulation of mouse islets for 24 h has previously been shown to double cytosolic free Zn^{2+} concentrations and to up-regulate genes involved in cellular zinc homeostasis [40] including ZIP6 and ZIP7 [41,42]. However, the consequences of chronic hyperglycaemia for β-cell zinc content remains poorly understood and experimental exploration of the ZIP paralogues in β-cell function remains limited to a few studies [40,43–46]. We have previously shown through a systematic review complemented with experimental data that ZIP6, ZIP7, ZIP9 and ZIP14 in human and rodent, and ZIP1 in rodent are potentially biologically important for β-cell zinc trafficking [46]. Here, we postulated these ZIP paralogues are involved in intracellular zinc homeostasis during β-cell stimulation. We also hypothesised that prolonged stimulation may lead to cellular zinc loss through enhanced zinc/insulin co-secretion, and that this may affect expression of β-cell markers, which as a consequence could influence β-cell phenotype. Thus, the aim of the present study was to characterise the consequences of prolonged stimulation for β-cell zinc content and expression of key ZIP transporters and zinc-responsive β-cell markers.

We show that prolonged stimulation decreases the total zinc content of MIN6 cells but increases mRNA expression for *Mt1* and *Mt2*, indicative of an early surge in cytosolic Zn^{2+} followed by increased buffering capacity as MT1 and MT2 proteins are being produced [47]. Unexpectedly, this effect on MT was coupled with a decrease in *Mtf1* mRNA. Using a combination of quantitative PCR (qPCR), immunocytochemistry and Western blot, we observed an increase in ZIP1 and a decrease in ZIP7 protein, down-regulation of mRNA for *Slc39a1*, *Slc39a6*, *Slc39a7*, *Slc39a14,* and down-regulation of multiple zinc-responsive β-cell markers. Our data demonstrate that prolonged stimulation depletes β-cells of zinc, presumably as a result of a decrease of multiple ZIP transporters along with loss of gene expression of several markers of β-cell differentiation.

2. Methods and materials

2.1. Cell line and culture

The adherent insulinoma β-cell line MIN6 (*Mus musculus*) was a kind gift from Dr. Jun-ichi Miyazaki [48]. Cells were maintained within 25 mM glucose Dulbecco's Modified Eagle's Medium (DMEM) supplemented with 15% foetal bovine serum (FBS), 4 mM L-glutamine, 50 μM β-mercaptoethanol, 100 μg/ml streptomycin and 100 units/ml penicillin (both Thermo Fisher) at 37 °C in a humidified atmosphere of 95% air and 5% CO_2. Cells were cultured for 24 h prior to experimentation. *For cell stimulation:* growth media were replaced with glucose-free DMEM containing 15% FBS, 4 mM L-glutamine, 50 μM β-mercaptoethanol, 100 μg/ml streptomycin and 100 units/ml penicillin supplemented with either 3 mM glucose (control) or 3 mM glucose and 40 mM potassium chloride (KCl) for 4 h or 24 h. KCl was used to depolarise MIN6 cells to induce insulin secretion since the cells were not glucose-responsive. *For zinc depletion:* FBS was depleted of metal ions through incubation with 5% (w/v) Chelex-100 (Sigma) for 1 h, and sterile-filtered through a 0.22 μm syringe filter. Chelex-100 treated FBS was diluted 1:100 in 0.5% nitric acid (HNO_3) and heavy metal analysis carried out through inductively-coupled plasma mass spectrometry (ICP-MS) [49]. Chelex-100 treated FBS was supplemented with Ca^{2+}, K^+ and Na^+ to original concentrations. Growth media were replaced with 25 mM glucose DMEM containing 15% Chelex-100 treated-FBS, 4 mM L-glutamine, 50 μM β-mercaptoethanol, 100 μg/ml streptomycin and 100 units/ml penicillin, supplemented with $ZnCl_2$ to total concentrations of 1 μM or 8 μM (control) Zn^{2+} for 24, 48 or 96 h.

2.2. Determination of total zinc content

Cells were lysed in hot 0.2% sodium dodecyl sulfate (SDS). Samples were diluted 1:100 with 0.5% HNO_3 (trace element grade) and the zinc concentration determined through ICP-MS. The total zinc content was normalised to protein content, determined through Bradford assays (Bio-Rad) [50], which were standardised to dilutions of bovine serum albumin (BSA) in phosphate-buffered saline (PBS). Statistical significance of differences in cellular zinc content was examined through unpaired *t*-tests.

2.3. RNA extraction, cDNA synthesis and quantitative PCR

Total RNA was extracted using TRIzol Reagent (Thermo Fisher), reverse transcribed to cDNA using the high capacity RNA-to-cDNA kit (Thermo Fisher), and diluted ≥1:10 prior to experimentation. Quantitative PCR (qPCR) assays were designed using the online Universal Probe Library (UPL) assay design tool (Roche). Assay designs are provided in Additional file 1. PCR plates were loaded using the Biomek FX liquid handling robot (Beckman Coulter) and reactions (20–40 ng cDNA, 0.1 μM UPL probe, 0.2 μM forward primer, 0.2 μM reverse primer and 1X TaqMan Fast Advanced Mastermix (Applied Biosystems) amplified using the Prism7900HT sequence detection system (Applied Biosystems) and analysed with SDS (sequence detection systems) 2.4 software. All gene expression values were normalised to the housekeeping gene ubiquitin C, and relative expression calculated using the ΔΔCT method [51]. The efficiencies for all primers ranged from 81 to 120%. Significance of differences in mRNA expression were examined through unpaired t-tests. Data show an average of three biological repeats.

2.4. Immunocytochemistry

MIN6 cells were seeded onto sterile glass coverslips and treated as described above. Cells were fixed using 4% paraformaldehyde for 15 min, permeabilised in 0.25% (v/v) Triton X-100 for 10 min and blocked in 3% (w/v) BSA/PBS for 1 h. Cells were immunolabelled

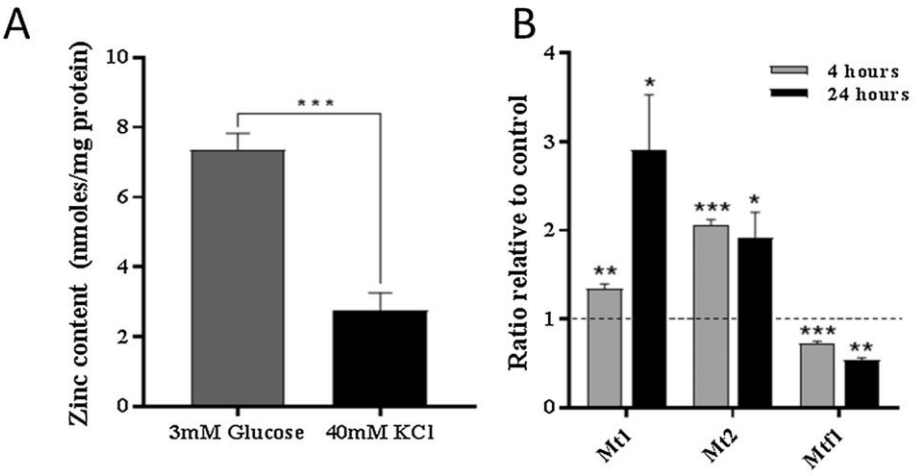

Fig. 1. MIN6 cell zinc content following prolonged stimulation. **(A)** Total cellular zinc content after 24 h treatment with 40 mM KCl determined through ICP-MS and normalised to protein content. N = 4. **(B)** mRNA expression of *Mt1*, *Mt2* and *Mtf1*, assessed through qPCR. Expression was calculated as a ratio compared to cells cultured under the same conditions but without KCl (3 mM glucose; control). N = 3. Error bars show ± SEM. $^{*}p < 0.05$, $^{**}p < 0.005$, $^{***}p < 0.001$.

through incubation with primary antibodies targeting ZIP1 (SAB3500592; Sigma Aldrich), ZIP6 (PA5-21071; Thermo Fisher), ZIP7 (19429-1-AP; Proteintech), ZIP9 (PA5-21074; Thermo Fisher) and ZIP14 (PA5-21077; Thermo Fisher) overnight at 4 °C, followed by incubation with Alexafluor 595-linked secondary antibodies (A11012; Thermo Fisher) for 1 h at room temperature. Cells were extensively washed in PBS between each step. Coverslips were mounted onto coverslides using VECTASHIELD Antifade Mounting Media containing 4′,6-diamidino-2-phenylindole (DAPI) (VECTOR Laboratories) and imaged using an AR1 confocal microscope (Nikon). We quantified the average Alexafluor 595 fluorescence intensities of six images taken across each slide using Fiji, ImageJ software [52], calculated as a ratio relative to DAPI. Significance of differences in protein abundances were examined through unpaired *t*-tests.

2.5. Western blotting

Protein lysates were prepared in 2x loading dye (Thermo Fisher) and boiled (10 min, 72 °C). Lysates (20 µg) were separated on 12% acrylamide SDS-PAGE gels using SDS-PAGE buffer (both Thermo Fisher) supplemented with 0.1% (w/v) SDS (200 V, 40 min). Proteins were transferred onto nitrocellulose membranes [GE Healthcare Life Sciences (1 h, 100 V)] using transfer buffer (25 mM Tris, 192 mM glycine, 10% methanol (pH 8.3)), and membranes blocked through incubation in 5% (w/v) BSA/Tris-buffered saline [TBS (50 mM Tris-Cl pH 7.5, 150 mM NaCl)] and 0.05% (v/v) TWEEN-20 [TBST (1 h, 25 °C)]. Membranes were incubated with primary antibodies targeting ZIP1 [SAB3500592; Sigma Aldrich (1:400)] or α-Tubulin [T9026, Sigma (1:15,000)] diluted in 1% BSA/TBST (16 h, 4 °C), followed by HRP-linked secondary antibodies [α-mouse: Amersham, NA931V (1:20,000); α-rabbit: Amersham, NA934V (1:15,000)] diluted in 1% BSA/TBST (1 h, 25 °C). Membranes were extensively washed with TBST between each step. Membranes were treated with ECL Western Blotting Detection Reagent (GE Healthcare Life Sciences) and visualised on X-ray film (GE Healthcare Life Sciences) using a film imager. For membrane stripping, immunoblots were washed in TBST, incubated in stripping buffer [Thermo Fisher (15 min, 25 °C)] and washed with TBST (10 min, 25 °C). Membranes were blocked with 5% (v/v) BSA/TBST (1 h, 25 °C) before further antibody incubation.

2.6. Proliferation assays

The rate of cell proliferation was determined using the Cell Proliferation ELISA, BrdU (colorimetric) assay (Roche), following manufacturer's instructions.

2.7. Apoptosis assays

The rate of cell apoptosis was determined through Caspase-Glo® 3/7 assays (Thermo Fisher), following manufacturer's instructions.

2.8. Transcription factor network analysis

MetaCore (GeneGo) Bioinformatics software from Thomson Reuters (https://portal.genego.com/) was used to create a network from qPCR data of transcription factor expression after zinc depletion for 48 h. The experimental data were uploaded to MetaCore version 6.32 build 69,020 and analysed through the 'Build Network' function, generating sub-networks enriched with the seed nodes from the qPCR data using canonical pathways and limiting the number of nodes in a network to 50. The top network was pruned to remove all objects with less than three links to analysed genes, leaving only FOXA2 (HNF-3B) in addition to the analysed genes. Data showing the basis of this network are provided in Additional file 2.

3. Results

3.1. Prolonged stimulation decreases the total zinc content of MIN6 cells

Zinc is co-released with insulin from β-cells during stimulation with glucose- or KCl–induced depolarisation. However, the consequences of prolonged stimulation for β-cell zinc content remain poorly understood. We stimulated MIN6 cells for 24 h and found a 2.8-fold depletion in total cellular zinc (Fig. 1A). Total cell zinc depletion was associated with elevated mRNA expression of the metallothioneins *Mt1* and *Mt2* (1.3-fold and 2.1-fold, respectively, at 4 h and 2.9-fold and 1.9-fold, respectively, at 24 h), indicative of an increase in cytosolic Zn^{2+} and consequent MTF1-mediated transactivation [53]. We further noted down-regulation of mRNA for *Mtf1* 1.4-fold at 4 h and 1.8-fold at 24 h (Fig. 1B).

3.2. Prolonged stimulation disrupts expression of multiple β-cell ZIP transporters

Increased zinc uptake during β-cell stimulation is likely influenced by changes in activity and/or abundance of ZIP and ZnT paralogues important for β-cell function. We therefore explored protein and mRNA expression of ZIP paralogues we previously highlighted as important for β-cell function [46] and mRNA expression for ZnT1 and ZnT8. We identified up-regulation of ZIP1 protein (1.5-fold) and a small but statistically significant down-regulation of ZIP7 protein (1.1-fold) through immunocytochemistry following 24 h sustained stimulation (Fig. 2**A-B**). ZIP1 protein up-regulation was verified using Western blot ($p = 0.04$)

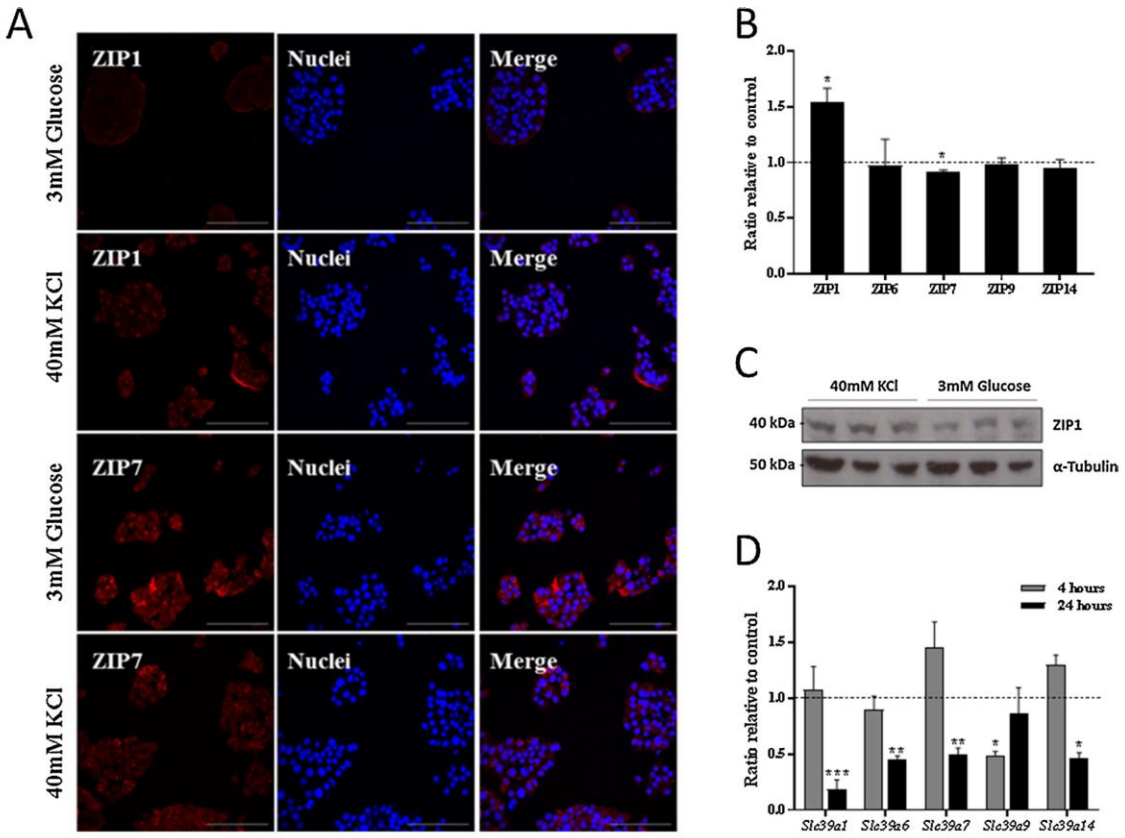

Fig. 2. Changes in ZIP/*Slc39a* expression in MIN6 cells following prolonged stimulation. **(A–C)** ZIP protein abundances following culture with 40 mM KCl for 24 h, imaged by immunocytochemistry. **(A)** Representative immunocytochemistry images for ZIP1 and ZIP7 after 24 h. Scale bar: 100 μm. **(B)** Average changes in ZIP protein abundances after 24 h. **(C)** Western blot for ZIP1 protein abundance after 24 h. **(D)** *Slc39a* mRNA abundances following culture with 40 mM KCl for 4 h (grey) and 24 h (black), assayed through qPCR. Expression was calculated as a ratio compared to cells cultured under the same conditions but without KCl (3 mM glucose; control). N = 3. Error bars show ± SEM. *p < 0.05, **p < 0.005, ***p < 0.001.

(Fig. 2C). Whilst we did not observe any differences in the mRNA abundances for these paralogues at 4 h, mRNA for *Slc39a1* and *Slc39a7* showed statistically significant down-regulation (*Slc39a1*: 6.8-fold, *Slc39a7*: 2.0-fold) along with those for *Slc39a6* (2.3-fold), and *Slc39a14* (2.2-fold) at 24 h (Fig. 2D). Conversely, *Slc39a9* mRNA was 2.0-fold downregulated at 4 h, but recovered after 24 h. We further observed statistically significant down-regulation of mRNA for *Slc30a8* (1.8-fold) at 24 h, but mRNA for *Slc30a1* remained unchanged. These data suggest prolonged β-cell stimulation induces initial up- and down-regulation of ZIP1 and ZIP7 proteins, respectively, followed by downregulation of mRNA for ZIP1, ZIP6, ZIP7, ZIP14 and ZnT8.

3.3. Prolonged stimulation disrupts expression of zinc-responsive β-cell markers

β-cell proliferation and function are controlled by multiple transcription factors, many of which are required to maintain the β-cell phenotype. Changes in the expression/function of important β-cell proteins are suggestive of loss of cellular identity and indicate mechanisms contributing to β-cell dedifferentiation [18,54]. We examined the expression of the transcription factors *Foxa1, Foxo1, Hnf1b, Hnf4a, MafA, Mnx1, Neurod1, Nkx2.2, Nkx6.1, Pax4, Pax6* and *Pdx1* in MIN6 cells following stimulation with KCl for 24 h and found significant up-regulation of mRNA expression for *Hnf1b* 2.9-fold, and down-regulation of mRNA expression for *Foxa1* (1.8-fold), *MafA* (3.8-fold), *Mnx-1* (2.6-fold), *Nkx2*.2 (2.6-fold) and *Pax6* (2.7-fold) (Fig. 3A). Although not statistically significant, mRNA for *Hnf4a* showed 3.1-fold numerical increase ($p < 0.2$) and *Neurod1* 2.0-fold decrease ($p < 0.06$). These data indicate an association between prolonged stimulation and changes in expression of key β-cell transcription factors with the predominant trend being down-regulation.

The transcription factors NEUROD1, HNF1B, HNF4A, FOXA1, NKX2.2 and PAX6 have previously been identified as zinc-responsive [34–37]. Since prolonged stimulation decreases intracellular zinc content, we asked whether changes in β-cell transcription factor expression may be consequential of cellular zinc depletion. We treated MIN6 cells with growth medium containing low (1 μM) zinc for 24 h to show no differences in mRNA expression for these key transcription factors compared to control cells cultured in growth medium with 8 μM zinc (Fig. 3B). However, after 48 h we observed statistically significant down-regulation of mRNA for *Hnf1b* (3.3-fold), *Hnf4a* (2.9-fold), *MafA* (1.8-fold), *Mnx-1* (3.6-fold), *Nkx2.2* (1.2-fold), *Nkx6.1* (2.5-fold) *Pax4* (1.5-fold), *Pax6* (3.2-fold) and *Pdx1* (2.7-fold) (Fig. 3C). These data demonstrate loss of *Hnf1b, Hnf4a, MafA, Mnx-1, Nkx2.2, Nkx6.1*, *Pax4, Pax6* and *Pdx1* in response to zinc depletion in mammalian β-cells and suggest changes in expression following chronic stimulation may be a result of zinc depletion caused by prolonged zinc secretion in combination with down-regulation of zinc importers.

Suppression of β-cell markers is suggestive of loss of β-cell identity and numbers. To explore the biologically relevant consequences of zinc depletion-induced transcription factor down-regulation we examined mRNA expression for *Arx,* which is activated to induce β-to-α-cell reprogramming [55], and MIN6 cell survival. We recorded a comparable increase in *Arx* mRNA abundance for cells cultured with 40 mM KCl for 24 h and low (1 μM) zinc for 48 h (4.0-fold and 2.9-fold, respectively). Although we did not observe any differences in MIN6 cell proliferation or apoptosis following 48 h zinc depletion (data not shown), by 96 h, cells exhibited a 1.3-fold decrease in proliferation ($p < 0.05$) and 1.4-

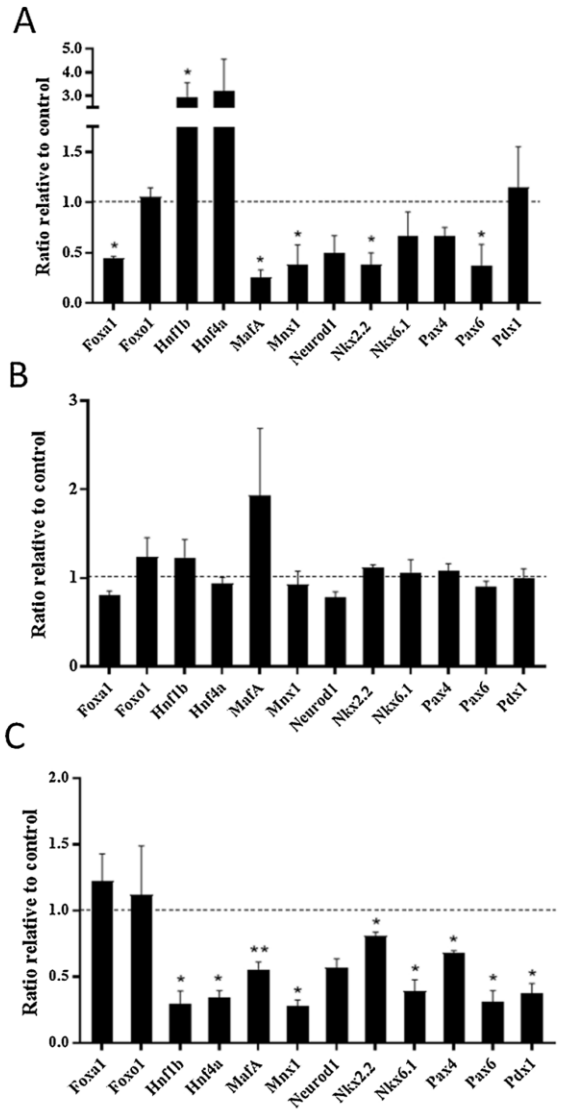

Fig. 3. Changes in mRNA expression of transcription factors in MIN6 cells. **(A)** Expression in response to stimulation with 40 mM KCl for 24 h. Expression was calculated as a ratio compared to cells cultured under the same conditions but without KCl (3 mM glucose; control). **(B–C)** Expression in response to extracellular zinc depletion for **(B)** 24 h or **(C)** 48 h. Expression was assayed through qPCR and calculated as a ratio compared to cells cultured with 8 μM extracellular zinc (control). N = 3. $*p < 0.05$, $**p < 0.005$.

fold increase in apoptosis ($p < 0.005$). These data support the contribution of chronic stimulation-induced MIN6 cell zinc depletion to loss of β-cell markers and decreased survival.

4. Discussion

4.1. Zinc depletion of MIN6 cells causes loss of β-cell markers

Zinc is an inter- and intracellular signalling component, regulating almost all aspects of cellular function including gene expression. In the current study, we demonstrate the transcription factors *Hnf1b, Hnf4a, MafA, Mnx-1, Nkx2.2, Nkx6.1*, *Pax4, Pax6* and *Pdx1* are down-regulated by zinc depletion in mammalian β-cells. These transcription factors have important roles in maintaining β-cell identity and their deregulation impacts cellular phenotype and function, including insulin pathway regulation, β-cell mass and islet architecture (Fig. 4). PDX1 is considered the key transcription factor in mature β-cells mediating β-cell survival and mass [56] and controlling a large array of genes [57,58]. PDX1 [59], HNF4A [60], MAFA [61] and PAX6 [62,63] are required for maximal insulin production. NKX6.1 stimulates islet cell proliferation [64], and MNX1 facilitates proliferation in aged cells [65]. Similarly, PAX4 stimulates proliferation and promotes survival of mature β-cells through protecting against stress-induced apoptosis [66,67]. NKX2.2 acts upstream of GLUT2, the transporter responsible for glucose uptake into rodent β-cells, and is necessary for proper β-cell clustering and islet architecture [68], and HNF1B regulates pathways mediating glucose signalling in β-cells [69]. Critically, monogenetic mutations in Hnf1b, Hnf4a, Pdx1 and Pax4 result in 'maternity-onset diabetes of the young' (MODY) [70] and, recently, mutations in Nkx2.2 and Mnx-1 have additionally been linked to the neonatal disease [71]. Consistent with our results, *hnf1ß*, *hnf4a, nkx2.2*, and *pax6* exhibit zinc-responsive expression in zebrafish [34–37], and PDX1 and PAX4 show up-regulation in response to zinc in human exfoliated deciduous tooth stem cells induced into insulin-secreting β-cell like stem cells [38]. Importantly, β-cells and glucagon-secreting α-cells are derived from common progenitors and share expression of many transcription factors at differing equilibria, many of which are specific to the endocrine pancreas; suppression of important β-cell transcription factors induces β-cell dedifferentiation and transdifferentiation into α-cells. PDX1, NKX2.2 and NKX6.1 are essential for maintaining β-cell phenotype in early β-cell development, proceeded by a prominent role of PAX4, MAFA and the related transcription factor MAFB. In mature β-cells, loss of PDX1 and NKX2.2 causes complete loss of β-cell identity and PAX4, NKX6.1 and PDX1 inhibit glucagon expression to prevent α-cell transdifferentiation [54,72]. Concurrently, we demonstrate zinc-depletion in MIN6 cells increases mRNA expression for *Arx,* which is indicative of loss of β-cell identity and α-cell reprogramming, and reduces MIN6 cell numbers through both reduced proliferation and increased apoptosis. Our data further suggest the systemic hypozincaemia present in some Type 2 Diabetic patients may contribute to loss of β-cell mass through promoting β-cell dedifferentiation or transdifferentiation into α-cells.

4.2. Prolonged stimulation of MIN6 cells causes zinc depletion and deregulation of β-cell markers

Chronic hyperglycaemia elevates the requirement for zinc replenishment through extending the duration of secretory pathway activation and β-cell zinc loss. Following prolonged KCl stimulation in MIN6 cells, we observed down-regulation of *Foxa1*, *MafA*, *Mnx-1*, *Nkx2.*2 and *Pax6*. We also found that a massive amount of the cellular zinc was lost during this treatment, probably reflecting the zinc lost from insulin granules, which has been previously observed following chronic exposure of rat INS-1E cells to high extracellular glucose [73]. Since depletion of zinc from the culture medium caused down-regulation of mRNA for nine out of the 12 β-cell markers measured, including *MafA*, *Mnx-1*, *Nkx2.*2 and *Pax6,* suppressed expression of these genes following prolonged stimulation may be a direct result of zinc depletion. The effects on β-cell markers were apparent following 24 h of KCl-induced depolarisation, but only after 48 h of treatment with reduced zinc concentration in the culture medium. This difference in time-course of the effect might be explained by temporal differences in depleting the cellular zinc content, which was very rapid during KCl treatment. However, treatment with a low zinc concentration in the culture medium did not completely mimic the effect triggered by prolonged stimulation using KCl. Interestingly, we show that depletion of zinc from the medium down-regulates *Hnf1b.* However the mRNA for this transcript was up-regulated following 24 h KCl stimulation; a similar relationship was observed for *Hnf4a* which was downregulated by zinc depletion for 48 h but not by the 24 h KCl-induced stimulation. Like most β-cell markers, expression of both *Hnf1b* and *Hnf4a* is tightly regulated by multiple factors, and an alternative pathway likely dominates regulation during cellular stimulation. Nevertheless, since major differences in *Hnf1b* and *Hnf4a* expression profiles are reported

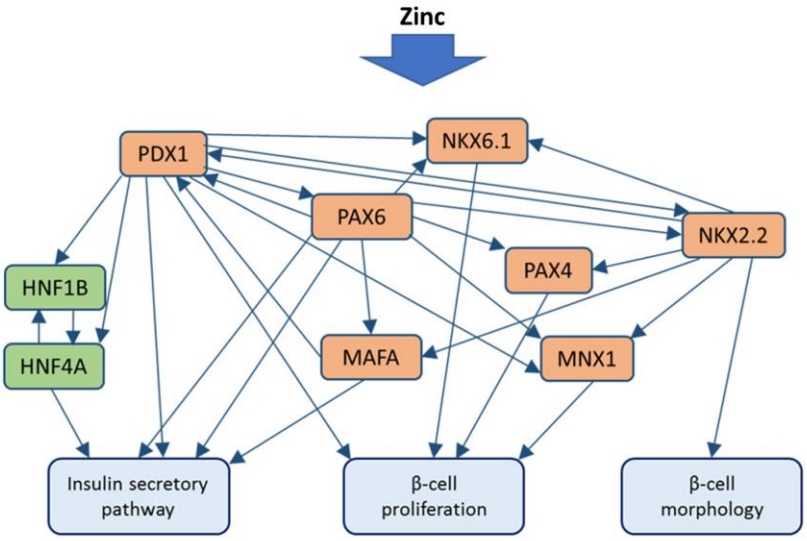

Fig. 4. Schematic illustrating key roles of the zinc-responsive transcription factors in mature β-cells. All transcription factors shown are down-regulated in response to zinc depletion in MIN6 cells. Transcription factors highlighted in orange show down-regulation in response to prolonged stimulation with KCl and those highlighted in green show up-regulation in response to prolonged stimulation with KCl. The arrows represent known signal transduction pathways between the transcription factors in β-cells.

between healthy human and rodent cells [74], these results may not be easily translatable to the human Type 2 Diabetes.

4.3. The role of zinc in maintenance of key transcription factors in MIN6 cells

Complex coordination and cross-regulation exist between transcription factors to tightly regulate β-cell phenotype and function. Based on published interactions between these transcription factors and our experimental data showing zinc depletion-mediated changes in gene expression, we are able to speculate zinc might target this network at MAFA, NEUORD1 or NKX2.2 (Fig. 5). Zinc may influence changes in gene expression via MTF1 or another zinc-signalling pathway such as via the zinc-finger transcription factors KLF4 [75] or ZNF658 [76]. Alternatively, the results may stem from altered transcription factor phosphorylation affecting protein activation and/or localisation, which has been previously shown for MAFA [77] and NEUROD1 [78]. Pinpointing the molecular action of zinc in this network requires further investigation and could prove important for understanding loss of β-cell identity and insulin secretory function during hyperglycaemia-induced β-cell dedifferentiation.

4.4. Fluctuations in markers for cytosolic Zn^{2+} during β-cell stimulation

Cellular zinc depletion was accompanied by up-regulation of mRNA expression for the metallothioneins *Mt1* and *Mt2*, which is suggestive of an early surge in cytosolic Zn^{2+} [40] followed by increased buffering capacity as MT1 and MT2 proteins are produced [79]. An early surge in Zn^{2+} uptake might be explained by increased zinc trafficking to insulin granules. We further demonstrated a decrease in mRNA expression for MTF1 within MIN6 cells, which cannot be readily explained. Zn^{2+} binds MTF1 at six Cys_2His_2-type zinc-finger domains, which exhibit differing binding affinities. Zn^{2+} binding promotes translocation of MTF1 from the cytosol to the nucleus, where MTF1 binds metal-response elements (MRE) in the promoters of zinc-regulated genes [80]. Although MTF1 transcript and protein levels increase with zinc treatment, MTF1 activity is mainly believed to be regulated post-translationally through nuclear-cytoplasmic shuttling, DNA-binding, phosphorylation and interaction with other transcriptional co-activators [13]. The observed increases in *Mt* mRNA could be a result of epigenetic regulation, increased MTF1 post-translational activation, or MTF1-independent mechanisms governing MT gene expression [81].

Stimulation-induced increases in cytosolic Zn^{2+} are consistent with a previous study on mouse islets [40], however these authors observed

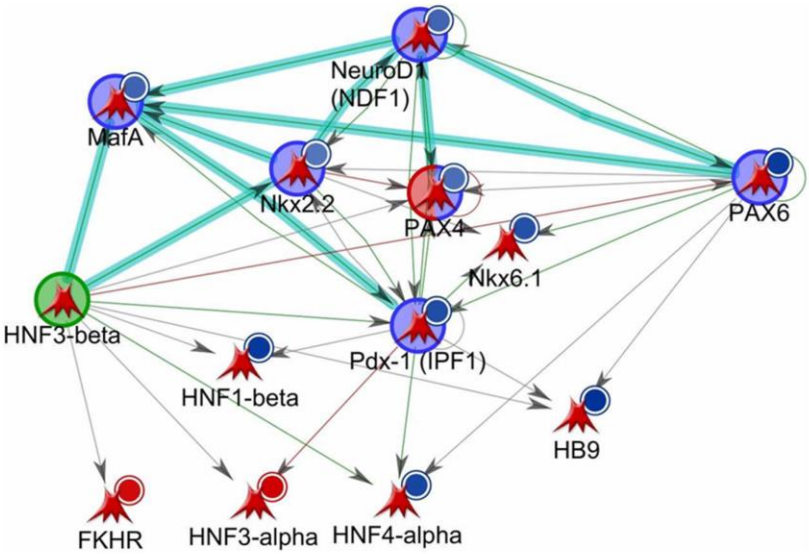

Fig. 5. Network of interactions between the transcription factors FOXA1 (HNF3A), FOXA2 (HNF3B), FOXO1 (FKHR), HNF1B, HNF4A, MAFA, MNX1 (HB9), NEUROD1, NKX2.2, NKX6.1, PAX4, PAX6 AND PDX1 in β-cells. The pathways highlighted in blue are the 'nodes' considered to drive the network in response to zinc. The red circles indicate the respective gene is up-regulated and the blue circles indicate the respective gene is down-regulated in response to zinc. Created using GeneGo MetaCore Bioinformatics software from Thomson Reuters (https://portal.genego.com/). Data showing the basis of this network are provided in Additional file 2.

MT1 and MT2 decrease and did not assess the total cellular zinc content. This variation could be explained by differences in the experimental design, including use of glucose rather than KCl to induce cellular stimulation or the use of primary islets containing 70–80% β-cells rather than a β-cell line which exist as a monolayer. We acknowledge that it is possible these differences in results could be an artefact of tissue culture rather than a physiological response, but our observations would still lend valuable information for interpreting future data on changes to the zinc status of β-cells. Furthermore, the variation may only represent temporal differences between conditions, perhaps influenced by the time required to induce intracellular zinc depletion. These observations need to be explored further to distinguish between physiological state and the pathological state proceeding loss of β-cell identity and β-cell dedifferentiation.

4.5. Regulation of zinc transporter expression during prolonged stimulation of MIN6 cells

L-VGCCs are activated during stimulation of the insulin secretory pathway [28] but are not thought to play the pivotal role in cellular zinc uptake [40], indicating important roles for the ZIP transporters. Our results suggest that an early post-transcriptional or post-translational up-regulation of ZIP1 protein may be integral in the physiological response to increased stimulation in murine MIN6 cells. ZIP1 is a plasma membrane-bound paralogue which we previously identified as highly expressed and potentially biologically important for rodent but not human β-cells [46]. It is therefore possible human β-cells encompass a different mechanism from rodents to adapt to increased zinc replenishment during elevated insulin secretion, perhaps through up-regulating expression of transporters functionally substituting in β-cells for the rodent ZIP1. Contrary to our expectation of what would happen following KCl-induced cellular zinc depletion, we observed down-regulation of *Slc39a1*, *Slc39a6*, *Slc39a7* and *Slc39a14* mRNA after 24 h KCl stimulation. This could be in response to elevations in cytosolic Zn^{2+}, either representing a protective mechanism to prevent cytosolic Zn^{2+} accumulation to pathological concentrations or reflecting zinc-responsive changes to mRNA transcript levels. Down-regulation of mRNA for ZIP4, ZIP5, ZIP6, ZIP7 and ZIP10 has previously been identified as a mechanism to protect against cytosolic zinc overload [41,42,82,83]. ZIP7 is localised to the Golgi apparatus [42], which stores zinc at high concentrations [84], and functions to release zinc spatially and temporally in response to stimuli [42]; ZIP7 down-regulation could be indicative of zinc depletion from the Golgi apparatus or represent a protective mechanism to prevent further depletion. Furthermore, ZIP14 facilitates import of non-haem iron in addition to zinc [85,86], indicating stimulation-induced ZIP14 downregulation could be a protective mechanism against accumulation of iron to cytotoxic concentrations. It is possible the observed ZIP suppression is simply a pathological response to prolonged stimulation rather than serving a physiological purpose. Since ZIP6, ZIP7 and ZIP14 additionally exhibit potent roles in stimulating cellular proliferation [87–92], chronic stimulation is likely to be detrimental to β-cell proliferation, and this may help to explain the loss of β-cell mass observed in Type 2 Diabetic patients.

ZnT transporters likely function co-operatively with the ZIPs to mediate β-cell zinc trafficking in response to chronic stimulation. A recent study has reported appreciable expression of all ZnT exporters in pancreatic β-cells [93]. Of potential notable importance, ZnT1 is detected with high abundance at the plasma membrane and ZnT8 at the insulin granule membranes. We demonstrate *Slc30a8* mRNA down-regulation in MIN6 cells following 24 h KCl stimulation. ZnT8 down-regulation has been suggested to increase β-cell survival [94,95]; however, studies using rat INS-1E cells demonstrate repression reduces cellular insulin content and GSIS [96] and overexpression stimulates increase in total intracellular zinc and protects against zinc-depletion induced cellular death [97], indicating loss of ZnT8 reduces β-cell identity and survival. Accordingly, there is currently no clear consensus on the role of ZnT8 for β-cell phenotype and function. There was no observed difference in mRNA expression for ZnT1. ZnT1 is regulated by MTF1 [98] and dietary zinc [99] at the transcriptional, post-transcriptional and post-translational level, including through presumed subcellular redistribution [100], and knockdown increases cadmium influx and toxicity [101]. We are therefore unable draw conclusions about ZnT1 regulation in response to chronic MIN6 cell stimulation from our data without first exploring the abundance and subcellular localisation of the expressed protein.

5. Conclusion

In this study, we explored the consequences of prolonged β-cell stimulation, characteristic of the hyperglycaemia universal in Type 2 Diabetic patients, for cellular zinc status and markers of β-cell function. We show sustained stimulation depletes β-cells of zinc and down-regulates multiple ZIP transporters of importance for β-cell function [46]. Potentially important for understanding human Type 2 Diabetes development, we demonstrate key β-cell transcription factors disrupted by prolonged stimulation are zinc-responsive in mammalian β-cells and their mRNA levels depressed by zinc depletion. We further anchored these findings to β-cell function, by showing that zinc depletion decreases proliferation and increases apoptosis. Critically, our results reveal a plausible causative link between hyperglycaemia-induced zinc depletion of pancreatic β-cells and loss of expression of transcription factors of importance for β-cell differentiation, proliferation and endocrine function.

Funding

RL was supported by the King's Bioscience Institute and the Guy's and St Thomas' Charity Prize PhD Programme in Biomedical and Translational Science.

Declarations of interest

None

Acknowledgements

Metal analysis was performed by the London Metallomics Facility funded by the Wellcome trust (grant reference 202902/Z/16/Z). The authors wish to thank Andy Cakebread for carrying out the ICP-MS, Dr Han Lu (Genomics Centre, King's College London) for help with the qPCR and Ben Robinson (Nikon Centre, King's College London) for help with the confocal microscopy.

Appendix A. Supplementary data

Supplementary material related to this article can be found, in the online version, at doi:https://doi.org/10.1016/j.jtemb.2018.04.020.

References

[1] D.A. Scott, A.M. Fisher, The insulin and the zinc content of normal and diabetic patients, J. Clin. Invest. 17 (6) (1938) 725–728.
[2] V.K. Garg, R. Gupta, R.K. Goyal, Hypozincemia in diabetes mellitus, J. Assoc. Phys. India 42 (9) (1994) 720–721.
[3] G.B. de Carvalho, P.N. Brandão-Lima, C.S. Maia, K.B. Barbosa, L.V. Pires, Zinc's role in the glycemic control of patients with type 2 diabetes: a systematic review, Biometals 30 (2) (2017) 151–162.
[4] S.F. Simon, C.G. Taylor, Dietary zinc supplementation attenuates hyperglycemia in db/db mice, Exp. Biol. Med. (Maywood) 226 (1) (2001) 43–51.
[5] N. Begin-Heick, M. Dalpe-Scott, J. Rowe, H.M. Heick, Zinc supplementation attenuates insulin secretory activity in pancreatic islets of the ob/ob mouse, Diabetes 34 (2) (1985) 179–184.
[6] J. Flannick, J.C. Florez, Type 2 diabetes: genetic data sharing to advance complex disease research, Nat. Rev. Genet. 17 (9) (2016) 535–549.

[7] P. Almgren, M. Lehtovirta, B. Isomaa, L. Sarelin, M.R. Taskinen, V. Lyssenko, T. Tuomi, L. Groop, B.S. Group, Heritability and familiality of type 2 diabetes and related quantitative traits in the botnia study, Diabetologia 54 (11) (2011) 2811–2819.

[8] T. Kambe, T. Tsuji, A. Hashimoto, N. Itsumura, The physiological, biochemical, and molecular roles of zinc transporters in zinc homeostasis and metabolism, Physiol. Rev. 95 (3) (2015) 749–784.

[9] W. Maret, Zinc in pancreatic Islet biology, insulin sensitivity, and diabetes, Prev. Nutr. Food Sci. 22 (1) (2017) 1–8.

[10] C. Hogstrand, P.M. Verbost, S.E. Wendelaar Bonga, Inhibition of human erythrocyte Ca^{2+}-ATPase by Zn^{2+}, Toxicology 133 (2–3) (1999) 139–145.

[11] W. Maret, Zinc in cellular regulation: the nature and significance of "zinc signals", Int. J. Mol. Sci. 18 (11) (2017).

[12] A. Krezel, Q. Hao, W. Maret, The zinc/thiolate redox biochemistry of metallothionein and the control of zinc ion fluctuations in cell signaling, Arch. Biochem. Biophys. 463 (2) (2007) 188–200.

[13] V. Günther, U. Lindert, W. Schaffner, The taste of heavy metals: gene regulation by MTF-1, Biochim. Biophys. Acta 1823 (9) (2012) 1416–1425.

[14] L.A. Gaither, D.J. Eide, Eukaryotic zinc transporters and their regulation, Biometals 14 (3–4) (2001) 251–270.

[15] K.M. Taylor, R.I. Nicholson, The LZT proteins; The LIV-1 subfamily of zinc transporters, Biochim. Biophys. Acta 1611 (1-2) (2003) 16–30.

[16] T. Fukada, T. Kambe, Molecular and genetic features of zinc transporters in physiology and pathogenesis, Metallomics 3 (7) (2011) 662–674.

[17] C. Talchai, S. Xuan, H.V. Lin, L. Sussel, D. Accili, Pancreatic β cell dedifferentiation as a mechanism of diabetic β cell failure, Cell 150 (6) (2012) 1223–1234.

[18] S. Guo, C. Dai, M. Guo, B. Taylor, J.S. Harmon, M. Sander, R.P. Robertson, A.C. Powers, R. Stein, Inactivation of specific β cell transcription factors in type 2 diabetes, J. Clin. Invest. 123 (8) (2013) 3305–3316.

[19] G.D. Gutiérrez, A.S. Bender, V. Cirulli, T.L. Mastracci, S.M. Kelly, A. Tsirigos, K.H. Kaestner, L. Sussel, Pancreatic β cell identity requires continual repression of non-β cell programs, J. Clin. Invest. 127 (1) (2017) 244–259.

[20] Y.V. Li, Zinc and insulin in pancreatic beta-cells, Endocrine. 45 (2) (2014) 178–189.

[21] P. Chabosseau, G.A. Rutter, Zinc and diabetes, Arch. Biochem. Biophys. 611 (2016) 79–85.

[22] J.C. Hutton, E.J. Penn, M. Peshavaria, Low-molecular-weight constituents of isolated insulin-secretory granules. Bivalent cations, adenine nucleotides and inorganic phosphate, Biochem. J. 210 (2) (1983) 297–305.

[23] L. Huang, Zinc and its transporters, pancreatic β-cells, and insulin metabolism, Vitam. Horm. 95 (2014) 365–390.

[24] F.Y. Liu, D.O. Kildsig, A.K. Mitra, Insulin aggregation in aqueous media and its effect on alpha-chymotrypsin-mediated proteolytic degradation, Pharm. Res. 8 (7) (1991) 925–929.

[25] G.M. Grodsky, A threshold distribution hypothesis for packet storage of insulin and its mathematical modeling, J. Clin. Invest. 51 (8) (1972) 2047–2059.

[26] P.D. Zalewski, S.H. Millard, I.J. Forbes, O. Kapaniris, A. Slavotinek, W.H. Betts, A.D. Ward, S.F. Lincoln, I. Mahadevan, Video image analysis of labile zinc in viable pancreatic islet cells using a specific fluorescent probe for zinc, J. Histochem. Cytochem. 42 (7) (1994) 877–884.

[27] W.J. Qian, K.R. Gee, R.T. Kennedy, Imaging of Zn2+ release from pancreatic beta-cells at the level of single exocytotic events, Anal. Chem. 75 (14) (2003) 3468–3475.

[28] A.V. Gyulkhandanyan, S.C. Lee, G. Bikopoulos, F. Dai, M.B. Wheeler, The Zn2+-transporting pathways in pancreatic beta-cells: a role for the L-type voltage-gated Ca2+ channel, J. Biol. Chem. 281 (14) (2006) 9361–9372.

[29] M. Komatsu, M. Takei, H. Ishii, Y. Sato, Glucose-stimulated insulin secretion: a newer perspective, J. Diabetes Investig. 4 (6) (2013) 511–516.

[30] R. Sladek, G. Rocheleau, J. Rung, C. Dina, L. Shen, D. Serre, P. Boutin, D. Vincent, A. Belisle, S. Hadjadj, B. Balkau, B. Heude, G. Charpentier, T.J. Hudson, A. Montpetit, A.V. Pshezhetsky, M. Prentki, B.I. Posner, D.J. Balding, D. Meyre, C. Polychronakos, P. Froguel, A genome-wide association study identifies novel risk loci for type 2 diabetes, Nature 445 (7130) (2007) 881–885.

[31] G.A. Rutter, F. Chimienti, SLC30A8 mutations in type 2 diabetes, Diabetologia 58 (1) (2015) 31–36.

[32] J. Flannick, G. Thorleifsson, N.L. Beer, S.B. Jacobs, N. Grarup, N.P. Burtt, A. Mahajan, C. Fuchsberger, G. Atzmon, R. Benediktsson, J. Blangero, D.W. Bowden, I. Brandslund, J. Brosnan, F. Burslem, J. Chambers, Y.S. Cho, C. Christensen, D.A. Douglas, R. Duggirala, Z. Dymek, Y. Farjoun, T. Fennell, P. Fontanillas, T. Forsén, S. Gabriel, B. Glaser, D.F. Gudbjartsson, C. Hanis, T. Hansen, A.B. Hreidarsson, K. Hveem, E. Ingelsson, B. Isomaa, S. Johansson, T. Jørgensen, M.E. Jørgensen, S. Kathiresan, A. Kong, J. Kooner, J. Kravic, M. Laakso, J.Y. Lee, L. Lind, C.M. Lindgren, A. Linneberg, G. Masson, T. Meitinger, K.L. Mohlke, A. Molven, A.P. Morris, S. Potluri, R. Rauramaa, R. Ribel-Madsen, A.M. Richard, T. Rolph, V. Salomaa, A.V. Segrè, H. Skärstrand, V. Steinthorsdottir, H.M. Stringham, P. Sulem, E.S. Tai, Y.Y. Teo, T. Teslovich, U. Thorsteinsdottir, J.K. Trimmer, T. Tuomi, J. Tuomilehto, F. Vaziri-Sani, B.F. Voight, J.G. Wilson, M. Boehnke, M.I. McCarthy, P.R. Njølstad, O. Pedersen, L. Groop, D.R. Cox, K. Stefansson, D. Altshuler, G.-T.D. Consortium, T.D.-G. Consortium, Loss-of-function mutations in SLC30A8 protect against type 2 diabetes, Nat. Genet. 46 (4) (2014) 357–363.

[33] G.A. Rutter, P. Chabosseau, E.A. Bellomo, W. Maret, R.K. Mitchell, D.J. Hodson, A. Solomou, M. Hu, Intracellular zinc in insulin secretion and action: a determinant of diabetes risk? Proc. Nutr. Soc. 75 (1) (2016) 61–72.

[34] D. Zheng, G.P. Feeney, R.D. Handy, C. Hogstrand, P. Kille, Uptake epithelia behave in a cell-centric and not systems homeostatic manner in response to zinc depletion and supplementation, Metallomics 6 (1) (2014) 154–165.

[35] D. Zheng, P. Kille, G.P. Feeney, P. Cunningham, R.D. Handy, C. Hogstrand, Dynamic transcriptomic profiles of zebrafish gills in response to zinc supplementation, BMC Genom. 11 (2010) 553.

[36] D. Zheng, P. Kille, G.P. Feeney, P. Cunningham, R.D. Handy, C. Hogstrand, Dynamic transcriptomic profiles of zebrafish gills in response to zinc depletion, BMC Genom. 11 (2010) 548.

[37] C. Hogstrand, D. Zheng, G. Feeney, P. Cunningham, P. Kille, Zinc-controlled gene expression by metal-regulatory transcription factor 1 (MTF1) in a model vertebrate, the zebrafish, Biochem. Soc. Trans. 36 (Pt 6) (2008) 1252–1257.

[38] G. Kim, K.H. Shin, E.K. Pae, Zinc up-regulates insulin secretion from β cell-like cells derived from stem cells from human exfoliated deciduous tooth (SHED), Int. J. Mol. Sci. 17 (12) (2016) 2092.

[39] B. Formby, F. Schmid-Formby, G.M. Grodsky, Relationship between insulin release and 65zinc efflux from rat pancreatic islets maintained in tissue culture, Diabetes 33 (3) (1984) 229–234.

[40] E.A. Bellomo, G. Meur, G.A. Rutter, Glucose regulates free cytosolic Zn^{2+} concentration, Slc39 (ZiP), and metallothionein gene expression in primary pancreatic islet β-cells, J. Biol. Chem. 286 (29) (2011) 25778–25789.

[41] W. Chowanadisai, B. Lönnerdal, S.L. Kelleher, Zip6 (LIV-1) regulates zinc uptake in neuroblastoma cells under resting but not depolarizing conditions, Brain Res. 1199 (2008) 10–19.

[42] L. Huang, C.P. Kirschke, Y. Zhang, Y.Y. Yu, The ZIP7 gene (Slc39a7) encodes a zinc transporter involved in zinc homeostasis of the golgi apparatus, J. Biol. Chem. 280 (15) (2005) 15456–15463.

[43] A.B. Hardy, K.J. Prentice, S. Froese, Y. Liu, G.K. Andrews, M.B. Wheeler, Zip4 mediated zinc influx stimulates insulin secretion in pancreatic beta cells, PLoS One 10 (3) (2015) e0119136.

[44] Y. Liu, B. Batchuluun, L. Ho, D. Zhu, K.J. Prentice, A. Bhattacharjee, M. Zhang, F. Pourasgari, A.B. Hardy, K.M. Taylor, H. Gaisano, F.F. Dai, M.B. Wheeler, Characterization of zinc influx transporters (ZIPs) in pancreatic Beta cells: roles in regulating cytosolic zinc homeostasis and insulin secretion, J. Biol. Chem. (2015) 18757–18769.

[45] E.K. Pae, G. Kim, Insulin production hampered by intermittent hypoxia via impaired zinc homeostasis, PLoS One 9 (2) (2014) e90192.

[46] R. Lawson, W. Maret, C. Hogstrand, Expression of the ZIP/SLC39A transporters in β-cells: a systematic review and integration of multiple datasets, BMC Genom. 18 (1) (2017) 719.

[47] K.M. Taylor, S. Hiscox, R.I. Nicholson, C. Hogstrand, P. Kille, Protein kinase CK2 triggers cytosolic zinc signaling pathways by phosphorylation of zinc channel ZIP7, Sci. Signal. 5 (210) (2012) ra11.

[48] J. Miyazaki, K. Araki, E. Yamato, H. Ikegami, T. Asano, Y. Shibasaki, Y. Oka, K. Yamamura, Establishment of a pancreatic beta cell line that retains glucose-inducible insulin secretion: special reference to expression of glucose transporter isoforms, Endocrinologya. 127 (1) (1990) 126–132.

[49] A.A. Ammann, Inductively coupled plasma mass spectrometry (ICP MS): a versatile tool, J. Mass Spectrom. 42 (4) (2007) 419–427.

[50] M.M. Bradford, A rapid and sensitive method for the quantitation of microgram quantities of protein utilizing the principle of protein-dye binding, Anal. Biochem. 72 (1976) 248–254.

[51] K.J. Livak, T.D. Schmittgen, Analysis of relative gene expression data using real-time quantitative PCR and the 2(-delta delta C(T)) method, Methods 25 (4) (2001) 402–408.

[52] J. Schindelin, I. Arganda-Carreras, E. Frise, V. Kaynig, M. Longair, T. Pietzsch, S. Preibisch, C. Rueden, S. Saalfeld, B. Schmid, J.Y. Tinevez, D.J. White, V. Hartenstein, K. Eliceiri, P. Tomancak, A. Cardona, Fiji: an open-source platform for biological-image analysis, Nat. Methods 9 (7) (2012) 676–682.

[53] A. Grzywacz, J. Gdula-Argasińska, B. Muszyńska, M. Tyszka-Czochara, T. Librowski, W. Opoka, Metal responsive transcription factor 1 (MTF-1) regulates zinc dependent cellular processes at the molecular level, Acta Biochim. Pol. 62 (3) (2015) 491–498.

[54] T. van der Meulen, M.O. Huising, Role of transcription factors in the transdifferentiation of pancreatic islet cells, J. Mol. Endocrinol. 54 (2) (2015) R103–117.

[55] J.B. Papizan, R.A. Singer, S.I. Tschen, S. Dhawan, J.M. Friel, S.B. Hipkens, M.A. Magnuson, A. Bhushan, L. Sussel, Nkx2.2 repressor complex regulates islet β-cell specification and prevents β-to-α-cell reprogramming, Genes Dev. 25 (21) (2011) 2291–2305.

[56] K. Fujimoto, K.S. Polonsky, Pdx1 and other factors that regulate pancreatic beta-cell survival, Diabetes Obes. Metab. 11 (Suppl. 4) (2009) 30–37.

[57] P. Svensson, C. Williams, J. Lundeberg, P. Rydén, I. Bergqvist, H. Edlund, Gene array identification of Ipf1/Pdx1-/- regulated genes in pancreatic progenitor cells, BMC Dev. Biol. 7 (2007) 129.

[58] H. Wang, P. Maechler, B. Ritz-Laser, K.A. Hagenfeldt, H. Ishihara, J. Philippe, C.B. Wollheim, Pdx1 level defines pancreatic gene expression pattern and cell lineage differentiation, J. Biol. Chem. 276 (27) (2001) 25279–25286.

[59] T. Iype, J. Francis, J.C. Garmey, J.C. Schisler, R. Nesher, G.C. Weir, T.C. Becker, C.B. Newgard, S.C. Griffen, R.G. Mirmira, Mechanism of insulin gene regulation by the pancreatic transcription factor Pdx-1: application of pre-mRNA analysis and chromatin immunoprecipitation to assess formation of functional transcriptional complexes, J. Biol. Chem. 280 (17) (2005) 16798–16807.

[60] R. Bartoov-Shifman, R. Hertz, H. Wang, C.B. Wollheim, J. Bar-Tana, M.D. Walker, Activation of the insulin gene promoter through a direct effect of hepatocyte nuclear factor 4 alpha, J. Biol. Chem. 277 (29) (2002) 25914–25919.

[61] H. Wang, T. Brun, K. Kataoka, A.J. Sharma, C.B. Wollheim, MAFA controls genes implicated in insulin biosynthesis and secretion, Diabetologia 50 (2) (2007) 348–358.

[62] A. Hamasaki, Y. Yamada, T. Kurose, N. Ban, K. Nagashima, A. Takahashi, S. Fujimoto, D. Shimono, M. Fujiwara, S. Toyokuni, Y. Seino, N. Inagaki, Adult pancreatic islets require differential pax6 gene dosage, Biochem. Biophys. Res. Commun. 353 (1) (2007) 40–46.
[63] J.H. Wen, Y.Y. Chen, S.J. Song, J. Ding, Y. Gao, Q.K. Hu, R.P. Feng, Y.Z. Liu, G.C. Ren, C.Y. Zhang, T.P. Hong, X. Gao, L.S. Li, Paired box 6 (PAX6) regulates glucose metabolism via proinsulin processing mediated by prohormone convertase 1/3 (PC1/3), Diabetologia 52 (3) (2009) 504–513.
[64] H.L. Hayes, L.G. Moss, J.C. Schisler, J.M. Haldeman, Z. Zhang, P.B. Rosenberg, C.B. Newgard, H.E. Hohmeier, Pdx-1 activates islet α- and β-cell proliferation via a mechanism regulated by transient receptor potential cation channels 3 and 6 and extracellular signal-regulated kinases 1 and 2, Mol. Cell Biol. 33 (20) (2013) 4017–4029.
[65] F.C. Pan, M. Brissova, A.C. Powers, S. Pfaff, C.V. Wright, Inactivating the permanent neonatal diabetes gene Mnx1 switches insulin-producing β-cells to a δ-like fate and reveals a facultative proliferative capacity in aged β-cells, Development 142 (21) (2015) 3637–3648.
[66] T. Brun, I. Franklin, L. St-Onge, A. Biason-Lauber, E.J. Schoenle, C.B. Wollheim, B.R. Gauthier, The diabetes-linked transcription factor PAX4 promotes {beta}-cell proliferation and survival in rat and human islets, J. Cell Biol. 167 (6) (2004) 1123–1135.
[67] J. Lu, G. Li, M.S. Lan, S. Zhang, W. Fan, H. Wang, D. Lu, Pax4 paired domain mediates direct protein transduction into mammalian cells, Endocrinology 148 (11) (2007) 5558–5565.
[68] M.J. Doyle, L. Sussel, Nkx2.2 regulates beta-cell function in the mature islet, Diabetes 56 (8) (2007) 1999–2007.
[69] L. Wang, C. Coffinier, M.K. Thomas, L. Gresh, G. Eddu, T. Manor, L.L. Levitsky, M. Yaniv, D.B. Rhoads, Selective deletion of the Hnf1beta (MODY5) gene in beta-cells leads to altered gene expression and defective insulin release, Endocrinology 145 (8) (2004) 3941–3949.
[70] M. Vaxillaire, P. Froguel, Genetic basis of maturity-onset diabetes of the young, Endocrinol. Metab. Clin. North Am. 35 (2) (2006) 371–384.
[71] S.E. Flanagan, E. De Franco, H. Lango Allen, M. Zerah, M.M. Abdul-Rasoul, J.A. Edge, H. Stewart, E. Alamiri, K. Hussain, S. Wallis, L. de Vries, O. Rubio-Cabezas, J.A. Houghton, E.L. Edghill, A.M. Patch, S. Ellard, A.T. Hattersley, Analysis of transcription factors key for mouse pancreatic development establishes NKX2-2 and MNX1 mutations as causes of neonatal diabetes in man, Cell Metab. 19 (1) (2014) 146–154.
[72] G.A. Rutter, Diabetes: controlling the identity of the adult pancreatic β cell, Nat. Rev. Endocrinol. 13 (3) (2017) 129–130.
[73] L.G. Søndergaard, B. Brock, M. Stoltenberg, A. Flyvbjerg, O. Schmitz, K. Smidt, G. Danscher, J. Rungby, Zinc fluxes during acute and chronic exposure of INS-1E cells to increasing glucose levels, Horm. Metab. Res. 37 (3) (2005) 133–139.
[74] L.W. Harries, J.E. Brown, A.L. Gloyn, Species-specific differences in the expression of the HNF1A, HNF1B and HNF4A genes, PLoS One 4 (11) (2009) e7855.
[75] J.P. Liuzzi, L. Guo, S.M. Chang, R.J. Cousins, Krüppel-like factor 4 regulates adaptive expression of the zinc transporter Zip4 in mouse small intestine, Am. J. Physiol. Gastrointest. Liver Physiol. 296 (3) (2009) G517–523.
[76] O.A. Ogo, J. Tyson, S.J. Cockell, A. Howard, R.A. Valentine, D. Ford, The zinc finger protein ZNF658 regulates the transcription of genes involved in zinc homeostasis and affects ribosome biogenesis through the zinc transcriptional regulatory element, Mol. Cell Biol. 35 (6) (2015) 977–987.
[77] S. Benkhelifa, S. Provot, E. Nabais, A. Eychène, G. Calothy, M.P. Felder-Schmittbuhl, Phosphorylation of MafA is essential for its transcriptional and biological properties, Mol. Cell Biol. 21 (14) (2001) 4441–4452.
[78] A.E. Castro, S.G. Benitez, L.E. Farias Altamirano, L.E. Savastano, S.I. Patterson, E.M. Muñoz, Expression and cellular localization of the transcription factor NeuroD1 in the developing and adult rat pineal gland, J. Pineal Res. 58 (4) (2015) 439–451.
[79] W. Maret, A. Krezel, Cellular zinc and redox buffering capacity of metallothionein/thionein in health and disease, Mol. Med. 13 (7-8) (2007) 371–375.
[80] G.K. Andrews, Cellular zinc sensors: MTF-1 regulation of gene expression, Biometals 14 (3–4) (2001) 223–237.
[81] D.H. Petering, J. Zhu, S. Krezoski, J. Meeusen, C. Kiekenbush, S. Krull, T. Specher, M. Dughish, Apo-metallothionein emerging as a major player in the cellular activities of metallothionein, Exp. Biol. Med. (Maywood) 231 (9) (2006) 1528–1534.
[82] B.P. Weaver, J. Dufner-Beattie, T. Kambe, G.K. Andrews, Novel zinc-responsive post-transcriptional mechanisms reciprocally regulate expression of the mouse Slc39a4 and Slc39a5 zinc transporters (Zip4 and Zip5), Biol. Chem. 388 (12) (2007) 1301–1312.
[83] L.A. Lichten, M.S. Ryu, L. Guo, J. Embury, R.J. Cousins, MTF-1-mediated repression of the zinc transporter Zip10 is alleviated by zinc restriction, PLoS One 6 (6) (2011) e21526.
[84] Q. Lu, H. Haragopal, K.G. Slepchenko, C. Stork, Y.V. Li, Intracellular zinc distribution in mitochondria, ER and the golgi apparatus, Int. J. Physiol. Pathophysiol. Pharmacol. 8 (1) (2016) 35–43.
[85] J.P. Liuzzi, L.A. Lichten, T. Lanata, R.J. Cousins, Zip14 protein is induced in mouse liver by endotoxin injection and functions as a zinc transporter, Faseb J. 19 (5) (2005) A974-A974.
[86] J.P. Liuzzi, F. Aydemir, H. Nam, M.D. Knutson, R.J. Cousins, Zip14 (Slc39a14) mediates non-transferrin-bound iron uptake into cells, Proc. Natl. Acad. Sci. U. S. A. 103 (37) (2006) 13612–13617.
[87] T.B. Aydemir, H.S. Sitren, R.J. Cousins, The zinc transporter Zip14 influences c-Met phosphorylation and hepatocyte proliferation during liver regeneration in mice, Gastroenterology 142 (7) (2012) 1536–1546 e1535.
[88] K.M. Taylor, I.A. Muraina, D. Brethour, G. Schmitt-Ulms, T. Nimmanon, S. Ziliotto, P. Kille, C. Hogstrand, Zinc transporter ZIP10 forms a heteromer with ZIP6 which regulates embryonic development and cell migration, Biochem. J. 473 (2016) 2531–2544.
[89] C. Hogstrand, P. Kille, M.L. Ackland, S. Hiscox, K.M. Taylor, A mechanism for epithelial-mesenchymal transition and anoikis resistance in breast cancer triggered by zinc channel ZIP6 and STAT3 (signal transducer and activator of transcription 3), Biochem. J. 455 (2013) 229–237.
[90] K.M. Taylor, S. Hiscox, R.I. Nicholson, C. Hogstrand, P. Kille, Protein kinase CK2 triggers cytosolic zinc signaling pathways by phosphorylation of zinc channel ZIP7, Sci. Signal. 5 (210) (2012) ra11-.
[91] C. Hogstrand, W. Maret, Genetics of Human Zinc Deficiencies, eLS: John Wiley & Sons, Ltd, 2016.
[92] K. Thorsen, F. Mansilla, T. Schepeler, B. Øster, M.H. Rasmussen, L. Dyrskjøt, R. Karni, M. Akerman, A.R. Krainer, S. Laurberg, C.L. Andersen, T.F. Ørntoft, Alternative splicing of SLC39A in colorectal cancer is regulated by the Wnt pathway, Mol. Cell Proteom. 10 (1) (2011) M110.002998.
[93] Y. Cai, C.P. Kirschke, L. Huang, SLC30A family expression in the pancreatic islets of humans and mice: cellular localization in the β-cells, J. Mol. Histol. 49 (2018) 133.
[94] C. Merriman, Q. Huang, G.A. Rutter, D. Fu, Lipid-tuned zinc transport activity of human ZnT8 protein correlates with risk for type-2 diabetes, J. Biol. Chem. 291 (53) (2016) 26950–26957.
[95] L. Huang, C.P. Kirschke, Down-regulation of zinc transporter 8 (SLC30A8) in pancreatic beta-cells promotes cell survival, Austin J. Endocrinol. Diabetes 3 (1) (2016) 1037.
[96] Y. Fu, W. Tian, E.B. Pratt, L.B. Dirling, S.L. Shyng, C.K. Meshul, D.M. Cohen, Down-regulation of ZnT8 expression in INS-1 rat pancreatic beta cells reduces insulin content and glucose-inducible insulin secretion, PLoS One 4 (5) (2009) e5679.
[97] F. Chimienti, S. Devergnas, F. Pattou, F. Schuit, R. Garcia-Cuenca, B. Vandewalle, J. Kerr-Conte, L. Van Lommel, D. Grunwald, A. Favier, M. Seve, In vivo expression and functional characterization of the zinc transporter ZnT8 in glucose-induced insulin secretion, J. Cell Sci. 119 (Pt 20) (2006) 4199–4206.
[98] S.J. Langmade, R. Ravindra, P.J. Daniels, G.K. Andrews, The transcription factor MTF-1 mediates metal regulation of the mouse ZnT1 gene, J. Biol. Chem. 275 (44) (2000) 34803–34809.
[99] R.J. McMahon, R.J. Cousins, Regulation of the zinc transporter ZnT-1 by dietary zinc, Proc. Natl. Acad. Sci. U. S. A. 95 (9) (1998) 4841–4846.
[100] S.L. Kelleher, Y.A. Seo, V. Lopez, Mammary gland zinc metabolism: regulation and dysregulation, Genes Nutr. 4 (2) (2009) 83–94.
[101] E. Ohana, I. Sekler, T. Kaisman, N. Kahn, J. Cove, W.F. Silverman, A. Amsterdam, M. Hershfinkel, Silencing of ZnT-1 expression enhances heavy metal influx and toxicity, J. Mol. Med. (Berl.) 84 (9) (2006) 753–763.

4.3. Additional files in publication

Table 4.1. Additional table 1: Designs for qPCR assays undertaken.

Transcript	RefSeq ID	Forward primer (5' – 3')	Reverse primer (5' – 3')	Amplicon	UPL Probe
Slc39a1	NM_013901.2	CGACAGCAATGGAGTGAGAC	TCCGATGCGACTGCTTCT	119	#81
Slc39a6	NM_139143.3	CCAGTCCCTTCGGACCTC	CTGTGGCCATTGCACCTT	89	#70
Slc39a7	NM_008202.2	GGATTTTGCCATCCTGGTC	TTGCAGTCACGAGTTGCAG	71	#71
Slc39a9	NM_026244.2	CGTGGCAATAATGCTACACAA	CATGCATCAGGAAGGAAACC	62	#67
Slc39a14	NM_001135151.1	GCTCTCTAACGCCCTTTTCC	ATTGTCCTGAGGGTTGAAGC	61	#110
Mtf1	NM_008636.4	CCAAGAGACTAGTTGGCAGCA	GGTGGGACCAAGATCACCT	65	#10
Mt1	NM_013602.3	CAAGTGCACCTCCTGCAA	TTCGTCACATCAGGCACAG	124	#18
Mt2	NM_008630.2	CATGGACCCCAACTGCTC	AGCAGGAGCAGCAGCTTT	110	#04
Foxa1	NM_008259.3	GAACAGCTACTACGCGGACA	CGGAGTTCATGTTGCTGACA	65	#82
Foxo1	NM_019739.3	GTGGGGCAACCTGTCGTA	TTCTCGGCTGAGCTCTCG	60	#9
Hnf1b	NM_009330.2	AATCCCCAGCAATCTCAGAA	GGCTTGGGAGGTGTTGAG	84	#109
Hnf4a	NM_008261.2	CAGCAATGGACAGATGTGTGA	TGGTGATGGCTGTGGAGTC	76	#27
MafA	NM_194350.1	CTCCAGAGCCAGGTGGAG	GTACAGGTCCCGCTCCTTG	66	#10

Mnx1	NM_019944.2	GATGCCGGACTTCAGCTC	AGCTGCTGGCTGGTGAAG	84	#60
Neurod1	NM_010894.2	CGCAGAAGGCAAGGTGTC	TTTGGTCATGTTTCCACTTCC	90	#01
Nkx2.2	NM_010919.2	GCAGCGACAACCCCTACA	ATTTGGAGCTCGAGTCTTGG	105	#20
Nkx6.1	NM_144955.2	CCCGGAGTGATGCAGAGT	GAACGTGGGTCTGGTGTGTT	114	#103
Pax4	NM_011038.2	AAGACCAGACCACCAGCAA	AAGTTTCTCTTTGGGACTGGTTC	107	#01
Pax6	NM_001244198.1	CACCAGACTCACCTGACACC	ACCGCCCTTGGTTAAAGTC	62	#96
Pdx-1	NM_008814.3	GAAATCCACCAAAGCTCACG	CGGGTTCCGCTGTGTAAG	65	#51
Ubc	NM_019639.4	GACCAGCAGCAGGCTGATCTT	CCTCTGAGGCGAAGGACTAA	110	#11

Additional file 2. Interactions report (excel file available online; DOI: 10.1016/j.jtemb.2018.04.020).

5. Extracellular zinc depletion lowers β-cell zinc content, disrupts the transcriptome and reduces cellular survival

5.1. Abstract

Large amounts of zinc are lost from pancreatic β-cells during GSIS. Adequate zinc replenishment is therefore required to maintain normal intracellular concentrations, mediated by ZIP transporters at the plasma membrane and membranes of intracellular organelles. However, hypozincaemia present in many type 2 diabetic patients and animal models of diabetes reduces the amount of zinc available for β-cell zinc uptake. We hypothesised that changes to extracellular zinc alter the β-cell zinc content and phenotype. We cultured MIN6 cells with depleted (1μM), adequate (8μM) and excess (42μM) zinc to show that zinc depletion lowers total cellular zinc and downregulates mRNA for *Mt1* and *Mt2*, indicative of decreased cytosolic free Zn^{2+}, but upregulates expression of *Slc39a8* and *Slc39a14*, presumably to increase cellular zinc uptake. Concurrently, excess zinc upregulates *Mt1* and *Mt2*. Culture of MIN6 cells with each of depleted or excess zinc lowers cellular proliferation and increases apoptosis compared to cells cultured with adequate zinc, each associated with reduced signalling via mTOR and MAPK cascades. To further investigate the impact of zinc depletion for β-cells, we carried out RNA-seq on MIN6 cells and mouse islets to show differentially expressed genes were enriched for phosphatases and that HIF1A regulation may be a key pathway disrupted by zinc depletion. These data indicate hypozincaemia present in some type 2 diabetic patients may lower the zinc content of β-cells to mediate intracellular signalling and reduce cellular survival.

5.2. Introduction

Zinc is fundamental for a multitude of biological processes as a structural, catalytic, and signalling component [127, 128]. β-cells contain one of the highest zinc contents of any known cell type, with total concentrations reaching 150-200μM [281]. The predominantly β-cell-specific zinc transporter ZnT8 facilitates zinc uptake into insulin secretory granules, where zinc in involved in proper insulin processing and is secreted with insulin during GSIS. Large amounts of zinc are therefore lost from β-cells during Zn^{2+}/insulin co-exocytosis and β-cells must maintain exceptionally high turnovers to replenish normal concentrations [266], mediated by members of the ZIP family of zinc importer proteins. Upon high glucose stimulation and enhanced ZnT8-facilitated granule zinc uptake, β-cells exhibit significant increases in cytosolic free Zn^{2+} and expression of Zn^{2+}-regulated genes (chapter 4 [405] and [192]), suggestive of additional roles for the elevated zinc aside from in insulin granules.

In human, normal serum zinc concentrations range from 0.66 to 1.10 mg/mL [406]. Metabolically obese individuals, type 2 diabetic patients and animal models of diabetes often exhibit systemic hypozincaemia [140, 283, 284, 407] and lowered zinc intakes have been shown to increase the relative risk of Type 2 Diabetes development by 17% [285]. In healthy individuals, approximately 80% of absorbed zinc is transported through the bloodstream associated with the serum protein Human Serum Albumin (HSA) [408]. Persistent hyperglycaemia present in diabetes induces non-enzymatic glycation of HSA, which alters its tertiary structure and lowers its zinc binding ability, reducing transport and distribution of zinc around the body and promoting hypozincaemia [409]. Diabetic hypozincaemia is further induced by increased urinary zinc loss [410]. Since zinc cannot be stored in mammals for more than a few days [411], hypozincaemia reduces the

amounts of zinc available for β-cell zinc replenishment following GSIS and this may promote dysfunction. Concurrently, zinc supplementation enhances β-cell function in high fat-fed mice [393], and increases insulin sensitivity [139] and improves glycaemic control in multiple animal models of diabetes [391-393] and in hypozincaemic type 2 diabetic patients [412, 413].

RNA-seq is a high-throughput sequencing technique used to quantify genome-wide changes to transcript expression. A population of RNA is fragmented and converted into a cDNA library containing adaptors at one or both ends. cDNA is amplified and sequenced to obtain 30-400 bp sequences, which generate high resolution expression profiles for multiple types of coding and noncoding RNA species, including mRNA, microRNA, long noncoding RNA, small nuclear RNA, small nucleolar RNA and Piwi-interacting RNA [414, 415]. Reads are mapped to the respective reference genome to produce a genome-wide transcriptomics map containing the structure and/or level of expression for each part of the genome. For accurate bioinformatic analysis, read counts are normalised to correct for systematic variability including sequence composition bias, differences in read depth and reads mapping to multiple transcripts, such as to gene isoforms [414]. RNA-seq can be used to detail genome annotations at base resolution, allowing genomic variations such as SNPs to be identified with low or non-existent background signals. RNA-seq offers further benefits over alternative expression analysis techniques (hybridization-based microarrays and Sanger sequencing) including increased sensitivity for genes expressed at low and very high levels, the requirement for less sample, novel gene discovery and enabling analysis of alternative splicing and allele-specific expression [414, 415].

A constant supply of zinc is essential to maintain β-cell zinc contents and both disrupted β-cell zinc [416] and hypozincaemia [140, 283, 284, 407] are linked to loss of glycaemic control. We therefore hypothesised that changes to extracellular zinc alter β-cell zinc uptake and accumulation and that subsequent changes to cellular zinc alter the β-cell phenotype. We aimed to characterise MIN6 cells in response to depleted and excess zinc and to identify pathways deregulated by zinc depletion that may help explain the phenotypes observed in hypozincaemic type 2 diabetic patients.

In this study, we stressed MIN6 cells with low, adequate (control) and high concentrations of zinc for 24, 48 and 96 h. We showed that zinc depletion reduces the zinc content of MIN6 cells but upregulates mRNA expression for *Slc39a8* and *Slc39a14* and increases the cellular zinc uptake capacity. Moreover, incubation of MIN6 cells with both depleted and excess zinc lowers cellular proliferation and increases apoptosis at 96 h, associated with reduced activation of MAPK and mTOR cascades. However, we did not record any differences in insulin gene expression or secretion. Finally, we used RNA-seq to explore transcriptomic changes induced by zinc depletion in MIN6 cells and mouse islets. We demonstrated that differentially expressed genes were enriched for phosphatases and that HIF1A regulation may be a key pathway mediated by zinc depletion. Critically, these data demonstrate the hypozincaemia present in some type 2 diabetic patients may lower the zinc content of β-cells to alter intracellular signalling and reduce cellular survival.

5.3. Methods

5.3.1. Cell line and culture

MIN6 cells were cultured as described in **2.1**. For experimentation, standard growth medium was replaced with growth media containing 25mM glucose and 1μM, 8μM or 42μM zinc for 24, 48 or 96 h (section **2.2**).

5.3.2. Cellular zinc parameters

The total cellular zinc content was determined through ICP-MS (section **2.3)**. The kinetics of zinc uptake into MIN6 cells were assessed through ^{65}Zinc uptake assays (section **2.8).**

5.3.3. Gene expression analysis

RNA was extracted from MIN6 cells, reverse transcribed to cDNA and relative expression assayed through qPCR. The full methodology and details of primers used are provided in section **2.6**. All results are presented as fold changes (Log2) in expression.

5.3.4. Cellular proliferation, apoptosis and oxidative stress

MIN6 cell proliferation, apoptosis and oxidative stress were determined as described in sections **2.9-2.11**. To explore signalling via MAPK and mTOR cascades, protein was extracted from cells and phosphorylation of ERK1/2 (MAPK) and RPS6 (mTOR) were determined by immunoblot (section **2.7**), expressed as a ratio to total ERK1/2 or RPS6. Primary antibodies used, with dilutions in 1% BSA/TBST, were ERK1/2 [#9102, Cell Signalling Technologies (1:1,000)], p42/44 ERK1/2 [#4370, Cell Signalling Technologies (1:2,000)], RPS6 [#2217, Cell Signalling Technologies (1:1,000)], Ser235/236 RPS6 [#4858, Cell Signalling Technologies (1:2,000)]. The HRP-linked secondary antibody used, diluted in 1% BSA/TBST, was α-rabbit [Amersham, NA934V (1:15,000)].

5.3.5. Mouse islets

5.3.5.1. Pancreas isolation

Male CD-1 mice were used as pancreatic donors. Mice were sacrificed by cervical dislocation at 12 weeks and pancreases isolated through collagenase digestion [1mg/ml (w/v) clostridium histolyticum, type X1 (Sigma Aldrich) in Modified Eagle's Medium (MEM; Sigma Aldrich)]. Isolated pancreases were heated at 37^{o}C for 10 mins and immediately placed on ice.

5.3.5.2. Islet isolation and purification

Isolated pancreases were washed three times with 25ml MEM containing 10% newborn calf serum, 100μg/ml streptomycin and 100 units/ml penicillin (all Sigma Aldrich; supplemented MEM) through vigorous shaking and centrifugation (1400rpm, 1 min 15, RT). Pancreases were resuspended in supplemented MEM and the islets isolated by passing through a 425mm sieve. The islets were pelleted (1500rpm, 1 min 30, RT), airdried, and resuspended in 15ml histopaque-1077 (Sigma Aldrich). Supplemented MEM (10ml) was added slowly to create two distinct layers, the suspension centrifuged (3510rpm, 24 mins, 10^{o}C), and the islets removed from just below the interface. Islets were washed three times with 50ml supplemented MEM (replacing only the top 25ml MEM each time) through vortex and centrifugation (1500rpm, 1.5 min, RT). Purified islets were placed into non-stick Sterlin® petri-dishes (Thermo Fisher) and removed using a 19G needle.

5.3.5.3. Islet culture

Isolated islets were resuspended in RPMI medium containing 11mM glucose (Thermo Fisher) supplemented with 10% FBS, 4mM L-glutamine, 50μM β-mercaptoethanol, 100μg/ml streptomycin and 100 units/ml penicillin. Media contained total zinc

concentrations of 1µM or 8µM (section **2.3**). Islets were cultured in 60ml Sterlin® petri-dishes at 37^{o}C in a humidified atmosphere of 95% air and 5% CO_2.

5.3.6. Transcriptomic analysis

5.3.6.1. RNA extraction

Total RNA was extracted from MIN6 cells and mouse islets using the RNeasy Mini Kit (Qiagen) with on-column DNase I treatment, according to manufacturer's instructions. Purified RNA was assessed for purity and quantity using a Nanodrop 1000 spectrophotometer and for quality using the RNA 6000 Nano Kit on a Bioanalyzer 2100 (both Agilent Technologies). Agilent Bioanalyzer analysis assigns RIN numbers (estimations of RNA integrity) to indicate RNA quality. The RIN numbers for all samples ranged between 9 and 10, indicating high quality RNA. Electropherograms and corresponding RIN numbers are provided in **Appendix 8**. To proceed onwards with RNA-seq, three biological repeats for MIN6 cells and five biological repeats for islets were chosen. These samples were annotated as follows during Agilent Bioanalyzer analysis: MIN6 cells (1µM zinc, samples 1, 2 and 3; 8µM zinc, samples 1, 3 and 4) and islets (both 1µM and 8µM zinc for samples 1, 2, 4, 7 and 10).

5.3.6.2. RNA-seq

Intact high-quality total RNA (RIN >9; 100ng) was used as input RNA to generate libraries for RNA-seq using the NEBNext Ultra II Directional kit (NEB, Cat.no: E7760S), as per manufacturer's recommendations. This protocol involved an initial step of ribosomal RNA depletion before the remaining RNA is fragmented. The first cDNA strand is then synthesised followed by the second strand, which is barcoded with indices for Illumina sequencing for final library amplification (13-cycles). The resulting libraries (330-380 bp full size) were assessed on a Bioanlyzer 2100 for purity. The NEBNext®

Library Quant Kit for Illumina (E7630L) was used to calculate the quantity of each library. The quantification data were used to pool the libraries in equal molarity prior to performing a QC run on the MiSeq [MiSeq Reagent Kit v3 (150-cycle); Cat no: MS-102-3001]. Further deep sequencing was performed on the pooled library using a HiSeq4000 to generate approximately 65 million reads per sample.

5.3.6.3. Data pre-processing

RNA-seq output data were provided as fastq files as two reads per lane for each sample. Reads were merged to make a composite for each sample. The quality of the sequencing data was assessed using FastQC to assess parameters such as per base sequencing quality and duplication. The adapters were trimmed using the FastQ toolkit on BaseSpace (5' adaptor: CAA GCA GAA GAC GGC ATA CGA T; 3' adapter: GTG ACT GGA GTT CAG ACG TGT GCT CTT CCG ATC T) and aligned using STAR to mm10 (GRCm38.90) to detect novel splice variants and fusion callings. Following alignment, Seqmonk (Babraham) was used to view the mapped data (**Appendices 9-11**). The RNA-seq QC plot showed ~100% reads mapped to genes, ~75% mapped to exons, with some spliced transcripts present, and 0% mapped to ribosomal RNA. The cumulative distribution plot showed there was no contamination of samples with ribosomal RNA or guide DNA, and the data store tree showed predicted grouping of the biological replicates with no obvious technical bias.

5.3.6.4. Differential expression analysis

Aligned data files were uploaded into Qlucore Omics Explorer (version 3.2; Qlucore AB, Lund, Sweden) bioinformatics software. Data were normalised by trimmed mean of M values (TMM) normalisation, which uses a weighted trimmed mean of the log expression ratios to estimate the ratio of RNA production and account for dataset composition bias

[417]. We visualised similarities in gene expression between different samples through generating principal component analysis (PCA) plots. Fold differences (FD) in gene expression were derived for the relevant conditions: MIN6 cells (1µM vs 8µM zinc), islets (1µM vs 8µM zinc) and MIN6 cells and islets (1µM vs 8µM zinc, eliminating the effect of sample origin during statistical analysis). We optimised the gene lists by filtering the variance (σ/σ_{max}) to 0.33. Differential expression was calculated through unpaired t-tests ($\neq$), adjusted for multiple comparison testing, and q-values <0.1 were used to indicate statistically significant differences. The literature was searched for previous associations between differentially expressed genes and zinc, and genes lists were inserted into DisGeNET software (http://www.disgenet.org) [418] to explore previous associations with diabetes.

Since only a limited number of genes were identified as differentially expressed (q <0.01), we used variance-optimised (σ/σ_{max}: 0.57) gene lists that were not corrected for multiple comparison testing (p-values <0.05) for further analysis. This is still a reasonable robust approach as subsequent enrichment analysis entails another layer of statistics. If tested gene lists are random, it is unlikely there will be any statistically significant enrichment or depletion of networks or gene categories. The intersection between comparisons (MIN6 cells: 1µM vs 8µM zinc; islets: 1µM vs 8µM zinc, and MIN6 cells and islets: 1µM vs 8µM zinc; p <0.05) were visualised in Venn diagrams created using GeneVenn software (http://genevenn.sourceforge.net/) [419].

5.3.6.5. Gene enrichment and network analysis

We used GeneGo MetaCore™ bioinformatics software version 6.35 (Thomson Reuters; https://portal.genego.com/) to analyse the gene list for our combined data [MIN6 cells and islets (1µM vs 8µM zinc), p <0.05]. We explored enriched protein functions, enriched

gene ontology (GO) cellular processes and enriched pathways for differentially expressed genes and identified transcription factors overly connected to differentially expressed genes in the dataset. For analysis of enriched protein functions and overly connected transcription factors, we recorded the ratio of hits in the dataset compared to the number expected by chance and the p-values for the significances. For enriched GO cellular processes and pathways, we recorded the number of hits in the dataset compared to the total number of genes associated with the process/pathway, the p-values for the significances and the false discovery rates (FDRs). For the pathway 'negative regulation of HIF1A function', we explored where zinc impacts the pathway through generating a pathway map, which highlights the differentially expressed genes alongside their relative levels of expression.

5.3.6.6. Comparison of RNA-seq and qPCR data

We compared differential expression of genes in MIN6 cells assessed through both RNA-seq and qPCR (data presented in chapters 4 [405] and 5) following 48 h culture with 1µM or 8µM zinc. We collated and compared FD in expression and the significances for differential expression. For RNA-seq data, the p-values presented were not corrected for multiple comparison testing since we were interrogating a specific set of genes in this instance and not looking genome-wide.

5.4. Results

5.4.1. Zinc depletion decreases the zinc content of MIN6 cells

β-cells exhibit exceptionally high turnovers of zinc [266] to maintain normal zinc contents following Zn^{2+}/insulin co-exocytosis. Zinc is delivered to islets through the bloodstream [408], however the amounts of serum zinc available for β-cell uptake is decreased in many type 2 diabetic patients [140, 283, 284]. To explore if changes to extracellular zinc

influence β-cell zinc content, we incubated MIN6 cells with depleted (1μM), adequate (8μM; control) or excess (42μM) zinc for 24, 48 or 96 h.

MIN6 cells cultured with depleted zinc medium exhibited lowered total zinc contents compared to cells cultured with adequate (48 h: 1.26-fold; 96 h: 1.90-fold) or excess zinc (48 h: 1.37-fold; 96 h: 2.01-fold). However, we did not record any differences in total cellular zinc between MIN6 cells cultured with excess zinc or controls (**Fig 5.1A**). To explore changes to cytosolic zinc, we assayed mRNA expression for *Mt1*, *Mt2* and *Mtf1*. Zinc depletion downregulated *Mt1* and *Mt2* compared to controls at 24 h (*Mt1*: 3.46-fold; *Mt2:* 4.02-fold), 48 h (*Mt1*: 5.40-fold; *Mt2:* 6.98-fold) and 96 h (*Mt1*: 1.73-fold; *Mt2:* 2.48-fold), whereas excess zinc upregulated both transcripts at 48 h (*Mt1*: 2.76-fold; *Mt2:* 3.46-fold) and 96 h (*Mt1*: 2.94-fold; *Mt2:* 4.78-fold) (**Fig 5.1B-C**). These results are consistent with a positive correlation between extracellular and cytosolic zinc. However, we did not record any differences in mRNA expression for *Mtf1* following culture of cells with depleted, adequate or excess zinc (**Fig 5.1D**).

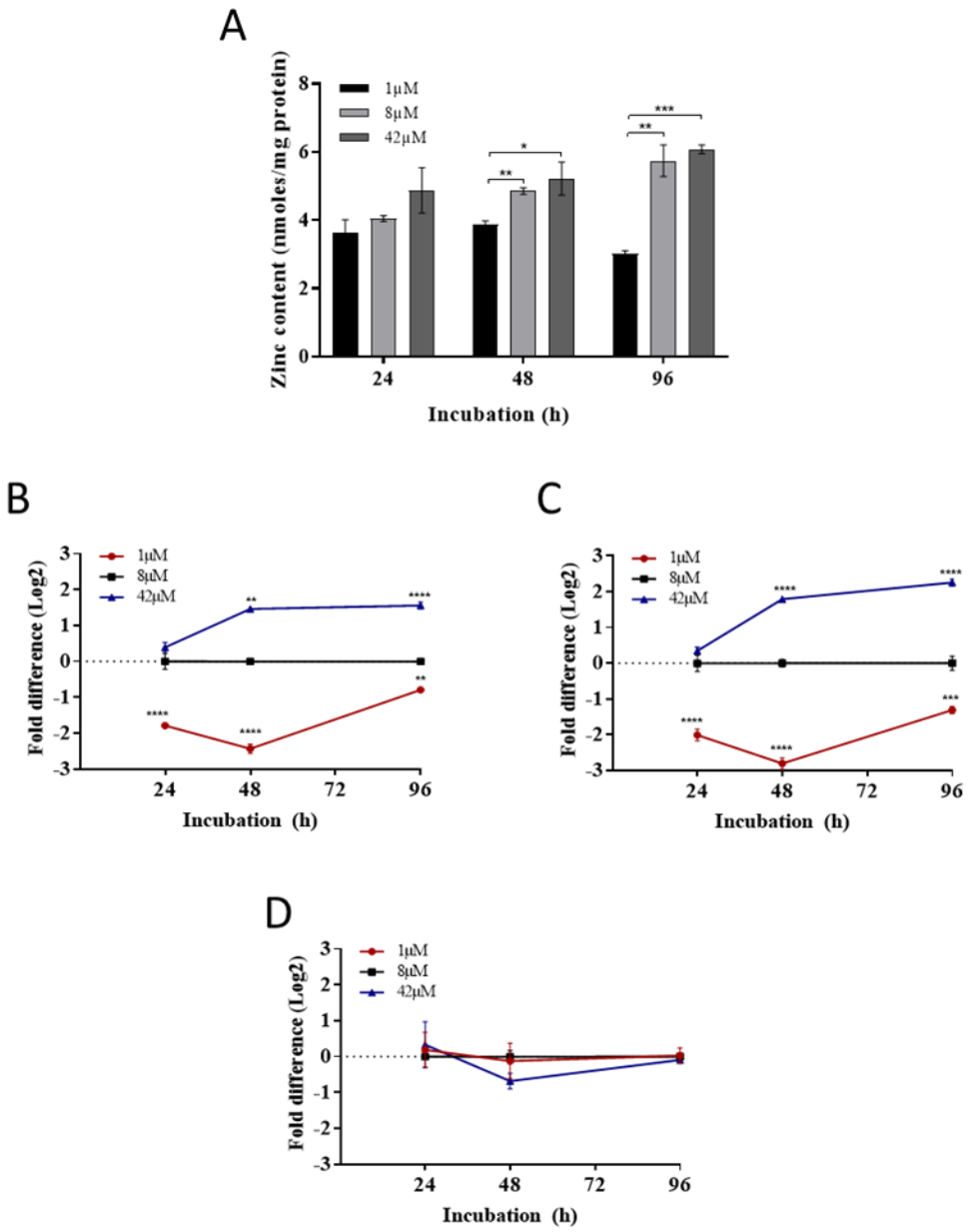

Fig 5.1. Zinc content of MIN6 cells in response to changes in extracellular zinc. (A) Total MIN6 cell zinc content following culture with 1µM, 8µM or 42µM zinc for 24, 48 or 96 h. Total zinc was determined through ICP-MS and normalised to protein. N=4. **(B-D)** mRNA expression for **(B)** *Mt1*, **(C)** *Mt2* and **(D)** *Mtf1* following culture with 1µM, 8µM or 42µM zinc for 24, 48 or 96 h. Changes in mRNA expression were calculated through qPCR and FD (Log_2) in expression presented relative to MIN6 cells cultured with 8µM zinc (control) at each time-point. N=3. All data were analysed by 2-way ANOVA followed by Tukey's multiple comparison test. Error bars show ± SEM. *p <0.05, **p <0.005, ****p <0.0001.

5.4.2. Zinc depletion increases the MIN6 cell zinc uptake capacity

Cytosolic zinc uptake is facilitated by ZIP transporters at the plasma membrane and membranes of intracellular organelles [420, 421]. We and others suggest ZIP1, ZIP6, ZIP7, ZIP8, ZIP9 and ZIP14 [192, 218, 404] are important for zinc trafficking into β-cells. Moreover, the abundance of ZnT8, which functions to transport zinc into insulin secretory granules, is associated with increased cytosolic zinc [201, 278] and is downregulated by stresses that negatively impact β-cell function [179, 186, 227]. To examine the role of the ZIP transporters for maintaining β-cell zinc homeostasis, we characterised zinc influx into MIN6 cells in response to changes in extracellular zinc.

MIN6 cells cultured with zinc depletion exhibited upregulation of mRNA for *Slc39a8* (2.13-fold) and *Slc39a14* (1.60-fold) at 48 h, however only *Slc39a8* remained upregulated (*2*.71-fold) at 96 h compared to controls. Whereas cells cultured with excess zinc downregulated mRNA for *Slc39a8* at both 24 h (1.67-fold) and 96 h (1.78-fold), and upregulated mRNA for *Slc39a6* 1.56-fold at 96 h (**Fig 5.2**). To attribute these changes in mRNA abundance to cytosolic zinc influx, we examined the zinc uptake kinetics for MIN6 cells. We cultured cells in 1μM, 8μM or 42μM zinc for 24, 48 or 96 h and then assayed ^{65}Zn uptake over a range of concentrations. Following pre-treatment with zinc depletion, we observed higher zinc influx into MIN6 cells at the highest two ^{65}Zn concentrations tested (23.85μM and 14.30μM) at 48 h compared to cells pre-treated with adequate zinc. Although not statistically significant, a similar trend was observed at both 24 and 96 h (**Fig 5.3**). However, these observations did not translate into significant differences for either J_{max} or $K_{0.5}$.

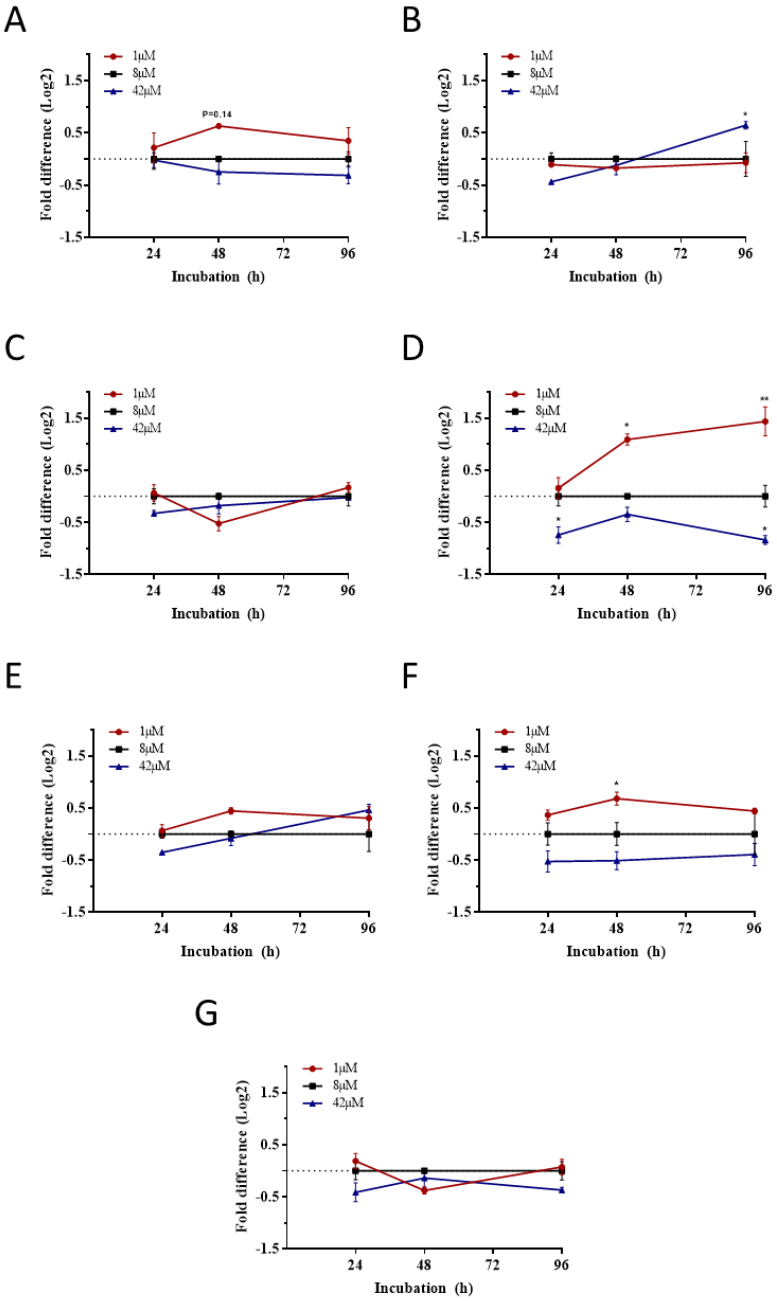

Fig 5.2. Abundances of *Slc39a* and *Slc30a8* mRNA in MIN6 cells in response to changes in extracellular zinc. Expression of **(A)** *Slc39a1*, **(B)** *Slc39a6*, **(C)** *Slc39a7*, **(D)** *Slc39a8*, **(E)** *Slc39a9*, **(F)** *Slc39a14*, and **(G)** *Slc30a8*. Experiments were carried out following culture with 1μM, 8μM or 42μM zinc for 24, 48 or 96 h. Expression was determined through qPCR and expressed as FD (Log_2) in expression relative to control cells (8μM zinc) at each time-point. Data were analysed by 2-way ANOVA followed by Tukey's multiple comparison test. N=3. Error bars show ± SEM. *p <0.05, **p <0.005.

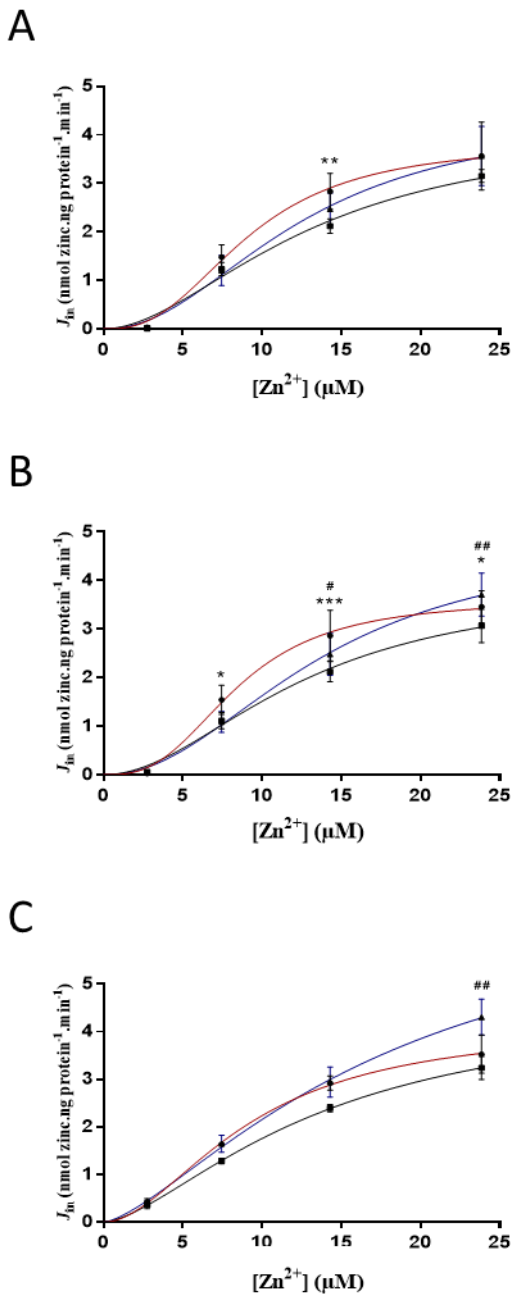

Fig 5.3. Kinetics of zinc uptake into MIN6 cells in response to changes in extracellular zinc. Uptake kinetics of ^{65}Zn into MIN6 cells following pre-treatment with 1µM, 8µM or 42µM zinc for **(A)** 24, **(B)** 48 or **(C)** 96 h. The rates of zinc uptake were assessed through ^{65}Zn uptake assays. N=3. Red: 1µM zinc, black: 8µM zinc, blue: 42µM zinc. Data were analysed by 2-way ANOVA followed by Tukey's multiple comparison test. Error bars show ± SEM. For 1µM vs 8µM zinc: *p <0.05**,** **p <0.005, ***p <0.001. For 42µM vs 8µM zinc: $^{\#}$p <0.05**,** $^{\#\#}$p <0.005.

5.4.3. Zinc depletion and excess decrease MIN6 cell survival

Adequate zinc is essential for cellular survival and growth. Zinc promotes survival through mediating numerous signalling pathways as a protein-binding and signalling component, with roles described in AKT [59], JAK/STAT [317], MAPK (including ERK1/2 [314], c-JNK and p38 [310]) and mTORC1 [313] signalling cascades. However, excess zinc decreases viability of human islets and mouse MIN6N8 cells [374]. We therefore examined whether changes to MIN6 cell zinc impact cellular viability.

MIN6 cells cultured in medium containing either depleted (1µM) or excess (42µM) zinc for 96 h exhibited decreased proliferation (1µM: 1.25-fold; 42µM: 1.35-fold) compared to controls. We further observed increased apoptosis (1.37-fold) for cells cultured with depleted zinc and increased amounts of oxidative stress (1.78-fold), as measured by the abundance of oxidizing metabolites that are increased by oxidant stress [422, 423], for cells cultured with excess zinc (**Fig 5.4A-C**). To explore if zinc may signal via MAPK or mTOR cascades to drive these changes to MIN6 cell viability, we examined phosphorylation of the downstream effectors ERK1/2 (MAPK cascades) and RPS6 (mTOR cascades), which are both activated by phosphorylation. Diagrams illustrating how ERK1/2 and RPS6 phosphorylation relate to cellular survival are provided in **Fig 5.5**. We examined phosphorylation at both 48 and 96 h since these changes may occur at an earlier time-point to drive the changes in proliferation and apoptosis. At 96 h, we observed decreased phosphorylation for both RPS6 and ERK1/2 in MIN6 cells cultured with either depleted (RPS6: 1.43-fold; ERK1/2: 1.79-fold) or excess (RPS6: 1.55-fold; ERK1/2: 1.35-fold) zinc compared to controls (**Fig 5.4D-E**). We did not record any differences in proliferation, apoptosis, oxidative stress or signalling via MAPK or mTOR cascades between MIN6 cells cultured with deficient, adequate or excess zinc for 48 h (data provided in appendix 14).

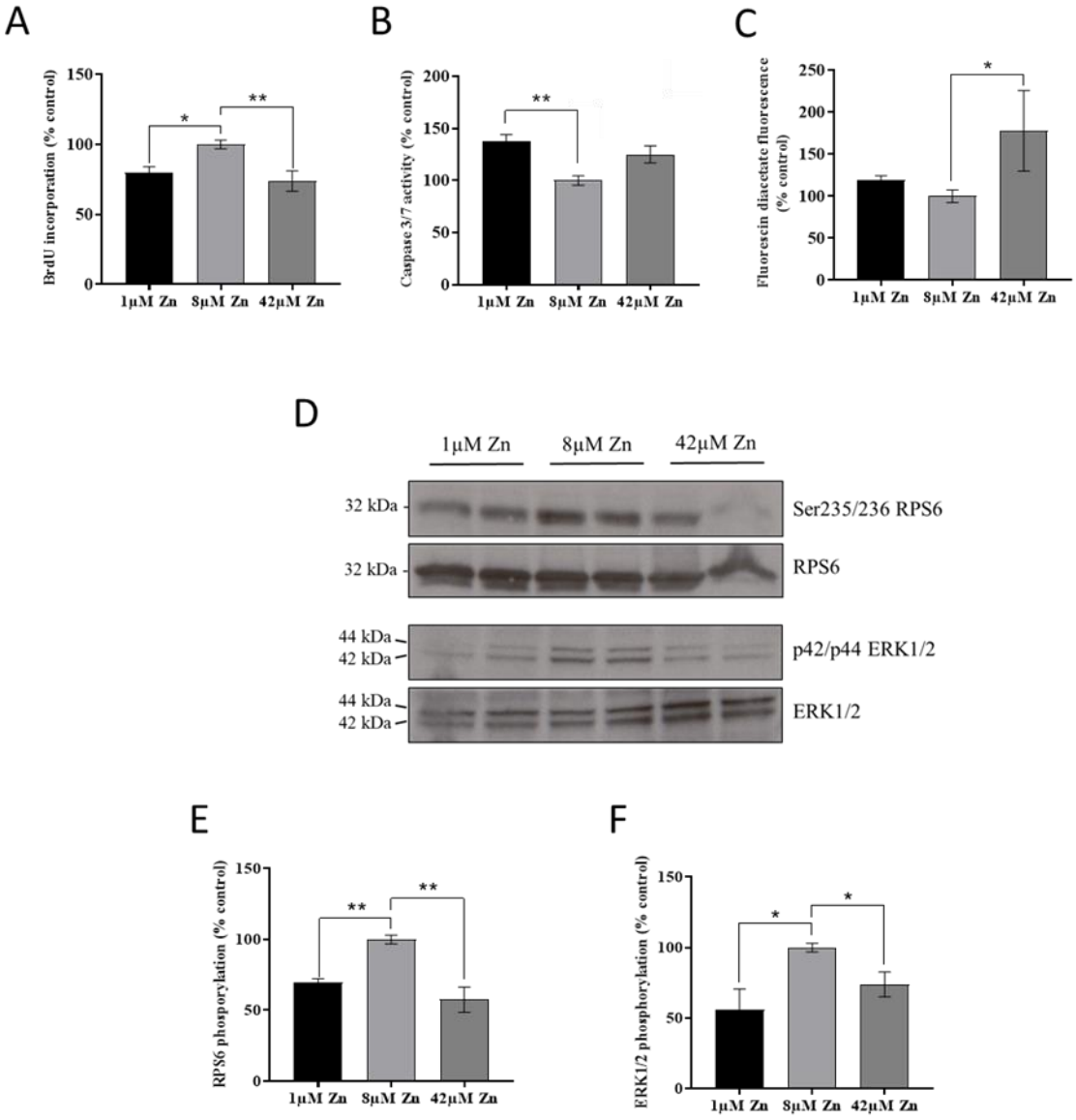

Fig 5.4. Survival of MIN6 cells in response to changes in extracellular zinc. (A) MIN6 cell proliferation, calculated by BrdU incorporation. **(B)** MIN6 cell apoptosis, measured by Caspase 3/7 assays. **(C)** MIN6 cell oxidative stress, measured by dihydrofluorescin diacetate fluorescence. **(D-F)** Phosphorylation of RPS6 and ERK1/2. **(D)** Immunoblots for Ser235/236 RPS6, RPS6, p42/p44 ERK1/2 and ERK1/2. **(E-F)** Quantification of immunoblots for **(E)** Ser235/236 RPS6 vs RPS6 and **(F)** p42/p44 ERK1/2 vs ERK1/2. Immunoblot quantification was carried out using ImageJ software. All experiments were carried out following culture of MIN6 cells with 1μM, 8μM or 42μM zinc for 96 h. Results are relative to MIN6 cells in 8μM zinc (control). Data were analysed by 2-way

ANOVA followed by Tukey's multiple comparison test. Error bars show ± SEM. N=3-5. *p <0.05**,** **p <0.005.

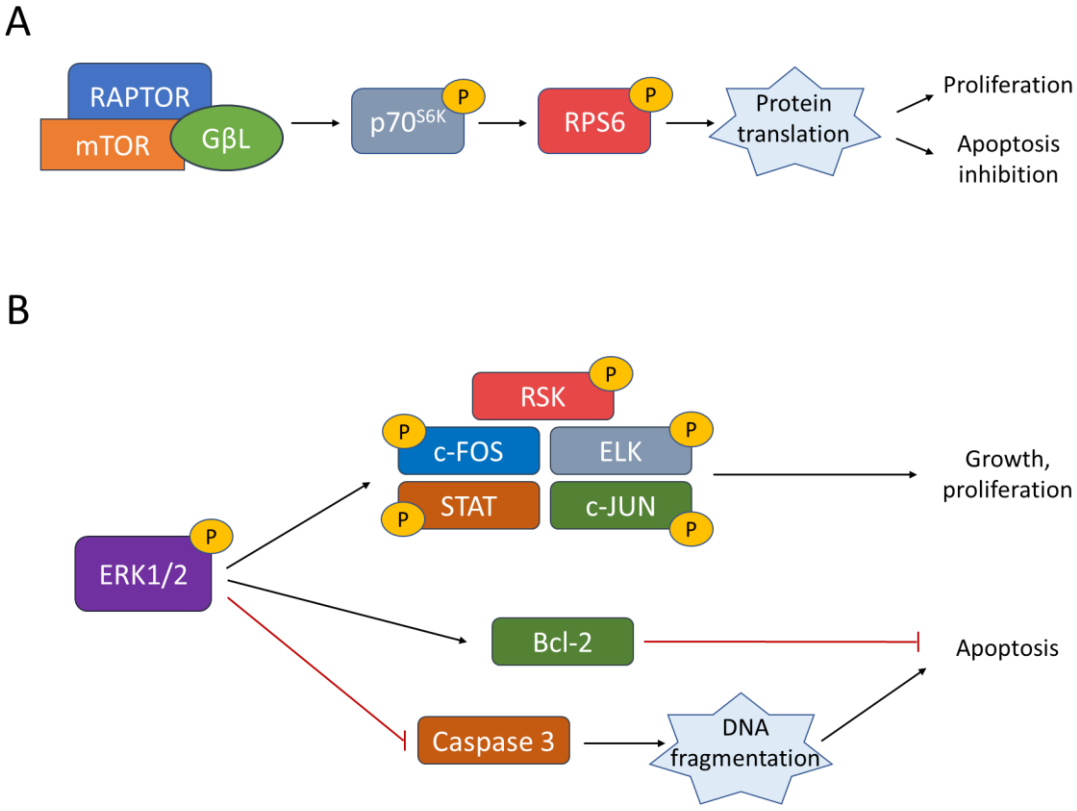

Fig 5.5. RPS6, ERK1/2 and cellular survival. (A) mTOR (mTORC1) activates $p70^{S6K}$, which phosphorylates and activates RPS6. Phosphorylated RPS6 activates protein translation to drive proliferation and inhibit apoptosis. **(B)** Phosphorylated ERK1/2 promotes cellular growth and proliferation through phosphorylating and activating RSK, c-FOS, ELK, STAT and c-JUN. Phosphorylated ERK1/2 inhibits apoptosis through activating Bcl-2 and suppressing Caspase 3, which induces DNA fragmentation. (P) = the protein is phosphorylated.

5.4.4. Zinc does not affect MIN6 cell insulin expression or secretion

β-cells function to mount adequate insulin secretory responses to glucose to maintain glycaemic control. Disruption of insulin gene regulation and insulin secretion is characteristic of β-cell dysfunction and represents a hallmark of β-cell failure during diabetes. Zinc is reported to promote both stimulatory [219, 329] and inhibitory [424] effects on β-cell insulin secretion. We therefore explored expression of insulin, of which two paralogues exist in rodent, in MIN6 cells and insulin secretion from MIN6 cells in response to changes in extracellular zinc. We did not observe any differences in mRNA abundances for *Ins1* or *Ins2* in cells cultured with depleted or excess zinc compared to controls. Moreover, we did not record any differences in basal or KCl-stimulated insulin release from MIN6 cells grown in either 1, 8 or 42μM zinc for 24, 48 or 96 h. Data for 96 h are presented in **Fig 5.6**. Data for 24 and 48 h are provided in appendix 15.

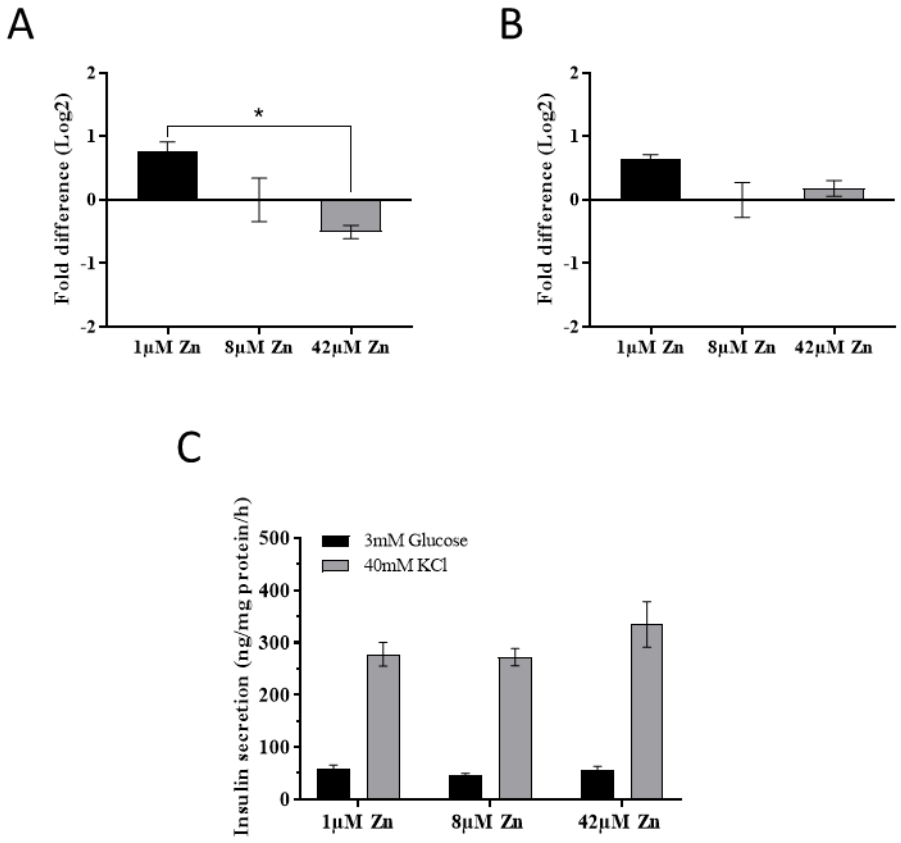

Fig 5.6. MIN6 cell insulin gene expression and insulin secretion in response to changes in extracellular zinc. (A-B) Abundance of **(A)** *Ins1* or **(B)** *Ins2* mRNA expression following culture with 1µM, 8µM or 42µM zinc for 96 h. Expression was assayed through qPCR and calculated as FD (Log2) relative to MIN6 cells cultured with 8µM zinc (control). **(C)** Insulin secretion from MIN6 cells in response to 3mM glucose (basal) or 40mM KCl (stimulated) following culture with 1µM, 8µM or 42µM zinc for 96 h. The amounts of secreted insulin were calculated through insulin secretion assays and normalised to total protein. Data were analysed by 2-way ANOVA followed by Tukey's multiple comparison test. Error bars show ± SEM. N=3.

5.4.5. Zinc and the β-cell transcriptome

In chapter 4 [405], we showed that multiple important β-cell markers are Zn^{2+}-responsive. Zinc binds ~3000 proteins in mammals [129] that are involved in diverse arrays of cellular processes [130, 301]. However, this does not mean that Zn^{2+}-responsive genes encode zinc(II)-binding proteins since regulation may be secondary to the cellular phenotype induced by zinc depletion. To avoid restricting investigation to pre-defined gene lists, we sought to explore the full set of processes to which zinc deficiency causes alterations in β-cells through transcriptomic analysis. We carried out RNA-seq on MIN6 cells and mouse islets following culture with depleted (1μM) or adequate (8μM) zinc for 48 h. Mouse islets were included in this study to increase the confidence of applying results from monolayer MIN6 cells to a physiological system, whilst being mindful that rodent islets do not only comprise of β-cells but also contain 20-40% other islet cell types [425]. The data produced during this analysis should generate a comprehensive view of zinc-induced β-cell dysfunction and may lead to discovery of novel Zn^{2+}-responsive genes and pathways.

5.4.5.1. Examination of RNA-seq data

PCA is used to reduce complex data so that variations and patterns can be readily visualised [426]. High-dimensional multivariate data are transformed into a small set of orthogonal variables that capture most of the dataset variation whilst maintaining as much information as possible [427, 428]. We generated PCA plots to visualise the similarities between each of MIN6 cells and islets following culture with 1μM or 8μM zinc (**Fig 5.7**). We observed high similarities between all MIN6 cell replicates cultured with 8μM zinc. However, only two of the three replicates cultured with 1μM zinc grouped together, and large variation, primarily in the second principal component, was observed between these and the third. Since we only obtained three replicates, we were unable to exclude the

outlier from analysis, despite this sample probably occluding identification of differential expression. For islets, the replicates did not group by treatment (1µM or 8µM zinc), indicating there was limited overall variation in gene expression in response to zinc depletion.

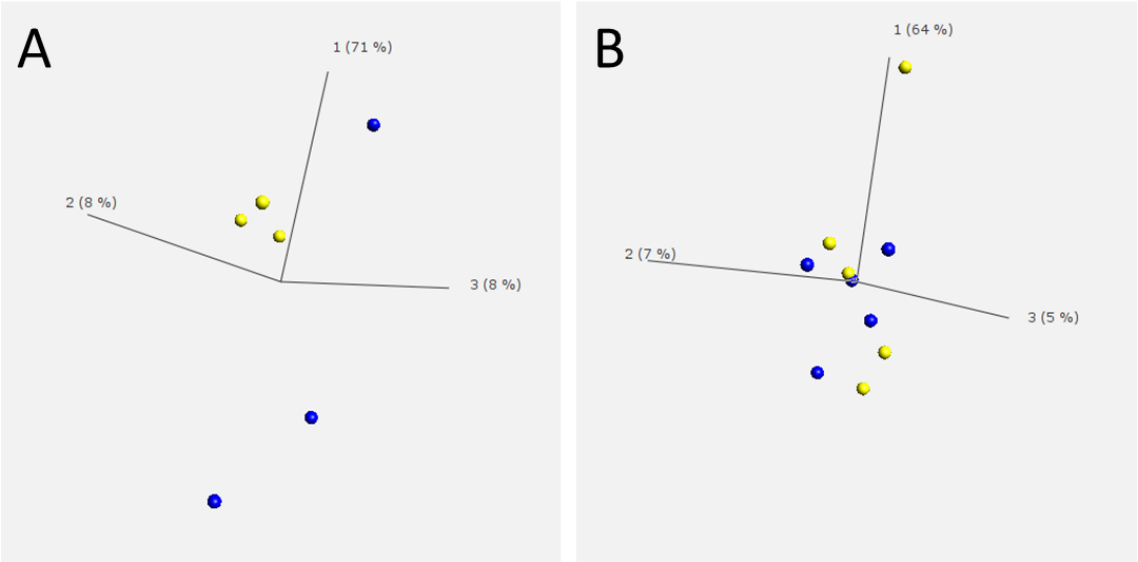

Fig 5.7. PCA plots for MIN6 cells and islets cultured with 1µM or 8µM zinc. Variation of expression for all genes in **(A)** MIN6 cells or **(B)** Islets following culture with 1µM (blue) or 8µM (yellow) zinc for 48 h. The PCA plots were created using Qlucore Omics Explorer (v3.4).

5.4.5.2. Differential gene expression

To identify genes differentially expressed in MIN6 cells and islets following culture with 1µM or 8µM zinc, we performed the following comparisons using Qlucore Omics Explorer (v3.4):

(1) MIN6 cells: 1µM vs 8µM zinc.

(2) Islets: 1µM vs 8µM zinc.

(3) MIN6 cells and islets: 1µM vs 8µM zinc (eliminating the effect of sample origin).

We filtered gene lists by variance (σ/σ_{max}: 0.33) and the significances of differential expression were corrected for multiple comparison testing (q-values). However, when using q <0.1 to indicate differential expression, we only identified 21 differentially expressed genes (all downregulated by zinc depletion) for MIN6 cells (1µM vs 8µM zinc; comparison 1) and 7 differentially expressed genes (3 upregulated and 4 downregulated by zinc depletion) for islets (1µM vs 8µM zinc; comparison 2). These genes are listed in **Tables 5.1** and **5.2**, alongside any known associations with zinc.

Genes downregulated in MIN6 cells by zinc depletion included genes involved in signal transduction (*Tenm2*), pH regulation and cellular signalling (*Otop3*), mitochondrial regulation (*Nlrx1*), RTK signalling (*Plch2*), protein degradation (*Prss27* and *Psmb11*), steroid synthesis (*Hsd17b11*), tethering (*Ubxn10*), cellular adhesion (*Lrrn4*), development (*Edaradd*) and gene expression regulation (*Ercc5*, *Zfg334*, *Zbtb44*). Six of the identified genes encode proteins that either bind zinc or are involved in zinc-mediated pathways and, therefore, adequate amounts of zinc are essential for their normal function. ZFP334 and ZBTB44 are zinc-finger transcription factors that require zinc for DNA binding [429], ERCC5 mediates DNA repair with the zinc(II)-binding metalloprotein XPA [430, 431] and SEC23B requires zinc binding to couple with SEC23A and form a GTPase activating protein (GAP) in the membranes of coat complex II-coated vesicles [432]. Moreover, PXN binds zinc to function as a docking site at focal adhesions for cytoskeletal proteins, kinases, GAPs and other adaptor proteins [433] and is suppressed

by ZIP6:ZIP10 heteromers [206], and OTOP3 forms a proton-selective ion channel required for zinc-sensitive proton conductance [434].

For islets, differentially expressed genes included genes involved in cell cycle regulation (*Cep126* was upregulated and *Spc24* was downregulated following zinc depletion). We additionally noted downregulation of genes involved in metabolic breakdown (*Uox*) and RNA transcription (*Mov1011*) and upregulation of two components of metal ion channels (*Kcnn3* and *Lrriq4*), suggesting zinc may control cellular metal ion distributions via transporter regulation. We did not identify any previously documented associations between any of these differentially expressed genes and zinc.

We additionally explored associations between the Zn^{2+}-responsive genes identified in MIN6 cells and islets with diabetes. We noted that *Uox* (downregulated in islets in response to zinc depletion) is associated with both obesity in diabetic patients [435] and metabolic disturbances [436], which are characteristic of diabetes. However, we did not identify any previously documented associations with diabetes for any other differentially expressed genes.

Table 5.1. Genes differentially expressed in MIN6 cells in response to zinc depletion. Gene lists were identified through RNA-seq analysis following culture of MIN6 cells with 1μM or 8μM zinc for 48 h. Gene lists were filtered by variance (σ/σ_{max}: 0.33) and genes were considered differentially expressed when q <0.01. # = no known associations with zinc.

Gene symbol	Gene name	q-value	Fold change	Previous associations with zinc
Zfp334	Zinc finger protein 334	1.52E-03	-4.302	Zinc binding protein [429]
Ercc5	Excision Repair 5, Endonuclease	1.52E-03	-4.302	Involved in zinc finger-regulated DNA repair pathways [437]
Plch2	Phospholipase C Eta 2	1.52E-03	-4.302	#
Hsd17b11	Hydroxysteroid 17-Beta Dehydrogenase 11	1.52E-03	-4.302	#
Nlrx1	NLR Family Member X1	1.52E-03	-4.302	#
Ubxn10	UBX Domain Protein 10	1.52E-03	-4.302	#
Tenm2	Teneurin Transmembrane Protein 2	1.52E-03	-4.302	#
Prss27	Serine protease 27	1.52E-03	-4.303	#
Psmb11	Proteasome Subunit Beta 11	1.52E-03	-4.303	#
Gm7847	Non-protein coding	1.52E-03	-4.303	#

AC154592.1	Non-protein coding	1.52E-03	-4.302	#
Sec23b	Sec23 Homolog B, Coat Complex II Component	1.63E-02	-4.813	Zinc binding protein [438]
Pxn	Paxillin	1.63E-02	-4.813	Zinc binding protein [134] Suppressed by ZIP6:ZIP10 heteromers at focal adhesions [206]
Lrrn4	Leucine Rich Repeat Neuronal 4	1.63E-02	-4.813	#
Gm12808	Non-protein coding	1.63E-02	-4.813	#
Zbtb44	Zinc Finger and BTB Domain Containing 44	2.73E-02	-6.205	Zinc binding protein [429]
Edaradd	EDAR Associated Death Domain	4.67E-02	-5.101	#
Gm43121	Non-protein coding	4.67E-02	-5.101	#
Gm19219	Non-protein coding	4.67E-02	-5.101	#
4930597O21Rik	RIKEN cDNA 4930597O21	6.48E-02	-6.634	#
Otop3	Otopetrin 3	8.98E-02	-5.707	Zinc binding protein [439]

Table 5.2. Genes differentially expressed in islets in response to zinc depletion. Gene lists were identified through RNA-seq analysis following culture of mouse islets with 1µM or 8µM zinc for 48 h. Gene lists were filtered by variance (σ/σmax: 0.33) and genes were considered differentially expressed when q <0.01. # = no known associations with zinc.

Gene Symbol	Gene name	q-value	Fold change	Previous associations with zinc
Kcnn3	Potassium Calcium-Activated Channel Subfamily N Member 3	8.67E-02	3.601	#
Mov10l1	Mov10 RISC Complex RNA Helicase Like 1	8.67E-02	-3.976	#
Lrriq4	Leucine Rich Repeats and IQ Motif Containing 4	8.67E-02	3.406	#
Uox	Urate Oxidase	8.67E-02	-3.976	#
Cep126	Centrosomal Protein 126	8.67E-02	3.988	#
Spc24	Kinetochore Protein Spc24	8.67E-02	-3.976	#
Gm17112	Non-protein coding	8.67E-02	-3.590	#

We next sought to compare zinc depletion-induced differential gene expression ($q < 0.1$) between MIN6 cells and islets. However, we did not highlight any commonly regulated genes. Above (section **5.4.5.1**), we show that large variation existed between MIN6 cell replicates (1µM zinc) but that there was not much variation between the islet replicates (1µM and 8µM zinc); using $q < 0.1$ to indicate differential expression may be too stringent to identify potentially important results. We therefore used $p < 0.05$ (not corrected for multiple comparison testing) to indicate differential expression in gene lists for use in subsequent data analysis. Accordingly, the following results should be taken with caution due to the relatively high possibility they may have occurred by chance.

We identified 1439 differentially expressed genes (1059 upregulated and 380 downregulated; $p < 0.05$) between MIN6 cells cultured with 1µM or 8µM zinc (comparison 1). Whereas between islets cultured with 1µM or 8µM zinc (comparison 2), we revealed differential expression for 826 genes (396 upregulated and 430 downregulated; $p < 0.05$). When the effect of sample type was eliminated (MIN6 cells and islets cultured with 1µM or 8µM zinc; comparison 3), we uncovered differential expression for 715 genes (439 upregulated and 276 downregulated; $p < 0.05$) (**Fig 5.8**). We noted that a total of 60 genes were commonly regulated between MIN6 cells and islets (28 upregulated and 32 downregulated); these genes are listed in **Appendices 12-13**.

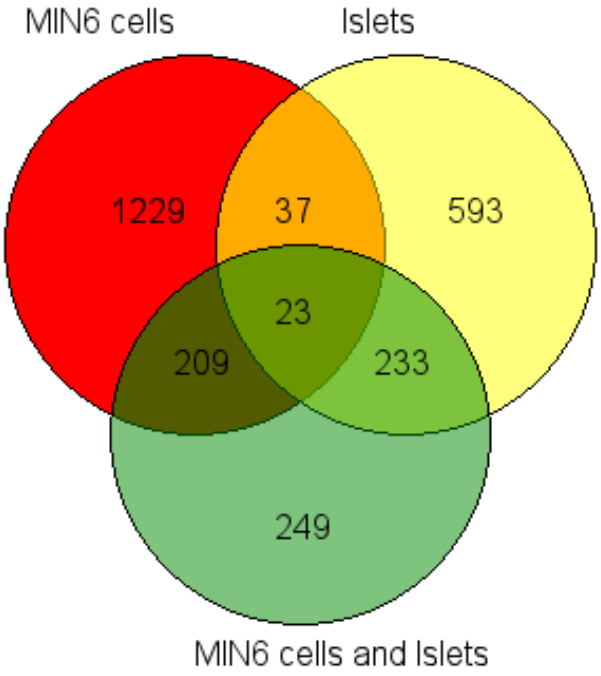

Fig 5.8. Gene differentially expressed in response to zinc depletion (p <0.05). Venn diagram showing differential gene expression in MIN6 cells (comparison 1), islets (comparison 2) and MIN6 cells and islets (eliminating the effects of sample origin; comparison 3) following culture of cells with 1µM or 8µM zinc. Gene lists were filtered by variance (σ/σ_{max}: 0.57). The numbers of genes showing differential expression (p <0.05) are indicated. Created using GeneVenn software [419].

5.4.6. Enrichment and pathway analysis

GeneGo MetaCore^{TM} bioinformatics software allows for analysis of a given list of genes based on relative changes in gene expression. Enrichment analysis consists of matching genes to functional ontologies to identify protein functions, processes and pathways (amongst others) over- or underrepresented in the dataset. Since we did not record adequate numbers of differentially expressed genes (q <0.1) for investigation, we focused

analysis on gene lists created using p <0.05. This approach is reasonable when the data is subjected to an additional level of robust statistical analysis. To increase the power of this analysis by including a greater number of replicates, we decided to analyse data derived from both MIN6 cells and islets (eliminating the effect of sample origin) cultured with 1µM or 8µM zinc (comparison 3). We generated PCA plots to confirm that, based on differential expression (p <0.05), samples grouped by treatment (1µM or 8µM zinc) and, therefore, similar processes and/or pathways may be altered in each MIN6 cells and islets by zinc depletion (**Fig 5.9**).

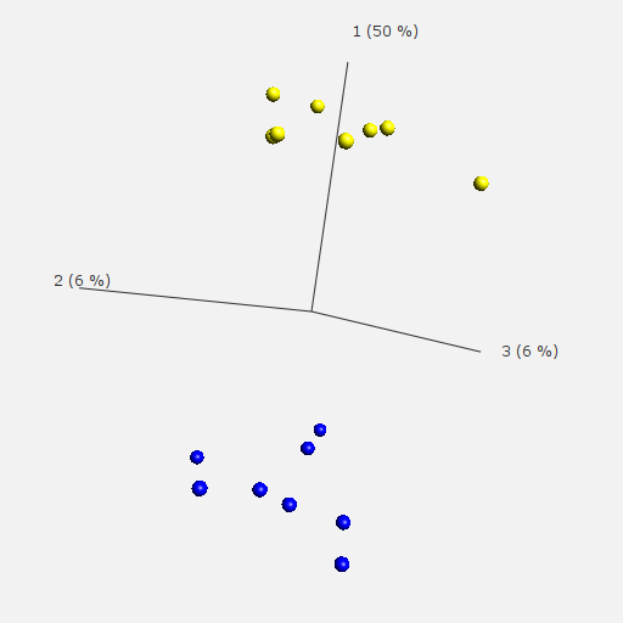

Fig 5.9. PCA plot for differential gene expression in MIN6 cells and islets (p <0.05). Variation of gene expression in MIN6 cells and islets (eliminating the effect of sample origin) following culture with 1µM (blue) or 8µM (yellow) zinc (comparison 3). Gene lists were filtered by variance (σ/σ_{max}: 0.57). The PCA plots were created using Qlucore Omics Explorer (v3.4).

5.4.6.1. Identification of enriched protein functions

We first sought to investigate protein functions either enriched or depleted for differentially expressed genes (**Table 5.3**). These functions correspond to a higher or lower fraction of genes in the gene list than is expected in the global genome. We noted enrichment for enzymes (ratio: 1.353) and phosphatases (ratio: 1.943) and depletion for proteins classed as 'other' (ratio: 0.9398).

Table 5.3. Protein functions enriched or depleted for genes differentially expressed (p <0.05) in response to zinc depletion. Enrichment and depletion for MIN6 cells and islets cultured with 1µM or 8µM zinc. For each protein function, the number of actual and expected mapped genes are listed, alongside the p-value for the significance.

Protein function	Actual/Expected	p-value
Enzymes	107/79.1	6.90E-04
Other	464/493.7	7.89E-03
Phosphatases	13/6.7	1.75E-02
Transcription factors	26/32.6	1.33E-01
Kinases	23/19.2	2.12E-01
Receptors	43/45.2	4.01E-01
Ligands	14/14.4	5.27E-01
Proteases	17/17.2	5.47E-01

5.4.6.2. Identification of enriched GO cellular processes

We next identified GO cellular processes enriched for differentially expressed genes (**Table 5.4**). Hits indicate that a higher fraction of genes in the gene lists are involved in

the respective process than is expected in the global genome. Top hits included enrichment of genes involved in the response to oxygen-containing compounds (hits: 140/2780), negative regulation of phosphorus metabolic processes (hits: 61/901), organophosphate metabolic processes (hits: 79/1311), regulation of protein kinase (hits: 70/1110) and transferase (hits: 86/1490) activities, and the cellular response to stress (hits: 120/2342).

Table 5.4. GO cellular processes enriched for genes differentially expressed in response to zinc depletion (p <0.05). Enrichment for MIN6 cells and islets cultured with 1µM or 8µM zinc. For each GO cellular process, the number of hits in the dataset compared to the total number encoded in the genome, the p-value for the significance and FDR are presented.

GO Process	Hits	p-value	FDR
Response to oxygen-containing compound	140/2780	1.132E-09	8.676E-06
Negative regulation of phosphorus metabolic process	61/901	5.562E-09	1.103E-05
Organophosphate metabolic process	79/1311	5.751E-09	1.103E-05
Regulation of protein kinase activity	70/1110	7.474E-09	1.103E-05
Regulation of transferase activity	86/1490	8.607E-09	1.103E-05
Cellular response to stress	120/2342	8.638E-09	1.103E-05
Regulation of purine nucleotide metabolic process	35/385	1.034E-08	1.132E-05
Negative regulation of phosphate metabolic process	60/900	1.310E-08	1.183E-05
Nervous system development	160/3438	1.536E-08	1.183E-05
Regulation of nucleotide metabolic process	35/393	1.745E-08	1.183E-05

5.4.6.3. Identification of overly connected transcription factors

We further identified transcription factors overly connected to differentially expressed genes (**Table 5.5**). These transcription factors regulate a greater or lower fraction of genes in the gene list than is expected in the global genome and may therefore represent potential hubs for driving changes to β-cell function. We noted 13 overly connected transcription factors, which are involved in cell cycle regulation, proliferation, survival and growth [p53 (ratio: 1.58), c-Myc (ratio: 1.36), CUX1 (ratio: 1.69) and RelA (ratio: 1.47)], cellular responses to hormone stimulation [CREB1 (ratio: 1.34)] and hypoxia [HIF1A (ratio: 1.63)], and fatty acid storage and glucose metabolism [PPAR-γ (ratio: 1.97)]. Of the listed transcription factors, only HIF1A showed differential expression in MIN6 cells and islets (eliminating the effect of sample origin, comparison 3; $p < 0.05$) following culture with depleted or adequate zinc.

Table 5.5. Transcription factors overly connected to genes differentially expressed in response to zinc depletion (p <0.05). Data for MIN6 cells and islets cultured with 1µM or 8µM zinc. For each transcription factor, the ratio of actual and expected connection hits are listed, alongside the p-value for the significance.

Transcription factor	Actual/Expected	p-value
CREB1	213/158.9	1.04E-06
p53	102/64.7	2.51E-06
CUX1 (p110)	66/39.1	2.38E-05
PPAR-γ	40/20.3	4.19E-05
DPF2	9/1.9	1.22E-04
TIF1-β	80/52.9	1.38E-04
c-Myc	126/92.5	1.63E-04
RelA (p65 NF-kB subunit)	86/58.5	1.94E-04
YY1	116/84.7	2.54E-04
RXRA	24/11	3.24E-04
HIF1A	52/31.9	3.98E-04
ZNF131	5/0.7	5.25E-04
p63	37/21	6.97E-04

5.4.6.4. Identification of enriched pathways

Finally, we identified intracellular pathways enriched for differentially expressed genes (**Table 5.6**). These pathways include a higher fraction of genes in the gene list than is expected in the global genome. Top hits included possible regulation of the HSF-1/chaperone pathway (hits: 7/21), negative regulation of HIF1A function (hits: 9/69) and anti-apoptotic TNFs/NF-kB/Bcl-2 pathways (hits: 6/42).

Table 5.6. Pathways enriched for genes differentially expressed in response to zinc depletion (p <0.05). Enrichment for MIN6 cells and islets cultured with 1µM or 8µM zinc. For each pathway, the number of gene hits in the dataset compared to total number of genes in the pathway, the p-value for the significance and FDR are presented.

Pathway	Hits	p-value	FDR
Possible regulation of HSF-1/chaperone pathway in Huntington's disease	7/21	2.961E-07	3.251E-04
Rheumatoid arthritis (general schema)	8/50	1.754E-05	9.630E-03
Transcription: negative regulation of HIF1A function	9/69	2.874E-05	1.052E-02
Regulation of Tissue factor signalling in cancer	7/43	5.300E-05	1.209E-02
Colorectal cancer (general schema)	6/30	5.504E-05	1.209E-02
Stellate cells activation and liver fibrosis	8/70	2.067E-04	3.782E-02
Apoptosis and survival: Anti-apoptotic TNFs/NF-kB/Bcl-2 pathway	6/42	3.851E-04	6.040E-02
Macrophage and dendritic cell phenotype shift in cancer	9/100	5.162E-04	6.585E-02
Inhibition of Ephrin receptors in colorectal cancer	5/30	5.756E-04	6.585E-02
FGF signalling in pancreatic cancer	6/46	6.363E-04	6.585E-02

5.4.6.5. Regulation of HIF1A

HIF1A mediates a vast array of cellular processes including apoptosis [440], angiogenesis [441] and the adaptive response to hypoxia [442]. HIF1A is stabilised by inflammation [443], growth factors [444] and increased levels of ROS [445], and is regulated by insulin via PI3K/AKT cascades [446]. HIF1A is mediated by the Zn^{2+}-responsive transcription factor MTF1 during hypoxic stress [447] and facilitates hypoxia-induced MT activation [165]. Targeted knockout of HIF1A in the β-cells of C57BL/6 mice induces glucose

intolerance, impairs GSIS and contributes to onset of Type 2 Diabetes [448]. Moreover, we identified above that HIF1A is overly connected to genes differentially expressed in response to zinc depletion (section **5.4.6.3**). To explore how zinc may impact pathways mediating HIF1A expression and/or activity, we generated a pathway map for HIF1A regulation to reveal the locations of Zn^{2+}-responsive genes in HIF1A regulatory pathways and their relative changes in expression (**Fig 5.10**). We demonstrate these Zn^{2+}-responsive genes encode proteins involved in oxygen-dependent HIF1A regulation (EGLIN2, OS-9, SIRTUIN2 and ARD1), HIF1A transcription (RUVBL2), activation of HIF1A via protein folding (HSP70 and HSP90) and cell cycle regulation (PTEN).

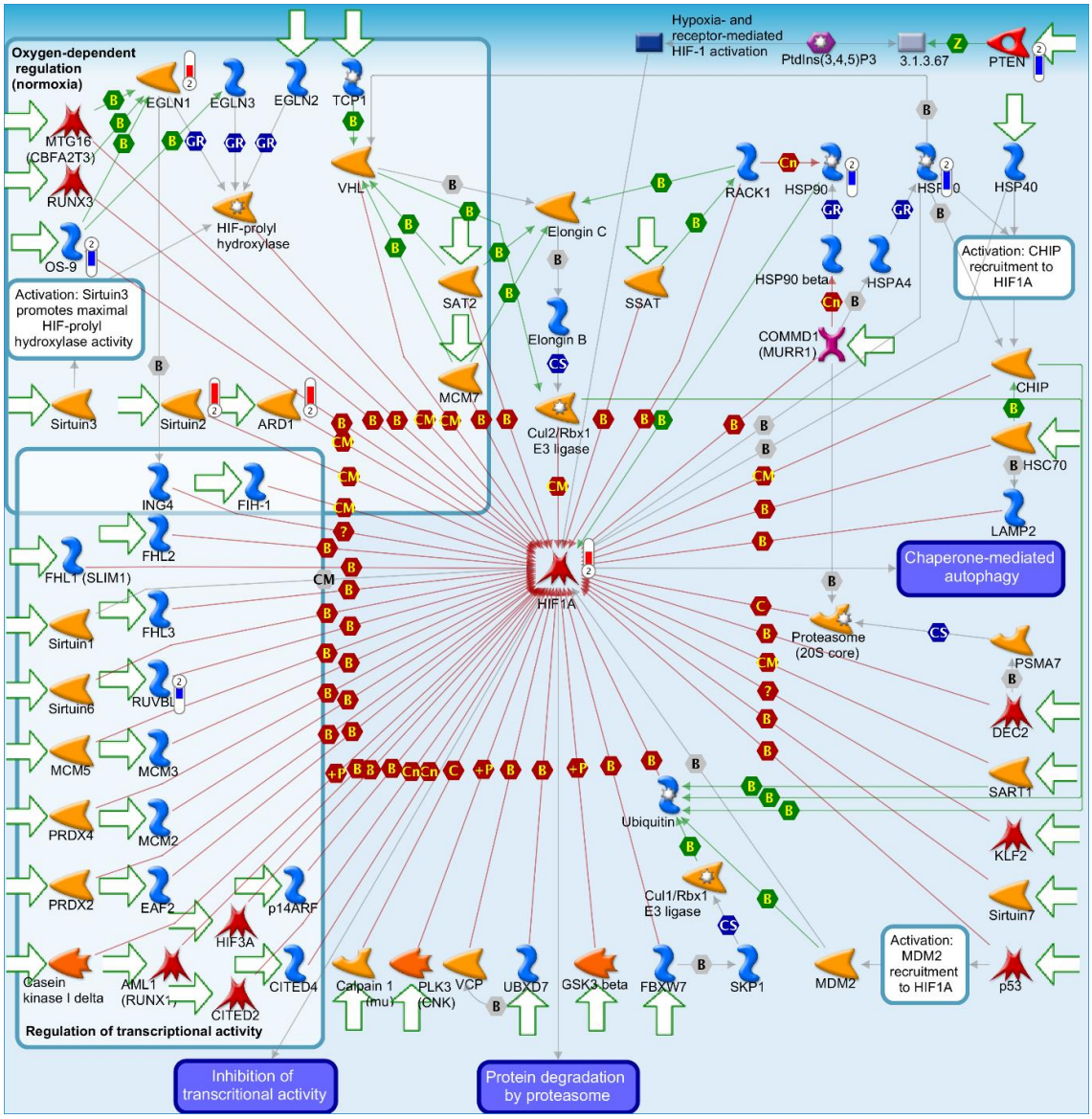

Fig 5.10. Negative regulation of HIF1A function. Pathway map created using GeneGo MetaCore™ from Thomson Reuters. For genes showing differential expression in MIN6 cells and islets cultured with 1µM or 8µM zinc for 48 h ($p < 0.05$), relative changes in gene expression are indicated by scaled expression bars. Red bar: upregulation. Blue bar: downregulation.

5.4.7. Comparison with qPCR data

In chapter 4 [405], we showed that multiple markers of β-cell identity and function are Zn^{2+}-responsive, indicating important roles for zinc in mediating β-cell phenotype. Moreover, earlier in the present chapter we showed that zinc depletion downregulates *Mt1* and *Mt2* and upregulates *Slc39a8* and *Slc39a14* in MIN6 cells. To validate our RNA-seq results, we next compared expression of these genes in the RNA-seq dataset to previous qPCR data [β-cell transcription factors: chapter 4 [405]; *Slc39a* paralogues, *Slc30a8*, *Mt1*, *Mt2* and *Mtf1*: chapter 5 (sections **5.4.1** and **5.4.2**)]. However, we only revealed significant downregulation of mRNA for *Mt1* and *Hnf4a* in the RNA-seq dataset. In line with our qPCR data, in response to zinc depletion we further noted a trend for *Slc39a14* upregulation and downregulation of mRNA for all other Zn^{2+}-responsive transcription factors investigated aside from *Pax4*, including >1.2-fold downregulation of *Nkx2.2*, *Nkx6.1* and *Pdx-1* (**Table 5.7**).

Table 5.7. Expression of qPCR-verified genes in the RNA-seq dataset. FD in expression are presented for MIN6 cells cultured with 1µM or 8µM zinc for 48 h, as measured by RNA-seq and qPCR. p-values for the significances of differential expression are indicated.

Transcript	RNA-seq		qPCR	
	Fold change	**p-value**	**Fold change**	**p-value**
Mt1	-2.041	0.028	-5.400	<0.0001
Mt2	-1.007	0.981	-6.976	<0.0001
Mtf1	-1.091	0.443	-1.087	0.968
Slc39a1	-1.170	0.608	1.550	0.148
Slc39a6	-1.078	0.867	-1.129	0.615
Slc39a7	-1.824	0.163	-1.438	0.055
Slc39a8	-1.321	0.609	2.128	0.014
Slc39a9	-1.344	0.424	1.360	0.209
Slc39a14	1.127	0.774	1.601	0.050
Slc30a8	-1.249	0.325	-1.301	0.022
Hnf1b	-1.022	0.979	-3.346	0.040
Hnf4a	-2.135	0.009	-2.918	0.010
MafA	-1.126	0.342	-1.797	0.004
Mnx-1	-1.068	0.720	-3.564	0.007
Nkx2.2	-1.221	0.178	-1.238	0.007
Nkx6.1	-1.219	0.219	-2.539	0.029
Pax4	1.293	0.240	-1.461	0.048
Pax6	-1.031	0.713	-3.234	0.009
Pdx-1	-1.231	0.285	-2.674	0.023

5.5. Discussion

Systemic hypozincaemia is present in many metabolically obese individuals, type 2 diabetic patients and animal models of diabetes [140, 283, 284, 407]. Since zinc is important for β-cell function in glycaemic control, a constant zinc supply is essential to restore intracellular concentrations following Zn^{2+}/insulin co-exocytosis [266, 411]. Hypozincaemia reduces the amounts of zinc available for β-cell uptake and may therefore alter β-cell zinc homeostasis and induce dysfunction.

5.5.1. Cellular zinc content and survival

The total zinc contents of human β-cells are sustained at 150-200μM [127, 146]. Zinc concentrations reach 20mM in insulin secretory granules [281] whereas cytosolic free Zn^{2+} is maintained within the pM range [127]. Extracellular zinc depletion (48 and 96 h) lowered the total zinc contents of MIN6 cells and downregulated mRNA expression for *Mt1* and *Mt2*, indicative of decreased cytosolic free Zn^{2+} and downregulation of Zn^{2+}-regulated genes [449]. Since 70% of β-cell zinc is contained in insulin secretory granules [281], cellular zinc depletion may reflect a reduced amount of zinc in the secretory pathway, and/or result from depletion of intracellular zinc stores to compensate for reduced uptake from outside the cell. Concurrently, excess zinc only upregulated *Mt1* and *Mt2*, indicative of an increased cytosolic free Zn^{2+} buffering capacity [449] without changes to the zinc contents of the secretory granule or zinc-containing organelles.

Zinc transporters are tightly regulated to maintain adequate intracellular zinc [147, 420]. Previous investigations highlight ZIP1, ZIP6, ZIP7, ZIP8, ZIP9 and ZIP14 as potentially biologically important for β-cell function (chapters 3-4 [404, 405] and [192, 218]); we therefore focused analysis on these paralogues. Zinc depletion upregulated mRNA expression for *Slc39a8* and *Slc39a14* and, in response to excess zinc, we observed

downregulation of *Slc39a8*. ZIP8 and ZIP14 may therefore be key paralogues regulating β-cell zinc in response changes in extracellular zinc. ZIP8 and ZIP14 upregulation in cells cultured with depleted zinc was coupled with increased cellular zinc uptake capacities, presumably to compensate for lowered amounts of available zinc. ZIP8 and ZIP14 are phylogenetically closely related [450] and both localise to the plasma membrane and membranes of intracellular zinc-storing organelles and vesicles [171, 209]. ZIP8 and ZIP14 have both been reported to regulate zinc accumulation into mitochondria, implicating zinc and these transporters in β-cell energy synthesis [451]. ZIP14 expression is induced during zinc deficiency via activation by ATF6 and JNK [452] and ZIP14 facilitates GPCR-mediated cAMP-CREB signalling through suppressing phosphodiesterase activity [325]. ZIP8 and ZIP14 both transport other metal ions in addition to zinc including non-transferrin bound iron [171, 172], cadmium [173] and manganese [453, 454], and altered transporter expression may therefore induce off-target effects consequential to redistribution of these metal ions. We further observed a trend for zinc depletion-induced upregulation of mRNA for *Slc39a1* at 48 h and show that *Slc39a6* is upregulated in response to high zinc at 96 h. Time-dependent changes to ZIP1 and ZIP6 abundances may fine-tune the β-cell response to extracellular zinc. ZIP1 and ZIP6 are ubiquitously expressed zinc transporters that facilitate cellular zinc influx at the plasma membrane [216, 319]. ZIP1 is highly expressed in mouse β-cells (chapter 3 [404]) and is important for mediating the initial zinc response to chronic MIN6 cell stimulation (chapter 4 [405]). ZIP6 expression is induced by STAT3 and the absence of ZIP10 [209] and ZIP6 forms a heteromer with ZIP10 (ZIP6:ZIP10) to interact with GLP-1R and potentiate GSIS [319]. ZIP6:ZIP10 heteromers facilitate inhibitory phosphorylation of GSK-3 [206, 311] and activation of downstream ERK1/2 cascades [320, 321] to promote

proliferation; ZIP6 may therefore be upregulated to compensate for lowered MIN6 cell proliferation.

Cells require intracellular zinc to be maintained within a narrow concentration range to avoid dysfunction [455]. Since culture of MIN6 cells with depleted and excess zinc alters cellular zinc homeostasis and since disrupted β-cell zinc is associated with loss of cellular phenotype (chapter 4 [405]), changes to extracellular zinc may impact β-cell survival. MIN6 cells cultured with either depleted or excess zinc exhibited increased apoptosis and decreased proliferation. We showed that the lowered cellular survival may be promoted by reduced mTOR and MAPK signalling. mTOR cascades are activated by growth factors and nutrients [51] to promote protein synthesis and maintain β-cell mass [62], and MAPK cascades respond to growth factors and mitogens to mediate cell cycle progression [69]. For MIN6 cells cultured with depleted zinc, the lowered cytosolic free Zn^{2+} may suppress mTOR and MAPK signalling cascades. Zinc inhibits PTP1B [79] leading to increases in IR and IGF-1R signalling [309] and activation of downstream MAPK and mTOR cascades. PTP1B inhibition ameliorates high-fat-diet and obesity-induced insulin resistance in mice [305], and genome-wide and tissue-specific PTP1B ablation increases insulin sensitivity and protects against obesity and diabetes [306, 307]. Zinc activates RAS upstream of ERK1/2 [314] and inactivates the dual specificity phosphatase DUSP, which dephosphorylates and inactivates ERK1/2 [456]. Moreover, the zinc transporter ZnT1 interacts with RAF-1 via its CTD to promote ERK1/2 activation [322] and activation of ZIP7-mediated zinc release from intracellular stores drives MAPK, mTOR and PI3K-AKT cascades [457]. MIN6 cells cultured with excess zinc exhibited elevated cytosolic free Zn^{2+}, which may explain the observed increase in apoptosis since cells require free Zn^{2+} to be maintained within a narrow range to avoid toxicity [455]. Concurrently, we noted increased amounts of oxidizing reagents in MIN6 cells cultured

with excess zinc, which are indicative of elevated oxidative stress [422, 423]. Although zinc exhibits potent anti-oxidant properties and protects against oxidative stress-induced β-cell dysfunction [270, 458], supraphysiological concentrations of zinc were used in this study which may have induced chronic oxidative stress [459]. Critically, we did not observe differences in cellular proliferation, apoptosis or oxidative stress at 24 or 48 h, suggesting MIN6 cells temporarily cope with changes in zinc concentrations.

Zinc co-secreted with insulin from β-cells exhibits autocrine effects for suppressing further insulin secretion by targeting K_{ATP} and L-VGCC channels [373]. It is therefore plausible that changes to serum zinc induce similar effects. However, we did not observe any differences for insulin expression in MIN6 cells or KCl-stimulated insulin secretion from MIN6 cells cultured with depleted or excess zinc. This observation may stem from differing roles of secreted and serum zinc for β-cells such as due to differing zinc coordination environments. Moreover, since the MIN6 cells used in this study were not glucose-responsive, we used KCl to stimulate insulin secretion and the high potency of KCl stimulation may mask zinc-induced suppression of insulin secretion. Alternatively, zinc may require the presence of additional stimuli to induce inhibitory effects that were not present in our experimental conditions. A further study indicates that zinc may affect the half-time but not the amplitude of the secretory response [460]; detailed analysis of the first and second phases of insulin secretion could therefore be required to identify temporal changes indicative of defective secretory function [461].

5.5.2. The β-cell transcriptome

Zinc binds over 10% of proteins in mammals [129] and influences expression of hundreds of genes [462, 463]. Zinc therefore has potential to affect virtually all aspects of β-cell physiology and function [130-133]. We carried out RNA-seq analysis on MIN6 cells and

islets cultured with deficient and adequate zinc to identify novel Zn^{2+}-responsive genes and pathways that could be deregulated in β-cells by hypozincaemia.

The genes we identified as differentially expressed ($q < 0.1$) in response to zinc depletion reflect the diverse roles of zinc in cells. For MIN6 cells, differentially expressed genes are involved in signal transduction, pH regulation and cellular signalling, mitochondrial regulation, receptor tyrosine kinase signalling, protein degradation, steroid synthesis, tethering, cellular adhesion, development and gene expression regulation. Whereas for islets, differentially expressed genes are involved in cell cycle regulation, metabolic breakdown, RNA transcription and metal ion transport. However, we only uncovered previous associations between six of these genes with zinc or zinc-mediated pathways (all of these were noted in MIN6 cells) and only *Uox* has been previously associated with the diabetic phenotype [435, 436]. Moreover, a total of six differentially expressed genes were identified as non-protein coding. Non-protein coding DNA makes up almost 98.5% of the genome, most of which is transcribed into RNA, including microRNAs, long noncoding RNAs, Piwi-interacting RNAs and small nuclear RNAs [464]. These transcripts have potential to regulate transcription and stability of mRNA to determine how much is translated into protein [465] and may contribute to the observed changes in expression of protein-coding genes. However, we could not find anything documented about the regulatory roles of the transcripts that we uncovered during this study. We did not identify enough differentially expressed genes to carry out enrichment and pathway analysis and, therefore, used gene lists for genes differentially expressed when $p < 0.05$ for subsequent analysis since a further level of robust statistical analysis would be undertaken.

Zinc is required for the catalytic activities of >300 metalloenzymes [466-468] and differential expression may be consequential to reduced formation of zinc(II)-enzyme complexes. In response to depleted zinc, we noted differentially expressed genes ($p < 0.05$) were enriched for enzymes, in particular phosphatases. Protein phosphorylation is the most prevalent post-translational modification in cells and regulates over 30% of cellular proteins [469]. Kinases facilitate protein phosphorylation through catalysing transfer of γ-phosphate from ATP or GTP to a protein substrate and phosphatases facilitate protein dephosphorylation through catalysing transfer of phosphate from a phosphoprotein to a water molecule [470]. Consistently, GO cellular processes enriched for differentially expressed genes ($p < 0.05$) included negative regulation of phosphorus metabolic processes, organophosphate metabolic processes, negative regulation of phosphate metabolic process and regulation of protein kinase activity. Zinc is a known negative regulator of phosphatase activity and zinc depletion may lead to increased activation of PTP1B [79], resulting in lowered phosphorylation of IRs and suppression of mTOR and ERK1/2 cascades [471]. This is consistent with our immunoblot data, albeit we did not observe differences in these signalling pathways until 96 h following treatment with depleted or sufficient zinc.

We demonstrated that the Zn^{2+}-responsive genes in MIN6 cells and islets are enriched for genes involved in the cellular response to oxygen-containing compounds. The transcription factor HIF1A is a key regulator of cellular hypoxia [442], and is directly regulated by ROS, including nitric oxide and superoxide [472]. Although we did not observe increases in oxidative stress for MIN6 cells cultured with depleted zinc, zinc is known to exhibit potent antioxidant properties: zinc mediates expression of many antioxidant genes including superoxide dismutase, for which zinc additionally acts as an important cofactor [301]. During pathway analysis, we highlighted regulation of HIF1A

by zinc depletion and we noted that HIF1A is an overly connected transcription factor to genes showing differential expression ($p < 0.05$) in response to depleted zinc. HIF1A may therefore represent a hub for mediating the β-cell response to zinc depletion. Zinc induces accumulation of transcriptionally active HIF1A in mammary epithelial cells in normoxic conditions [473] to upregulate genes involved in glucose transport, angiogenesis, pH control and cell cycle progression [474-476]. However, our data suggest that zinc depletion upregulates HIF1A abundance through disrupting expression of genes involved in oxygen-dependent HIF1A regulation, HIF1A transcription and HIF1A activation via protein folding and cell cycle progression. Confusingly, in response to zinc depletion we noted upregulation of the HIF1A inhibitor Sintuin2, which requires zinc binding for normal function [477], and downregulation of the upstream effector PTEN, which is inhibited and degraded in response to zinc [478]. *HIF1A* mRNA expression is additionally induced by STAT3 [479] and mTORC1 cascades [480], which we demonstrate are downregulated following incubation with zinc depletion for 96 h. Moreover, HIF1A is a direct substrate of GSK-3 [481], indicating HIF1A may be activated by ZIP6:ZIP10/GSK-3 interactions [207]. Of potential importance, the abundance of HIF1A is decreased in type 2 diabetic individuals and loss of HIF1A in the β-cells of C57BL/6 mice impairs ATP generation and GSIS to induce glucose intolerance [482]. These data suggest β-cells adapt to hypozincaemia through upregulating HIF1A, thus decreasing cellular sensitivity to oxidative-stress induced dysfunction.

Amongst the transcription factors overly connected to Zn^{2+}-responsive genes ($p < 0.05$) in MIN6 cells and islets, we additionally identified PPAR-γ and CREB. PPAR-γ controls expression of genes required for fatty acid synthesis and esterification [483] and exhibits important roles in β-cell proliferation and hyperplasia [484]. Activation of PPAR-γ in β-cells increases intracellular calcium signalling, insulin secretion and β-cell gene

expression [485]. The DNA binding domains of PPAR-γ and its binding partner RXR both consist of two zinc fingers [486, 487] and PPAR-γ signalling is inhibited during zinc deficiency [488]. Whereas CREB controls expression of pro-survival and pro-adaptive genes in response to a range of external stimuli. In β-cells, CREB induces IRS-2 expression to promote cell survival signalling downstream of the IR [489] and IRS-2-dependent increases in insulin signalling promote cellular growth through mTORC1 activation and induction of HIF1A [490]. Sustained CREB activation increases β-cell proliferation [491] and depletion of intracellular zinc downregulates CREB in hippocampal neurons [492]. PPAR-γ and CREB are both activated by mTOR signalling [493, 494], which we demonstrate is suppressed following zinc depletion for 96 h, and by post-translational phosphorylation [495, 496], which may explain why we did not observe differential expression for these transcription factors in our RNA-seq dataset.

In chapter 4 [405], we revealed that multiple markers for β-cell identity are Zn^{2+}-responsive. Earlier in this chapter, we additionally showed that extracellular zinc depletion downregulates the Zn^{2+}-responsive cytosolic zinc buffering proteins MT1 and MT2 and upregulates ZIP8 and ZIP14 in MIN6 cells. However, when we examined expression of these genes in our RNA-seq dataset, we only observed statistically significant differential expression for *Mt1* and the β-cell transcription factor *Hnf4a*. MT1 and MT2 are highly sensitive to zinc and zinc supplementation should promote MTF1-induced *Mt1* and *Mt2* upregulation to mediate cellular zinc availability and distribution by zinc chelation and donation [156], which is consistent with our qPCR data. However, in our RNA-seq dataset we did not observe *Mt2* downregulation following zinc depletion. This is likely due to low similarities between the MIN6 cell replicates cultured with depleted zinc, which we show included one outlier, and may explain why only a limited

number of genes exhibited differential expression (q <0.1). Our RNA-seq data should therefore be taken with caution prior to experimental confirmation.

5.6. Conclusion

In this study, we explored the impact of changes to extracellular zinc on MIN6 cell zinc content, phenotype and survival. We showed that depleted zinc reduces the total and cytosolic zinc contents of MIN6 cells but increases cellular zinc uptake capacities through upregulation of ZIP8 and ZIP14, probably as an adaptive response to counteract zinc depletion-induced dysfunction. Whereas excess zinc increases the cytosolic zinc content of MIN6 cells but downregulates ZIP8 and ZIP14, and both depleted and excess zinc decrease cellular survival through suppressing MAPK and mTOR cascades. For MIN6 cells and islets, depleted zinc alters expression of genes involved in protein phosphorylation and we identified regulation of HIF1A as a key pathway mediated by zinc depletion. However, inconsistencies between qPCR and RNA-seq data suggest further experimentation is needed to confirm these results. Moreover, since our experiments explored the effects of short-term severe zinc depletion rather than long-term relatively mild hypozincaemia (potentially over years) of type 2 diabetic patients, whether these results can be translated to physiological conditions *in vivo* remains to be determined. Overall, we suggest hypozincaemia present in Type 2 Diabetes lowers the zinc content β-cells, and that this may alter expression of genes involved in protein phosphorylation and HIF1A signalling and decrease cellular survival.

6. ZnT8 haploinsufficiency impacts MIN6 cell zinc content and phenotype via ZnT8-ZIP coregulation

6.1. Abstract

The predominantly β-cell-specific zinc transporter ZnT8 localises to insulin secretory granules where it facilitates zinc uptake and accumulation. Prior to ZnT8-mediated granule zinc influx, zinc is imported into the cytosol by members of the ZIP family of zinc transporters. ZnT8 abundance is linked to β-cell survival and phenotype, however the consequences of ZnT8 haploinsufficiency for β-cell zinc trafficking and function remain unknown. We hypothesised ZnT8-ZIP coregulation maintains β-cell zinc in response to hypozincaemia present in some type 2 diabetic patients and that ZnT8 haploinsufficiency induces dysfunction. We used CRISPR/Cas9 technology to generate ZnT8 haploinsufficient MIN6 cells and showed that lowered ZnT8 abundance is associated with downregulation of mRNA for *Slc39a8* and *Slc39a14*, lowered cellular zinc and a reduced cellular zinc uptake capacity in zinc deficient culture. Moreover, ZnT8 haploinsufficiency disrupts expression of a distinct array of important β-cell markers, decreases cellular proliferation via MAPK cascades and downregulates insulin gene expression. We additionally demonstrate that the major β-cell transcriptional regulator PDX-1 may mediate zinc trafficking via transcriptional co-regulation of ZIP6 and ZIP9 alongside ZnT8. Critically, we suggest that ZnT8-ZIP cooperation maintains β-cell zinc homeostasis and that lowered ZnT8 expression reduces MIN6 cell zinc content and survival.

6.2. Introduction

In mammals, the 14 ZIP paralogues influx zinc into the cytosol and the 10 ZnT paralogues function in cytosolic zinc efflux and compartmentalisation of zinc into intracellular organelles and vesicles [420, 421]. Approximately 50% of cellular zinc is distributed to the cytosol [145], where it is buffered at 0.4nM in β-cells [497] by MTs, which occupy 5-15% of the total zinc pool [156]. Cytosolic zinc is further involved in cellular signalling and tightly binds to metalloproteins as a structural component and/or cofactor [498]. The predominantly islet-specific zinc transporter ZnT8 is the most highly expressed zinc transporter in β-cells. ZnT8 localises to the membranes of insulin secretory granules where it regulates granule zinc uptake and accumulation, important for normal insulin maturation [198]. Disruption of ZnT8 activity is associated with β-cell dysfunction and polymorphisms are strongly linked to Type 2 Diabetes risk [234, 236, 262].

The role of ZnT8 for β-cell function has been extensively explored [198], although the precise mechanism of action remains inconclusive. Decreased ZnT8 abundance is associated with stresses that negatively impact β-cell function and mass including hypoxia [227], lipotoxicity [186] and cytokine stimulation [179]. ZnT8 overexpression protects against palmitate- and TPEN-induced decreases in GSIS in human islets [186] and increases cellular zinc content and protects against zinc depletion-induced apoptosis in INS-1E cells [191]. However, an additional study indicates ZnT8 is upregulated in islets of diabetic and insulin-resistant patients whilst knockdown in MIN6 cells increases proliferation and protects against inflammation-induced cell death [229]. Consistent with a positive correlation between ZnT8 and Type 2 Diabetes risk, twelve rare loss-of-function nonsense and missense polymorphisms are protective against the disease [271]. Islets from mice containing knock-in mutations of the most common loss-of-function

variant R138X exhibit reduced ZnT8 activity coupled with increased insulin secretory function [280]. ZnT8 knockout in mouse induces large changes to secretory granule morphologies and lowers β-cell zinc contents, however few differences in glycaemic parameters have been recorded [201, 202, 273, 276]. In human, only ZnT8 haploinsufficient genotypes are described and the effects of absolute loss of function remain unknown.

The polymorphic variant rs13266634 in the ZnT8 gene *SLC30A8* is strongly associated with Type 2 Diabetes risk [234, 236, 262], however it remains unclear whether the mutation induces a loss- or gain-of-function. The CTD of ZnT8-R exhibits a higher thermostability but lower dimerization affinity than that of ZnT8-W, suggesting the mutation impacts transporter stability [269]. The ZnT8-R risk variant is more active than ZnT8-W when reconstituted with artificial phospholipids [265] but is less able to promote granule zinc accumulation when overexpressed in MIN6 cells [201]. Mouse islets transgenic for hZnT8-W exhibit reduced zinc contents compared to hZnT8-R controls [279] and human ZnT8-R variant carriers present with increased proinsulin:insulin ratios [260], lowered β-cell function [261] and impaired insulin secretion during intravenous glucose tolerance tests [262, 263].

The transcription factor PDX-1 governs development and differentiation of the endocrine pancreas [91, 101, 499]. In mature islets, high PDX-1 expression is restricted to β-cells where it exhibits critical roles in maintaining cellular phenotype and function, including transcriptional regulation of the insulin gene [500] and repression of genes characteristic of other islet cell types, such as glucagon [91]. PDX-1 knockout is embryonically lethal [94] and heterozygous frameshift and missense mutations in human result in MODY4 development [4]. Animal models suggest PDX-1 downregulation in mature β-cells

induces loss of cellular identity and promotes β- to α-cell reprogramming [114], and that this underlies secretory failure and Type 2 Diabetes development [501, 502]. PDX-1 regulates β-cell zinc by targeting two promoters for the ZnT8 gene *SLC30A8* [200] and mediates expression of the Zn^{2+}-responsive transcription factor PAX4 [503]. Our previous data suggest that PDX-1 may additionally regulate expression of multiple ZIP paralogues, in particular ZIP1, ZIP5, ZIP6, ZIP8 and ZIP14 (chapter 3 [404]). PDX-1 therefore represents a plausible β-cell-specific regulator of zinc trafficking to ensure β-cells maintain their unique requirement for zinc in insulin secretory granules.

In chapters 4 [405] and 5, we demonstrated that prolonged stimulation and extracellular zinc depletion decrease the total zinc contents of MIN6 cells and disrupt expression of genes involved in zinc regulation. Since ZnT8 abundance is linked to β-cell survival and function [179, 186, 191, 227, 229, 271] and that increased ZnT8 activity during cellular stimulation elevates cytosolic free Zn^{2+} [192], ZnT8 is likely central to β-cell zinc trafficking and homeostasis. In this chapter, we postulated that ZnT8 functions cooperatively with ZIP transporters to mediate β-cells zinc homeostasis, phenotype and survival in response to hypozincaemia. We additionally hypothesised that PDX-1 co-regulates ZnT8-ZIP transcription to ensure normal β-cell zinc trafficking. We aimed to generate and characterise ZnT8 haploinsufficient MIN6 cells, representing lowered ZnT8 activity *in vivo*, in response to zinc depletion and to explore binding of PDX-1 to *SLC39A* regulatory regions.

6.3. Methods

6.3.1. Cell line and culture

MIN6 cells were cultured as described in section **2.1**. For zinc depletion experiments, standard growth medium was replaced with growth media containing 25mM glucose and 1μM or 8μM zinc for 48 h (section **2.2**).

6.3.2. CRISPR/Cas9 gene editing

ZnT8/*Slc30a8* gene editing was carried out using CRISPR/Cas9 gene technology, as detailed in section **2.5**. Primers to assess the occurrence of genome editing were designed through computationally aligning ZnT8 Cas9 nickase guide sequences to the mouse genome assembly mm10 (forward: TCATCTCCGTGCTCAAACCC, reverse: TCTGTCATCGTGGCACTCAA (Sigma Aldrich); **Fig 6.1A**). Six potential clonal *Slc30a8* knockout populations were generated by serial dilution. PCR amplifications of the Cas9-targeted genomic loci were separated by agarose gel electrophoresis to reveal multiple variants in three of the six colonies (clones 3, 4 and 5; **Fig 6.1B**), consistent with editing of one *Slc30a8* copy variant to result in heterogeneous knockdown populations, which was confirmed through Sanger sequencing for clone 3.

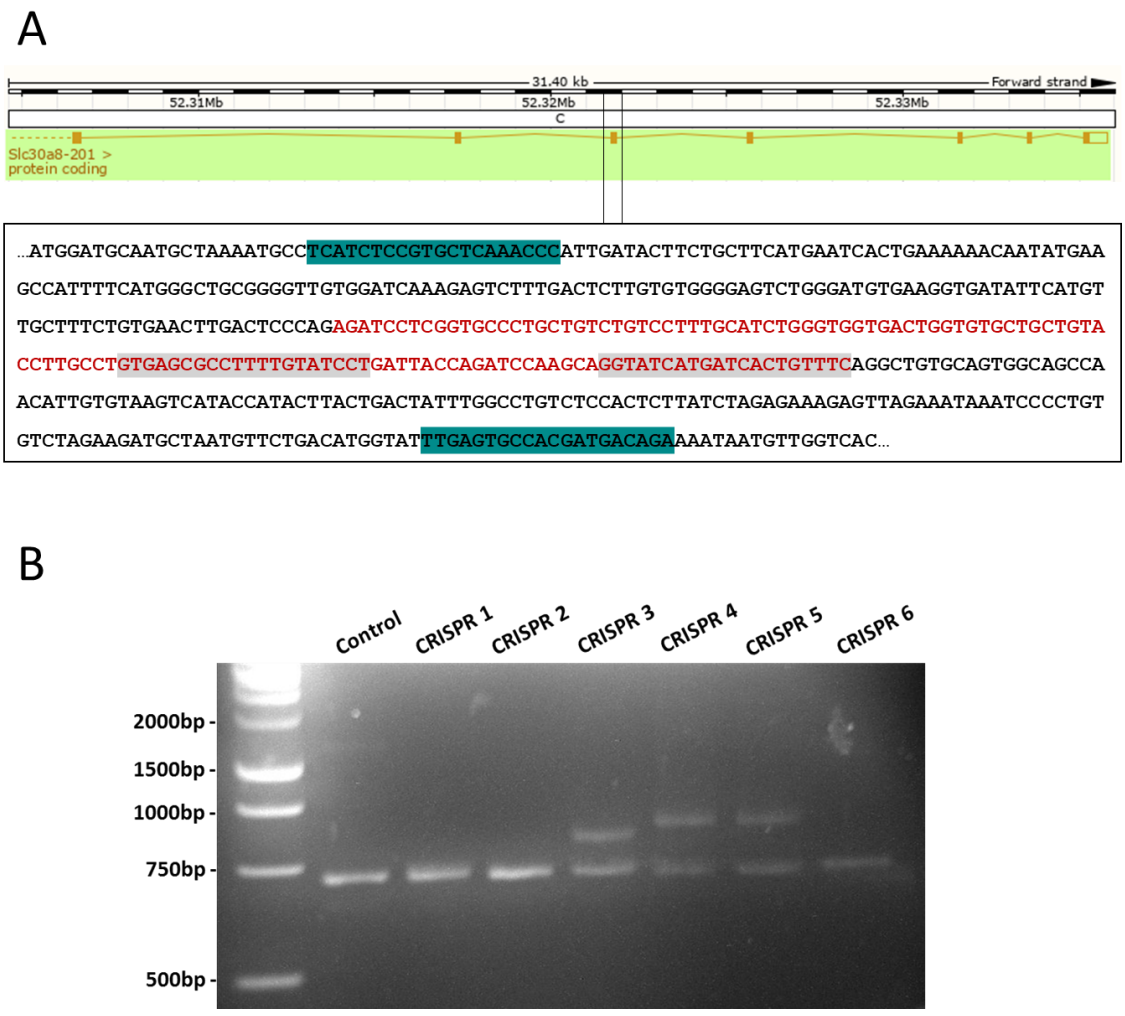

Fig 6.1. Amplification of the ZnT8 CRISPR/Cas9-targeted genomic DNA. (A) Binding of CRISPR/Cas9 constructs to *Slc30a8* genomic DNA. ZnT8 was mapped to chromosome 15 (52,295,553-52,335,798) on mouse genome GRCm38.p6 using the NCBI Ensembl genome browser 92. The Cas9 nuclease binds at the sequences highlighted in grey. Primers to assess knockdown bind at the sequences highlighted in turquoise. Red: exon 4. **(B)** Agarose gel electrophoresis showing PCR-amplified regions of *Slc30a8* from clonal MIN6 cell populations, transfected with ZnT8 CRISPR/Cas9 or control nickase constructs. The gel was imaged using GeneSnap software.

6.3.3. Cell transfection

For gene knockdown experiments, MIN6 cells were transfected with siRNA targeting *Slc30a8* mRNA [s108999; 5'-3' sequence: CUUUAAGCCUGACUACAAAtt (Thermo Fisher)] or with Silencer® Select negative control siRNA (4390844; Thermo Fisher). For overexpression experiments, MIN6 cells were transfected with plasmid DNA encoding the open reading frame for mouse PDX-1 [Myc-DDK-tagged (MR227421; Origene)] or water as a control (mock transfected). Details for MIN6 cell transfection with siRNA and plasmid DNA are provided in section **2.4.**

6.3.4. Gene expression analysis

RNA was extracted from MIN6 cells, reverse transcribed to cDNA and relative expression assayed through qPCR. The full methodology and details of primers used are provided in section **2.6**. All results are presented as expression ratios compared to control cells except for insulin gene expression, where values for FD (Log2) in expression are presented.

6.3.5. Cellular zinc parameters

Total cellular zinc contents were determined through ICP-MS (section **2.3**). The kinetics of zinc uptake into MIN6 cells were assessed through ^{65}Zinc uptake assays (section **2.8**).

6.3.6. Cellular proliferation and apoptosis

The rates of MIN6 cell proliferation and apoptosis were determined as described in sections **2.9**-**2.10**.

6.3.7. Immunoblotting

Immunoblotting was carried out as previously described (section **2.7**) using antibodies listed in section **5.3.4.** The additional primary antibodies used in this chapter, with

dilutions in 1% BSA/TBST, were α-MYC [9E10, Thermo Fisher (1:1,000)] and α-Tubulin [T9026, Sigma (1:15,000)]. The additional HRP-linked secondary antibody used, diluted in 1% BSA/TBST, was α-mouse [NA931V, Amersham (1:20,000)].

6.3.8. Insulin secretion assays

The amounts of secreted insulin were determined through insulin secretion assays and quantified using insulin ELISA assays, as described in section **2.12**.

6.3.9. Prediction of PDX-1 binding sites

6.3.9.1. ChIP-Seq data analysis

The Pubmed database was searched for chromatin immunoprecipitation sequencing (ChIP-Seq) datasets of PDX-1 binding to human and rodent β-cell or islet DNA. Datasets were filtered for binding loci in *SLC39A/Slc39a* genes. The binding loci from differing genome assemblies were lifted and the coordinates converted to Human Genome, Dec. 2013 (GRCh38/hg38) using the Batch Coordinate Conversion (LiftOver) software from the UCSC Genome Browser [504]. The identified loci were visualised schematically using GraphPad Prism 7.

6.3.9.2. Binding to intronic, 3'UTR, 5'UTR and promoter regions

The intronic, 3'UTR and 5'UTR regions of human *SLC39A* genomic sequences were aligned to genomes from 26 species using the ConTra v2 web server [505]. The major *SLC39A* transcripts in β-cells (as shown in **Fig 3.1**) were used as the reference sequences for alignment. Conserved PDX-1 binding loci were identified using the TRANSFAC stringency minimise database [506].

6.3.9.3. Alignment of candidate PDX-1 binding sites

Predicted transcription factor biding sites from ChIP-Seq datasets and bioinformatic alignments were collectively aligned. Loci overlapping between experiments were considered to include potentially important PDX-1 binding sites within β-cells and were identified as candidates for further investigation.

6.4. Results

6.4.1. ZnT8 is associated with expression of ZIP8 and ZIP14

ZnT8 transports zinc out of the cytosol and into insulin granules [198]. However, ZnT8 activity is positively correlated with cytosolic free Zn^{2+}: overexpression of human orthologues in MIN6 cells elevates free Zn^{2+} [201] whereas knockdown in mouse islets reduces free Zn^{2+} [201, 278]. ZnT8 activity is therefore likely to be co-regulated with the expression and/or activities of ZIP zinc importers.

ZnT8 is downregulated by cellular stresses that negatively impact β-cell function [179, 186, 227]. To explore the temporal ZIP response as cells adjust to ZnT8 deficiency, we knocked down *Slc30a8* mRNA in MIN6 cells using siRNA and assayed expression of the *Slc39a* paralogues that we and others previously identified as important for β-cell function (chapter 3 [404] and [192, 218]) at 48, 72 and 96 h (**Fig 6.2**). *Slc30a8* showed >2-fold depletion at all three time-points. At 48 h, we observed upregulation of mRNA for *Slc39a14* (8.56-fold), and downregulation for *Slc39a1* (5.39-fold), *Slc39a8* (2.20-fold) and *Slc39a9* (2.22-fold). At both 72 and 96 h, only *Slc39a8* remained differentially expressed compared to control cells (2.02-fold and 1.52-fold downregulation, respectively).

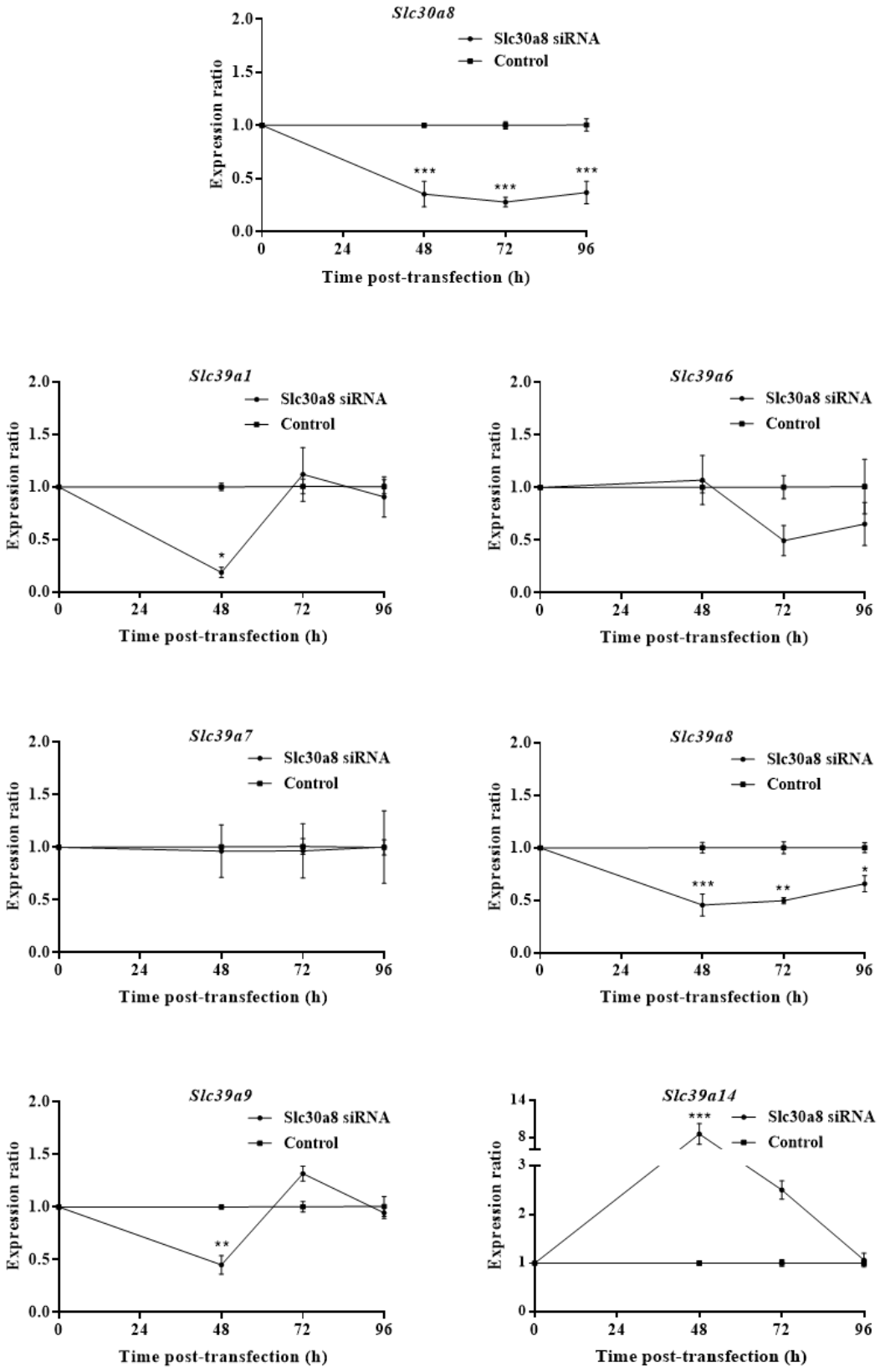

Fig 6.2. *Slc39a* mRNA expression following temporal *Slc30a8* knockdown in MIN6 cells. mRNA expression for *Slc30a8*, *Slc39a1*, *Slc39a6*, *Slc39a7*, *Slc39a8*, *Slc39a9* and

Slc39a14 following knockdown of *Slc30a8* by siRNA. Expression was assayed at 48, 72 and 96 h post-transfection. Changes in mRNA abundances were calculated through qPCR and presented as expression ratios relative to MIN6 cells transfected with Silencer® Select negative control siRNA (control) at each time-point. Data were analysed by 2-way ANOVA followed by Sidak's multiple comparison test. Error bars show ± SEM. N=3. *p <0.05, **p <0.005, ***p <0.001.

We next examined the final state of reducing ZnT8 abundance through examining the expression profiles for ZnT and ZIP paralogues in ZnT8 haploinsufficient MIN6 cells. *In silico* sequence analysis revealed that ZnT8 CRISPR close 3 MIN6 cells are predicted to encode a 187 amino truncated version of ZnT8 in addition to the 367 amino wildtype (**Fig 6.3**). However, we observed a 2.1-fold decrease in mRNA abundance for *Slc30a8*, suggesting that genome editing either prevented transcription of the truncated *Slc30a8* copy variant or resulted in transcription of unstable, rapidly degraded mRNA, therefore confirming the ZnT8 haploinsufficient genotype. We did not record differences in mRNA abundances for any other ZnT paralogues (**Fig 6.4A**), indicating lack of transporter redundancy and/or a compensatory response. When we examined expression of the ZIP paralogues in ZnT8 haploinsufficient MIN6 cells, we recorded downregulation of mRNA for both *Slc39a8* (2.37-fold) and *Slc39a14* (2.32-fold) (**Fig 6.4B**).

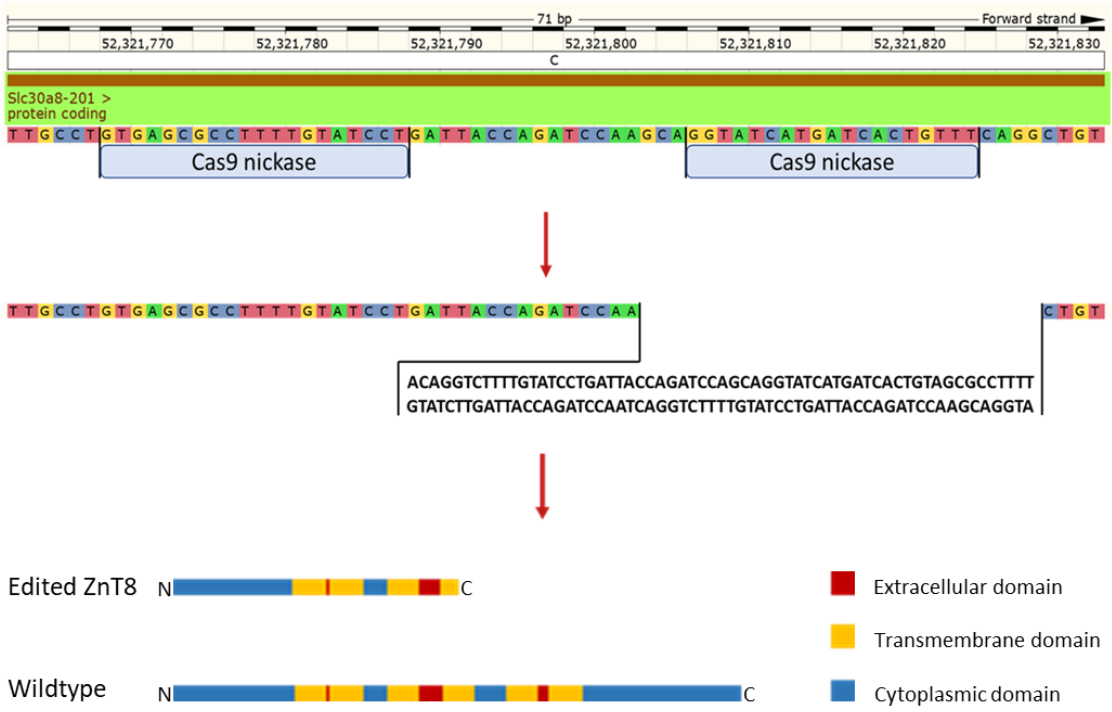

Fig 6.3. *Slc30a8* genome editing. Editing at *Slc30a8* exon 4 for ZnT8 CRISPR clone 3 MIN6 cells. The reference sequence was downloaded from the NCBI Ensembl genome browser 92 and binding of the ZnT8 Cas9 nickase constructs illustrated. The region shown spans Chr15:52321762-52321832 (mouse genome GRCm38.p6). The sequence of the edited genome and the protein domains of the translated proteins are shown.

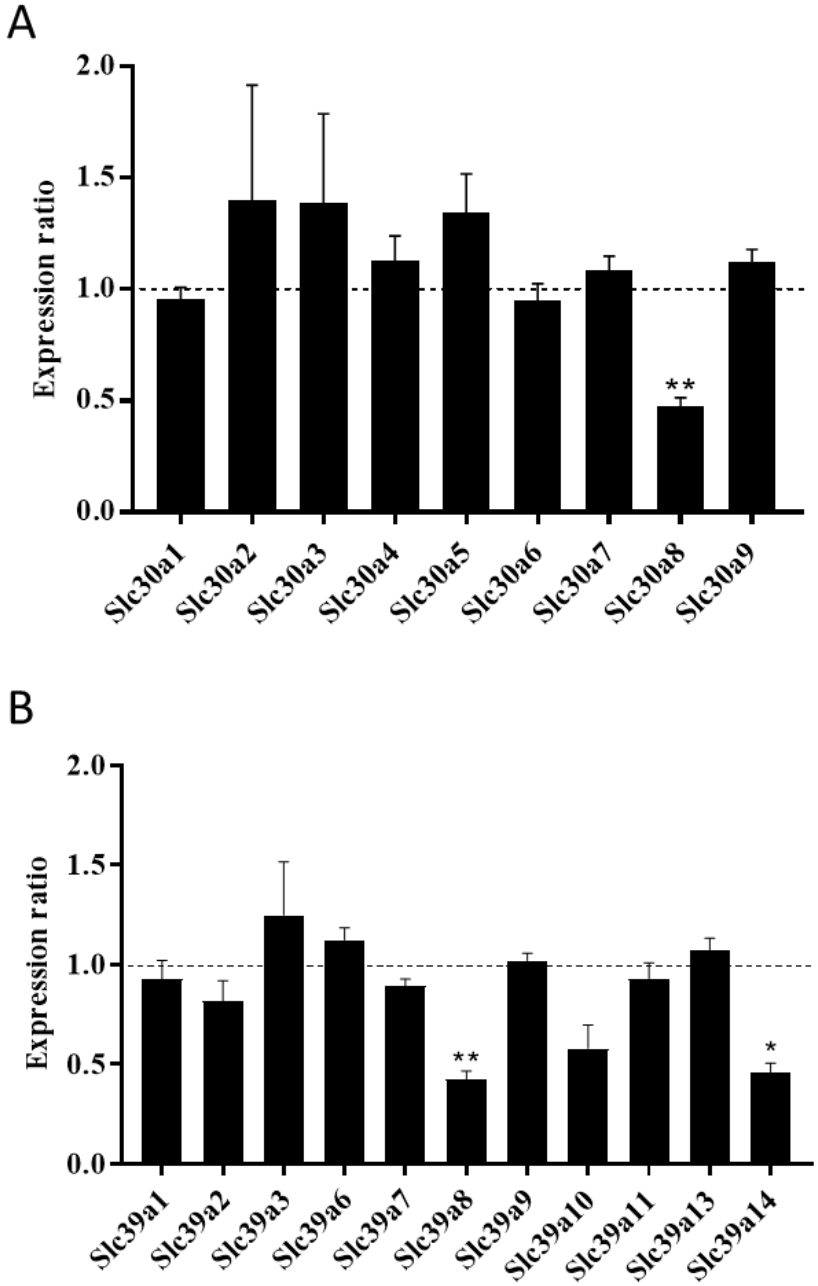

Fig 6.4. Zinc transporter expression in ZnT8 haploinsufficient MIN6 cells. mRNA expression for **(A)** *Slc30a* and **(B)** *Slc39a* paralogues in ZnT8 haploinsufficient MIN6 cells generated by CRISPR/Cas9 technology. We were unable to detect quantifiable expression for *Slc30a10*, *Slc39a4*, *Slc39a5* or *Slc39a12*. Changes in mRNA expression were calculated through qPCR and are presented relative to sham-CRISPR MIN6 cells (control). Data were analysed through t-tests and corrected for multiple comparisons. Error bars show ± SEM. N=3. *p <0.05, **p <0.005.

6.4.2. ZnT8 haploinsufficiency decreases zinc uptake into MIN6 cells

ZnT8 knockout in mouse decreases the zinc content of islets [201, 202, 272-274, 276], indicating ZnT8 is important for normal zinc uptake and accumulation. Above, we show that ZnT8 haploinsufficient MIN6 cells have lowered expression of mRNA encoding for ZIP8 and ZIP14, suggesting ZnT8 coordinates cellular zinc uptake through cooperating with these paralogues. We next aimed to characterise the impact of ZnT8 haploinsufficiency on zinc uptake and accumulation into MIN6 cells and explore whether these responses are influenced by extracellular zinc depletion.

We incubated ZnT8 haploinsufficient MIN6 cells in both zinc deficient (1μM) and adequate (8μM) culture for 48 h to show that ZnT8 haploinsufficiency lowers total cellular zinc contents compared to sham-CRISPR MIN6 cells (1μM: 1.34-fold and 8μM: 1.43-fold) (**Fig 6.5A**). Cellular zinc depletion was not associated with any differences in mRNA abundances for *Mt1* or *Mt2*, suggesting haploinsufficiency does not alter the cytosolic zinc content. However, we observed 1.5-fold depletion of mRNA for *Mtf1* in ZnT8 haploinsufficient MIN6 cells cultured with 1μM but not 8μM zinc (**Fig 6.5B**). To attribute these changes in mRNA abundance to cytosolic zinc influx, we examined the zinc uptake kinetics. We cultured MIN6 cells with 1μM or 8μM zinc for 48 h and then assayed ^{65}Zn uptake over a range of concentrations. We revealed that pre-treatment with zinc depletion decreased zinc influx into ZnT8 haploinsufficient cells at the highest two ^{65}Zn concentrations tested (27.25μM and 13.63μM) compared to sham-CRISPR controls (**Fig 6.5C-D**). However, this did not translate into significant differences in either J_{max} or $K_{0.5}$.

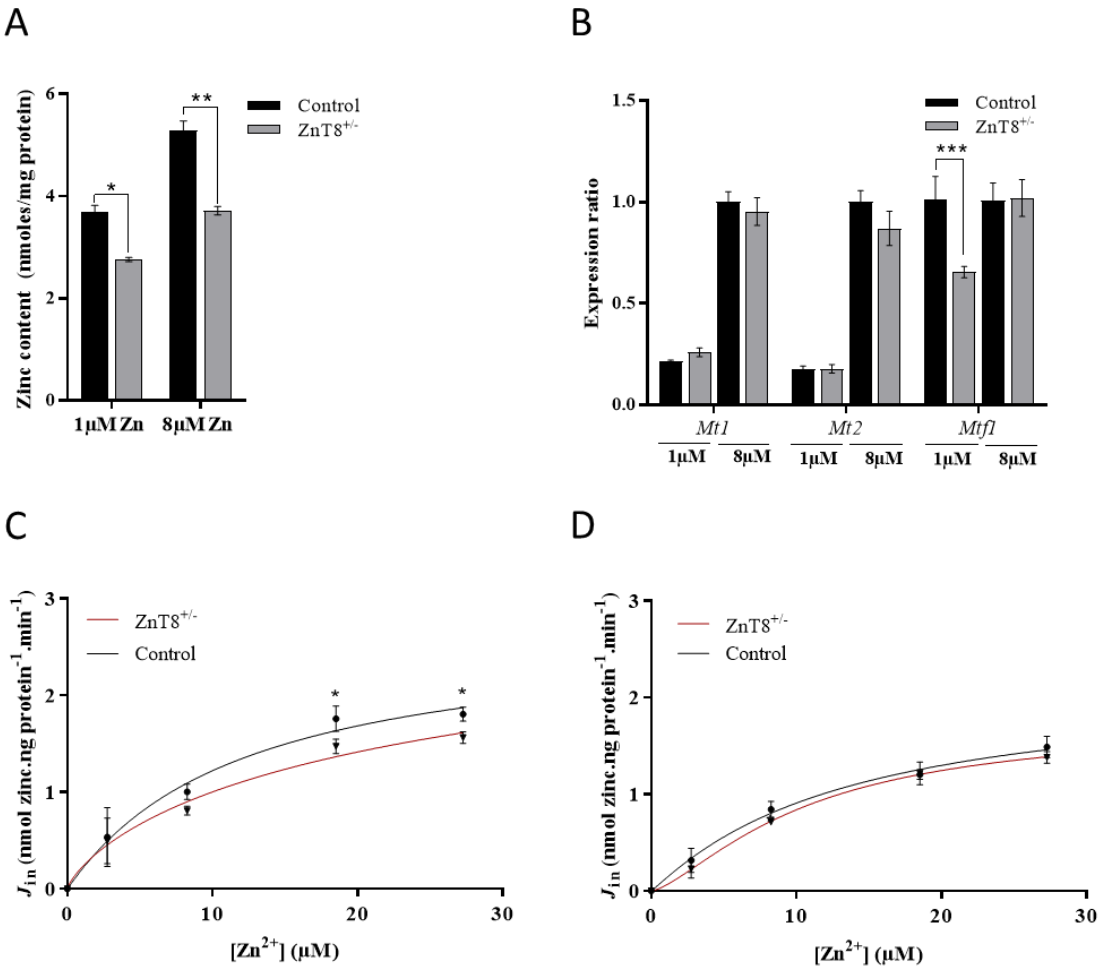

Fig 6.5. Zinc content and uptake kinetics of ZnT8 haploinsufficient MIN6 cells in response to extracellular zinc depletion. (A) Total cellular zinc content. Zinc content was determined through ICP-MS and normalised to protein. **(B)** mRNA expression for *Mt1*, *Mt2* and *Mtf1*. Changes in mRNA expression were calculated by qPCR and expressed as an expression ratio relative to sham-CRISPR MIN6 cells cultured with 8µM zinc (control). **(C-D)** Uptake kinetics of zinc into cells cultured with **(C)** 1µM or **(D)** 8µM zinc. Red: ZnT8 haploinsufficient MIN6 cells; black: sham-CRISPR MIN6 cells (control). ZnT8 haploinsufficient MIN6 cells: $ZnT8^{+/-}$. All experiments were carried out following culture with 1µM or 8µM zinc for 48 h. Data were analysed by 2-way ANOVA followed by **(A-B)** Tukey's multiple comparison test or **(C-D)** Sidak's multiple

comparison test. Error bars show ± SEM. For **(A)** N=4 and **(B-D)** N=3. *p <0.05, **p <0.005, ***p <0.001.

6.4.3. ZnT8 haploinsufficiency alters expression of important β-cell markers

We have previously shown that multiple markers for β-cell identity and function are zinc responsive *[Hnf1b, Hnf4a, MafA, Mnx-1, Nkx2.2, Nkx6.1, Pax4, Pax6* and *Pdx-1]* (chapter 4 [405]). Since lowered ZnT8 activity alters β-cell zinc trafficking and induces a depleted zinc phenotype, it is likely ZnT8 haploinsufficiency impacts expression of these transcription factors. We therefore examined mRNA abundances for the Zn^{2+}-responsive transcription factors *Hnf1b, Hnf4a, MafA, Mnx-1, Nkx2.2, Nkx6.1, Pax4, Pax6* and *Pdx-1* in ZnT8 haploinsufficient MIN6 cells following culture with 1μM or 8μM zinc. We additionally included *Foxa1*, *Foxa2*, *Foxo1* and *Neurod1* in our analysis to account for Zn^{2+}-independent roles of β-cell ZnT8.

We observed altered expression for a small but distinct array of β-cell markers in ZnT8 haploinsufficient MIN6 cells (**Fig 6.6**). In response to both 1μM and 8μM zinc, we recorded upregulation of mRNA for *Pax4* (1μM: 2.37-fold; 8μM: 2.03-fold) and downregulation for *Foxa1* (1μM: 4.06-fold; 8μM: 2.48-fold). We further noted 1.61-fold upregulation of *Hnf4a* mRNA following culture with 8μM zinc and decreases in mRNA abundances for *Foxo1* (1.38-fold) and *MafA* (1.64-fold) in cells cultured with 1μM zinc.

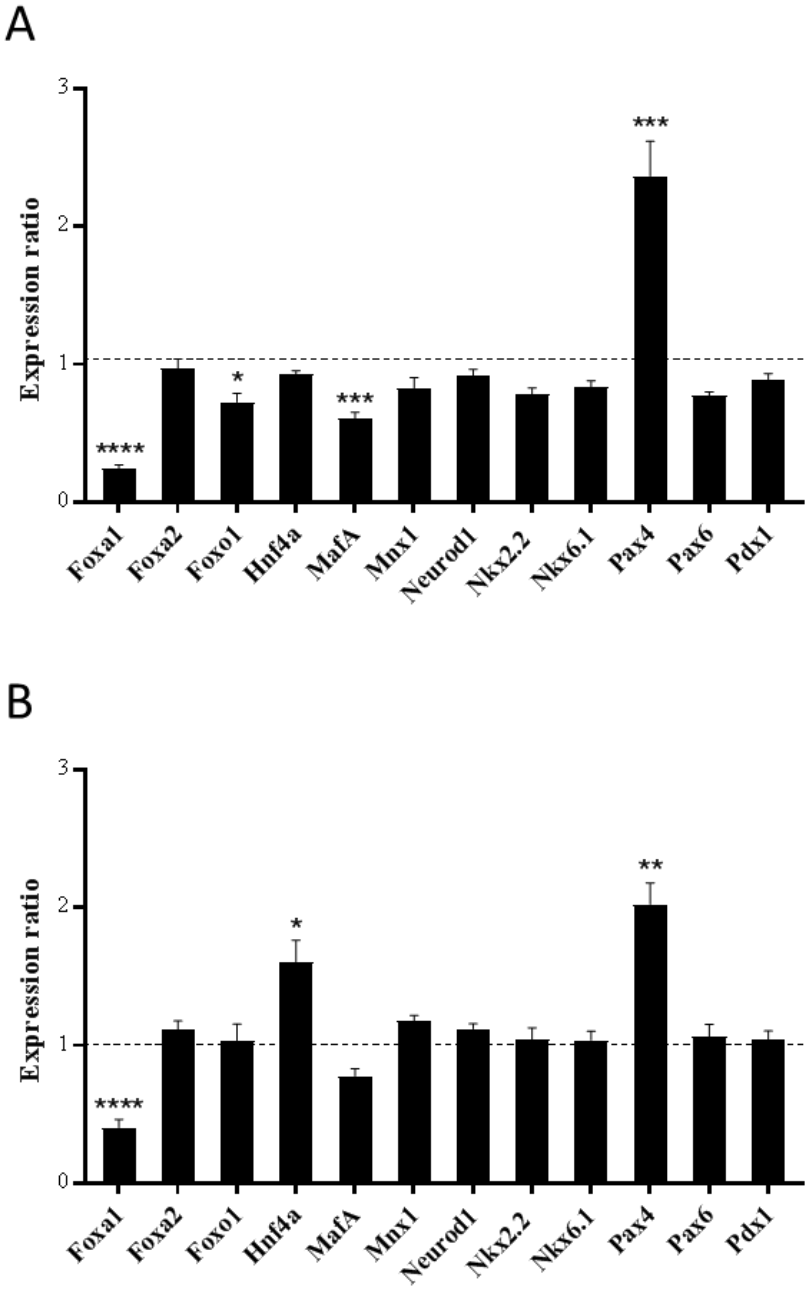

Fig 6.6. mRNA expression for transcription factors in ZnT8 haploinsufficient MIN6 cells. Expression in MIN6 cells in response to culture with **(A)** 1µM or **(B)** 8µM zinc. Expression was assayed through qPCR and calculated as a ratio compared to sham-CRISPR MIN6 cells cultured with **(A)** 1µM or **(B)** 8µM zinc (control). Experiments were carried out at 48 h. Data were analysed through t-tests and corrected for multiple comparisons. Error bars show ± SEM. N=3. *p <0.05**,** **p <0.005, ***p <0.001, ****p <0.0001.

6.4.5. ZnT8 haploinsufficiency reduces MIN6 cell proliferation and *Ins1* expression

We demonstrate above that ZnT8 haploinsufficiency disrupts expression of a distinct array of markers for β-cell identity, with differences observed based on extracellular zinc. To investigate whether these transcriptional changes alter the β-cell functional phenotype, we examined the survival parameters and insulin secretory response of ZnT8 haploinsufficient MIN6 cells following culture with zinc depletion.

ZnT8 haploinsufficient MIN6 cells cultured with either 1μM or 8μM zinc for 48 h exhibited lowered rates of proliferation compared to sham-CRISPR controls (1μM zinc: 1.24-fold; 8μM zinc: 1.30-fold). We additionally observed a 1.59-fold increase in apoptosis for cells in response to 8μM zinc (**Fig 6.7A-B**). MAPK cascades mediate proliferation through cell cycle regulation [69] and mTOR cascades promote proliferation through mediating mRNA translation [51] (depicted in chapter 5, **Fig 5.5**); both MAPK and mTOR pathways can be regulated by zinc [313, 314]. To explore if the decreased proliferation of ZnT8 haploinsufficient MIN6 cells may be driven by MAPK or mTOR cascades, we examined phosphorylation of the downstream effectors ERK1/2 (MAPK) and RPS6 (mTOR), which are both activated by phosphorylation. We observed decreased phosphorylation of ERK1/2 at p42/p44 compared to sham-CRISPR MIN6 cells (1μM zinc: 1.61-fold; 8μM zinc: 1.79-fold) and a small but significant increase in phosphorylation of RPS6 at Ser235/236 (1.22-fold) following culture with zinc depletion (**Fig 6.7C-E**). We further examined the abundance of STAT3, which mediates key roles in growth, survival and development [507] (**Fig 6.8**) and is activated by zinc-dependent phosphorylation [317]. We noted a 2.15-fold (p=0.03, n=3) decrease in *Stat3* mRNA expression in ZnT8 haploinsufficient MIN6 cells compared to controls cultured with zinc depletion.

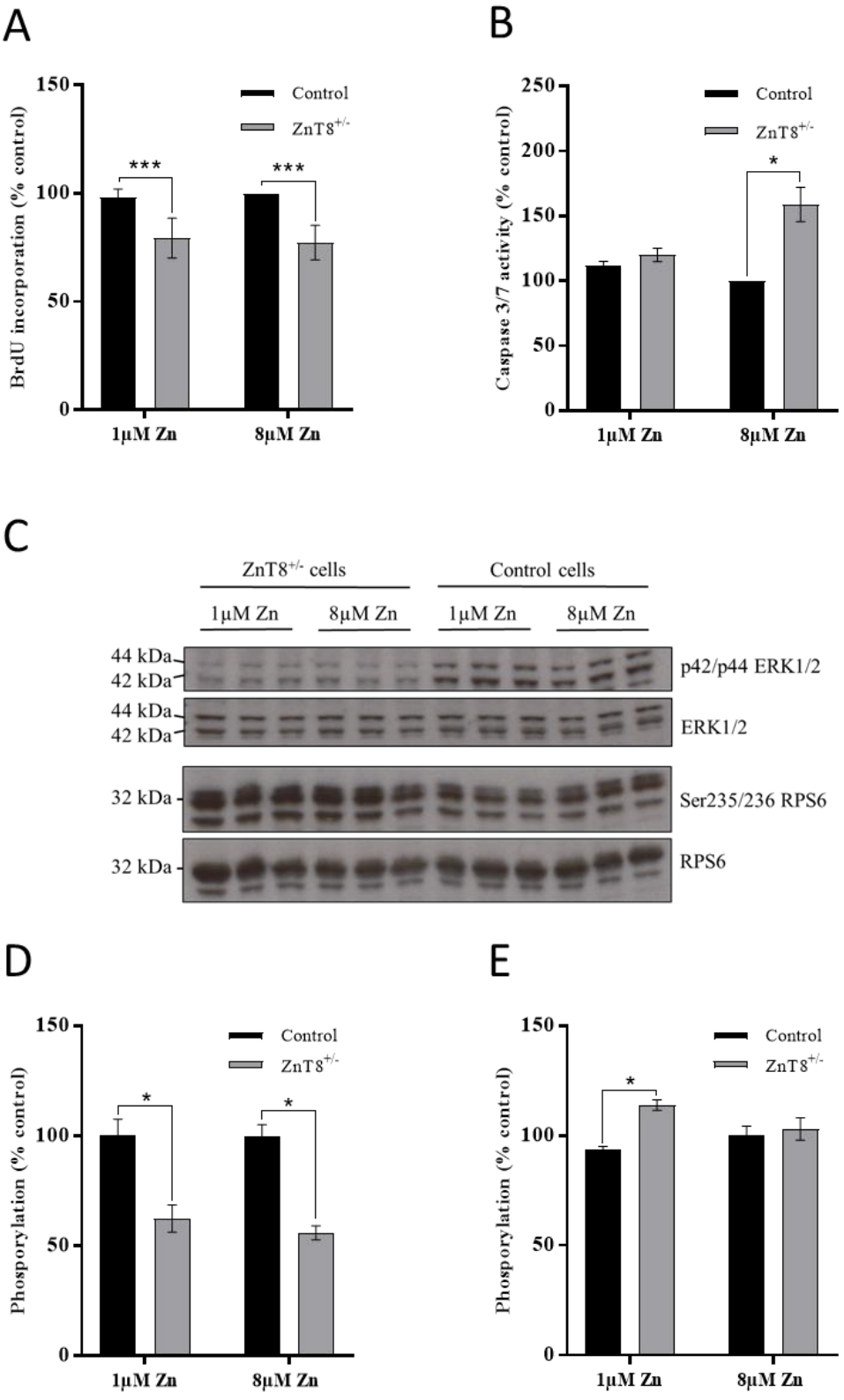

Fig 6.7. Survival of ZnT8 haploinsufficient MIN6 cells in response to zinc depletion. **(A)** MIN6 cell proliferation, determined by BrdU incorporation. **(B)** MIN6 cell apoptosis, determined by Caspase 3/7 assays. **(C-E)** Phosphorylation of ERK1/2 and RPS6. **(C)**

Immunoblots of p42/p44 ERK1/2, ERK1/2, Ser235/236 RPS6 and RPS6. **(D-E)** Quantification of immunoblots for **(D)** p42/p44 ERK1/2 vs ERK1/2 and **(E)** Ser235/236 RPS6 vs RPS6. Immunoblot quantification was carried out using ImageJ software. All experiments were carried out following culture of cells with 1µM or 8µM zinc for 48 h. **(A-B, D-E)** Results are relative to sham-CRISPR MIN6 cells cultured with 8µM zinc (control). Data were analysed by 2-way ANOVA followed by Sidak's multiple comparison test. ZnT8 haploinsufficient MIN6 cells: $ZnT8^{+/-}$. Error bars show ± SEM. N=3. *p <0.05**,** ***p <0.001.

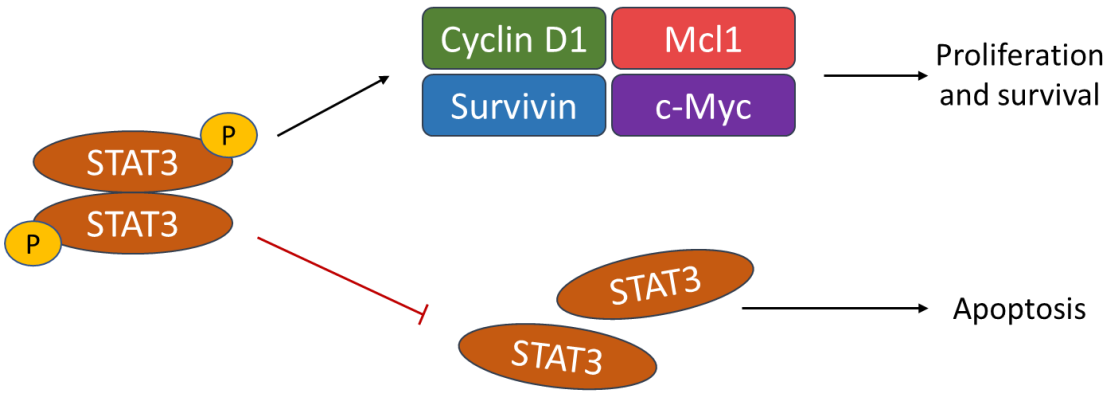

Fig 6.8. STAT3 and cellular survival. STAT3 is activated by phosphorylation. Phosphorylated STAT3 translocates to the nucleus where it mediates expression of genes driving proliferation and survival, including Cyclin D1, Mcl1, Survivin and c-Myc. STAT3 dephosphorylation drives apoptosis.

Finally, we explored the impact of ZnT8 haploinsufficiency on insulin expression and secretion, downregulation of which is a hallmark of β-cell dysfunction and failure. Unlike in human, rodents encode two insulin genes, *Ins1* and *Ins2*, however the contribution of each for glucose regulation remain inconclusive [508]. We observed downregulation of *Ins1* mRNA in ZnT8 haploinsufficient MIN6 cells following culture with both 1μM (2.01-fold) and 8μM (1.65-fold) zinc. However, we did not observe any differences in KCl-stimulated insulin secretion (**Fig 6.9)**.

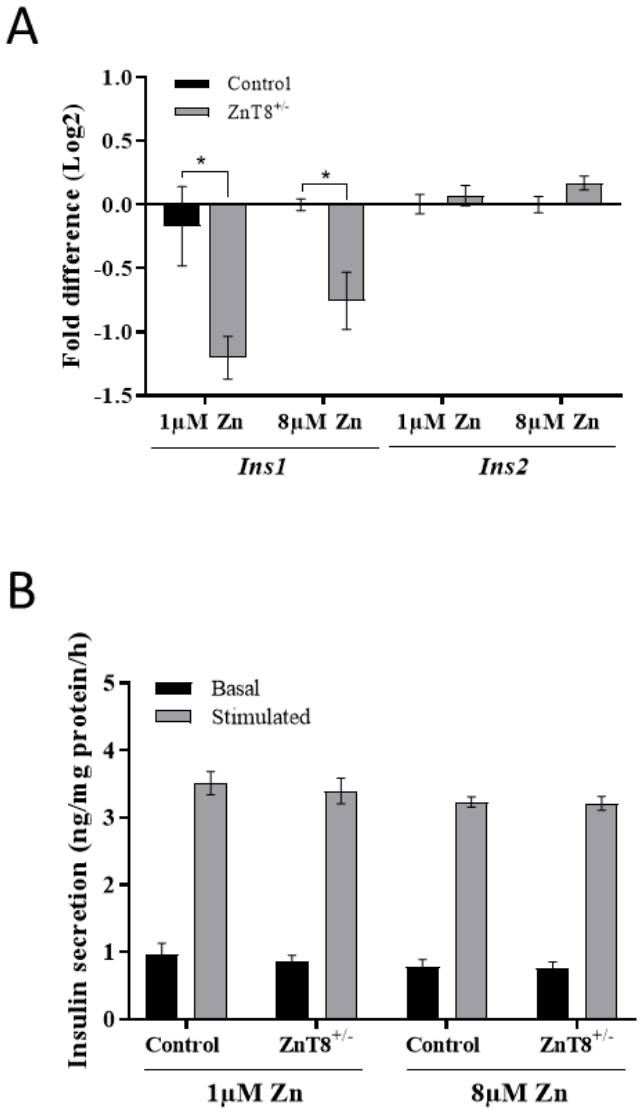

Fig 6.9. Insulin parameters for ZnT8 haploinsufficient MIN6 cells in response to zinc depletion. (A) *Ins1* and *Ins2* mRNA expression. Expression was assayed through qPCR and calculated as FD (Log2) compared sham-CRISPR MIN6 cells cultured with 8µM zinc (control). **(B)** Insulin secretion from MIN6 cells following addition of 3mM glucose (basal) or 40mM KCl (stimulated). The amounts of secreted insulin were calculated through insulin secretion assays and normalised to protein. All experiments were carried out following culture with 1µM or 8µM zinc for 48 h. Data were analysed by 2-way ANOVA followed by Tukey's multiple comparison test. ZnT8 haploinsufficient MIN6 cells: $ZnT8^{+/-}$. Error bars show ± SEM. N=3. *p <0.05.

6.4.6. Prediction of PDX-1 binding to *SLC39A* DNA

PDX-1 regulates zinc homeostasis in β-cells through targeting enhancers for ZnT8 [200]. Results presented in our systematic review (chapter 3 [404]) indicate PDX-1 abundance is additionally associated with mRNA expression for *Slc39a1, Slc39a5, Slc39a6, Slc39a8* and *Slc39a14.* In the present chapter, we show that ZnT8 functions corporately with ZIP8 and ZIP14 to facilitate zinc trafficking and accumulation in β-cells, indicating potential ZnT8-ZIP coregulation. To examine whether PDX-1 may be involved in mediating coordinated ZnT8-ZIP expression, we examined transcriptional regulation of *SLC39A* mRNA in β-cells by PDX-1.

We collated three independent PDX-1 ChIP-seq datasets for analysis of significant PDX-1 binding to *SLC39A* exons and/or regulatory regions. Datasets included binding in nondiabetic human islets, mouse islets [509] and human embryonic stem cells differentiated into proliferative PDX-1^+ pancreatic progenitor cells, representative of β-cell progenitors [510]. To account for differences in genome annotations between assemblies, we lifted coordinates to the Human Genome, Dec. 2013 (GRCh38/hg38). We aligned PDX-1 binding coordinates to show overlap of significant binding sites between three independent studies for *SLC39A3* and *SLC39A6,* and two independent studies for *SLC39A9* and *SLC39A13* (human and mouse islets) (**Fig 6.10)**. We additionally identified significant PDX-1 binding to *SLC39A9, SLC39A11, SLC39A12* and *SLC39A14* in human islets, *SLC39A8, SLC39A10, SLC39A812* and *SLC39A14* in human PDX-1^+ pancreatic progenitor cells, and *Slc39a1, Slc39a9, Slc39a10* and *Slc39a11* in mouse islets (**Table 6.1**).

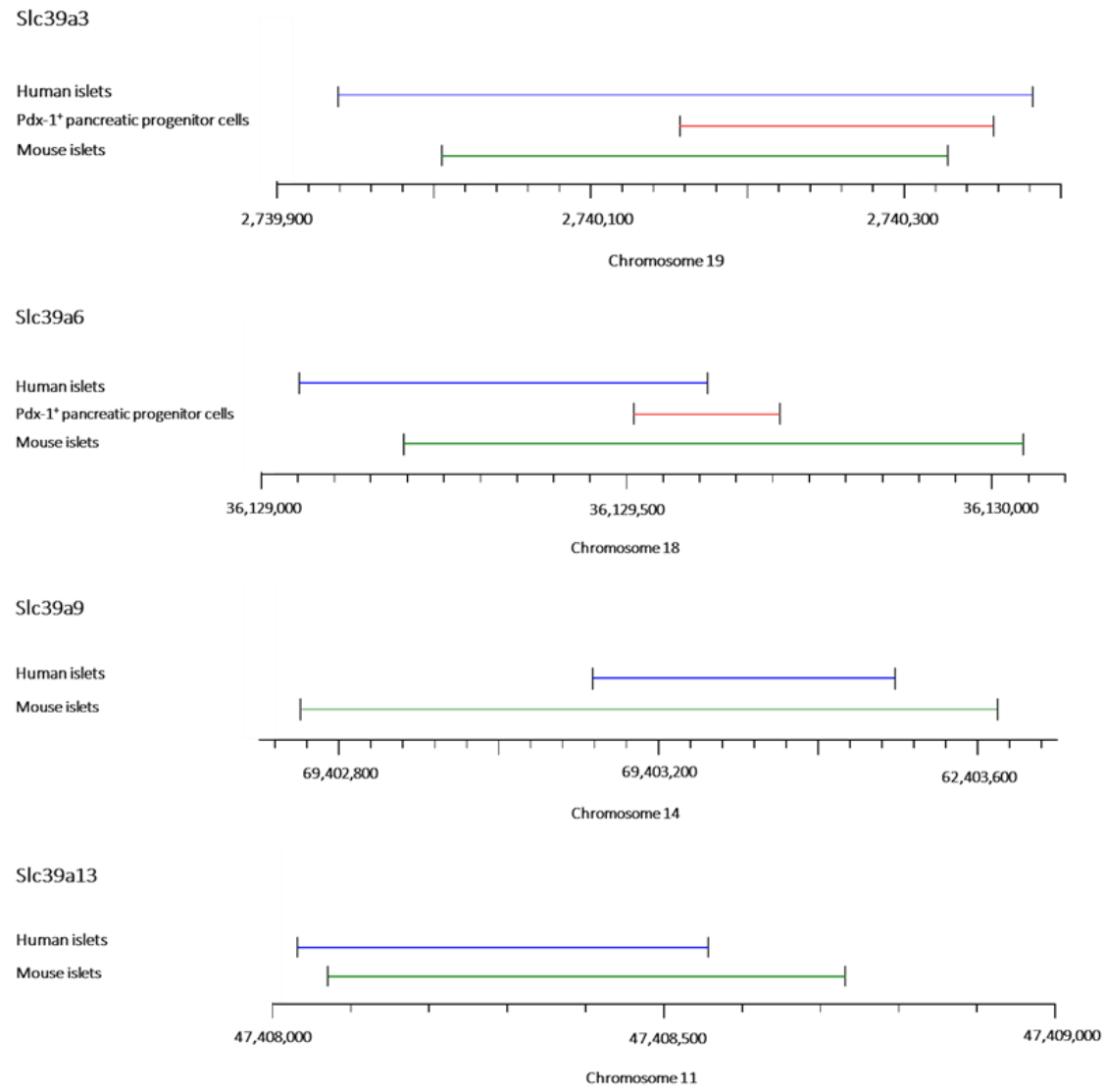

Fig 6.10. Genomic regions harbouring significant PDX-1 binding sites. Loci were identified through analysis of published ChIP-seq datasets. Only identified genomic regions overlapping between independent studies are presented.

Table 6.1. Significant PDX-1 binding coordinates identified through ChIP-seq dataset analysis. Data were derived from human islets, mouse islets [509] and embryonic stem cell derived proliferative PDX-1^{+} pancreatic progenitor cells [510]. Coordinates overlapping between ChIP-seq studies are highlighted. Repeated coordinates that mapped to multiple *SLC39A* isoforms are excluded.

Gene	Human islets	PDX-1^{+} pancreatic progenitor cells	Mouse islets
SLC39A1			chr1:153963390-153963774
SLC39A3	chr19:2739939-2740382	chr19:2740157-2740357	chr19:2740005-2740328
SLC39A6	chr18:36129052-36129611	chr18:36129510-36129710	chr18:36129195-36130043
SLC39A8		chr4:102092583-102092783	
SLC39A9	chr14:69386220-69386512 chr14:69403118-69403497 chr14:69460107-69460476		chr14:69348064-69348371 chr14:69397590-69398842 chr14:69402752-69403625
SLC39A10	chr2:195576024-195576422	chr2:195156244-195156444 chr2:195307830-195308030 chr2:195612770-195612970 chr2:195687569-195687769 chr2:194908477-194908677 chr2:195724138-195724338 chr2:195668053-195668253 chr2:194421363-194421563 chr2:195817926-195818126 chr2:194924717-194924917 chr2:194326082-194326282	chr2:195614544-195615579
SLC39A11	chr17:72749167-72749492 chr17:72759261-72759688 chr17:72778396-72779057 chr17:72853606-72853965 chr17:72890767-72891036 chr17:72954477-72955009 chr17:73027458-73027712 chr17:73089901-73090309 chr17:73118779-73119457	chr17:72924236-72924436 chr17:72903554-72903754 chr17:72972403-72972603	chr17:72945157-72945740 chr17:72977653-72978378
SLC39A12	chr10:17961962-17962505	chr10:18005565-18005765	
SLC39A13	chr11:47408032-47408557		chr11:47408071-47408732
SLC39A14	chr8:22392243-22393914	chr8:22365551-22365751	

To predict the PDX-1 binding sites at the identified *SLC39A3, SLC39A6, SLC39A9* and *SLC39A13* coordinates, we resorted to comparative genomics. We used ConTra V2 to map potential binding sites to the promoter (and up to 5000 bases upstream), 5'UTR, 3'UTR and intronic regions, using the 'minimize false positive' position weight matrix and the TRANSFAC database. We then aligned the coordinates identified through ChIP-Seq and ConTra V2 analysis (**Table 6.2**) to uncover a potential PDX-1 binding site within the 5'UTR of *SLC39A6* (Hg38 loci chr18:36129333-36129348), conserved between 20 of the 27 species assessed (**Table 6.3**). This loci maps to coordinates identified through analysis of ChIP-seq data from human and mouse islets and resides <200 bases from coordinates identified in PDX-1^{+} pancreatic progenitor cells.

We further noted a potential PDX-1 binding site within intron 1 of *SLC39A9* (Hg38 loci chr14:69403222-69403231), which maps to coordinates identified through analysis of ChIP-seq data from human and mouse islets and is conserved in 11 out of the 26 species assessed (**Table 6.4)**. However, TRANSFAC did not predict binding in rodents. There was no predicted PDX-1 binding by TRANSFAC within the coordinates identified for *SLC39A3* or *SLC39A13*.

Table 6.2. Predicted PDX-1 binding loci within *SLC39A* genomic DNA. All coordinates are expressed in Hg38 nomenclature. * = No PDX-1 binding predicted in rodent by TRANSFAC.

Gene	Human islets	PDX-1^{+} pancreatic progenitor cells	Mouse islets	Predicted binding by TRANSFAC?
SLC39A3	chr19:2739939-2740382	chr19:2740157-2740357	chr19:2740005-2740328	No
SLC39A6	chr18:36129052-36129611	chr18:36129510-36129710	chr18:36129195-36130043	chr18:36129333-36129348
SLC39A9	chr14:69403118-69403497	-	chr14:69402752-69403625	chr14:69403222-69403231*
SLC39A13	chr11:47408032-47408557	-	chr11:47408071-47408732	No

Table 6.3. Predicted PDX-1 binding loci in the 5'UTR of *SLC39A6* (Hg38: chr18:36129333-36129348). The core PDX-1 binding sequence (TAAT) is conserved in 20 of the 27 species assessed.

SPECIES	GENOME SEQUENCE
HUMAN	----CGCG-------AAGCTGGAAG-ACAA-TCACTAATTAC--CGCCGCGC-GCA----------GCGC
CHIMP	----CGCG-------AAGCTGGAAG-ACAA-TCACTAATTAC--CGCCGCGC-GCA----------GCGC
ORANGUTAN	----CGCG-------AAGCTGGAGG-ACAA-TCACTAATTAC--CGCCGCGC-GCA----------GCGC
RHESUS	----TGCG-------GAGCTGGAGG-ACAA-TCACTAATTAC--CGCCGCGC-GCA----------GCGC
BABOON	----TGCG-------GAGCTGGAGG-ACAA-TCACTAATTAC--CGCCGCGC-GCA----------GCGC
MARMOSET	----CGCG-------GAGCTGGAGG-ACAA-TCACTAATTAC--CGCCGAGC-GCA----------GCGC
MOUSE	----CTCC-------AAGC---AGG-ACAA-TCGGTAATTAC--CGCCGC----------
RAT	----CTCC-------AAGC---AGG-ACAA-TCGGTAATTAC--CGCCGC----------
KANGAROO RAT	----CCCA-------GATC---CGG-ACAA-TCGGTAATTAC--CGCCGCGC-GCC----------
GUINEA PIG	----CCCG-------GAGC---AGG-ACAA-TCAGGAGTCACAACGCCGCGC-GCCACGCGCCA-AGCAA
SQUIRREL	----CCCG-------GAGC---AGG-ACAA-TCAGTAATTAA--CGCCGCGC-GCA-------G-CGCGA
RABBIT	----TCGG-------GAGAAGGAGG-ACAA-TCGGTAATTAC--CGCCCCGC-GCG-----CGG-CGCGC
ALPACA	----CCGG-------CAGCAGGAGGAACAT-TTACTAATTAC--CGCCGCGC-TCA-------ATCGCGC
DOLPHIN	----CCGG-------G---AGGAGG-ACAA-TTACTAATTAC--CGCCGCTC-GTA-------G-CGCGC
COW	----CCGG-------GAGCAGGAGG-ACAA-TCACTAATTAG--CGCCGCGC-GCA-------G-CGCGC
HORSE	----CCGG-------GAGCAGGAGG-ACAA-TTACTAATTGC--CGCCGCGC-GCA-------G-CGCGC
CAT	----CCAG-------GAGC-TGAGG-ACAA-TTACTAATTAC--CGCCGCGC-GCA-------G-CGCGC
DOG	----CCGG-------GAGCAGGAGG-ACAA-TTACTAATTAC--CGCCGCGC-GCA-------G-CGCGC
MEGABAT	----CCTG-------GAGC---AGG-ACAA-TTACTAATTAC--CGCCGCGC-GCA-------G-CGCGC
HEDGEHOG	----CCCACCCCCCCGAGTCCGAGG-ACAA-TCACCAATTAG--CGCCGCGC-GCC-------G-CGCGC
TETRAODON	----ACCA-------CAGCCCGGGG-TCAA-AGGTCAGCGCC--TTCTTCCT-GAG-------G------
OPOSSUM	----CCCG-------ACCCACGAGG-ACGG-TCCCTCACCTG--CGGCGTCT-GGC-------T-AGCGC
SLOTH	----CCGG-------CTGCACGAGG-ACAA-TCACTAATTAC--CGCCGCGC-GCA-------G-CGCGC
TENREC	----CCCG-------GAGCACGAGG-ACAA-TCGCTAATCAC--CGCCGCGC-GTC-------G-CGCGC
ROCK HYRAX	----CGGG-------GAACACGAGG-ACAA-TCACTGATTAC--CGCCGCGC-GTA-------G-AGCGC
ELEPHANT	----CCCG-------GACCACGAGG-ACAATTCAGTAATTTC--CGCCGCGCGGTG-------A-AGCGC
TREESHREW	CTCCCGCG-------A----GCAAG-ACAA-TCAGTAATTAC--CGCCGCGC-GCA-------G-CGCGC

Table 6.4. Predicted PDX-1 binding loci in exon 1 of *SLC39A9* (Hg38: chr14:69403222-69403231). The core PDX-1 binding sequence (TAAT) is conserved in 11 of the 26 species assessed.

SPECIES	SEQUENCE
HUMAN	TTAACACT----------G---TCTTATG----TTTTTTCGATTG-AATTGCTAATGAGTAGTTT
MARMOSET	TTGGCACT----------G---TCTTATG----TTTTTTAGATTTCAATTGCTAGTGAGTAGTTT
BABOON	TTAACACT----------A---TCTTATG----TTTTTTCAATTG-AATTGCTAATGAGTAGTTT
RHESUS	TTAACACT----------G---TCTTATG----TTTTTTCAATTG-AATTGCTAATGAGTAGTTT
ORANGUTAN	TTAACACT----------G---TCTTATG----TTTTTTCGATTG-AATTGCTAATGAGTAGTTT
GORILLA	TTAACACT----------G---TCTTATG----TTTTTTCGATTG-AATTGCCAATGAGTAGTTT
CHIMP	TTAACACT----------G---TCTTATG----TTTTTTCGATTG-AATTGCTAATGAGTAGTTT
TREESHREW	----CACT----------G---TCTTGTA----TTTTTCATATTC-AGTTGGTAGTG---AGTTT
RAT	----------TCCTGAC----ATTT--AGAT---GGTTG----------GTTT
MOUSE	----------TCTTGTG----TTTT--GGATTC-AGTTGCTAAGGAGCTGTTT
GUINEA PIG	----------TG----TTTT--GGATTC-AGTTCTATGACAG--GTTT
SQUIRREL	----------GCCATCTGATA----TTTT--AGATTC-AGTCGCAAATGAGC-AGTT
PIKA	TTAACACT----------G---CCTTGTT----TTC------TTA-AGTTGCTAATGAGATGTTT
RABBIT	TTA--GCT----------G----CTTGTG----TTCT--AGATTC-AGTTGCTGATGAGCAGTTT
COW	-----ACT----------A---CATTGTG----TTTTTAAGATTC-AGCTGT---TGAGCAGTTT
SHREW	--AGTACTGACGAAGATATTAGCA---CCATTTG----GGTAGGTGATTC-AGTTGTGATTGAGCAGTTT
MICROBAT	--AGTACT----------A---GCTTAGG----TTTTTTAGATTC-AGTTGTTAATGAGCAGTTT
DOLPHIN	--AGTACT----------A---TATTGTG-----TTTTAAGATTC-AGTTGTTAATGAGTAGTTT
MEGABAT	----------AGTTGTTAATGAGCAGTTT
CAT	--AGTACT----------A---TCTTACG-----ATGTTAGATTC-AGTTGGTAACGAGCAGTTT
DOG	--AGCACT----------A---TCTTATA-----ATGTTAGATTC-AGTTGTTAACGAGC---TC
HORSE	--AGCACC----------G---TCTTATG----TTTTTTAGATTC-ACTTGTTCATGAGCAGTTT
ALPACA	--AGCACT----------G---TCTTGTG----TTTTTCAGATTT-AGTTGTTATTGAGCCCTTT
ELEPHANT	TTAGCACT----------A---TCTTATGTTTTTTTTTTAGATTC-AGATGTTAGTGAGTGGAGC
ARMADILLO	TTAGCACT----------T---GCTTATG---TTTTTTTAGACTC-A---TTTAATGAGTAGTTT
SLOTH	---GCA----------CTCATG---TTTTTTTAGATTC-A---TTTAATGAGCAGTTT
OPOSSUM	----------AACATTCTTA----TTATTCAGATTC-AGTT-------AATAATTT

6.4.7. PDX-1 and abundances of *Slc39a* mRNA

To explore regulation of the ZIP paralogues by PDX-1, we overexpressed PDX-1 transgenes in MIN6 cells. We first confirmed overexpression by detecting high transgene abundance using immunoblot (**Fig 6.11**).

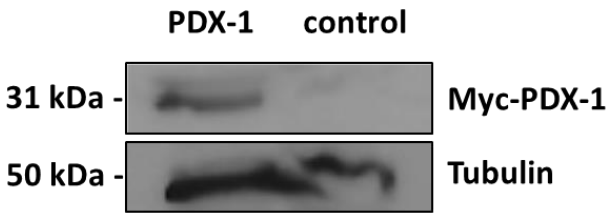

Fig 6.11. PDX-1 transgene overexpression in MIN6 cells. Overexpression was detected by immunoblot using antibodies targeting the PDX-1 Myc synthetic tag.

Overexpression of PDX-1 in MIN6 cells for 72 h increased the abundance of *Pdx-1* mRNA 43.29-fold. Overexpression was accompanied with upregulation of mRNA for eight *Slc39a* paralogues under investigation (*Slc39a1:* 2.09-fold, *Slc39a3:* 2.24-fold, *Slc39a6:* 1.61-fold, *Slc39a8:* 2.13-fold, *Slc39a9:* 1.75-fold, *Slc39a10:* 1.32-fold, *Slc39a11:* 2.49-fold and *Slc39a13:* 2.13-fold). We additionally assayed mRNA abundances for *Oct-4*, *Ins1*, *Ins2*, *Slc30a8* and *Slc39a7* as controls. PDX-1 downregulates *Oct-4*, a marker of endocrine pluripotency [510], upregulates *Ins1*, *Ins2* and *Slc30a8* [200, 511] and is not predicted to transcriptionally regulate *Slc39a7* (above). Consistent with elevated PDX-1 activity, we observed *Oct-4* downregulation 3.56-fold and *Slc30a8* upregulation 1.41-fold; however, we could not detect any differences in mRNA abundances for *Ins1* nor *Ins2*. We further noted *Slc39a7* upregulation 1.78-fold despite not harbouring a significant PDX-1 binding site identified during ChIP-seq dataset

analysis (**Table 6.1**). These discrepancies may be explained by time-dependent responses, dominant additional regulatory mechanisms or regulation via pathways secondary to PDX-1.

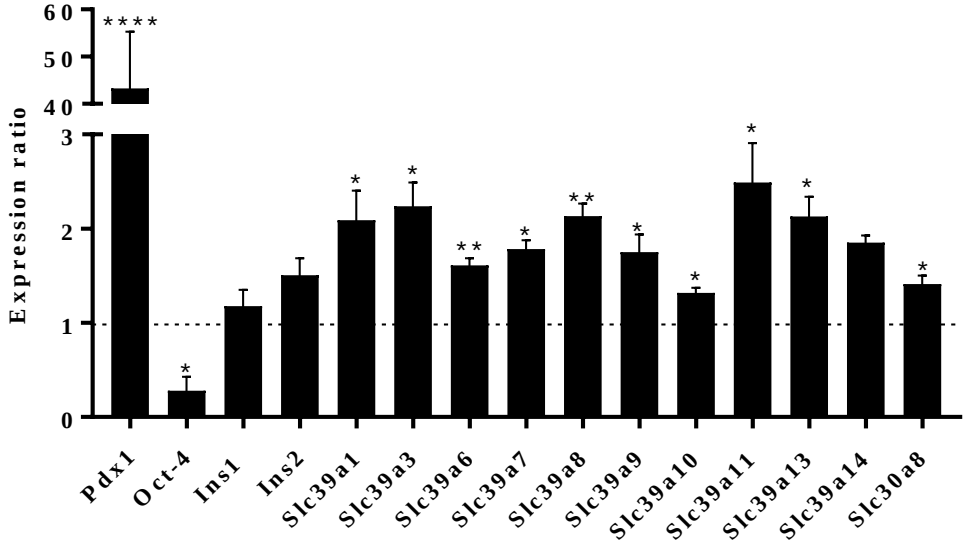

Fig 6.12. *Slc39a* mRNA abundances in MIN6 cells in response to PDX-1 overexpression. Expression of *Slc39a1*, *Slc39a3*, *Slc39a6*, *Slc39a8*. *Slc39a9*, *Slc39a10*, *Slc39a11*, *Slc39a13* and *Slc39a14* mRNA. Positive controls: *Pdx-1*, *Ins1*, *Ins2* and *Slc30a8*; neutral control: *Slc39a7*; negative control: *Oct-4*. Expression was assayed through qPCR and calculated as a ratio compared to mock transfected cells (controls) at 72 h. N=3. *p <0.05**,** **p <0.005, ****p <0.0001.

Finally, to infer whether PDX-1-mediated ZIP upregulation is likely to increase cellular zinc, we assayed mRNA expression for *Mtf1* and the metallothioneins *Mt1* and *Mt2*. MTF1 responds to zinc to mediate expression of Zn^{2+}-responsive genes [148] and the MTs bind and buffer cytosolic zinc to maintain optimal free Zn^{2+} concentrations [145]. Following overexpression of PDX-1 for 72 h, we did not observe any differences in the

abundances of *Mt1* or *Mt2*, however *Mtf1* was upregulated 1.88-fold (p=0.02) (data not shown).

6.5. Discussion

Lowered ZnT8 activity is associated with both protective and destructive effects for β-cell phenotype and function. Twelve rare ZnT8 nonsense or missense loss-of-function variants collectively represent a 65% decrease in Type 2 Diabetes risk [271] whereas ZnT8 overexpression protects against zinc depletion-induced reductions in human islet and rat INS-1E cell function [186, 191]. Furthermore, it is unclear whether the diabetes-susceptibility ZnT8 polymorphic variant at amino acid position 325 encodes a gain- or loss-of-function mutation [201, 265]. Since complete loss of abundance has not been reported for ZnT8 in human, ZnT8 haploinsufficient cells represent a model to examine the dampened ZnT8 expression that is induced by polymorphisms [271] and/or stresses that negatively impact β-cell function and mass [179, 186, 227].

6.5.1. Zinc characteristics of ZnT8 haploinsufficient MIN6 cells

Prior to uptake of zinc into insulin granules by ZnT8, β-cells exhibit increases in cytosolic free Zn^{2+} [192], suggesting ZnT8 activity is coordinated with ZIP-facilitated cytosolic zinc influx at the plasma membrane and/or membranes of intracellular zinc stores [146]. Concurrently, temporal loss of ZnT8 expression induced during β-cell dysfunction is coupled with decreased cytosolic free Zn^{2+} and a reduced insulin secretory capacity [179, 186, 227]. The lowered cytosolic Zn^{2+} is probably mediated by rapid changes to ZIP expression and/or activities coordinated with ZnT8 abundance. Following ZnT8 depletion with siRNA, we observed initial transcriptional upregulation of *Slc39a14* and downregulation of *Slc39a1*, *Slc39a8* and *Slc39a9*. Expression of ZIP1, ZIP8 and ZIP9 may be supressed to prevent excess cytosolic free Zn^{2+} accumulation in response to

decreased granule uptake. Of potential importance, ZIP9 functions as an androgen receptor in addition to as a zinc transporter, and downregulation may further impact β-cell function via associated G-protein signal transduction pathways [512]. The spike in ZIP14 abundance could reflect an adaptive response to increase cytosolic free Zn^{2+}, which we have previously shown is promoted by zinc depletion (chapter 5).

ZnT8 haploinsufficient cells may represent the final state of stress-induced downregulation of ZnT8 abundance. In MIN6 cells, ZnT8 haploinsufficiency was not associated with disrupted mRNA expression for any other ZnT paralogues, indicating MIN6 cells do not induce *Slc30a* transcription to compensate for partial loss of ZnT8, consistent with observations recorded for ZnT8 null mouse islets [202]. ZnT8 haploinsufficiency was associated with lowered mRNA expression for *Slc39a8* and *Slc39a14*, suggesting ZIP8 and ZIP14 are important for coordinating cytosolic zinc influx in the steady state with ZnT8 activity. MIN6 cells may downregulate ZIP8 and ZIP14 to prevent destructive effects of cytosolic free Zn^{2+} overload (chapter 5 and [459]) when efflux into secretory granules is reduced. The implications of changes to ZIP8 and ZIP14 abundances in MIN6 cells are discussed in chapter 5 (section **5.5.1**). Our previous studies demonstrate that stresses associated with β-cell dysfunction deregulate expression of multiple ZIP paralogues (chapters 3-5 [404, 405]); our present data demonstrate these transcriptional changes could be consequential to lowered ZnT8 activity or result from disruption of a factor co-regulating ZnT8 and coordinated ZIP paralogues.

Lowered ZnT8 activity decreases β-cell/islet zinc contents [201, 202, 273, 276]. Consistently, we demonstrate that ZnT8 haploinsufficient MIN6 cells exhibit reduced total zinc contents compared to controls. Since we did not observe differences in MT expression, the decrease in zinc likely represents lowered granule rather than cytosolic

free Zn^{2+}, which has previously been observed for ZnT8 null mouse models [201, 202, 273]. We noted that reduced cellular zinc was coupled with a trend for a lowered zinc influx capacity for cells cultured with depleted zinc, probably representing reduced trafficking of zinc to secretory granules due to downregulated ZIP expression and decreased amounts of available zinc. These differences to the zinc uptake capacity suggest that ZIP abundances are mediated simultaneously by both ZnT8 activity and zinc availability to regulate β-cell zinc homeostasis.

6.5.2. Phenotypes of ZnT8 haploinsufficient MIN6 cells

An array of endocrine-specific markers function to tightly maintain β-cell phenotype [114]. We have previously demonstrated that multiple transcription factors important for β-cell identity and endocrine function show Zn^{2+}-responsive expression *(*HNF1B, HNF4A, MAFA, MNX-1, NKX2.2, NKX6.1, PAX4, PAX6 and PDX-1; Chapter 4 [405]). Since ZnT8 haploinsufficient MIN6 cells exhibit lowered zinc contents compared to controls, it is likely that a lowered ZnT8 abundance additionally impacts β-cell transcription factor expression and identity. In MIN6 cells, ZnT8 haploinsufficiency induced upregulation of *Pax4* and downregulation of *Foxa1*. We additionally recorded small but significant upregulation of mRNA for *Hnf4a* in response to adequate zinc culture and downregulation for *Foxo1* and *MafA* following zinc depletion. Although PAX4 and HNF4A are Zn^{2+}-responsive [329, 405], their expression is tightly maintained by multiple factors; upregulation in ZnT8 haploinsufficient cells suggests they are additionally regulated by other roles of ZnT8, which likely dominate under these conditions. PAX4 is a major transcriptional regulator of β-cell development, phenotype and function [513], promotes cellular survival by protecting against stress-induced apoptosis [513, 514] and prevents β- to α-cell transdifferentiation through inhibiting glucagon expression [515], whereas HNF4A functions to regulate insulin gene expression

[339]. Downregulation of FOXA1, FOXO1 and MAFA additionally has potential to disrupt β-cell function. FOXA1 acts in combination with FOXA2 to regulate insulin secretion and carbohydrate metabolism [516] and MAFA mediates GSIS [517], with loss of function disrupting mature β-cell identity [103]. Moreover, FOXO1 is essential for β-cells to increase insulin secretion to compensate for increased peripheral insulin resistance [518] and regulates expression of NEUROD1 and MAFA to protect against oxidative damage [108].

Tightly maintained zinc homeostasis is required for cellular signalling, differentiation and proliferation [519]. We have previously shown that lowered cellular zinc negatively impacts MIN6 cell survival and intracellular signalling (chapters 4 [405] and 5). The changes to transcription factor expression observed in ZnT8 haploinsufficient cells suggest that ZnT8 downregulation has potential to impact β-cell survival. We demonstrated that ZnT8 haploinsufficiency lowers proliferation of MIN6 cells and increases apoptosis only in adequate zinc culture, possibly due to toxicity resulting from a reduced zinc storage capacity. The lowered proliferation may be promoted by reduced MAPK signalling. MAPK cascades are activated by physiological concentrations of Zn^{2+} [520, 521] to regulate gene expression, mitosis, differentiation, metabolism and programmed cell death [522]. We further observed downregulation of mRNA for *Stat3* following zinc depletion, which may contribute to the reduced β-cell survival. STAT3 is activated by cytokines and non-receptor tyrosine kinases to mediate β-cell function, proliferation and survival [523-526] and maintains the β-cell steady state through regulating cell cycle progression [527]. STAT3 activity is linked to cellular zinc homeostasis through inducing transcription of ZIP6 and ZIP10 [207, 316]. However, mice harbouring β-cell-specific STAT3 ablation (PDX-1-Cre transgene inactivation) do not develop glucose intolerances, suggesting STAT3 may be dispensable for β-cell function

[528]. It should be acknowledged that a recent study reported CRISPR/Cas9 genome editing induces a p53-driven DNA damage response and cell cycle arrest in immortalised human retinal pigment epithelial cells; it is therefore conceivable that decreased MIN6 cell proliferation may be secondary to the technique rather than consequential of transporter knockdown [529]. However, the use of sham-CRISPR cells as controls reduces the likelihood for this explanation.

Contradictive to our results, previous studies suggest that loss-of-function ZnT8 variants are protective against Type 2 Diabetes in human [271] and that the most common loss-of-function variant R138X elevates insulin secretion in response to high glucose [280]. Moreover, another study reported that lowered β-cell zinc consequential to reduced ZnT8 activity is protective for β-cell function and increases cellular proliferation via insulin-stimulated AKT activation [229]. ZnT8 loss-of-function variants may induce additional function(s) in β-cells, and/or may be coordinated differently with ZIP transporters than haploinsufficient genotypes, therefore inducing differing phenotypes. Alternatively, species-specific differences in the function of ZnT8 may exist, preventing us from replicating this observation in a rodent model. Our ZnT8 haploinsufficient MIN6 cells likely represent the downregulated ZnT8 phenotype of β-cells in response to stresses negatively impacting β-cell function [179, 186, 227].

Inadequate insulin secretion in response to elevated concentrations of glucose is a hallmark of β-cell failure and diabetic onset. The insulin secretory pathway is tightly controlled by temporal expression of multiple transcription factors and may therefore be impacted by the changes in expression consequential to ZnT8 abundance. In ZnT8 haploinsufficient MIN6 cells, we recorded lowered mRNA expression for *Ins1* compared to control cells, indicating reduced ZnT8 abundance may prevent cells mounting

appropriate secretory responses. However, we did not observe any differences in basal or KCl-stimulated insulin release, which is contradictive of a previous study exploring ZnT8 knockdown in MIN6 cells [229]. In mouse, ZnT8 ablation has been reported to either negatively impact [201, 202] or have no effect [274] on glucose tolerance, nevertheless circulating insulin is generally lowered in ZnT8 null animals [277]. However, as previously noted (chapter 5, section **5.5.1**), stimulation of MIN6 cells with KCl may not replicate differences in the secretory response that exist following glucose stimulation.

6.5.3. ZnT8-ZIP coregulation by PDX-1

The transcription factor PDX-1 is largely confined to β-cells in the mature pancreas [91]. PDX-1 regulates β-cell-specific roles of widely expressed genes, and mediates zinc homeostasis by promoting expression of ZnT8 [200]. We demonstrate that PDX-1 may bind genomic enhancers for ZIP6 and ZIP9 and could therefore co-regulate ZIP6 and ZIP9 alongside ZnT8 [200]. However, mechanistic investigations, such as reporter gene and promoter bashing assays, are required before conclusions can be drawn. Following PDX-1 overexpression in MIN6 cells, we further observed upregulation of mRNA for additional ZIP paralogues and MTF1. PDX-1 mediates expression of thousands of genes in β-cells with roles in almost all areas of β-cell function, including metabolism, gene expression and cellular survival [509]. ZIP abundance may be regulated by PDX-1-induced expression of a *SLC39A*-targeting transcription factors or via another mechanism functioning to maintain β-cell homeostasis. MTF1 is the main transactivator of MT1 and MT2 expression [162, 163]; upregulation of MTF1 but not MT1 or MT2 in cells overexpressing PDX-1 suggests that PDX-1 might prime the β-cell zinc response, possibly to induce more potent responses following addition of zinc or further stimuli, which is consistent with our previous observations that PDX-1 primes the β-cell ZIP/zinc response to cytokines (chapter 3 [404]).

If PDX-1 is found to transcriptionally regulate ZIP6 and/or ZIP9 in addition to ZnT8, PDX-1 could be key for understanding zinc trafficking in β-cells. PDX-1 portrays critical regulatory roles during development of the endocrine pancreas [100] and is important for mediating a diverse range of functions in mature β-cells including cellular survival [101], identity [91], action of GLP-1 [530] and ER stress susceptibility [531], many of which are additionally regulated by zinc and its transporters [218, 519, 532, 533]. Our data would implicate a role of zinc for β-cell dysfunction in patients with MODY4, which arises from inactivating PDX-1 mutations [4]. Taken with our previous data, these results may suggest ZnT8 is transcriptionally coregulated with ZIP6 and ZIP9 by PDX-1 to maintain adequate zinc uptake into the cytosol, and that expression of ZIP8 and ZIP14 are altered by ZnT8 activity to rapidly adapt cytosolic zinc flux following ZnT8 downregulation. ZIP6, ZIP8, ZIP9 and ZIP14 have all previously been identified as important candidates for regulating β-cell function [192, 404] and may function cooperatively to fine-tune β-cell zinc homeostasis and endocrine function.

6.6. Conclusion

In this study we explored the impact of loss of ZnT8 abundance for the phenotype of MIN6 cells following zinc depletion. ZnT8 haploinsufficient MIN6 cells exhibited downregulation of ZIP8 and ZIP14 and decreased β-cell zinc uptake and accumulation. Moreover, loss of ZnT8 abundance altered expression of key β-cell transcription factors in MIN6 cells and reduced cellular survival via MAPK cascades, consistent with the destructive role of stress-induced ZnT8 suppression [179, 186, 227] but contradictive of the protective effects induced by loss-of-function ZnT8 variants [271]. The existence of differing pathways associated with loss of ZnT8 abundance in mature cells compared to expression of a truncated protein probably explain this variation. We additionally showed

that PDX-1 may transcriptionally co-regulate ZIP6 and ZIP9 alongside ZnT8. PDX-1-induced β-cell dysfunction could therefore, at least in part, be driven by zinc deregulation. Overall, we demonstrate coordinated ZnT8-ZIP zinc trafficking is important for β-cell zinc homeostasis and that ZnT8 haploinsufficiency impacts β-cell phenotype and reduces cellular survival.

7. ZIP6 deficiency increases the cytosolic zinc content of MIN6 cells to disrupt Zn^{2+}-responsive β-cell markers and cellular survival

7.1. Abstract

The zinc importer ZIP6 is highly expressed in β-cells. Whilst ZIP6 is a plasma membrane zinc channel, its principal role in a variety of cell types is zinc-mediated cellular signalling, notably to stimulate proliferation and anoikis resistance. However, the role of ZIP6 for maintaining β-cell phenotype and mass remains poorly described. We hypothesised ZIP6 is important for β-cell zinc homeostasis and that ZIP6 plays key roles in the adaptive response to hypozincaemia. We used CRISPR/Cas9 technology to generate ZIP6 knockout MIN6 cell populations and stressed cells with zinc depletion. We showed that ZIP6 abundance is associated with expression of multiple ZIP and ZnT paralogues and the zinc-responsive proteins MTF1, MT1 and MT2. ZIP6 knockout MIN6 cells cultured with depleted zinc exhibited lowered total zinc contents compared to controls, suggesting ZIP6 plays a role in adapting to zinc depletion. The disrupted zinc phenotype was accompanied with altered expression of multiple markers for β-cell identity including key transcription factors and the insulin gene, with potentially important differences observed between cells cultured with deficient and adequate zinc. Moreover, ZIP6 knockout cells exhibited decreased proliferation and apoptosis, coupled with suppression of mTOR cascades and increased abundance of *Stat3* mRNA. These data highlight ZIP6 as important for β-cell identity and survival and show that ZIP6 is critical for the cellular response to zinc depletion.

7.2. Introduction

Tightly controlled zinc homeostasis is important for maintaining β-cell identity and survival (chapters 4 [405] and 5). In mammals, the 14 ZIP and 10 ZnT zinc transporters mediate cellular zinc trafficking at the plasma membrane and membranes of intracellular vesicles and organelles. The predominantly β-cell-specific paralogue ZnT8 facilitates zinc uptake into insulin secretory granules and changes to its abundance and/or activity disrupt β-cell zinc content and induce dysfunction associated with Type 2 Diabetes [198]. Stimulation of islets with high glucose induces elevations in cytosolic free Zn^{2+} [192], presumably representing increased zinc trafficking to secretory granules to replenish zinc lost through increased Zn^{2+}/insulin co-exocytosis. The responsible ZIP influx transporters (possibly ZIP6, ZIP8, ZIP9 and ZIP14; chapter 6) must also therefore be important for normal β-cell zinc trafficking and function.

ZIP6 is a member of the LIV-1 subfamily of ZIP transporters and is ubiquitously expressed in mammals [534]. Following translation, ZIP6 is expressed as an inactive pro-protein at the ER and subsequent N-terminal cleavage promotes translocation of the active protein to the plasma membrane [204]. ZIP6 forms heteromers with the phylogenetically closely related LIV-1 paralogue ZIP10, which exhibit non-redundant cellular signalling roles compared to each homodimer alone [206]. ZIP6:ZIP10 heteromers are transcriptionally regulated downstream of JAK-STAT3/5 pathways involved in cellular survival [207, 316] and are implicated in regulating the potent kinases GSK-3α and GSK-3β [206, 311]. ZIP6 has been strongly linked to inducing epithelial-mesenchymal transition for tumour cell migration via transcriptionally repressing ERK1/2-SNAIL-SLUG signalling [320, 321] and loss of ZIP6 in the breast cancer cell line MCF-7 disturbs intracellular zinc to promote cellular survival during hypoxia [535]. ZIP6 additionally co-

localises with and is evolutionarily homologous to prion proteins, although the full significance of this remains to be determined [536].

Limited information is available about the role of ZIP6 in β-cells. We and others [192, 218, 404] show that ZIP6 exhibits relatively high expression in β-cells, suggestive of a potential biological importance. Moreover, ZIP6 abundance may be linked to β-cell dysfunction since ZIP6 downregulation is observed in islets from type 2 diabetic patients (chapter 3 [404]). Previous studies suggest that ZIP6 is important for maintaining β-cell and islet zinc homeostasis [218] and that ZIP6 may function to suppress β-cell apoptosis, promote insulin expression and biosynthesis, and interact with GLP-1R to potentiate GSIS [319].

Changes to β-cell zinc are induced by the availability of extracellular zinc and impact cellular signalling and survival (chapter 5). We previously demonstrated that ZIP6 expression is supressed in the islets of some type 2 diabetic patients (chapter 3 [404]). Moreover, that ZIP6 is downregulated in MIN6 cells by prolonged stimulation, associated with decreased cellular zinc (chapter 4 [405]), and in response to high zinc (chapter 5). Here, we hypothesised that ZIP6 maintains β-cell phenotype and promotes survival in response to hypozincaemia. We aimed to generate ZIP6 knockout MIN6 cells and explore changes to cellular zinc, phenotype and survival following zinc depletion.

In this chapter we used CRISPR/Cas9 technology to generate ZIP6 knockout MIN6 cells. We showed that ZIP6 knockout disrupts *Slc39a* and *Slc30a* expression profiles, upregulates mRNA abundances for *Mt1*, *Mt2* and *Mtf1*, and increases cellular zinc uptake capacities in adequate (8μM) but not deficient (1μM) zinc culture. Furthermore, ZIP6-induced changes to cellular zinc are coupled with differential expression of transcription

factors important for β-cell function and survival, lowered rates of proliferation and apoptosis associated with mTOR signalling and *Stat3* induction, and decreased abundance of *Ins1* mRNA. Critically, we demonstrate ZIP6 is required to maintain β-cell zinc content, phenotype and survival and that ZIP6 plays a small, but potentially significant, role in the cellular response to zinc depletion.

7.3. Methods

7.3.1. Cell line and culture

MIN6 cells were cultured as described in section **2.1**. For zinc depletion experiments, standard growth medium was replaced with growth media containing 25mM glucose and 1μM or 8μM zinc for 48 h (section **2.2**).

7.3.2. CRISPR/Cas9 gene knockout

ZIP6/*Slc39a6* gene knockout was carried out using CRISPR/Cas9 gene technology, as detailed in section **2.5**. Primers to assess the occurrence of genome editing were designed through computationally aligning ZIP6 Cas9 nickase guide sequences to the mouse genome assembly mm10 (forward: CTTTGGGTTACAAGCCCCCT; reverse: CCTAGGAGGACCAAACAGGC (Sigma Aldrich); **Fig 7.1A**). Seven potential *Slc39a6* knockout populations were generated by serial dilution. PCR amplifications of the Cas9-targeted genomic loci were separated by agarose gel electrophoresis to reveal multiple variants shifted from the control in two of the seven colonies (clones 4 and 5; **Fig 7.1B**), consistent with editing of both *Slc39a6* copy variants, which was confirmed through Sanger sequencing for clone 4.

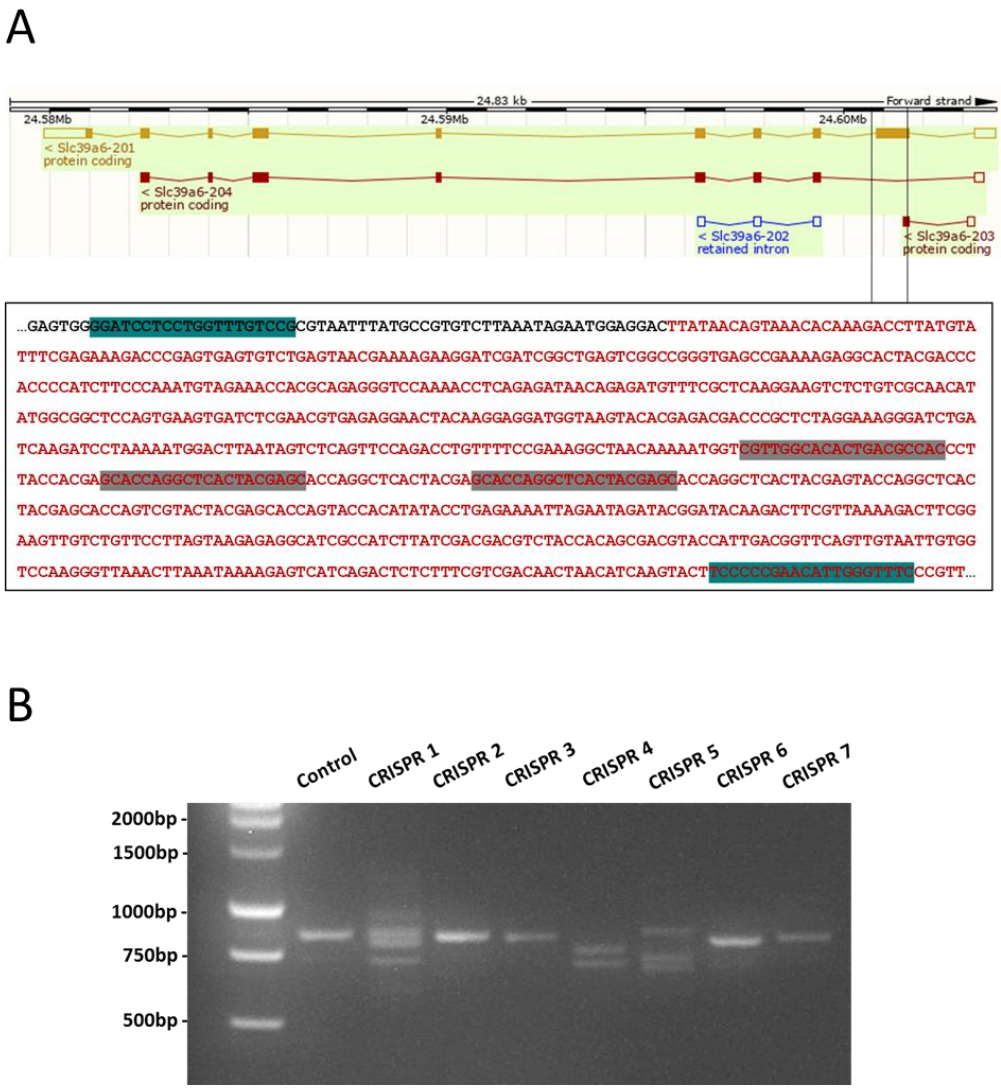

Fig 7.1. Amplification of ZIP6 CRISPR/Cas9-targeted genomic DNA. (A) Binding of CRISPR/Cas9 constructs to *Slc39a6* genomic DNA. ZIP6 was mapped to the reverse strand of chromosome 18 (24,579,881-24,603,817) on mouse genome GRCm38.p6 using the NCBI Ensembl genome browser 92. The Cas9 nuclease binds at the sequences highlighted in grey. The downstream nickase construct is predicted to bind at two identical *Slc39a6* loci in close proximity (depicted in **Fig 7.2**). Primers to assess knockdown bind at the sequences highlighted in turquoise. Red: exon 2. **(B)** Agarose gel electrophoresis showing PCR-amplified regions of *Slc39a6* from clonal MIN6 cell populations transfected with ZIP6 CRISPR/Cas9 or control nickase constructs. The gel was imaged using GeneSnap software.

7.3.3. Gene expression analysis

RNA was extracted from MIN6 cells, reverse transcribed to cDNA and relative expression assayed through qPCR. The full methodology and details of primers used are provided in section **2.6**. All results were presented as an expression ratio compared to control cells except for insulin gene expression, where values for FD (Log2) in expression are presented.

7.3.4. Cellular zinc parameters

Total MIN6 cell zinc contents were determined through ICP-MS (section **2.3)**. The kinetics of zinc uptake into MIN6 cells were assessed through ^{65}Zinc uptake assays (section **2.8**).

7.3.5. Cellular proliferation and apoptosis

The rates of MIN6 cell proliferation and apoptosis were determined as described in sections **2.9**-**2.10**. To investigate signalling via MAPK and mTOR signalling cascades, protein was extracted from cells and phosphorylation of the downstream components ERK1/2 (MAPK) and RPS6 (mTOR) were quantified by immunoblot (section **2.7**). The primary and secondary antibodies used are as detailed in section **6.3.7.**

7.3.6. Insulin secretion assays

The amounts of secreted insulin were determined through insulin secretion assays followed by quantification using insulin ELISA assays, as described in section **2.12**.

7.4. Results

7.4.1. ZIP6 knockout disrupts ZIP and ZnT expression

ZIP6 exists as homomers and heteromers with ZIP10 at the plasma membrane to facilitate zinc uptake into the cytosol [206]. ZIP6 expression is associated with multiple stresses that impact β-cell function (chapter 3-4 [404, 405]) and ZIP6 downregulation disrupts the cytosolic zinc content of MIN6 cells [218]. To explore which zinc transporters function in conjunction with ZIP6 to maintain β-cell zinc homeostasis, we examined expression profiles for the ZIP and ZnT paralogues in ZIP6 knockout MIN6 cells.

We first verified loss of ZIP6 abundance in CRISPR/Cas9-treated MIN6 cells. *In silico* sequence analysis revealed that ZIP6 CRISPR clone 4 is predicted to encode both 144 amino (protein A) and 728 amino (protein B) truncated versions of ZIP6 (wildtype: 765 amino acids) (**Fig 7.2**). Protein A consists of 144 amino acids of the ZIP6 NTD so is unlikely to be functionally active, whereas protein B only differs from the wildtype by the absence of 37 amino acids from the middle of its NTD; it is therefore possible protein B is active. Nevertheless, we only detected background expression for *Slc39a6* (9.73-fold depletion), suggesting genome editing probably resulted in translation of unstable mRNA, which was rapidly degraded, indicative of ZIP6 knockout. However, it should be noted that genome editing was not predicted to alter the sequence for ZIP6 variant 2 (ZIP6-204 in **Fig 7.1A**), nor are our primers predicted to recognise expression of this transcript. However, since ZIP6 variant 1 is the predominant ZIP6 isoform expressed in islets (chapter 3, **Fig 3.1** [404]) the impact of variant 2 is likely minimal.

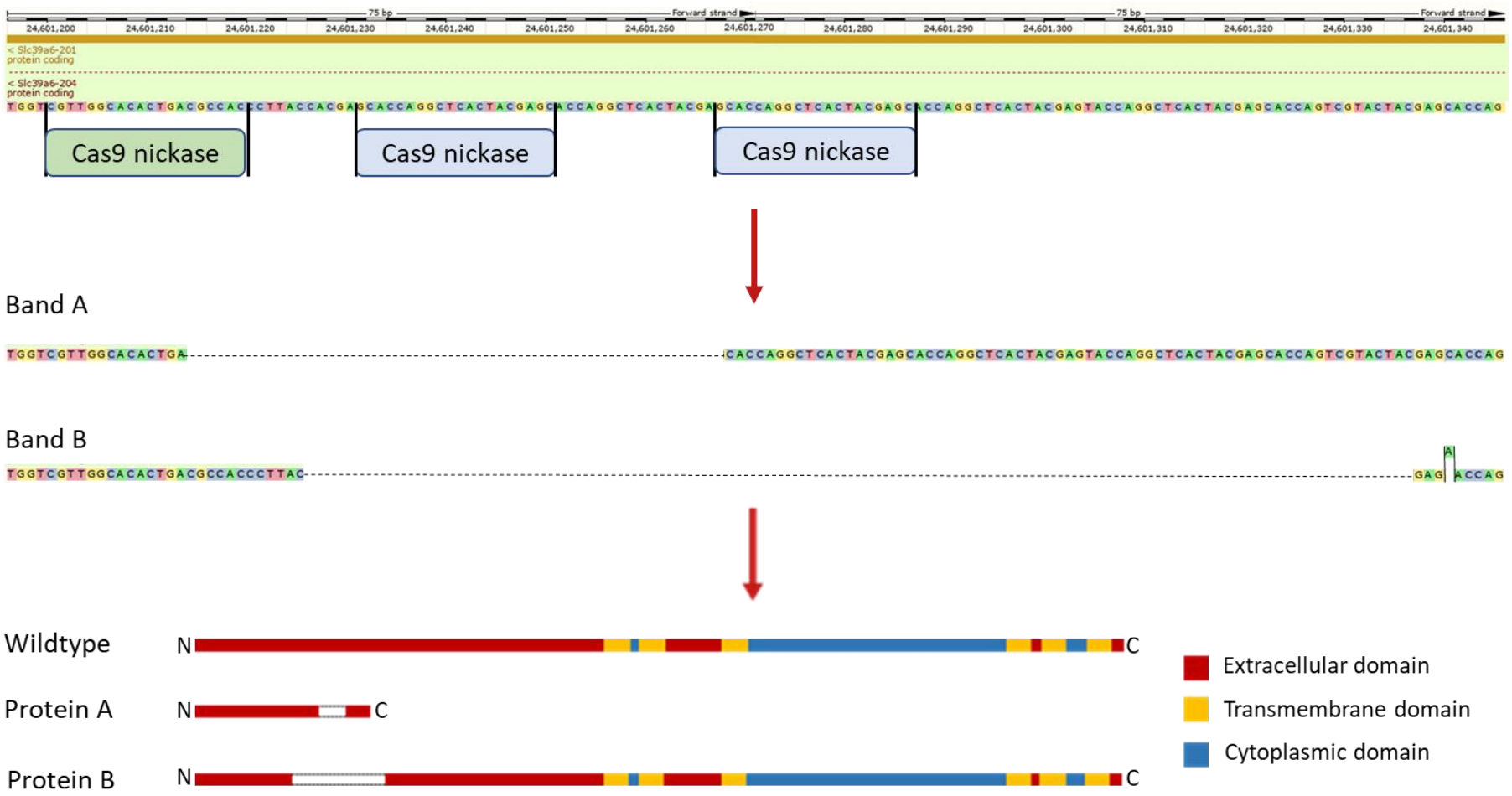

Fig 7.2. *Slc39a6* genome editing. Editing at *Slc30a6* exon 2 for ZIP6 CRISPR clone 4. The reference sequence was downloaded from the NCBI Ensembl genome browser 92 and binding of the ZIP6 Cas9 nickase constructs illustrated. The region shown spans Chr18:24601196-24601346 (mouse genome GRCm38.p6) on the negative strand. The sequences of the edited genome and protein domains of the translated proteins are shown.

ZIP6 knockout was coupled with downregulation of mRNA for *Slc39a2* (2.03-fold), *Slc39a10* (8.03-fold) and *Slc39a14* (1.64-fold), and upregulation for *Slc39a4* (4.58-fold) and *Slc39a13* (2.29-fold) compared to sham-CRISPR MIN6 cells (**Fig 7.3A**). When we examined expression of the ZnT paralogues, we recorded upregulation of mRNA for *Slc30a1* (1.92-fold), *Slc30a4* (1.88-fold), *Slc30a6* (1.50-fold) and *Slc30a7* (1.48-fold) (**Fig 7.3B**).

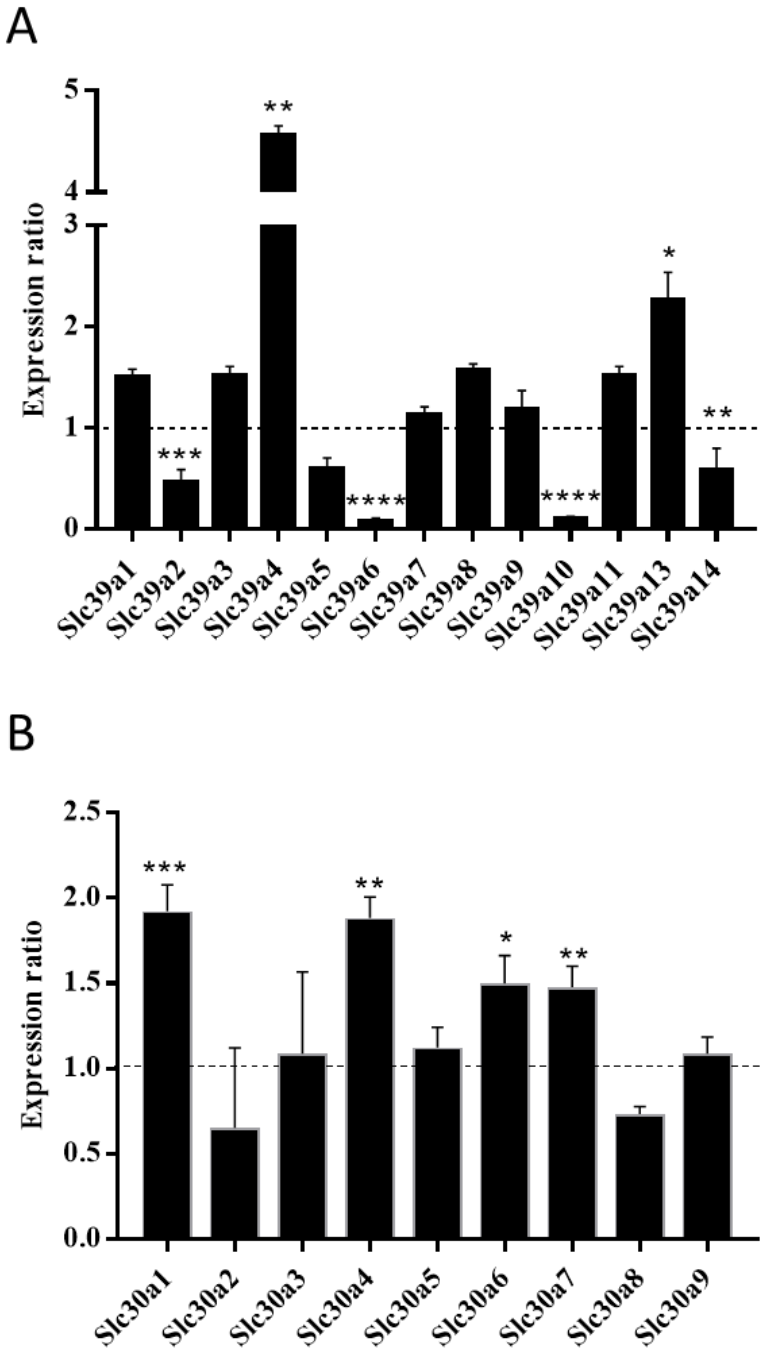

Fig 7.3. Zinc transporter expression in ZIP6 knockout MIN6 cells. mRNA expression for **(A)** *Slc39a* and (B) *Slc30a* paralogues in ZIP6 knockout MIN6 cells generated by CRISPR/Cas9 technology. We were unable to detect quantifiable expression for *Slc39a12* or *Slc30a10*. Expression is presented relative to sham-CRISPR MIN6 cells (control). Data were analysed using t-tests and corrected for multiple comparisons. Error bars show ± SEM. N=3. *p <0.05, **p<0.005, ***p<0.001, ****p<0.0001.

7.4.2. ZIP6 knockout increases cytosolic zinc in MIN6 cells

Extracellular zinc depletion decreases the zinc contents of MIN6 cells but increases the cellular zinc uptake capacities (chapter 5), presumably as an adaptive response to prevent zinc depletion-induced dysfunction [183]. To examine the role of ZIP6 in MIN6 cells for maintaining zinc homeostasis, we explored the zinc characteristics of ZIP6 knockout MIN6 cells cultured with depleted and adequate zinc.

Following culture of ZIP6 knockout MIN6 cells in zinc deficient (1µM zinc) media for 48 h, we observed a 1.35-fold reduction in total zinc compared to sham-CRISPR controls. However, we did not record a difference in cellular zinc content in response to 8µM zinc (**Fig 7.4A**). In ZIP6 knockout MIN6 cells, we noted upregulation of mRNA expression for *Mt1*, *Mt2* and *Mtf1* following culture with both 1µM (*Mt1*: 3.93-fold; *Mt2:* 3.58-fold; *Mtf1:* 1.41-fold) and 8µM (*Mt1*: 2.31-fold; *Mt2:* 2.37-fold*; Mtf1:* 1.49-fold) zinc (**Fig 7.4B**), suggestive of increased amounts of cytosolic free Zn^{2+} and activation of Zn^{2+}-responsive genes. To attribute these increases in mRNA abundances to cytosolic zinc influx, we examined the zinc uptake kinetics. We treated MIN6 cells with 1µM zinc or 8µM zinc for 48 h and then assayed ^{65}Zn uptake at a range of concentrations. We revealed pre-treatment with 8µM zinc increased zinc influx into ZIP6 knockout MIN6 cells at all ^{65}Zn concentrations tested compared to sham-CRISPR controls (**Fig 7.4C-D**). However, this did not translate into significant differences in either J_{max} or $K_{0.5}$.

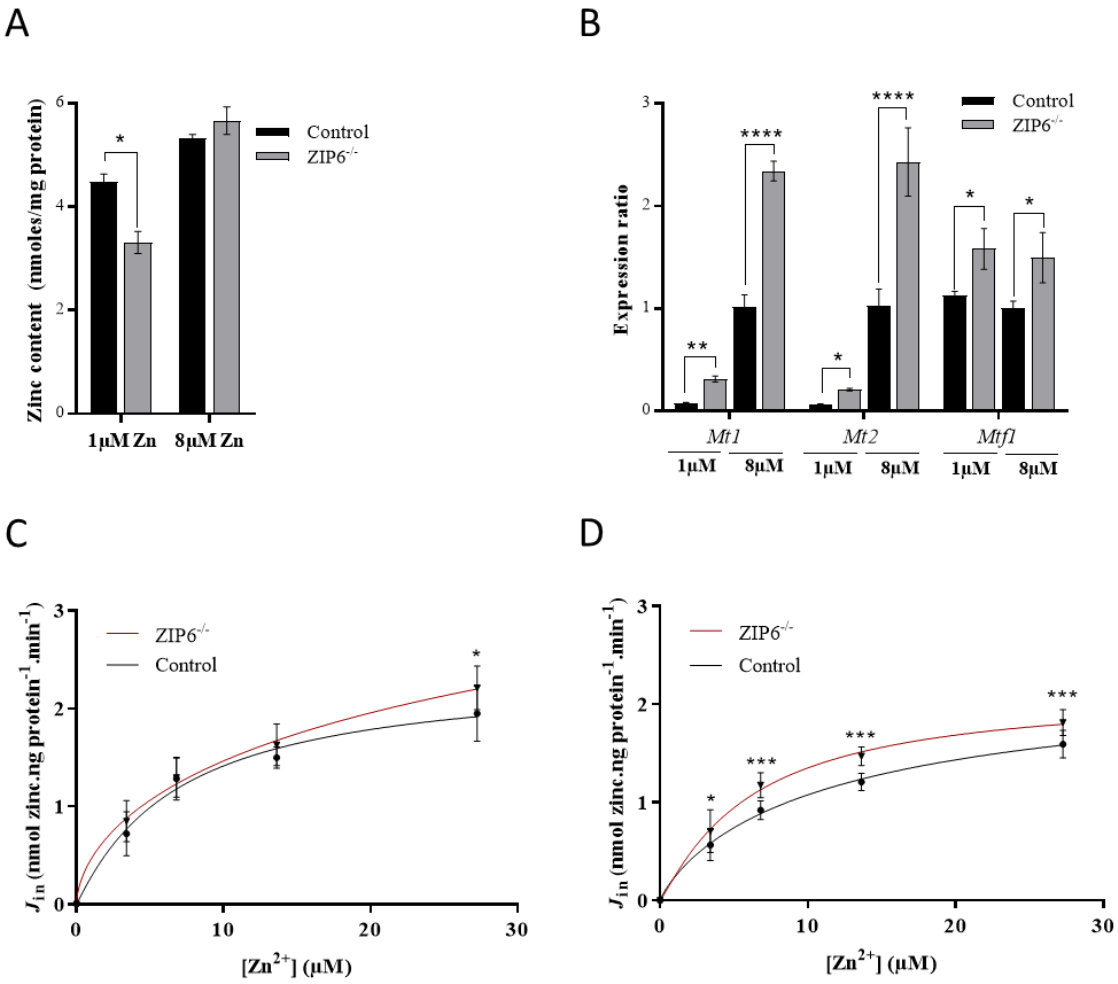

Fig 7.4. Zinc content and uptake kinetics for ZIP6 knockout MIN6 cells in response to zinc depletion. (A) Total cellular zinc content. Zinc content was determined through ICP-MS and normalised to protein. **(B)** mRNA expression for *Mt1*, *Mt2* and *Mtf1*. Changes in mRNA expression were calculated through qPCR and expressed as a ratio relative to sham-CRISPR MIN6 cells cultured with 8µM zinc (control). **(C-D)** Uptake kinetics for zinc into cells pre-treated with **(C)** 1µM or **(D)** 8µM zinc. Red: ZIP6 knockout MIN6 cells; black: sham-CRISPR MIN6 cells (control). All experiments were carried out following culture with 1µM or 8µM zinc for 48 h. Data were analysed by 2-way ANOVA followed by **(A-B)** Tukey's or **(C-D)** Sidak's multiple comparison test. ZIP6 knockout MIN6 cells: ZIP6$^{-/-}$. For **(A)** N=4 and **(B-D)** N=3. Error bars show ± SEM. *p <0.05, **p <0.005, ***p <0.001, ****p <0.0001.

7.4.3. ZIP6 knockout disrupts expression of important β-cell markers

Above, we indicate that ZIP6 has pronounced effects on expression of β-cell ZIP and ZnT transporters and cellular zinc uptake and accumulation. Critically, total cellular zinc and the cellular zinc uptake capacities differed dependent on pre-treatment of ZIP6 knockout cells with 1µM or 8µM zinc. To assess the impact of ZIP6-induced zinc disruption for β-cell phenotype, we examined expression of markers for β-cell identity and function [*Foxa1, Foxa2, Foxo1, Hnf1b, Hnf4a, MafA, Mnx-1, Nkx2.2, Nkx6.1, Neurod1, Pax4, Pax6* and *Pdx-1,* many of which show Zn^{2+}-responsive expression in β-cells (chapter 4 [405])] following loss of ZIP6 abundance.

ZIP6 knockout MIN6 cells cultured with either 1µM or 8µM zinc for 48 h exhibited upregulation of mRNA for *Foxa1* (1µM: 2.38-fold; 8µM: 2.24-fold), *MafA* (1µM: 1.70-fold; 8µM: 1.49-fold), *Nkx6.1* (1µM: 1.56-fold; 8µM: 1.31-fold) and *Pdx-1* (1µM: 1.45-fold; 8µM: 1.39-fold) and downregulation for *Hnf4a* (1µM: 5.69-fold; 8µM: 4.72-fold), *Nkx2*.2 (1µM: 1.51-fold; 8µM: 1.48-fold) and *Pax4* (1µM: 14.47-fold; 8µM: 13.03-fold) compared to sham-CRISPR controls. We additionally noted upregulation of mRNA for *Foxo1* (1.33-fold) in ZIP6 knockout MIN6 cells cultured with 1µM zinc and *Pax6* (1.55-fold) in cells cultured with 8µM zinc (**Fig 7.5**).

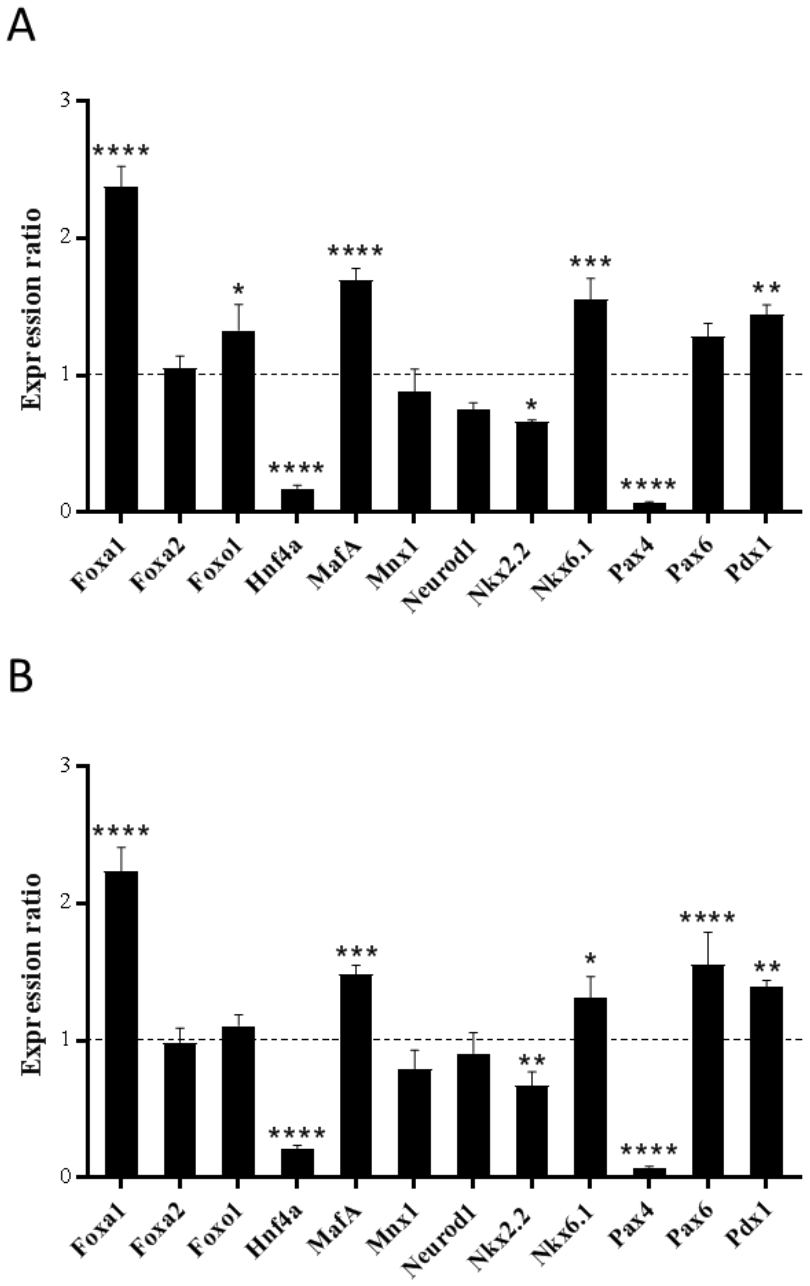

Fig 7.5. mRNA expression for transcription factors in ZIP6 knockout MIN6 cells. Expression in response to **(A)** 1µM or **(B)** 8µM extracellular zinc. Expression was assayed through qPCR and calculated as a ratio compared to sham-CRISPR MIN6 cells cultured with **(A)** 1µM or **(B)** 8µM extracellular zinc (controls). Experiments were carried out at 48 h. Data were analysed using t-tests and corrected for multiple comparisons. Error bars show ± SEM. N=3. *p <0.05**,** **p <0.005, ***p <0.001, ****p <0.0001.

7.4.4. ZIP6 knockout lowers MIN6 cell apoptosis and proliferation

ZIP6:ZIP10 heteromers stimulate proliferation and survival of mammalian cells [206]. We have shown that changes to extracellular zinc decrease MIN6 cell survival (chapter 5) and that ZIP6 abundance is associated with differential expression for multiple transcription factors important for β-cell phenotype, function and mass (above, section **7.4.3**). Disruption of ZIP6 expression and associated changes to MIN6 cell zinc may therefore impact cellular survival. We examined the survival characteristics of ZIP6 knockout MIN6 cells and, since ZIP6 induces differences to the cellular zinc content and the expression profiles of β-cell markers dependent on extracellular zinc, whether these differ following zinc depletion.

ZIP6 knockout MIN6 cells cultured with 1μM or 8μM zinc for 48 h exhibited lowered rates of proliferation (1μM: 1.35-fold; 8μM: 1.18-fold) and apoptosis (1μM: 1.62-fold; 8μM: 1.48-fold) compared to sham-CRISPR controls (**Fig 7.6A-B**); this observation is unexpected since ZIP6 deficiency has been associated with increased cellular survival [535]. MAPK and mTOR signalling pathways both regulate cell cycle progression, proliferation and apoptosis [51, 69] (depicted in chapter 5, **Fig 5.5**) and can be mediated by zinc [313, 314]. To examine if ZIP6-induced changes to MIN6 cell survival may be induced via MAPK or mTOR cascades, we assessed phosphorylation of their downstream components ERK1/2 (at p42/p44; MAPK) and RPS6 (at Ser235/236; mTOR) (**Fig 7.6C-E**). We did not observe any differences in p42/p44 ERK1/2 phosphorylation between ZIP6 knockout MIN6 cells and controls. However, there was an increase in Ser235/236 RPS6 phosphorylation following loss of ZIP6 abundance (1μM zinc: 1.63-fold; 8μM zinc: 1.34-fold). Finally, we examined expression of the transcription factor STAT3, which mediates key roles in growth, survival and development [507] (depicted in chapter 6, **Fig. 6.8**). *Stat3* mRNA was upregulated in ZIP6 knockout MIN6 cells compared to

sham-CRISPR controls in response to both 1µM [1.59-fold (p=0.03, n=3)] and 8µM [1.43-fold (p=0.04, n=3)] zinc.

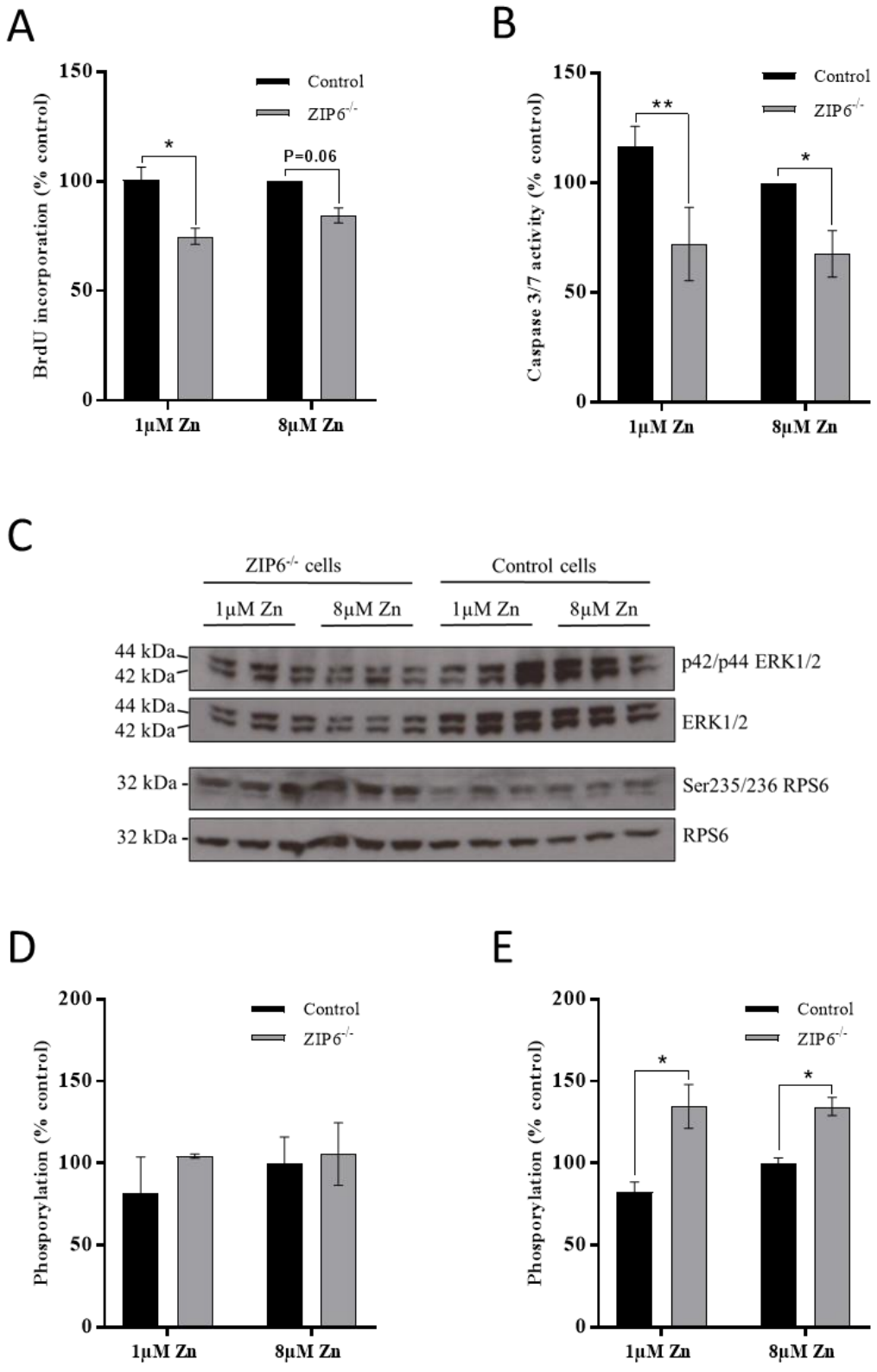

Fig 7.6. Survival of ZIP6 knockout MIN6 cells in response to zinc depletion. (A) MIN6 cell proliferation, determined by BrdU incorporation. **(B)** MIN6 cell apoptosis, determined by Caspase 3/7 assays. **(C-E)** Phosphorylation of ERK1/2 and RPS6. **(C)**

Immunoblots of p42/p44 ERK1/2, ERK1/2, Ser235/236 RPS6 and RPS6. **(D-E)** Quantification of immunoblots for **(D)** p42/p44 ERK1/2 vs ERK1/2 and **(E)** Ser235/236 RPS6 vs RPS6. Immunoblot quantification was carried out using ImageJ software. All experiments were carried out following culture of cells with 1µM or 8µM zinc for 48 h. Data were analysed by 2-way ANOVA followed by Sidak's multiple comparison test. **(A-B and D-E)** Results are relative to sham-CRISPR MIN6 cells cultured with 8µM zinc (control). ZIP6 knockout MIN6 cells: $ZIP6^{-/-}$. Error bars show ± SEM. N=3. *p <0.05**,** **p <0.005.

7.4.5. ZIP6 knockout alters insulin gene expression

Zinc is reported to promote both stimulatory [219, 329] and inhibitory [424] effects on β-cell insulin secretion. Moreover, the transcription factors impacted by ZIP6 knockout (above, section **7.4.3**) are all involved in regulating insulin production and/or secretion. To explore the role of ZIP6 and ZIP6-mediated zinc disruption on β-cell insulin secretory function, we examined expression of the two insulin genes present in rodent (*Ins1* and *Ins2*) in ZIP6 knockout MIN6 cells and insulin secretion from ZIP6 knockout MIN6 cells following culture with zinc depletion. We observed downregulation of *Ins1* mRNA in ZIP6 knockout MIN6 cells compared to sham-CRISPR controls (1µM zinc: 3.24-fold; 8µM zinc: 3.38-fold). We additionally recorded a modest 1.62-fold upregulation of *Ins2* mRNA for cells cultured with 8µM zinc (**Fig 7.7A**). However, we did not observe any differences in basal or KCl-stimulated insulin secretion from MIN6 cells dependent on ZIP6 abundance (**Fig 7.7B)**.

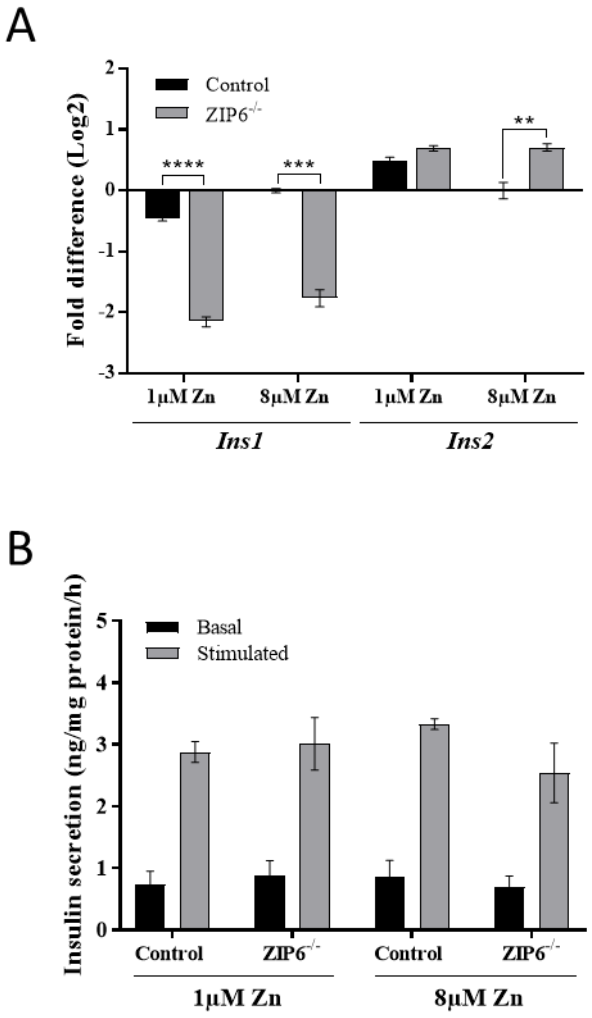

Fig 7.7. Insulin parameters for ZIP6 knockout MIN6 cells in response to zinc depletion. (A) *Ins1* and *Ins2* mRNA expression. Expression was assayed through qPCR and calculated as FD (Log2) in expression compared to sham-CRISPR MIN6 cells cultured with 8µM zinc (control). **(B)** Insulin secretion from MIN6 cells following addition of 3mM glucose (basal) or 40mM KCl (stimulated). The amounts of secreted insulin were calculated through insulin secretion assays and normalised to total protein. All experiments were carried out following culture with 1µM or 8µM zinc for 48 h. Data were analysed by 2-way ANOVA followed by Tukey's multiple comparison test. ZIP6 knockout MIN6 cells: $ZIP6^{-/-}$. Error bars show ± SEM. N=3. **p <0.005, ***p <0.001, ****p <0.0001.

7.5. Discussion

Extracellular zinc depletion reduces the total zinc content of MIN6 cells, induces changes to the transcriptome and decreases cellular survival (chapter 5). Previous studies by ourselves and others [192, 218, 404] suggest ZIP6 plays key roles in β-cell zinc uptake and that ZIP6 downregulation may impact intracellular zinc and induce dysfunction. Here, we generated and studied ZIP6 knockout MIN6 cells to explore the role of ZIP6 in the β-cell adaptive response to extracellular zinc depletion

Zinc transporters are regulated at transcriptional, post-transcriptional and post-translational levels in β-cells in response to nutrients, hormones, growth factors and stresses to maintain adequate supplies of zinc [147, 420]. Many ZIP and ZnT paralogues exhibit redundant functions [537, 538] and loss of transporters important for β-cells may induce differential expression and/or activities of coordinated paralogues to prevent zinc depletion-induced dysfunction. ZIP6 ablation was coupled with downregulation of mRNA encoding for ZIP2, ZIP10 and ZIP14 and upregulation for ZIP4, ZIP13, ZnT1, ZnT4, ZnT6 and ZnT7. Disruption of any of these transporters may alter cellular zinc trafficking and content. ZIP13 localises to the ER and Golgi apparatus, however the other disrupted ZIPs all present at the plasma membrane [147]. ZIP10 forms heteromers with ZIP6 to mediate proliferation [539] and act as a scaffold for GSK-3 binding [206], a critical regulator of proliferation and survival [540]. Interestingly, Zip10 knockdown induces expression of Zip6 in zebrafish embryos, presumably to compensate for loss of Zip10 function [206], however we did not observe the reverse in MIN6 cells. We previously identified ZIP14 as potentially important for β-cell zinc influx [404] and ZIP14 null mice exhibit higher islet insulin contents than controls [541], which is not easy to explain but indicates that downregulation may impact insulin secretory function.

Upregulation of ZIP4 and ZIP13 could represent compensatory mechanisms to increase β-cell cytosolic free Zn^{2+} in the absence of ZIP6. We previously identified ZIP13, which fluxes zinc out of the secretory pathway [542], as potentially important for β-cell function [404]. ZIP4 responds to zinc deficiency to induce rapid plasma membrane ZIP4 accumulation [543] and, although exhibiting relatively low expression in β-cells [404], may play important roles in β-cell zinc accumulation [219], contradictory to our conclusion in chapter 3 [404]. However, upregulation of ZnT1, ZnT4, ZnT6 and ZnT7 would be predicted to lower cytosolic zinc. Aside from ZnT1, which facilitates zinc efflux at the plasma membrane, these paralogues reside in the membranes of intracellular compartments including the trans-Golgi network and vesicles (ZnT4 and ZnT6) and the Golgi apparatus (ZnT7) in β-cells [185, 194, 195]. Upregulation may therefore increase the intracellular storage of zinc to ensure adequate supplies in the absence of ZIP6.

Changes to zinc transporter expression profiles may alter cellular function and phenotype through disrupting zinc accumulation and/or transporter-protein interactions involved in intracellular signalling. When we characterised the zinc phenotype of ZIP6 knockout MIN6 cells, we recorded upregulation of *Mt1*, *Mt2* and *Mtf1* mRNA, indicative of elevated cytosolic zinc [449], and cells exhibited higher zinc uptake capacities in adequate zinc culture. MTF1 responds to free Zn^{2+} fluctuations to mediate expression of genes involved in zinc homeostasis and anti-oxidative responses, including the MTs [544], which maintain cytosolic concentrations by zinc donation, sequestration and/or redox control [156]. Increases in cytosolic zinc uptake and accumulation suggest that predominant zinc trafficking following loss of ZIP6 may be mediated by the increased abundances of ZIP4 at the plasma membrane and ZIP13 at the ER and Golgi apparatus. However, we were unable to correlate elevated cytosolic zinc to an increase in total zinc. A previous study suggested simultaneous loss of ZIP6 and Golgi-localised ZIP7 is

required to inhibit $ZnSO_4^-$ and glucose-induced increases in cellular zinc [218]. The lowered total zinc content of ZIP6 knockout MIN6 cells cultured with depleted zinc indicates that ZIP6 is required for sufficient MIN6 cell zinc uptake in the presence of low extracellular zinc, such as the hypozincaemia observed in some human type 2 diabetic patients [140, 283, 284].

Zinc deficiency induces profound consequences for the β-cell transcriptome (chapter 5), including disruption of multiple β-cell/islet specific transcription factors (chapter 4 [405]). In this chapter, we showed that ZIP6-induced changes to MIN6 cell zinc are associated with distinct expression profiles for important β-cell markers. We observed upregulation of mRNA for *Foxa1*, *MafA*, *Nkx6.1*, *Pdx-1* and downregulation for *Hnf4a*, *Nkx2.2* and *Pax4*; changes to the abundances of any of these transcription factors have potential to disrupt cellular function in glycaemic control. MAFA, NKX6.1 and PDX-1 are major transcriptional regulators of β-cell development, phenotype and function [100, 116, 517] and exhibit Zn^{2+}-responsive expression in β-cells (chapter 4 [405]), whereas FOXA1 acts in combination with FOXA2 to mediate insulin secretion and carbohydrate metabolism [516]. HNF4A, NKX2.2 and PAX4 are all required to maintain mature β-cell identity and optimal insulin secretion [350, 545, 546]. HNF4A additionally regulates nutrient-induced insulin secretion [545] and PAX4 stimulates islet proliferation and survival [513]. Moreover, monogenetic mutations in HNF4A, PDX-1 and PAX4 result in MODY development [547]. We additionally observed upregulation of mRNA for *Foxo1* in ZIP6 knockout MIN6 cells in response to zinc depletion and *Pax6* in cells cultured with adequate zinc. FOXO1, which is ubiquitously expressed and is a major transcriptional regulator of cellular survival and function, inhibits proliferation by regulating cyclin-dependent kinase inhibitor 1B [548, 549] and can promote apoptosis [550]. PAX6 is required for maximum insulin production [551, 552] and upregulation is consistent with

the observed increase in *Ins2* mRNA expression. Consequences of disruption of these Zn^{2+}-responsive markers for β-cell function are discussed in more detail in chapter 4 [405].

Tightly maintained zinc homeostasis is required for cellular proliferation and mass [519]. We demonstrate the disrupted zinc phenotype of ZIP6 knockout MIN6 cells is coupled with lowered rates of cellular proliferation and apoptosis. ZIP6:ZIP10 heteromers promote proliferation [539], however ZIP6 deficiency increases survival in response to hypoxia [535] and can induce ROS without triggering apoptosis [218]. Simultaneous reductions in proliferation and apoptosis is unusual but may be indicative of differentiation, which has previously been shown for adipocytes and epidermal keratinocyte cells [553-555] and could explain the observed changes to β-cell transcription factor expression. Simultaneous decreases have additionally been recorded for macrophages stimulated by danger signals [556] and hepatic stellate cells in response to TNF-α and TNF-β [557]. We observed increased RPS6 phosphorylation in ZIP6 knockout MIN6 cells, indicative of enhanced signalling via mTOR cascades. ZIP6:ZIP10 heteromers act as a scaffold for GSK-3 binding and inhibitory phosphorylation; loss of ZIP6 may increase net activation of GSK-3, which phosphorylates upstream components of mTOR cascades including IRS-1, IRS-2, AKT, PTEN, RICTOR, TSC1 and TSC2, to regulate mTOR signalling [540, 558].

mTOR cascades promote protein synthesis and β-cell growth and secretory function via activation of the RPS6 kinase S6K. RPS6 is a critical component of the 40 S ribosomal subunit [559] and represents a point of regulatory convergence for pathways controlling translation initiation. RPS6 undergoes inducible phosphorylation at five C-terminal serine residues to mediate cell size through promoting growth and proliferation [560]. Islets

from $RPS6^{P-/-}$ mice contain less insulin compared to those from $RPS6^{P+/+}$ controls and present with impaired glucose tolerances [63], and mice deficient for the RPS6 upstream kinase S6K1 present with impaired glucose homeostasis [561]. Knockout of ZIP4 in the mouse intestine lowers cytosolic zinc (as measured by MT expression), which decreases the proportion of phosphorylated RPS6 in the villus epithelium, accompanied by diminished mTOR activity and impaired protein synthesis [313]. Consistently, we showed that ZIP6 knockout enhances RPS6 phosphorylation, which may result from the increased cytosolic zinc and/or upregulation of ZIP4. Loss of ZIP6 could therefore be beneficial for insulin tolerance and β-cell growth. However, we would expect this to be accompanied by increased insulin synthesis, which was not the case in our ZIP6 knockout MIN6 cells.

We additionally recorded upregulation of mRNA for *Stat3* in ZIP6 knockout MIN6 cells. The role of STAT3 for regulating β-cell function, proliferation and survival is discussed in chapter 6 (section **6.5.2**). Of potential importance, STAT3 activates ZIP6 and ZIP10 transcription [207, 316] and STAT3 upregulation may be a compensatory response for loss of ZIP6. Similarly, knockdown of Zip10 in zebrafish upregulates *stat3* and *zip6* mRNA [206]. STAT3 is activated by mTOR signalling [562, 563] and zinc, and has been specifically linked to enhanced ZIP4 signalling in pancreatic cancer [564]. Activating STAT3 mutations cause neonatal diabetes through premature induction of pancreatic differentiation [565]. However, the total β-cell mass, irrespective of cellular number and size, determines the insulin secretory response [63]. Larger cells may be secondary to the reduced metabolic state characteristic of decreased proliferation and apoptosis, and future work should investigate the sizes of individual ZIP6 knockout MIN6 cells compared to controls. As discussed in chapter 6 (section **6.5.2**), it is possible that decreased proliferation may be secondary to the CRISPR/Cas9 genome editing technique rather than

transporter knockdown [529], however the use of sham-CRISPR control cells reduce this likelihood.

The tightly regulated phenotype ensures β-cells mount appropriate insulin secretory responses to extracellular glucose. The phenotype induced in MIN6 cells by loss of ZIP6 lowered mRNA expression for *Ins1*, indicative of loss of insulin secretory function and onset of β-cell failure. We additionally noted modest upregulation of mRNA for *Ins2* in cells cultured with adequate zinc. Unlike in human where only one insulin gene exists, rodents encode two insulin paralogues, insulin 1 and insulin 2. Although mouse models suggest insulin 1 knockout induces insulin deficiency whereas loss of insulin 2 does not impact β-cell insulin content [566], the roles of each in systemic glucose regulation remains unclear [508]. Insulin 2 abundance may be induced to compensate for loss of insulin 1 and ZIP6-regulated pathways could be critical for enhancing insulin 2 expression in hypozincaemic conditions, which would directly link the supressed ZIP6 phenotype observed in some type 2 diabetic islets [404] to loss of insulin secretory function. However, we did not record any differences in basal or KCl-stimulated insulin release from ZIP6 knockout MIN6 cells, consistent with a previous study that showed simultaneous knockdown of both ZIP6 and ZIP7 is required to inhibit insulin secretion [218]. The role of zinc in regulating insulin secretion is discussed in more detail in chapter 5 (section **5.5.1**). However, as previously noted, stimulating cells with KCl may not replicate differences in the secretory response that exist following glucose stimulation.

7.6. Conclusion

In this study we explored the role of ZIP6 in the MIN6 cell adaptive response to extracellular zinc depletion. We showed that ZIP6 knockout disrupts expression of multiple ZIP and ZnT paralogues and MIN6 cell zinc trafficking and accumulation. Our

data suggest ZIP6 is required for adequate zinc uptake in response to zinc depletion and that loss of ZIP6 abundance disrupts regulation of the insulin gene. Moreover, ZIP6 mediates transcription of multiple markers important for β-cell identity and regulates survival of MIN6 cells through activating mTOR cascades and upregulating expression of STAT3. Critically, our data highlight the importance of ZIP6 for β-cell identity and survival and show that ZIP6 may be important for the β-cell adaptive response to hypozincaemia.

8. General Discussion

Multiple studies have associated zinc and its transporters with development and progression of Type 2 Diabetes. Systemic hypozincaemia is evident in some type 2 diabetic patients [140, 283, 284] due to reduced plasma zinc transport resulting from hyperglycaemia-induced HSA glycation [409], and increased urinary zinc loss [410]. Moreover, the R325W missense mutation in the predominantly β-cell-specific zinc transporter ZnT8 is associated with an odds ratio for Type 2 Diabetes predisposition of 1.14-1.15, with a ~16.5% increase in relative risk per risk allele [243, 256-259]. However, the mechanism whereby ZnT8 risk variants predispose patients to Type 2 Diabetes remains unclear: the R325W polymorphism disrupts zinc transport into granules through altering ZnT8 dimer formation and stability [269] but minimal differences in glycaemic parameters are observed following ZnT8 knockout in mouse [198]. The relatively limited existing evidence further suggests that loss-of-function ZnT8 mutants induced through SNPs or haploinsufficiency are collectively associated with a 65% reduced risk of Type 2 Diabetes [271]. A recent study examining the most abundant loss-of-function variant R138X, which encodes a premature stop codon, demonstrated that ZnT8 truncation increases the β-cells' capacity to secrete insulin in high glucose conditions [280]. Additional studies show ZnT8-mediated granule zinc uptake is coupled with cytosolic free Zn^{2+} elevations [192], presumably representing coordinated ZIP-facilitated zinc influx and trafficking. Spikes in cytosolic free Zn^{2+} may therefore induce further consequences for β-cells, which have not previously been examined, suggesting cytosolic zinc elevations are important for β-cells aside from insulin processing in secretory granules. ZnT8-induced β-cell dysfunction may reflect these additional roles. Moreover, links between the increased requirement for β-cell zinc uptake during hyperglycaemia

(due to elevated Zn^{2+}/insulin co-release), the reduced pool of available zinc present in hypozincaemic type 2 diabetic patients, and β-cell zinc content, phenotype and survival remain unexplored.

8.1. Overview of results

In this project we postulated that zinc uptake into insulin granules is coordinated with ZIP-facilitated cytosolic zinc influx and that different ZnT8 abundances and genotypes associated with Type 2 Diabetes interfere with ZIP-regulated zinc trafficking. We further hypothesized that alterations to the abundances/activities of these ZIP transporters impact β-cell phenotype and function. Through the research carried out during this PhD, we can partially accept this hypothesis. We can confirm that ZnT8-facilitated granule zinc uptake is associated with ZIP expression, however we are unable to comment on how this relates to the R325W genotype. Moreover, we can confirm that loss of ZIP6 abundance disrupts β-cell zinc content and phenotype and reduces cellular survival. Discussion of how we addressed the project aims are provided below.

Aim 1: To identify ZIP transporters that functionally coordinate with ZnT8 to maintain normal zinc trafficking in β-cells and explore whether these transporters are regulated differently based on ZnT8 activity.

Zinc transporters exhibit unique cell- and tissue-specific expression and responsiveness to tightly control zinc homeostasis [170]. We therefore first sought to identify ZIP paralogues important for β-cell function (Chapter 3 [404]). We hypothesised that important ZIP paralogues are regulated by stresses that negatively impact β-cell function and are associated with β-cell failure during Type 2 Diabetes. We used a systematic approach combined with experimental expression analysis to identify ZIP1 in rodent and

ZIP6, ZIP7, ZIP9, ZIP13 and ZIP14 in human and rodent as potentially biologically important for mediating β-cell zinc homeostasis, function and phenotype. We further aligned ZIP mRNA and protein sequences to show high human-rodent conservation, suggesting paralogues substitute functionally in both backgrounds and that the data generated from MIN6 cell studies during this project are likely translatable to human. The results from this analysis were used to focus further investigation of ZIP transporters in β-cells.

ZnT8 activity is associated with increases in cytosolic free Zn^{2+} and Type 2 Diabetes development [192]. To explore ZIP transporter expression in response to ZnT8 abundance, we hypothesised that ZnT8 functions cooperatively with ZIP transporters to regulate β-cell zinc homeostasis (chapter 6). Since ZnT8 abundance is lowered by multiple stresses that negatively impact β-cell function [179, 186, 227], we examined the initial and final ZIP responses to stress-induced ZnT8 downregulation. Using siRNA, we noted initial upregulation of ZIP14 and downregulation of ZIP1, ZIP8 and ZIP9. In the final state following loss of ZnT8 abundance (explored using our ZnT8 haploinsufficient MIN6 cell model), we demonstrated that ZIP8 and ZIP14 are downregulated. From these data, we concluded that ZIP8 and ZIP14 are the key paralogues mediating β-cell zinc trafficking to coordinate with ZnT8 activity, and that ZIP1 and ZIP9 may additionally play important roles in the initial response to loss of ZnT8 (summarised in **Fig 8.1**).

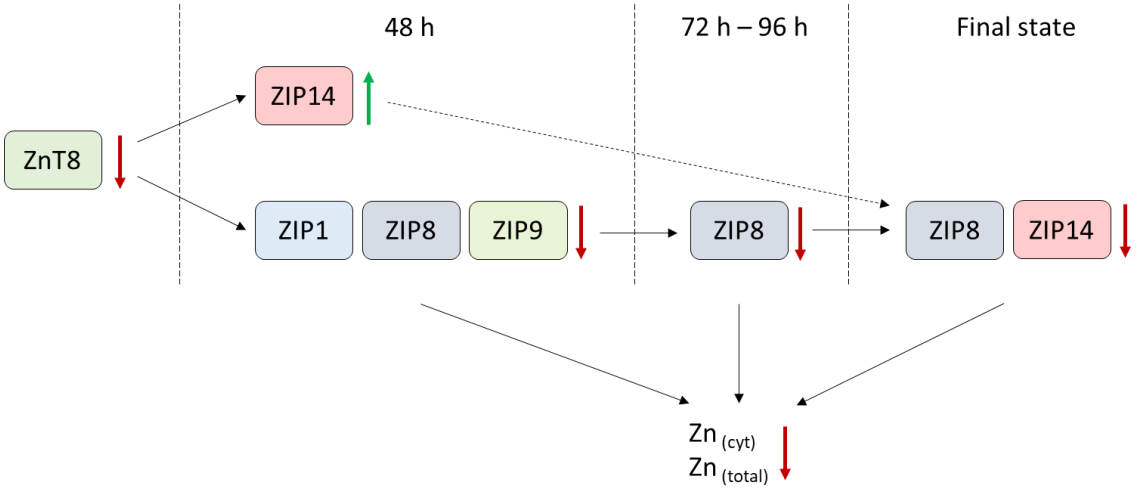

Fig 8.1. Proposed sequence of changes to ZIP transporter expression following stress-induced ZnT8 downregulation. Red arrows: downregulation. Green arrows: upregulation. $Zn_{(cyt)}$: cytosolic zinc content. $Zn_{(total)}$: total zinc content. The time-points indicate hours post-transfection.

We additionally explored transcriptional co-regulation of β-cell ZIP paralogues with ZnT8 by the key β-cell transcription factor PDX-1 (Chapter 6). PDX-1 regulates ZnT8 transcription through targeting two *SLC30A8* enhancers in β-cells [200] and we showed in our systematic review that PDX-1 abundance is associated with mRNA expression for multiple ZIP paralogues (chapter 3 [404]). We hypothesised that PDX-1 may be involved in regulating coordinated ZnT8-ZIP expression. We used bioinformatics to show that PDX-1 is predicted to bind enhancers for ZIP6 and ZIP9 and may therefore directly co-regulate their expression alongside ZnT8. Using PDX-1 overexpression studies, we demonstrated that PDX-1 upregulates multiple ZIP paralogues including ZIP6 and ZIP9, indicating PDX-1 may be important for transcriptionally mediating zinc trafficking in β-cells. However, mechanistic investigations are required to confirm these results. Taken together, our data indicate that ZnT8 may be transcriptionally co-regulated with ZIP6 and

ZIP9 by PDX-1 to maintain adequate zinc uptake into the cytosol, and that expression of ZIP8 and ZIP14 are altered in response to ZnT8 activity to rapidly adapt zinc influx following stress-induced ZnT8 downregulation.

Aim 2: To explore the consequences of the hyperglycaemia and hypozincaemia associated with Type 2 Diabetes for β-cell ZIP transporter expression, zinc content and cellular phenotype.

Hyperglycaemia is characteristic of all diabetic patients and is a major factor driving β-cell dysfunction. Of importance, hyperglycaemia induces increased Zn^{2+}/insulin co-exocytosis [567, 568] and is associated with downregulation of ZnT8 [228]. To explore the consequences of hyperglycaemia for the β-cell zinc response, we postulated that ZIP transporters are involved in intracellular zinc homeostasis during β-cell stimulation (chapter 4 [405]). We further hypothesised that prolonged stimulation, representative of hyperglycaemia *in vivo*, leads to cellular zinc loss and that this may influence β-cell phenotype. Our data suggest that prolonged stimulation decreases the zinc content of MIN6 cells, associated with initial upregulation of ZIP1 protein expression following by transcriptional downregulation of ZIP1, ZIP6, ZIP7 and ZIP14. We further demonstrated that multiple markers for β-cell identity are Zn^{2+}-responsive in a mammalian system and suggest that hyperglycaemia-induced downregulation of these markers and consequential loss of cellular phenotype may be driven by lowered cellular zinc. These data are summarised in **Fig 8.2**.

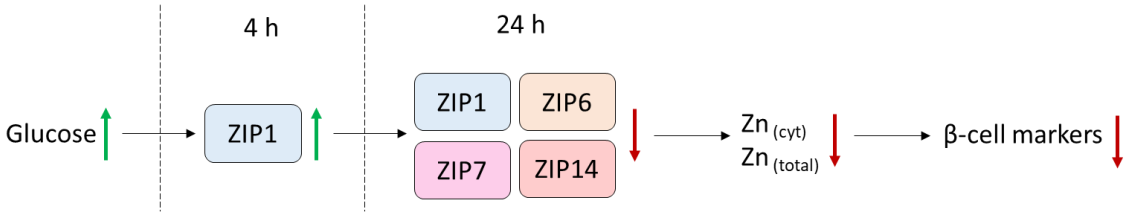

Fig 8.2. Proposed sequence of changes to β-cell signalling in response to hyperglycaemia. Data included: ZIP transporter expression, cellular zinc content and expression of β-cell markers. Red arrows: downregulation. Green arrows: upregulation. $Zn_{(cyt)}$: cytosolic zinc content. $Zn_{(total)}$: total zinc content. The time-points indicate hours following stimulation of cells with KCl.

The hypozincaemia present in some type 2 diabetic patients [140, 283, 284] presumably reduces the amounts of zinc available for uptake into β-cells. To explore the relationship between hypozincaemia and β-cell zinc, we hypothesised that changes to extracellular zinc, representing serum zinc *in vivo*, alter β-cell zinc content and phenotype (chapter 5). We showed that culture with depleted zinc decreases the zinc content of MIN6 cells but increases cellular zinc uptake capacities, presumably through upregulation of ZIP8 and ZIP14. Moreover, that depleted zinc decreases cellular survival, associated with decreased signalling via MAPK and mTOR cascades. These data are summarised in **Fig 8.3**. In addition, through transcriptomic analysis we demonstrated that genes differentially expressed in MIN6 cells and islets following culture with depleted zinc are enriched for phosphatases and that HIF1A regulation may be a key pathway mediated by zinc depletion. We therefore highlighted hypozincaemia as a potential stress driving zinc depletion-induced β-cell dysfunction. However, our experiments explored the effects of short-term severe zinc depletion rather than long-term relatively mild hypozincaemia

(potentially over years) of type 2 diabetic patients, and whether these results can be translated to physiological conditions *in vivo* remains to be determined.

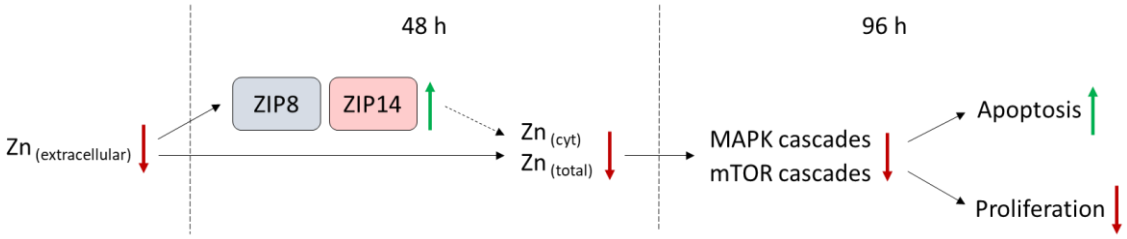

Fig 8.3. Proposed sequence of changes to β-cell signalling in response to hypozincaemia. Data included: ZIP transporter expression, cellular zinc content, cellular survival and expression of β-cell markers. Red arrows: downregulation. Green arrows: upregulation. $Zn_{(cyt)}$: cytosolic zinc content. $Zn_{(extracellular)}$: extracellular zinc content. $Zn_{(total)}$: total zinc content. The time-points indicate hours following addition of depleted or adequate zinc media.

Aim 3: To explore the roles of highlighted ZIP transporters for the β-cell response to hypozincaemia.

ZIP6 is highly expressed in β-cells [192, 218, 404] and, during this project, we linked decreased ZIP6 abundance to hyperglycaemia in MIN6 cells (chapter 4 [405]), PDX-1 overexpression in INS-1 cells, and Type 2 Diabetes in human (chapter 3 [404]). ZIP6 stimulates cellular proliferation and protects against anoikis in a number of cell types and contexts [206, 207] and protects against hypoxia in breast cancer cell lines [535]. We therefore decided to focus analysis on ZIP6. To address the role of ZIP6 in β-cells, we hypothesised that ZIP6 maintains β-cell phenotype and mass in response to extracellular

zinc depletion (chapter 7). We generated ZIP6 knockout MIN6 cells to show that ZIP6 abundance is associated with expression of multiple ZIP and ZnT paralogues, presumably to maintain adequate zinc uptake. We demonstrated that loss of ZIP6 increases cytosolic free Zn^{2+} but reduces total cellular zinc only in depleted zinc culture. Whereas in response to adequate zinc, loss of ZIP6 increases cellular zinc uptake capacities. We further showed that ZIP6 is important for expression of multiple markers for β-cell identity (transcription factors and insulin) and cellular survival associated with mTOR signalling, which has previously been linked to β-cell proliferation and insulin processing [569, 570]. In a previous study, mTORC1/S6K cascades were determined to regulate β-cell apoptosis, size and autophagy, which is consistent with our data [570]. We additionally noted upregulation of STAT3, which induces expression of ZIP6 and ZIP10 [207, 316], and suggested that increases in STAT3 abundance may be compensatory for loss of ZIP6:ZIP10 heteromers. These data indicate that ZIP6 is important for β-cell zinc trafficking and phenotype and is involved in the cellular response to zinc depletion. These data are summarised in **Fig 8.4**.

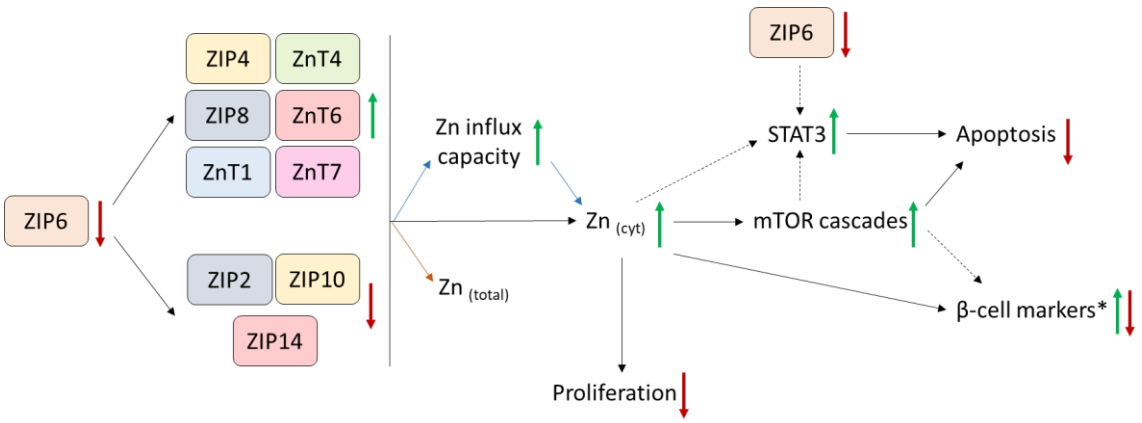

Fig 8.4. Proposed sequence of changes to β-cell signalling in ZIP6 knockout MIN6 cells. Data included: ZIP and ZnT transporter expression, cellular zinc parameters, cell

survival and expression of β-cell markers. *β-cell markers include data for transcription factors and insulin. Data shown is in response to both deficient and adequate zinc culture. Orange arrows: only regulated in cells in response to depleted zinc. Blue arrows: only regulated in cells in response to adequate zinc. Red arrows: downregulation. Green arrows: upregulation. $Zn_{(cyt)}$: cytosolic zinc content. $Zn_{(total)}$: total zinc content.

We concluded in chapter 6 that ZnT8 activity is associated with the abundances of ZIP8 and ZIP14. These cells therefore represent a model for investigating the role of coordinated ZnT8-ZIP8-ZIP14 activity in β-cells. To examine this further, we hypothesised that ZnT8-ZIP coordination mediates β-cell zinc homeostasis, survival and phenotype in response to extracellular zinc. We showed that ZnT8 haploinsufficiency lowers the total zinc contents of MIN6 cells and reduces cellular zinc uptake capacities following culture with depleted zinc. Moreover, ZnT8 haploinsufficiency decreases MIN6 cell proliferation and downregulates expression of insulin 1 and multiple important β-cell transcription factors. This contrasts with a recent investigation that showed ZnT8 R138X loss-of-function variants, which are protective against Type 2 Diabetes [271], increase the β-cell's insulin secretory capacity [280] but is consistent with ZnT8 suppression observed in response to stresses negatively impacting β-cell function [179, 186, 227]. These data indicate that decreased ZnT8-ZIP8-ZIP14-facilitated zinc trafficking impacts β-cellular survival and phenotype aside from insulin secretion and suggest that zinc deficiency may alter the response (summarised in **Fig 8.5**).

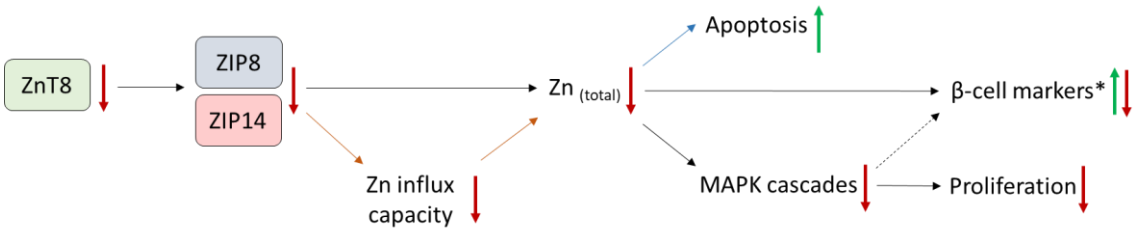

Fig 8.5. Proposed sequence of changes to β-cell signalling in ZnT8 haploinsufficient MIN6 cells. Data included: ZIP transporter expression, cellular zinc parameters, cellular survival and expression of β-cell markers. *= β-cell markers include data for transcription factors and insulin. Data shown is in response to both deficient and adequate zinc culture. Orange arrows: only regulated in cells in response to depleted zinc. Blue arrows: only regulated in cells in response to adequate zinc. Red arrows: downregulation. Green arrows: upregulation. $Zn_{(cyt)}$: cytosolic zinc content. $Zn_{(total)}$: total zinc content.

8.2. The importance of different β-cell ZIP transporters

Zinc impacts almost all aspects of cellular physiology and function [130-133]. It is therefore unsurprising that we identified a vast range of genes, processes and pathways to be regulated by zinc transporter deficiency/deregulation and zinc depletion in MIN6 cells and mouse islets. We revealed Zn^{2+}-mediated disruption of important β-cell markers, cellular survival and multiple signalling pathways (chapters 4 [405] and 5-7). This may simply reflect that Zn^{2+} binds ~10% of the genome [129] and changing the amount of Zn^{2+} available for protein binding inhibits zinc(II)-protein interactions and protein function. However, to target zinc dyshomeostasis it is important to understand the mechanism(s) driving zinc-mediated disruption; this may have differed between experiments and may explain the variation in our data. For example, we observed differences in cytosolic free Zn^{2+}, cellular signalling pathways and transcription factor

expression between ZIP6 knockout and ZnT8 haploinsufficient MIN6 cells compared to respective controls (chapter 6-7).

In this study, we revealed changes to the abundances of multiple ZIP and ZnT paralogues in MIN6 cells in response to hyperglycaemia (chapter 4 [405]) and hypozincaemia (chapter 5), probably driven by differing cellular zinc demand and/or the activities of preferable ZIP/ZnT paralogue(s). Multiple zinc transporters undertake additional roles aside from zinc transport [171-173, 206, 322] and might be regarded as membrane-bound Zn^{2+} chaperones. ZIP6:ZIP10 heteromers stimulate proliferation through promoting phosphorylation and inhibition of GSK-3 [207] and ZnT1 inhibits L-VGCC and activates the RAF-1 kinase, promoting RAS/ERK signalling [571]. Moreover, proteins that dock in the local vicinity of specific ZIP or ZnT paralogues, such as to organelle membranes, may require ZIP/ZnT-protein interactions for normal function. Although there are no known SNPs in any ZIP paralogues that are associated with β-cell dysfunction or Type 2 Diabetes, mutations or changes in expression of ZIP binding partners, due to pathological or maladaptive stimuli, or loss of transporter abundance may alter ZIP-protein interactions and downstream pathways. Delivery of zinc via certain transporters may additionally be critical for normal temporal release of free Zn^{2+} into the cytosol. For example, Golgi-localised ZIP7 is activated by CK2-regulated phosphorylation to drive MAPK, PI3K and mTOR growth and proliferation signalling pathways [457]. The results observed within this project may therefore not (entirely) stem from altered cellular zinc but from changes in ZIP-facilitated zinc trafficking and transporter abundances or from downstream effects of zinc- or ZIP-signalling. Zinc buffering by the MTs, which are readily induced in response to cytosolic free Zn^{2+} [572], may be adequate for cells to adapt to differences in cellular zinc.

Our lab has previously shown that the ZnT8 CTD interacts with PDLIM7 [573, 574], a scaffolding protein involved in cellular migration, signal transduction, differentiation, heart development, and oncogenesis [575, 576]. However, the significance of this interaction for β-cells is not yet known. The diabetes-associated rs13266634 polymorphism resides within the ZnT8 CTD [235] and may disrupt this interaction and any downstream processes, which could include proper regulation of zinc uptake via ZnT8, in addition to affecting the thermostability and dimerization affinity of the transporter [269]. Further ZnT8 binding partners likely exist and may help explain the phenotypes imposed by ZnT8-R/W variants *in vivo* [260-263].

8.3. The significance of this study

The work presented in this thesis has great significance for β-cell research because many stresses associated with Type 2 Diabetes disrupt ZIP transporter expression (chapter 3 [404]) and consequential changes to zinc trafficking may contribute to the observed β-cell phenotype. We experimentally showed that this holds true for a model of hyperglycaemia (chapter 4 [405]) and hypozincaemia (chapters 5-7). Moreover, although the data is only preliminary, in chapter 6 we suggested that PDX-1 co-regulates ZnT8 with ZIP6 and ZIP9 [200]; therefore, loss of PDX-1 function, such as in MODY4 [4], could result, in part, from zinc deregulation. In this project, we further demonstrated the vast range of genes exhibiting Zn^{2+}-responsive expression in mammalian β-cells (chapters 4 [405] and 5), including key β-cell markers. Zinc may mediate these genes via Zn^{2+}-responsive transcription factors (MTF1 [148], KLF4 [153] and ZNF658 [154]), chromatin stabilisation [577] or binding to zinc finger transcription factors, such as the diabetes-associated zinc finger protein 407 [578]. If changes to gene expression alongside disruption of any of the above are observed in future studies, plausible explanations

should include changes to cellular zinc. The data presented in this project should direct future research to consider zinc and its transporters as factors impacting β-cell function, phenotype and survival alongside stimuli under investigation (such as hyperglycaemia, cytokines, oxidative stress), and whether targeted addition of zinc could help alleviate the phenotype.

8.4. Study limitations

First, the mouse MIN6 cell line was used throughout this study. Ideally, we would use human β-cells for experimentation of human disease, however this proves impossible *in vivo* due to ethical and logistical constraints and limited *ex vivo* since islets from otherwise healthy cadaver donors are prioritised for type 1 diabetic transplant patients. We tried to obtain but could not get access to the one described human β-cell line (EndoC-βH1 cells [579]). Rodent β-cells and islets differ from human in terms of cellular compositions, orthologue properties and gene expression profiles: the proportion of β-cells in islets is 60-80% in mouse [425] and 50% in human [17], MT1 exists in eight functional isoforms in human but only one is present in mouse [160] and notable differences exist between human and rodent long non-coding RNA expression [580]. However, rodent models remain an important tool for β-cell study. We chose MIN6 cells for experimentation since they allow for relatively easy genomic manipulation and their popularity ensured we could directly compare results to previous studies. Nevertheless, MIN6 cells are not a pure β-cell line, instead existing as a mixture with other pancreatic endocrine cell types, including cells that express and secrete glucagon [581]. Immortalised cell lines exhibit significantly different transcriptomic profiles from their respective primary equivalents. MIN6 cells express increased levels of hexokinase mRNA, which leads to increased insulin secretion in response to sub-physiological levels of glucose, and MIN6 cells often

suddenly lose insulin sensitivity due to reduced expression of genes responsible for GSIS [582]; this occurred to our cells and we were therefore unable to use glucose as the stimulus during insulin secretion assays. Moreover, MIN6 cell phenotypes change with passage number, which can cause problems when comparing results carried out at different times [583]. Finally, MIN6 cells exist as a monolayer in tissue culture; our results may therefore not represent corresponding responses *in vivo*, where the islet structure, other endocrine cell types and additional stimuli (including hormones, integrins and nutrients) impact β-cell function in addition to the homologous β-cell interactions. This is the major limitation of this project: the conclusions were drawn from data generated in cell culture experiments and therefore need verification *in vivo*.

Second, we used the results from our systematic review (chapter 3 [404]) to determine which ZIP transporters to focus analysis on during this study. This hypothesis-driven approach was necessary due to time and cost restraints. However, the pre-defined criteria may have been too restrictive, and we could have missed critical paralogues. During the systematic review, we did not highlight ZIP4 or ZIP8 as important for β-cells; however, potentially important roles of these paralogues for β-cell zinc homeostasis have been previously described [192, 219]. We additionally identified ZIP8 alongside ZIP14 as important for coordinating zinc trafficking with ZnT8 (chapter 6) and suggested ZIP4 may be important for facilitating cellular zinc uptake in the absence of ZIP6 (chapter 7). However, since ZIP4 shows very low abundance in β-cells [218, 404], we sustain that we do not believe ZIP4 is of great importance for β-cells. Moreover, the nature of our data selection (from RNA-seq and microarray gene expression profiling studies) limited results to identifying ZIPs that respond to stimuli on a transcriptional level; we may therefore have missed paralogues regulated post-translationally.

Third, the majority of studies investigating the role of ZnT8 in β-cells are based on the rodent orthologue, which shows 80% amino acid conservation compared to human ZnT8 (determined through sequence alignment using NCBI BLAST [584]). The diabetes-associated loci at amino position 325 is not conserved between human and rodent: mouse ZnT8 harbours glutamine (Q) in contrast to arginine (R) or tryptophan (W) in human. ZnT8 rodent models may therefore not represent accurate models for the human protein. Although mice transgenic for human ZnT8 variants have been bred [278, 279], the full consequence of this polymorphism may not be observed due to continued expression of native mZnT8. Moreover, many rodent studies are based on absolute ZnT8 knockout [198], which has not been observed in human and which may explain the low apparent conservation of results cross-species. However, the protective effects of the ZnT8 loss-of-function R138X variant appears conserved between human [271] and mouse, since R138X knock-in mice exhibit increased insulin secretion in response to high glucose [280]. Although we showed that the ZIP paralogues we highlighted as important for β-cell function exhibit high human-rodent mRNA and protein similarities (chapter 3 [404]), species-specific differences remain, which could limit translation of the results throughout this thesis to human.

Finally, when we cultured MIN6 cells in media containing differing concentrations of zinc, we did not determine or control for zinc buffering, which is mainly mediated by binding to serum in tissue culture (FBS in our experiments). The serum present in growth media has a relatively high affinity for Zn^{2+} (K_D ~0.1 μmol/L [585]); zinc mainly binds to albumin but also to ligands such as histidine, cysteine and phosphate [455]. We can therefore only be confident about the total zinc content of the media and not the amount of zinc available for uptake. However, since we observed differences in the characteristics

of MIN6 cells cultured with depleted, adequate and excess zinc (chapter 5), we can be confident differences existed in the amounts of available zinc.

8.5. Future directions

Future studies should first expand on the work presented in this PhD project focusing on the ZIP transporters in MIN6 cells. To explore cooperation between paralogues and account for compensatory responses, the ZIPs of interest should be knocked out simultaneously and the described experiments repeated. Simultaneous knockdown of ZIP6 and ZIP7 with siRNA has previously been described in MIN6 cells, and results show an additive effect of loss of these two transporters for β-cell function [218]. Since there are no known SNPs in any ZIP paralogues that impact β-cell function or predispose to Type 2 Diabetes, ZIP deregulation during diabetes likely arises from disruption of a co-regulatory factor; therefore, a combination approach may be more representative of β-cell dysfunction *in vivo*.

Second, our RNA-seq data (chapter 5) should be further investigated. The top gene hits should first be confirmed through qPCR and the highlighted pathways explored in the context of zinc depletion by functional assays. If these pathways are impacted by depleted zinc, they should be investigated in models for diabetes-associated β-cell dysfunction (such as hyperglycaemia [192], hypoxia [227] and cytokine stimulation [359]) and it should be determined if zinc supplementation helps restore normal signalling.

Third, the results of this project should be explored *in vivo* through creation of β-cell-specific ZIP knockout mice (ZIP1, ZIP6, ZIP7, ZIP8, ZIP9, ZIP13 and ZIP14). The β-cell phenotypes and systemic glycaemic parameters should be described in the context of conditions relevant to human diabetes. Experimentation should be carried out in mice

with diabetic backgrounds (such as db/db), in response to high-fat and low zinc diets, and/or in response to disrupted ZnT8 expression (downregulated native mZnT8, mice transgenic for hZnT8-R/W and/or knock-in loss-of-function variants). These experiments will additionally be important for verifying if the phenotypes induced in MIN6 cells by KCl stimulation and severe short-term zinc deficiency are comparable to the milder long-term hyperglycaemia and hypozincaemia, respectively, that are characteristic of human type 2 diabetic patients. The results from these experiments should indicate if our current data can be translated to a mammalian *in vivo* model.

Finally, we should expand on our preliminary data indicating that PDX-1 co-regulates ZnT8-ZIP6/9 transcription via functional assays and site-directed mutagenesis of predicted binding loci. Additional candidates for ZnT8-ZIP or ZIP-ZIP coregulation in β-cells should additionally be identified using the methods described for PDX-1 (ChIP-seq analysis and bioinformatic alignments) and the candidates functionally assessed. Any associations should eventually be confirmed *in vivo*. If experiments confirm coordinated ZnT8-ZIP or ZIP-ZIP activities are important for β-cell identity, function and/or survival, results will help identify mechanisms directly governing the dysfunction observed throughout this study. Such mechanisms could potentially be targeted to restore normal β-cell zinc homeostasis.

Data from these described experiments could help explain β-cell failure in the context of polymorphisms and/or stresses that directly or indirectly alter β-cell zinc trafficking and homeostasis. Understanding the consequences of altered β-cell zinc may eventually help clinicians implement β-cell-targeted zinc supplementation therapies into personalised type 2 diabetic treatment plans to help suppress decline of β-cell function and mass and improve patient prognosis.

8.6. Concluding remarks

During this PhD project, we investigated the consequences of hyperglycaemia and hypozincaemia for β-cell zinc and the role(s) of the ZIP transporters for maintaining β-cell zinc homeostasis. Overall, we drew the following conclusions:

1. ZIP1 in rodent and ZIP6, ZIP7, ZIP8, ZIP9, ZIP13 and ZIP14 in human and rodent may be biologically important for β-cell phenotype and function.
2. Prolonged stimulation, representative of hyperglycaemia *in vivo*, and extracellular zinc depletion, representative of hypozincaemia *in vivo*, deplete MIN6 cells of zinc.
3. Depletion of zinc from MIN6 cells disrupts the transcriptome (including expression of key β-cell markers) and decreases cellular survival.
4. ZnT8 abundance is co-ordinated with expression of both ZIP8 and ZIP14.
5. Both ZnT8 haploinsufficiency and loss of ZIP6 alter the MIN6 cell response to extracellular zinc depletion.

Critically, this research demonstrates the importance of zinc and its transporters for β-cell phenotype, function and survival aside from its role in insulin granules. These results should guide future studies to consider zinc dyshomeostasis as a plausible explanation for observed declines in β-cell phenotype, function and mass.

VII. Bibliography

1. Association, A.D., *Diagnosis and classification of diabetes mellitus.* Diabetes Care, 2014. **37 Suppl 1**: p. S81-90.
2. Ranasinghe, P., et al., *Zinc and diabetes mellitus: understanding molecular mechanisms and clinical implications.* Daru, 2015. **23**: p. 44.
3. Csorba, T.R., A.W. Lyon, and M.D. Hollenberg, *Autoimmunity and the pathogenesis of type 1 diabetes.* Crit Rev Clin Lab Sci, 2010. **47**(2): p. 51-71.
4. Gardner, D.S. and E.S. Tai, *Clinical features and treatment of maturity onset diabetes of the young (MODY).* Diabetes Metab Syndr Obes, 2012. **5**: p. 101-8.
5. Konen, J.C., L.G. Curtis, and J.H. Summerson, *Symptoms and complications of adult diabetic patients in a family practice.* Arch Fam Med, 1996. **5**(3): p. 135-45.
6. Association, A.D., *(2) Classification and diagnosis of diabetes.* Diabetes Care, 2015. **38 Suppl**: p. S8-S16.
7. Twigg, S.M., et al., *Prediabetes: a position statement from the Australian Diabetes Society and Australian Diabetes Educators Association.* Med J Aust, 2007. **186**(9): p. 461-5.
8. Stuckler, D., *Population causes and consequences of leading chronic diseases: a comparative analysis of prevailing explanations.* Milbank Q, 2008. **86**(2): p. 273-326.
9. Flannick, J. and J.C. Florez, *Type 2 diabetes: genetic data sharing to advance complex disease research.* Nat Rev Genet, 2016. **17**(9): p. 535-49.
10. Almgren, P., et al., *Heritability and familiality of type 2 diabetes and related quantitative traits in the Botnia Study.* Diabetologia, 2011. **54**(11): p. 2811-9.
11. Medici, F., et al., *Concordance rate for type II diabetes mellitus in monozygotic twins: actuarial analysis.* Diabetologia, 1999. **42**(2): p. 146-50.
12. Ali, M.K., K.M. Bullard, and E.W. Gregg, *Achievement of goals in U.S. Diabetes Care, 1999-2010.* N Engl J Med, 2013. **369**(3): p. 287-8.
13. Khan, A.R. and F.R. Awan, *Metals in the pathogenesis of type 2 diabetes.* J Diabetes Metab Disord, 2014. **13**(1): p. 16.
14. Schlienger, J.L., *[Type 2 diabetes complications]*. Presse Med, 2013. **42**(5): p. 839-48.

15. Kulkarni, R.N., *The islet beta-cell.* Int J Biochem Cell Biol, 2004. **36**(3): p. 365-71.
16. Rutter, G.A. and D.J. Hodson, *Beta cell connectivity in pancreatic islets: a type 2 diabetes target?* Cell Mol Life Sci, 2015. **72**(3): p. 453-67.
17. Cabrera, O., et al., *The unique cytoarchitecture of human pancreatic islets has implications for islet cell function.* Proc Natl Acad Sci U S A, 2006. **103**(7): p. 2334-9.
18. Bonner-Weir, S. and A. Sharma, *Pancreatic stem cells.* J Pathol, 2002. **197**(4): p. 519-26.
19. Drucker, D.J., *The biology of incretin hormones.* Cell Metab, 2006. **3**(3): p. 153-65.
20. Brunetti, A., E. Chiefari, and D. Foti, *Recent advances in the molecular genetics of type 2 diabetes mellitus.* World J Diabetes, 2014. **5**(2): p. 128-40.
21. Goodge, K.A. and J.C. Hutton, *Translational regulation of proinsulin biosynthesis and proinsulin conversion in the pancreatic beta-cell.* Semin Cell Dev Biol, 2000. **11**(4): p. 235-42.
22. van de Bunt, M. and A.L. Gloyn, *A tale of two glucose transporters: how GLUT2 re-emerged as a contender for glucose transport into the human beta cell.* Diabetologia, 2012. **55**(9): p. 2312-5.
23. Newgard, C.B. and J.D. McGarry, *Metabolic coupling factors in pancreatic beta-cell signal transduction.* Annu Rev Biochem, 1995. **64**: p. 689-719.
24. Komatsu, M., et al., *Glucose-stimulated insulin secretion: A newer perspective.* J Diabetes Investig, 2013. **4**(6): p. 511-6.
25. Wollheim, C.B. and G.W. Sharp, *Regulation of insulin release by calcium.* Physiol Rev, 1981. **61**(4): p. 914-73.
26. Takahashi, N., et al., *Fusion pore dynamics and insulin granule exocytosis in the pancreatic islet.* Science, 2002. **297**(5585): p. 1349-52.
27. Bosco, D., L. Orci, and P. Meda, *Homologous but not heterologous contact increases the insulin secretion of individual pancreatic B-cells.* Exp Cell Res, 1989. **184**(1): p. 72-80.
28. Speier, S., et al., *Cx36-mediated coupling reduces beta-cell heterogeneity, confines the stimulating glucose concentration range, and affects insulin release kinetics.* Diabetes, 2007. **56**(4): p. 1078-86.

29. Grodsky, G.M., *A threshold distribution hypothesis for packet storage of insulin and its mathematical modeling.* J Clin Invest, 1972. **51**(8): p. 2047-59.
30. Petersen, K.F., et al., *Mechanism by which glucose and insulin inhibit net hepatic glycogenolysis in humans.* J Clin Invest, 1998. **101**(6): p. 1203-9.
31. Pilkis, S.J. and D.K. Granner, *Molecular physiology of the regulation of hepatic gluconeogenesis and glycolysis.* Annu Rev Physiol, 1992. **54**: p. 885-909.
32. Duncan, R.E., et al., *Regulation of lipolysis in adipocytes.* Annu Rev Nutr, 2007. **27**: p. 79-101.
33. Titchenell, P.M., et al., *Hepatic insulin signalling is dispensable for suppression of glucose output by insulin in vivo.* Nat Commun, 2015. **6**: p. 7078.
34. Leney, S.E. and J.M. Tavaré, *The molecular basis of insulin-stimulated glucose uptake: signalling, trafficking and potential drug targets.* J Endocrinol, 2009. **203**(1): p. 1-18.
35. De León, D.D. and C.A. Stanley, *Mechanisms of Disease: advances in diagnosis and treatment of hyperinsulinism in neonates.* Nat Clin Pract Endocrinol Metab, 2007. **3**(1): p. 57-68.
36. Rhodes, C.J., *Type 2 diabetes-a matter of beta-cell life and death?* Science, 2005. **307**(5708): p. 380-4.
37. Sakuraba, H., et al., *Reduced beta-cell mass and expression of oxidative stress-related DNA damage in the islet of Japanese Type II diabetic patients.* Diabetologia, 2002. **45**(1): p. 85-96.
38. Cernea, S. and M. Dobreanu, *Diabetes and beta cell function: from mechanisms to evaluation and clinical implications.* Biochem Med (Zagreb), 2013. **23**(3): p. 266-80.
39. Chang-Chen, K.J., R. Mullur, and E. Bernal-Mizrachi, *Beta-cell failure as a complication of diabetes.* Rev Endocr Metab Disord, 2008. **9**(4): p. 329-43.
40. Mori, M., *[Endoplasmic reticulum stress and diabetes]*. Tanpakushitsu Kakusan Koso, 2004. **49**(7 Suppl): p. 1131-2.
41. Federici, M., et al., *High glucose causes apoptosis in cultured human pancreatic islets of Langerhans: a potential role for regulation of specific Bcl family genes toward an apoptotic cell death program.* Diabetes, 2001. **50**(6): p. 1290-301.
42. Maedler, K., et al., *Glucose induces beta-cell apoptosis via upregulation of the Fas receptor in human islets.* Diabetes, 2001. **50**(8): p. 1683-90.

43. Zhang, Z., et al., *High glucose inhibits glucose-6-phosphate dehydrogenase, leading to increased oxidative stress and beta-cell apoptosis.* FASEB J, 2010. **24**(5): p. 1497-505.
44. Shimabukuro, M., et al., *Fatty acid-induced beta cell apoptosis: a link between obesity and diabetes.* Proc Natl Acad Sci U S A, 1998. **95**(5): p. 2498-502.
45. Roehrich, M.E., et al., *Insulin-secreting beta-cell dysfunction induced by human lipoproteins.* J Biol Chem, 2003. **278**(20): p. 18368-75.
46. Lenzen, S., *Oxidative stress: the vulnerable beta-cell.* Biochem Soc Trans, 2008. **36**(Pt 3): p. 343-7.
47. Kaneto, H., et al., *Oxidative stress and the JNK pathway in diabetes.* Curr Diabetes Rev, 2005. **1**(1): p. 65-72.
48. Wang, C., Y. Guan, and J. Yang, *Cytokines in the Progression of Pancreatic β-Cell Dysfunction.* Int J Endocrinol, 2010. **2010**: p. 515136.
49. Bhowmick, D.C., et al., *The Molecular Physiopathogenesis of Islet Amyloidosis.* Handb Exp Pharmacol, 2017.
50. Bernal-Mizrachi, E., et al., *Human β-cell proliferation and intracellular signaling part 2: still driving in the dark without a road map.* Diabetes, 2014. **63**(3): p. 819-31.
51. Elghazi, L. and E. Bernal-Mizrachi, *Akt and PTEN: beta-cell mass and pancreas plasticity.* Trends Endocrinol Metab, 2009. **20**(5): p. 243-51.
52. Brazil, D.P. and B.A. Hemmings, *Ten years of protein kinase B signalling: a hard Akt to follow.* Trends Biochem Sci, 2001. **26**(11): p. 657-64.
53. Belham, C., S. Wu, and J. Avruch, *Intracellular signalling: PDK1--a kinase at the hub of things.* Curr Biol, 1999. **9**(3): p. R93-6.
54. Sarbassov, D.D., et al., *Phosphorylation and regulation of Akt/PKB by the rictor-mTOR complex.* Science, 2005. **307**(5712): p. 1098-101.
55. Bernal-Mizrachi, E., et al., *Defective insulin secretion and increased susceptibility to experimental diabetes are induced by reduced Akt activity in pancreatic islet beta cells.* J Clin Invest, 2004. **114**(7): p. 928-36.
56. Tuttle, R.L., et al., *Regulation of pancreatic beta-cell growth and survival by the serine/threonine protein kinase Akt1/PKBalpha.* Nat Med, 2001. **7**(10): p. 1133-7.

57. Bernal-Mizrachi, E., et al., *Islet beta cell expression of constitutively active Akt1/PKB alpha induces striking hypertrophy, hyperplasia, and hyperinsulinemia.* J Clin Invest, 2001. **108**(11): p. 1631-8.
58. Kong, D.X. and T. Yamori, *ZSTK474, a novel phosphatidylinositol 3-kinase inhibitor identified using the JFCR39 drug discovery system.* Acta Pharmacol Sin, 2010. **31**(9): p. 1189-97.
59. Sun, W., et al., *The beneficial effects of Zn on Akt-mediated insulin and cell survival signaling pathways in diabetes.* J Trace Elem Med Biol, 2018. **46**: p. 117-127.
60. Tee, A.R., R. Anjum, and J. Blenis, *Inactivation of the tuberous sclerosis complex-1 and -2 gene products occurs by phosphoinositide 3-kinase/Akt-dependent and -independent phosphorylation of tuberin.* J Biol Chem, 2003. **278**(39): p. 37288-96.
61. Hahn-Windgassen, A., et al., *Akt activates the mammalian target of rapamycin by regulating cellular ATP level and AMPK activity.* J Biol Chem, 2005. **280**(37): p. 32081-9.
62. Huang, J. and B.D. Manning, *The TSC1-TSC2 complex: a molecular switchboard controlling cell growth.* Biochem J, 2008. **412**(2): p. 179-90.
63. Ruvinsky, I., et al., *Ribosomal protein S6 phosphorylation is a determinant of cell size and glucose homeostasis.* Genes Dev, 2005. **19**(18): p. 2199-211.
64. Balcazar, N., et al., *mTORC1 activation regulates beta-cell mass and proliferation by modulation of cyclin D2 synthesis and stability.* J Biol Chem, 2009. **284**(12): p. 7832-42.
65. Shigeyama, Y., et al., *Biphasic response of pancreatic beta-cell mass to ablation of tuberous sclerosis complex 2 in mice.* Mol Cell Biol, 2008. **28**(9): p. 2971-9.
66. Rachdi, L., et al., *Disruption of Tsc2 in pancreatic beta cells induces beta cell mass expansion and improved glucose tolerance in a TORC1-dependent manner.* Proc Natl Acad Sci U S A, 2008. **105**(27): p. 9250-5.
67. Manning, B.D., *Balancing Akt with S6K: implications for both metabolic diseases and tumorigenesis.* J Cell Biol, 2004. **167**(3): p. 399-403.
68. Barlow, A.D., M.L. Nicholson, and T.P. Herbert, *Evidence for rapamycin toxicity in pancreatic β-cells and a review of the underlying molecular mechanisms.* Diabetes, 2013. **62**(8): p. 2674-82.

69. McCubrey, J.A., et al., *Roles of the Raf/MEK/ERK pathway in cell growth, malignant transformation and drug resistance.* Biochim Biophys Acta, 2007. **1773**(8): p. 1263-84.
70. Jirakulaporn, T. and A.J. Muslin, *Cation diffusion facilitator proteins modulate Raf-1 activity.* J Biol Chem, 2004. **279**(26): p. 27807-15.
71. Pouysségur, J. and P. Lenormand, *Fidelity and spatio-temporal control in MAP kinase (ERKs) signalling.* Eur J Biochem, 2003. **270**(16): p. 3291-9.
72. Steelman, L.S., et al., *JAK/STAT, Raf/MEK/ERK, PI3K/Akt and BCR-ABL in cell cycle progression and leukemogenesis.* Leukemia, 2004. **18**(2): p. 189-218.
73. Allan, L.A., et al., *Inhibition of caspase-9 through phosphorylation at Thr 125 by ERK MAPK.* Nat Cell Biol, 2003. **5**(7): p. 647-54.
74. Deng, X., et al., *Survival function of ERK1/2 as IL-3-activated, staurosporine-resistant Bcl2 kinases.* Proc Natl Acad Sci U S A, 2000. **97**(4): p. 1578-83.
75. Nakano, H., et al., *Differential regulation of IkappaB kinase alpha and beta by two upstream kinases, NF-kappaB-inducing kinase and mitogen-activated protein kinase/ERK kinase kinase-1.* Proc Natl Acad Sci U S A, 1998. **95**(7): p. 3537-42.
76. Knebel, A., et al., *Dephosphorylation of receptor tyrosine kinases as target of regulation by radiation, oxidants or alkylating agents.* EMBO J, 1996. **15**(19): p. 5314-25.
77. Truong, T.H. and K.S. Carroll, *Redox regulation of epidermal growth factor receptor signaling through cysteine oxidation.* Biochemistry, 2012. **51**(50): p. 9954-65.
78. Catarzi, S., et al., *Redox regulation of platelet-derived-growth-factor-receptor: role of NADPH-oxidase and c-Src tyrosine kinase.* Biochim Biophys Acta, 2005. **1745**(2): p. 166-75.
79. Bellomo, E., et al., *Zinc ions modulate protein tyrosine phosphatase 1B activity.* Metallomics, 2014. **6**(7): p. 1229-39.
80. Wang, X.T., et al., *Oxidative stress-induced phospholipase C-gamma 1 activation enhances cell survival.* J Biol Chem, 2001. **276**(30): p. 28364-71.
81. Alejandro, E.U., et al., *Acute insulin signaling in pancreatic beta-cells is mediated by multiple Raf-1 dependent pathways.* Endocrinology, 2010. **151**(2): p. 502-12.
82. Lawrence, M., et al., *The protein kinases ERK1/2 and their roles in pancreatic beta cells.* Acta Physiol (Oxf), 2008. **192**(1): p. 11-7.

83. Gupta, R.K., et al., *Expansion of adult beta-cell mass in response to increased metabolic demand is dependent on HNF-4alpha.* Genes Dev, 2007. **21**(7): p. 756-69.

84. Santo-Domingo, J., et al., *Coordinated activation of mitochondrial respiration and exocytosis mediated by PKC signaling in pancreatic β cells.* FASEB J, 2017. **31**(3): p. 1028-1045.

85. Selway, J., et al., *Evidence that Ca2+ within the microdomain of the L-type voltage gated Ca2+ channel activates ERK in MIN6 cells in response to glucagon-like peptide-1.* PLoS One, 2012. **7**(3): p. e33004.

86. Briaud, I., et al., *Differential activation mechanisms of Erk-1/2 and p70(S6K) by glucose in pancreatic beta-cells.* Diabetes, 2003. **52**(4): p. 974-83.

87. Pratilas, C.A. and D.B. Solit, *Targeting the mitogen-activated protein kinase pathway: physiological feedback and drug response.* Clin Cancer Res, 2010. **16**(13): p. 3329-34.

88. Romeo, Y., X. Zhang, and P.P. Roux, *Regulation and function of the RSK family of protein kinases.* Biochem J, 2012. **441**(2): p. 553-69.

89. Liu, H., et al., *Systematically labeling developmental stage-specific genes for the study of pancreatic β-cell differentiation from human embryonic stem cells.* Cell Res, 2014. **24**(10): p. 1181-200.

90. Benner, C., et al., *The transcriptional landscape of mouse beta cells compared to human beta cells reveals notable species differences in long non-coding RNA and protein-coding gene expression.* BMC Genomics, 2014. **15**: p. 620.

91. Gao, T., et al., *Pdx1 maintains β cell identity and function by repressing an α cell program.* Cell Metab, 2014. **19**(2): p. 259-71.

92. Hayes, H.L., et al., *Pdx-1 activates islet α- and β-cell proliferation via a mechanism regulated by transient receptor potential cation channels 3 and 6 and extracellular signal-regulated kinases 1 and 2.* Mol Cell Biol, 2013. **33**(20): p. 4017-29.

93. Wang, L., et al., *Selective deletion of the Hnf1beta (MODY5) gene in beta-cells leads to altered gene expression and defective insulin release.* Endocrinology, 2004. **145**(8): p. 3941-9.

94. Chen, C., et al., *Pdx1 inactivation restricted to the intestinal epithelium in mice alters duodenal gene expression in enterocytes and enteroendocrine cells.* Am J Physiol Gastrointest Liver Physiol, 2009. **297**(6): p. G1126-37.

95. Fujitani, Y., et al., *Targeted deletion of a cis-regulatory region reveals differential gene dosage requirements for Pdx1 in foregut organ differentiation and pancreas formation.* Genes Dev, 2006. **20**(2): p. 253-66.
96. Johnson, J.D., et al., *Increased islet apoptosis in Pdx1+/- mice.* J Clin Invest, 2003. **111**(8): p. 1147-60.
97. Brissova, M., et al., *Reduction in pancreatic transcription factor PDX-1 impairs glucose-stimulated insulin secretion.* J Biol Chem, 2002. **277**(13): p. 11225-32.
98. Qiu, Y., et al., *Insulin gene transcription is mediated by interactions between the p300 coactivator and PDX-1, BETA2, and E47.* Mol Cell Biol, 2002. **22**(2): p. 412-20.
99. Qiu, Y., A. Sharma, and R. Stein, *p300 mediates transcriptional stimulation by the basic helix-loop-helix activators of the insulin gene.* Mol Cell Biol, 1998. **18**(5): p. 2957-64.
100. Oliver-Krasinski, J.M., et al., *The diabetes gene Pdx1 regulates the transcriptional network of pancreatic endocrine progenitor cells in mice.* J Clin Invest, 2009. **119**(7): p. 1888-98.
101. Fujimoto, K. and K.S. Polonsky, *Pdx1 and other factors that regulate pancreatic beta-cell survival.* Diabetes Obes Metab, 2009. **11 Suppl 4**: p. 30-7.
102. Artner, I., et al., *MafA and MafB regulate genes critical to beta-cells in a unique temporal manner.* Diabetes, 2010. **59**(10): p. 2530-9.
103. Nishimura, W., S. Takahashi, and K. Yasuda, *MafA is critical for maintenance of the mature beta cell phenotype in mice.* Diabetologia, 2015. **58**(3): p. 566-74.
104. Butler, A.E., et al., *Beta-cell deficit and increased beta-cell apoptosis in humans with type 2 diabetes.* Diabetes, 2003. **52**(1): p. 102-10.
105. Zhang, C., et al., *MafA is a key regulator of glucose-stimulated insulin secretion.* Mol Cell Biol, 2005. **25**(12): p. 4969-76.
106. Kaneto, H., et al., *Role of MafA in pancreatic beta-cells.* Adv Drug Deliv Rev, 2009. **61**(7-8): p. 489-96.
107. Aramata, S., S.I. Han, and K. Kataoka, *Roles and regulation of transcription factor MafA in islet beta-cells.* Endocr J, 2007. **54**(5): p. 659-66.
108. Kitamura, Y.I., et al., *FoxO1 protects against pancreatic beta cell failure through NeuroD and MafA induction.* Cell Metab, 2005. **2**(3): p. 153-63.
109. Raum, J.C., et al., *FoxA2, Nkx2.2, and PDX-1 regulate islet beta-cell-specific mafA expression through conserved sequences located between base pairs -8118*

and -7750 upstream from the transcription start site. Mol Cell Biol, 2006. **26**(15): p. 5735-43.

110. Nishimura, W., S. Bonner-Weir, and A. Sharma, *Expression of MafA in pancreatic progenitors is detrimental for pancreatic development.* Dev Biol, 2009. **333**(1): p. 108-20.
111. Hang, Y., et al., *The MafA transcription factor becomes essential to islet β-cells soon after birth.* Diabetes, 2014. **63**(6): p. 1994-2005.
112. Henseleit, K.D., et al., *NKX6 transcription factor activity is required for alpha- and beta-cell development in the pancreas.* Development, 2005. **132**(13): p. 3139-49.
113. Guo, S., et al., *Inactivation of specific β cell transcription factors in type 2 diabetes.* J Clin Invest, 2013. **123**(8): p. 3305-16.
114. Talchai, C., et al., *Pancreatic β cell dedifferentiation as a mechanism of diabetic β cell failure.* Cell, 2012. **150**(6): p. 1223-34.
115. Yokoi, N., et al., *Association studies of variants in the genes involved in pancreatic beta-cell function in type 2 diabetes in Japanese subjects.* Diabetes, 2006. **55**(8): p. 2379-86.
116. Schaffer, A.E., et al., *Nkx6.1 controls a gene regulatory network required for establishing and maintaining pancreatic Beta cell identity.* PLoS Genet, 2013. **9**(1): p. e1003274.
117. Watada, H., et al., *Transcriptional and translational regulation of beta-cell differentiation factor Nkx6.1.* J Biol Chem, 2000. **275**(44): p. 34224-30.
118. Fujita, Y., et al., *Human Pancreatic Alpha- to Beta-Cell Area Ratio Increases After Type 2 Diabetes Onset.* J Diabetes Investig, 2018.
119. Andersson, A., *Long-term effects of glucose on insulin release and glucose oxidation by mouse pancreatic islets maintained in tissue culture.* Biochem J, 1974. **140**(3): p. 377-82.
120. Taylor, B.L., F.F. Liu, and M. Sander, *Nkx6.1 is essential for maintaining the functional state of pancreatic beta cells.* Cell Rep, 2013. **4**(6): p. 1262-75.
121. Mitchell, R.K., et al., *The transcription factor Pax6 is required for pancreatic β cell identity, glucose-regulated ATP synthesis, and Ca2+ dynamics in adult mice.* J Biol Chem, 2017. **292**(21): p. 8892-8906.
122. Kone, M., et al., *LKB1 and AMPK differentially regulate pancreatic β-cell identity.* FASEB J, 2014. **28**(11): p. 4972-85.

123. Puri, S., H. Akiyama, and M. Hebrok, *VHL-mediated disruption of Sox9 activity compromises β-cell identity and results in diabetes mellitus.* Genes Dev, 2013. **27**(23): p. 2563-75.
124. Armour, S., et al. *A Novel Role for Tle3 in Maintaining Beta Cell Identity*. in *Diabetes*. 2016.
125. Metzger, D.E., et al., *Grg3/TLE3 and Grg1/TLE1 induce monohormonal pancreatic β-cells while repressing α-cell functions.* Diabetes, 2014. **63**(5): p. 1804-16.
126. Eide, D.J., *Zinc transporters and the cellular trafficking of zinc.* Biochim Biophys Acta, 2006. **1763**(7): p. 711-22.
127. Li, Y.V., *Zinc and insulin in pancreatic beta-cells.* Endocrine, 2014. **45**(2): p. 178-89.
128. Kambe, T., et al., *The Physiological, Biochemical, and Molecular Roles of Zinc Transporters in Zinc Homeostasis and Metabolism.* Physiol Rev, 2015. **95**(3): p. 749-784.
129. Andreini, C., et al., *Counting the zinc-proteins encoded in the human genome.* J Proteome Res, 2006. **5**(1): p. 196-201.
130. Wu, F.Y. and C.W. Wu, *Zinc in DNA replication and transcription.* Annu Rev Nutr, 1987. **7**: p. 251-72.
131. Vallee, B.L. and D.S. Auld, *Zinc coordination, function, and structure of zinc enzymes and other proteins.* Biochemistry, 1990. **29**(24): p. 5647-59.
132. Maret, W., *Zinc biochemistry: from a single zinc enzyme to a key element of life.* Adv Nutr, 2013. **4**(1): p. 82-91.
133. Chesters, J.K., *Trace element-gene interactions with particular reference to zinc.* Proc Nutr Soc, 1991. **50**(2): p. 123-9.
134. Cassandri, M., et al., *Zinc-finger proteins in health and disease.* Cell Death Discovery, 2017. **3**: p. 17071.
135. Religa, D., et al., *Elevated cortical zinc in Alzheimer disease.* Neurology, 2006. **67**(1): p. 69-75.
136. Dufner-Beattie, J., et al., *The mouse acrodermatitis enteropathica gene Slc39a4 (Zip4) is essential for early development and heterozygosity causes hypersensitivity to zinc deficiency.* Hum Mol Genet, 2007. **16**(12): p. 1391-9.
137. Taylor, K.M., et al., *The emerging role of the LIV-1 subfamily of zinc transporters in breast cancer*. Mol Med, 2007. **13**(7-8): p. 396-406.

138. Franklin, R.B., et al., *hZIP1 zinc uptake transporter down regulation and zinc depletion in prostate cancer.* Mol Cancer, 2005. **4**: p. 32.
139. Vashum, K.P., et al., *Is serum zinc associated with pancreatic beta cell function and insulin sensitivity in pre-diabetic and normal individuals? Findings from the Hunter Community Study*. PLoS One, 2014. **9**(1): p. e83944.
140. Garg, V.K., R. Gupta, and R.K. Goyal, *Hypozincemia in diabetes mellitus.* J Assoc Physicians India, 1994. **42**(9): p. 720-1.
141. Pidduck, H.G., P.J. Wren, and D.A. Evans, *Hyperzincuria of diabetes mellitus and possible genetical implications of this observation.* Diabetes, 1970. **19**(4): p. 240-7.
142. Capdor, J., et al., *Zinc and glycemic control: a meta-analysis of randomised placebo controlled supplementation trials in humans.* J Trace Elem Med Biol, 2013. **27**(2): p. 137-42.
143. Tang, X. and N.F. Shay, *Zinc has an insulin-like effect on glucose transport mediated by phosphoinositol-3-kinase and Akt in 3T3-L1 fibroblasts and adipocytes.* J Nutr, 2001. **131**(5): p. 1414-20.
144. Krezel, A., Q. Hao, and W. Maret, *The zinc/thiolate redox biochemistry of metallothionein and the control of zinc ion fluctuations in cell signaling.* Arch Biochem Biophys, 2007. **463**(2): p. 188-200.
145. Kimura, T. and T. Kambe, *The Functions of Metallothionein and ZIP and ZnT Transporters: An Overview and Perspective.* Int J Mol Sci, 2016. **17**(3).
146. Lu, Q., et al., *Intracellular zinc distribution in mitochondria, ER and the Golgi apparatus.* Int J Physiol Pathophysiol Pharmacol, 2016. **8**(1): p. 35-43.
147. Myers, S.A., A. Nield, and M. Myers, *Zinc transporters, mechanisms of action and therapeutic utility: implications for type 2 diabetes mellitus.* J Nutr Metab, 2012. **2012**: p. 173712.
148. Günes, C., et al., *Embryonic lethality and liver degeneration in mice lacking the metal-responsive transcriptional activator MTF-1.* EMBO J, 1998. **17**(10): p. 2846-54.
149. Laity, J.H. and G.K. Andrews, *Understanding the mechanisms of zinc-sensing by metal-response element binding transcription factor-1 (MTF-1).* Arch Biochem Biophys, 2007. **463**(2): p. 201-10.

150. Potter, B.M., et al., *The six zinc fingers of metal-responsive element binding transcription factor-1 form stable and quasi-ordered structures with relatively small differences in zinc affinities.* J Biol Chem, 2005. **280**(31): p. 28529-40.
151. Hogstrand, C., et al., *Zinc-controlled gene expression by metal-regulatory transcription factor 1 (MTF1) in a model vertebrate, the zebrafish.* Biochem Soc Trans, 2008. **36**(Pt 6): p. 1252-7.
152. Li, Y., et al., *Zinc-induced formation of a coactivator complex containing the zinc-sensing transcription factor MTF-1, p300/CBP, and Sp1.* Mol Cell Biol, 2008. **28**(13): p. 4275-84.
153. Liuzzi, J.P., et al., *Krüppel-like factor 4 regulates adaptive expression of the zinc transporter Zip4 in mouse small intestine.* Am J Physiol Gastrointest Liver Physiol, 2009. **296**(3): p. G517-23.
154. Ogo, O.A., et al., *The zinc finger protein ZNF658 regulates the transcription of genes involved in zinc homeostasis and affects ribosome biogenesis through the zinc transcriptional regulatory element.* Mol Cell Biol, 2015. **35**(6): p. 977-87.
155. Mao, X., et al., *A histidine-rich cluster mediates the ubiquitination and degradation of the human zinc transporter, hZIP4, and protects against zinc cytotoxicity.* J Biol Chem, 2007. **282**(10): p. 6992-7000.
156. Coyle, P., et al., *Metallothionein: the multipurpose protein.* Cell Mol Life Sci, 2002. **59**(4): p. 627-47.
157. Zeng, J., et al., *Thionein (apometallothionein) can modulate DNA binding and transcription activation by zinc finger containing factor Sp1.* FEBS Lett, 1991. **279**(2): p. 310-2.
158. Zeng, J., B.L. Vallee, and J.H. Kägi, *Zinc transfer from transcription factor IIIA fingers to thionein clusters.* Proc Natl Acad Sci U S A, 1991. **88**(22): p. 9984-8.
159. Krezel, A. and W. Maret, *Zinc-buffering capacity of a eukaryotic cell at physiological pZn.* J Biol Inorg Chem, 2006. **11**(8): p. 1049-62.
160. Moleirinho, A., et al., *Gains, losses and changes of function after gene duplication: study of the metallothionein family.* PLoS One, 2011. **6**(4): p. e18487.
161. Krężel, A. and W. Maret, *Different redox states of metallothionein/thionein in biological tissue.* Biochemical Journal, 2007. **402**(Pt 3): p. 551-558.
162. Stuart, G.W., P.F. Searle, and R.D. Palmiter, *Identification of multiple metal regulatory elements in mouse metallothionein-I promoter by assaying synthetic sequences.* Nature, 1985. **317**(6040): p. 828-31.

163. Westin, G. and W. Schaffner, *A zinc-responsive factor interacts with a metal-regulated enhancer element (MRE) of the mouse metallothionein-I gene.* EMBO J, 1988. **7**(12): p. 3763-70.
164. Schroeder, J.J. and R.J. Cousins, *Interleukin 6 regulates metallothionein gene expression and zinc metabolism in hepatocyte monolayer cultures.* Proceedings of the National Academy of Sciences of the United States of America, 1990. **87**(8): p. 3137-3141.
165. Murphy, B.J., et al., *Metallothionein induction by hypoxia involves cooperative interactions between metal-responsive transcription factor-1 and hypoxia-inducible transcription factor-1alpha.* Mol Cancer Res, 2008. **6**(3): p. 483-90.
166. Laukens, D., et al., *Human metallothionein expression under normal and pathological conditions: mechanisms of gene regulation based on in silico promoter analysis.* Crit Rev Eukaryot Gene Expr, 2009. **19**(4): p. 301-17.
167. Karin, M. and H.R. Herschman, *Dexamethasone stimulation of metallothionein synthesis in HeLa cell cultures.* Science, 1979. **204**(4389): p. 176.
168. Ghoshal, K., et al., *Suppression of metallothionein gene expression in a rat hepatoma because of promoter-specific DNA methylation.* J Biol Chem, 2000. **275**(1): p. 539-47.
169. Majumder, S., et al., *Silencing of metallothionein-I gene in mouse lymphosarcoma cells by methylation.* Oncogene, 1999. **18**(46): p. 6287-95.
170. Myers, S.A., *Zinc transporters and zinc signaling: new insights into their role in type 2 diabetes.* Int J Endocrinol, 2015. **2015**: p. 167503.
171. Wang, C.Y., et al., *ZIP8 is an iron and zinc transporter whose cell-surface expression is up-regulated by cellular iron loading.* J Biol Chem, 2012. **287**(41): p. 34032-43.
172. Liuzzi, J.P., et al., *Zip14 (Slc39a14) mediates non-transferrin-bound iron uptake into cells.* Proc Natl Acad Sci U S A, 2006. **103**(37): p. 13612-7.
173. El Muayed, M., et al., *Accumulation of cadmium in insulin-producing β cells.* Islets, 2012. **4**(6): p. 405-16.
174. Kambe, T., A. Hashimoto, and S. Fujimoto, *Current understanding of ZIP and ZnT zinc transporters in human health and diseases.* Cell Mol Life Sci, 2014. **71**(17): p. 3281-95.

175. Weaver, B.P. and G.K. Andrews, *Regulation of zinc-responsive Slc39a5 (Zip5) translation is mediated by conserved elements in the 3'-untranslated region.* Biometals, 2012. **25**(2): p. 319-35.
176. Weaver, B.P., et al., *Novel zinc-responsive post-transcriptional mechanisms reciprocally regulate expression of the mouse Slc39a4 and Slc39a5 zinc transporters (Zip4 and Zip5).* Biol Chem, 2007. **388**(12): p. 1301-12.
177. Fukada, T. and T. Kambe, *Molecular and genetic features of zinc transporters in physiology and pathogenesis.* Metallomics, 2011. **3**(7): p. 662-74.
178. Gaither, L.A. and D.J. Eide, *Eukaryotic zinc transporters and their regulation.* Biometals, 2001. **14**(3-4): p. 251-270.
179. Egefjord, L., et al., *Zinc transporter gene expression is regulated by pro-inflammatory cytokines: a potential role for zinc transporters in beta-cell apoptosis?* BMC Endocr Disord, 2009. **9**: p. 7.
180. Kambe, T., et al., *Cloning and characterization of a novel mammalian zinc transporter, zinc transporter 5, abundantly expressed in pancreatic beta cells.* J Biol Chem, 2002. **277**(21): p. 19049-55.
181. Lasry, I., et al., *In situ dimerization of multiple wild type and mutant zinc transporters in live cells using bimolecular fluorescence complementation.* J Biol Chem, 2014. **289**(11): p. 7275-92.
182. Murgia, C., et al., *Diabetes-linked zinc transporter ZnT8 is a homodimeric protein expressed by distinct rodent endocrine cell types in the pancreas and other glands.* Nutr Metab Cardiovasc Dis, 2009. **19**(6): p. 431-9.
183. Fukunaka, A., et al., *Demonstration and characterization of the heterodimerization of ZnT5 and ZnT6 in the early secretory pathway.* J Biol Chem, 2009. **284**(45): p. 30798-806.
184. Golan, Y., B. Berman, and Y.G. Assaraf, *Heterodimerization, altered subcellular localization, and function of multiple zinc transporters in viable cells using bimolecular fluorescence complementation.* J Biol Chem, 2015. **290**(14): p. 9050-63.
185. Cai, Y., C.P. Kirschke, and L. Huang, *SLC30A family expression in the pancreatic islets of humans and mice: cellular localization in the β-cells.* J Mol Histol, 2018.
186. Lefebvre, B., et al., *Regulation and functional effects of ZNT8 in human pancreatic islets.* J Endocrinol, 2012. **214**(2): p. 225-32.

187. Lopez, V. and S.L. Kelleher, *Zinc transporter-2 (ZnT2) variants are localized to distinct subcellular compartments and functionally transport zinc.* Biochem J, 2009. **422**(1): p. 43-52.

188. Linkous, D.H., et al., *Evidence that the ZNT3 protein controls the total amount of elemental zinc in synaptic vesicles.* J Histochem Cytochem, 2008. **56**(1): p. 3-6.

189. Smidt, K., et al., *SLC30A3 responds to glucose- and zinc variations in beta-cells and is critical for insulin production and in vivo glucose-metabolism during beta-cell stress.* PLoS One, 2009. **4**(5): p. e5684.

190. Zhong, M.L., et al., *Widespread expression of zinc transporter ZnT (SLC30) family members in mouse endocrine cells.* Histochem Cell Biol, 2012. **138**(4): p. 605-16.

191. Chimienti, F., et al., *In vivo expression and functional characterization of the zinc transporter ZnT8 in glucose-induced insulin secretion.* J Cell Sci, 2006. **119**(Pt 20): p. 4199-206.

192. Bellomo, E.A., G. Meur, and G.A. Rutter, *Glucose regulates free cytosolic Zn^{2+} concentration, Slc39 (ZiP), and metallothionein gene expression in primary pancreatic islet β-cells.* J Biol Chem, 2011. **286**(29): p. 25778-89.

193. Thornton, J.K., et al., *Differential subcellular localization of the splice variants of the zinc transporter ZnT5 is dictated by the different C-terminal regions.* PLoS One, 2011. **6**(8): p. e23878.

194. Huang, L., C.P. Kirschke, and J. Gitschier, *Functional characterization of a novel mammalian zinc transporter, ZnT6.* J Biol Chem, 2002. **277**(29): p. 26389-95.

195. Cai, Y., C.P. Kirschke, and L. Huang, *SLC30A family expression in the pancreatic islets of humans and mice: cellular localization in the β-cells.* J Mol Histol, 2018. **49**(2): p. 133-145.

196. Huang, L., et al., *Znt7-null mice are more susceptible to diet-induced glucose intolerance and insulin resistance.* J Biol Chem, 2012. **287**(40): p. 33883-96.

197. Bosomworth, H.J., et al., *Efflux function, tissue-specific expression and intracellular trafficking of the Zn transporter ZnT10 indicate roles in adult Zn homeostasis.* Metallomics, 2012. **4**(8): p. 771-9.

198. Davidson, H.W., J.M. Wenzlau, and R.M. O'Brien, *Zinc transporter 8 (ZnT8) and β cell function.* Trends Endocrinol Metab, 2014. **25**(8): p. 415-24.

199. Chimienti, F., A. Favier, and M. Seve, *ZnT-8, a pancreatic beta-cell-specific zinc transporter*. Biometals, 2005. **18**(4): p. 313-7.

200. Pound, L.D., et al., *The pancreatic islet β-cell-enriched transcription factor Pdx-1 regulates Slc30a8 gene transcription through an intronic enhancer.* Biochem J, 2011. **433**(1): p. 95-105.
201. Nicolson, T.J., et al., *Insulin storage and glucose homeostasis in mice null for the granule zinc transporter ZnT8 and studies of the type 2 diabetes-associated variants.* Diabetes, 2009. **58**(9): p. 2070-83.
202. Lemaire, K., et al., *Insulin crystallization depends on zinc transporter ZnT8 expression, but is not required for normal glucose homeostasis in mice.* Proc Natl Acad Sci U S A, 2009. **106**(35): p. 14872-7.
203. Taylor, K.M. and R.I. Nicholson, *The LZT proteins; the LIV-1 subfamily of zinc transporters.* Biochim Biophys Acta, 2003. **1611**(1-2): p. 16-30.
204. Hogstrand, C., et al., *A mechanism for epithelial-mesenchymal transition and anoikis resistance in breast cancer triggered by zinc channel ZIP6 and STAT3 (signal transducer and activator of transcription 3).* Biochem J, 2013. **455**(2): p. 229-37.
205. Kambe, T. and G.K. Andrews, *Novel proteolytic processing of the ectodomain of the zinc transporter ZIP4 (SLC39A4) during zinc deficiency is inhibited by acrodermatitis enteropathica mutations.* Mol Cell Biol, 2009. **29**(1): p. 129-39.
206. Taylor, K.M., et al., *Zinc transporter ZIP10 forms a heteromer with ZIP6 which regulates embryonic development and cell migration.* Biochemical Journal, 2016. **473**: p. 2531-2544.
207. Hogstrand, C., et al., *A mechanism for epithelial-mesenchymal transition and anoikis resistance in breast cancer triggered by zinc channel ZIP6 and STAT3 (signal transducer and activator of transcription 3).* Biochemical Journal, 2013. **455**: p. 229-237.
208. Hogstrand, C. and W. Maret, *Genetics of Human Zinc Deficiencies*, in *eLS*. 2016, John Wiley & Sons, Ltd.
209. Bafaro, E., et al., *The emerging role of zinc transporters in cellular homeostasis and cancer.* Signal Transduct Target Ther, 2017. **2**.
210. Guerinot, M.L., *The ZIP family of metal transporters.* Biochimica Et Biophysica Acta-Biomembranes, 2000. **1465**(1-2): p. 190-198.
211. Zhang, T., D. Sui, and J. Hu, *Structural insights of ZIP4 extracellular domain critical for optimal zinc transport.* Nat Commun, 2016. **7**: p. 11979.

212. Zhang, T., et al., *Crystal structures of a ZIP zinc transporter reveal a binuclear metal center in the transport pathway.* Sci Adv, 2017. **3**(8): p. e1700344.
213. Zhao, H. and D. Eide, *The yeast ZRT1 gene encodes the zinc transporter protein of a high-affinity uptake system induced by zinc limitation.* Proc Natl Acad Sci U S A, 1996. **93**(6): p. 2454-8.
214. Zhao, H. and D. Eide, *The ZRT2 gene encodes the low affinity zinc transporter in Saccharomyces cerevisiae.* J Biol Chem, 1996. **271**(38): p. 23203-10.
215. Gaither, L.A. and D.J. Eide, *Functional expression of the human hZIP2 zinc transporter.* J Biol Chem, 2000. **275**(8): p. 5560-4.
216. Gaither, L.A. and D.J. Eide, *The human ZIP1 transporter mediates zinc uptake in human K562 erythroleukemia cells.* J Biol Chem, 2001. **276**(25): p. 22258-64.
217. Nebert, D.W., et al., *ZIP14 and ZIP8 zinc/bicarbonate symporters in Xenopus oocytes: characterization of metal uptake and inhibition.* Metallomics, 2012. **4**(11): p. 1218-25.
218. Liu, Y., et al., *Characterization of Zinc Influx Transporters (ZIPs) in Pancreatic Beta Cells: Roles in Regulating Cytosolic Zinc Homeostasis and Insulin Secretion.* J Biol Chem, 2015: p. 18757-18769.
219. Hardy, A.B., et al., *Zip4 mediated zinc influx stimulates insulin secretion in pancreatic beta cells.* PLoS One, 2015. **10**(3): p. e0119136.
220. Dufner-Beattie, J., et al., *The adaptive response to dietary zinc in mice involves the differential cellular localization and zinc regulation of the zinc transporters ZIP4 and ZIP5.* J Biol Chem, 2004. **279**(47): p. 49082-90.
221. Wijesekara, N., F. Chimienti, and M.B. Wheeler, *Zinc, a regulator of islet function and glucose homeostasis.* Diabetes Obes Metab, 2009. **11 Suppl 4**: p. 202-14.
222. Pae, E.K. and G. Kim, *Insulin production hampered by intermittent hypoxia via impaired zinc homeostasis.* PLoS One, 2014. **9**(2): p. e90192.
223. Gyulkhandanyan, A.V., et al., *The Zn2+-transporting pathways in pancreatic beta-cells: a role for the L-type voltage-gated Ca2+ channel.* J Biol Chem, 2006. **281**(14): p. 9361-72.
224. Wagner, T.F., et al., *TRPM3 channels provide a regulated influx pathway for zinc in pancreatic beta cells.* Pflugers Arch, 2010. **460**(4): p. 755-65.
225. Andersson, D.A., et al., *Clioquinol and pyrithione activate TRPA1 by increasing intracellular Zn2+.* Proc Natl Acad Sci U S A, 2009. **106**(20): p. 8374-9.

226. Inoue, K., D. Branigan, and Z.G. Xiong, *Zinc-induced neurotoxicity mediated by transient receptor potential melastatin 7 channels.* J Biol Chem, 2010. **285**(10): p. 7430-9.
227. Gerber, P.A., et al., *Hypoxia lowers SLC30A8/ZnT8 expression and free cytosolic Zn2+ in pancreatic beta cells.* Diabetologia, 2014. **57**(8): p. 1635-44.
228. Tamaki, M., et al., *Downregulation of ZnT8 expression in pancreatic β-cells of diabetic mice.* Islets, 2009. **1**(2): p. 124-8.
229. Huang, L. and C. Kirschke, *Down-Regulation of Zinc Transporter 8 (SLC30A8) in Pancreatic Beta-Cells Promotes Cell Survival* Austin Journal of Endocrinology and Diabetes 2016. **3**(1): p. id1037.
230. Carvalho, S., et al., *Differential cytolocation and functional assays of the two major human SLC30A8 (ZnT8) isoforms.* J Trace Elem Med Biol, 2017. **44**: p. 116-124.
231. Eizirik, D.L., et al., *The human pancreatic islet transcriptome: expression of candidate genes for type 1 diabetes and the impact of pro-inflammatory cytokines.* PLoS Genet, 2012. **8**(3): p. e1002552.
232. Wenzlau, J.M., et al., *The cation efflux transporter ZnT8 (Slc30A8) is a major autoantigen in human type 1 diabetes.* Proc Natl Acad Sci U S A, 2007. **104**(43): p. 17040-5.
233. Grotz, A.K., A.L. Gloyn, and S.K. Thomsen, *Prioritising Causal Genes at Type 2 Diabetes Risk Loci.* Curr Diab Rep, 2017. **17**(9): p. 76.
234. Sladek, R., et al., *A genome-wide association study identifies novel risk loci for type 2 diabetes.* Nature, 2007. **445**(7130): p. 881-5.
235. Lu, M. and D. Fu, *Structure of the zinc transporter YiiP.* Science, 2007. **317**(5845): p. 1746-8.
236. Saxena, R., et al., *Genome-wide association analysis identifies loci for type 2 diabetes and triglyceride levels.* Science, 2007. **316**(5829): p. 1331-6.
237. Zeggini, E., et al., *Replication of genome-wide association signals in UK samples reveals risk loci for type 2 diabetes.* Science, 2007. **316**(5829): p. 1336-41.
238. Scott, L.J., et al., *A genome-wide association study of type 2 diabetes in Finns detects multiple susceptibility variants.* Science, 2007. **316**(5829): p. 1341-5.
239. Takeuchi, F., et al., *Confirmation of multiple risk Loci and genetic impacts by a genome-wide association study of type 2 diabetes in the Japanese population.* Diabetes, 2009. **58**(7): p. 1690-9.

240. Wu, Y., et al., *Common variants in CDKAL1, CDKN2A/B, IGF2BP2, SLC30A8, and HHEX/IDE genes are associated with type 2 diabetes and impaired fasting glucose in a Chinese Han population.* Diabetes, 2008. **57**(10): p. 2834-42.

241. Tabara, Y., et al., *Replication study of candidate genes associated with type 2 diabetes based on genome-wide screening.* Diabetes, 2009. **58**(2): p. 493-8.

242. Chang, Y.C., et al., *Validation of type 2 diabetes risk variants identified by genome-wide association studies in Han Chinese population: a replication study and meta-analysis.* PLoS One, 2014. **9**(4): p. e95045.

243. Cauchi, S., et al., *Meta-analysis and functional effects of the SLC30A8 rs13266634 polymorphism on isolated human pancreatic islets.* Mol Genet Metab, 2010. **100**(1): p. 77-82.

244. Lyssenko, V., et al., *Clinical risk factors, DNA variants, and the development of type 2 diabetes.* N Engl J Med, 2008. **359**(21): p. 2220-32.

245. Hertel, J.K., et al., *Genetic analysis of recently identified type 2 diabetes loci in 1,638 unselected patients with type 2 diabetes and 1,858 control participants from a Norwegian population-based cohort (the HUNT study).* Diabetologia, 2008. **51**(6): p. 971-7.

246. van Hoek, M., et al., *Predicting type 2 diabetes based on polymorphisms from genome-wide association studies: a population-based study.* Diabetes, 2008. **57**(11): p. 3122-8.

247. Horikoshi, M., et al., *Variations in the HHEX gene are associated with increased risk of type 2 diabetes in the Japanese population.* Diabetologia, 2007. **50**(12): p. 2461-6.

248. Xiang, J., et al., *Zinc transporter-8 gene (SLC30A8) is associated with type 2 diabetes in Chinese.* J Clin Endocrinol Metab, 2008. **93**(10): p. 4107-12.

249. Horikawa, Y., et al., *Replication of genome-wide association studies of type 2 diabetes susceptibility in Japan.* J Clin Endocrinol Metab, 2008. **93**(8): p. 3136-41.

250. Steinthorsdottir, V., et al., *A variant in CDKAL1 influences insulin response and risk of type 2 diabetes.* Nat Genet, 2007. **39**(6): p. 770-5.

251. Lewis, J.P., et al., *Association analysis in african americans of European-derived type 2 diabetes single nucleotide polymorphisms from whole-genome association studies.* Diabetes, 2008. **57**(8): p. 2220-5.

252. Sanghera, D.K., et al., *Impact of nine common type 2 diabetes risk polymorphisms in Asian Indian Sikhs: PPARG2 (Pro12Ala), IGF2BP2, TCF7L2 and FTO variants confer a significant risk.* BMC Med Genet, 2008. **9**: p. 59.
253. Cauchi, S., et al., *Post genome-wide association studies of novel genes associated with type 2 diabetes show gene-gene interaction and high predictive value.* PLoS One, 2008. **3**(5): p. e2031.
254. Teleginski, A., et al., *Leptin (rs7799039) and solute carrier family 30 zinc transporter (rs13266634) polymorphisms in Euro-Brazilian pregnant women with gestational diabetes.* Genet Mol Res, 2017. **16**(1).
255. Kwak, S.H., et al., *Clinical and genetic risk factors for type 2 diabetes at early or late post partum after gestational diabetes mellitus.* J Clin Endocrinol Metab, 2013. **98**(4): p. E744-52.
256. Cheng, L., et al., *Association between SLC30A8 rs13266634 Polymorphism and Type 2 Diabetes Risk: A Meta-Analysis.* Med Sci Monit, 2015. **21**: p. 2178-89.
257. Fan, M., et al., *Association of SLC30A8 gene polymorphism with type 2 diabetes, evidence from 46 studies: a meta-analysis.* Endocrine, 2016.
258. Xu, K., et al., *Association between rs13266634 C/T polymorphisms of solute carrier family 30 member 8 (SLC30A8) and type 2 diabetes, impaired glucose tolerance, type 1 diabetes--a meta-analysis.* Diabetes Res Clin Pract, 2011. **91**(2): p. 195-202.
259. Jing, Y.L., et al., *SLC30A8 polymorphism and type 2 diabetes risk: evidence from 27 study groups.* Nutr Metab Cardiovasc Dis, 2011. **21**(6): p. 398-405.
260. Kirchhoff, K., et al., *Polymorphisms in the TCF7L2, CDKAL1 and SLC30A8 genes are associated with impaired proinsulin conversion.* Diabetologia, 2008. **51**(4): p. 597-601.
261. Dimas, A.S., et al., *Impact of type 2 diabetes susceptibility variants on quantitative glycemic traits reveals mechanistic heterogeneity.* Diabetes, 2014. **63**(6): p. 2158-71.
262. Boesgaard, T.W., et al., *The common SLC30A8 Arg325Trp variant is associated with reduced first-phase insulin release in 846 non-diabetic offspring of type 2 diabetes patients--the EUGENE2 study.* Diabetologia, 2008. **51**(5): p. 816-20.
263. Staiger, H., et al., *Polymorphisms within novel risk loci for type 2 diabetes determine beta-cell function.* PLoS One, 2007. **2**(9): p. e832.

264. Kim, I., et al., *A low-risk ZnT-8 allele (W325) for post-transplantation diabetes mellitus is protective against cyclosporin A-induced impairment of insulin secretion.* Pharmacogenomics J, 2011. **11**(3): p. 191-8.
265. Merriman, C., et al., *Lipid-tuned Zinc Transport Activity of Human ZnT8 Protein Correlates with Risk for Type-2 Diabetes.* J Biol Chem, 2016. **291**(53): p. 26950-26957.
266. Wong, W.P., et al., *Exploring the Association Between Demographics, SLC30A8 Genotype, and Human Islet Content of Zinc, Cadmium, Copper, Iron, Manganese and Nickel.* Sci Rep, 2017. **7**(1): p. 473.
267. Weijers, R.N., *Three-dimensional structure of beta-cell-specific zinc transporter, ZnT-8, predicted from the type 2 diabetes-associated gene variant SLC30A8 R325W.* Diabetol Metab Syndr, 2010. **2**(1): p. 33.
268. Lu, M., J. Chai, and D. Fu, *Structural basis for autoregulation of the zinc transporter YiiP.* Nat Struct Mol Biol, 2009. **16**(10): p. 1063-7.
269. Parsons, D.S., C. Hogstrand, and W. Maret, *The C-terminal cytosolic domain of the human zinc transporter ZnT8 and its diabetes risk variant.* FEBS J, 2018. **285**(7): p. 1237-1250.
270. Rutter, G.A., et al., *Intracellular zinc in insulin secretion and action: a determinant of diabetes risk?* Proc Nutr Soc, 2016. **75**(1): p. 61-72.
271. Flannick, J., et al., *Loss-of-function mutations in SLC30A8 protect against type 2 diabetes.* Nat Genet, 2014. **46**(4): p. 357-63.
272. Tamaki, M., et al., *The diabetes-susceptible gene SLC30A8/ZnT8 regulates hepatic insulin clearance.* J Clin Invest, 2013. **123**(10): p. 4513-24.
273. Pound, L.D., et al., *Deletion of the mouse Slc30a8 gene encoding zinc transporter-8 results in impaired insulin secretion.* Biochem J, 2009. **421**(3): p. 371-6.
274. Pound, L.D., et al., *The physiological effects of deleting the mouse SLC30A8 gene encoding zinc transporter-8 are influenced by gender and genetic background.* PLoS One, 2012. **7**(7): p. e40972.
275. Wicksteed, B., et al., *Conditional gene targeting in mouse pancreatic ß-Cells: analysis of ectopic Cre transgene expression in the brain.* Diabetes, 2010. **59**(12): p. 3090-8.
276. Wijesekara, N., et al., *Beta cell-specific Znt8 deletion in mice causes marked defects in insulin processing, crystallisation and secretion.* Diabetologia, 2010. **53**(8): p. 1656-68.

277. Rutter, G.A. and F. Chimienti, *SLC30A8 mutations in type 2 diabetes.* Diabetologia, 2015. **58**(1): p. 31-6.
278. Mitchell, R.K., et al., *Molecular Genetic Regulation of Slc30a8/ZnT8 Reveals a Positive Association With Glucose Tolerance.* Mol Endocrinol, 2016. **30**(1): p. 77-91.
279. Li, L., S. Bai, and C.T. Sheline, *hZnT8 (Slc30a8) Transgenic Mice That Overexpress the R325W Polymorph Have Reduced Islet Zn2+ and Proinsulin Levels, Increased Glucose Tolerance After a High-Fat Diet, and Altered Levels of Pancreatic Zinc Binding Proteins.* Diabetes, 2017. **66**(2): p. 551-559.
280. Kleiner, S., et al., *Mice harboring the human SLC30A8 R138X loss-of-function mutation have increased insulin secretory capacity.* Proc Natl Acad Sci U S A, 2018. **115**(32): p. E7642-e7649.
281. Hutton, J.C., E.J. Penn, and M. Peshavaria, *Low-molecular-weight constituents of isolated insulin-secretory granules. Bivalent cations, adenine nucleotides and inorganic phosphate.* Biochem J, 1983. **210**(2): p. 297-305.
282. Scott, D.A. and A.M. Fisher, *The insulin and the zinc content of normal and diabetic patients.* J Clin Invest, 1938. **17**(6): p. 725-8.
283. Basaki, M., et al., *Zinc, copper, iron, and chromium concentrations in young patients with type 2 diabetes mellitus.* Biol Trace Elem Res, 2012. **148**(2): p. 161-4.
284. Jansen, J., et al., *Disturbed zinc homeostasis in diabetic patients by in vitro and in vivo analysis of insulinomimetic activity of zinc.* J Nutr Biochem, 2012. **23**(11): p. 1458-66.
285. Sun, Q., et al., *Prospective study of zinc intake and risk of type 2 diabetes in women.* Diabetes Care, 2009. **32**(4): p. 629-34.
286. Shan, Z., et al., *Interactions between zinc transporter-8 gene (SLC30A8) and plasma zinc concentrations for impaired glucose regulation and type 2 diabetes.* Diabetes, 2014. **63**(5): p. 1796-803.
287. Eshak, E.S., et al., *Associations between dietary intakes of iron, copper and zinc with risk of type 2 diabetes mellitus: A large population-based prospective cohort study.* Clin Nutr, 2018. **37**(2): p. 667-674.
288. Park, J.S., et al., *Longitudinal association between toenail zinc levels and the incidence of diabetes among American young adults: The CARDIA Trace Element Study.* Sci Rep, 2016. **6**: p. 23155.

289. Chu, A., M. Foster, and S. Samman, *Zinc Status and Risk of Cardiovascular Diseases and Type 2 Diabetes Mellitus-A Systematic Review of Prospective Cohort Studies.* Nutrients, 2016. **8**(11).

290. Prasad, A.S., et al., *Hypocupremia induced by zinc therapy in adults.* JAMA, 1978. **240**(20): p. 2166-8.

291. Ranasinghe, P., et al., *Effects of Zinc supplementation on serum lipids: a systematic review and meta-analysis.* Nutr Metab (Lond), 2015. **12**: p. 26.

292. Søndergaard, L.G., et al., *Zinc ions in the endocrine and exocrine pancreas of zinc deficient rats.* Histol Histopathol, 2006. **21**(6): p. 619-25.

293. Kloubert, V. and L. Rink, *Zinc as a micronutrient and its preventive role of oxidative damage in cells.* Food Funct, 2015. **6**(10): p. 3195-204.

294. Tyo, K.E., et al., *Imbalance of heterologous protein folding and disulfide bond formation rates yields runaway oxidative stress.* BMC Biol, 2012. **10**: p. 16.

295. Liemburg-Apers, D.C., et al., *Interactions between mitochondrial reactive oxygen species and cellular glucose metabolism.* Arch Toxicol, 2015. **89**(8): p. 1209-26.

296. Poitout, V. and R.P. Robertson, *Glucolipotoxicity: fuel excess and beta-cell dysfunction.* Endocr Rev, 2008. **29**(3): p. 351-66.

297. Sarre, A., et al., *Reactive oxygen species are produced at low glucose and contribute to the activation of AMPK in insulin-secreting cells.* Free Radic Biol Med, 2012. **52**(1): p. 142-50.

298. Sadri, H., N.N. Larki, and S. Kolahian, *Hypoglycemic and Hypolipidemic Effects of Leucine, Zinc, and Chromium, Alone and in Combination, in Rats with Type 2 Diabetes.* Biol Trace Elem Res, 2017.

299. Pace, N.J. and E. Weerapana, *Zinc-Binding Cysteines: Diverse Functions and Structural Motifs.* Biomolecules, 2014. **4**(2): p. 419-434.

300. Marreiro, D.D., et al., *Zinc and Oxidative Stress: Current Mechanisms.* Antioxidants (Basel), 2017. **6**(2).

301. Zheng, Y., et al., *The role of zinc, copper and iron in the pathogenesis of diabetes and diabetic complications: therapeutic effects by chelators.* Hemoglobin, 2008. **32**(1-2): p. 135-45.

302. Gazaryan, I.G., et al., *Zinc is a potent inhibitor of thiol oxidoreductase activity and stimulates reactive oxygen species production by lipoamide dehydrogenase.* J Biol Chem, 2002. **277**(12): p. 10064-72.

303. Carocho, M. and I.C. Ferreira, *A review on antioxidants, prooxidants and related controversy: natural and synthetic compounds, screening and analysis methodologies and future perspectives.* Food Chem Toxicol, 2013. **51**: p. 15-25.
304. Baynes, J.W., *Role of oxidative stress in development of complications in diabetes.* Diabetes, 1991. **40**(4): p. 405-12.
305. Ding, H., et al., *Norathyriol reverses obesity- and high-fat-diet-induced insulin resistance in mice through inhibition of PTP1B.* Diabetologia, 2014. **57**(10): p. 2145-54.
306. Elchebly, M., et al., *Increased insulin sensitivity and obesity resistance in mice lacking the protein tyrosine phosphatase-1B gene.* Science, 1999. **283**(5407): p. 1544-8.
307. Klaman, L.D., et al., *Increased energy expenditure, decreased adiposity, and tissue-specific insulin sensitivity in protein-tyrosine phosphatase 1B-deficient mice.* Mol Cell Biol, 2000. **20**(15): p. 5479-89.
308. Fernandez-Ruiz, R., et al., *Protein tyrosine phosphatase-1B modulates pancreatic β-cell mass.* PLoS One, 2014. **9**(2): p. e90344.
309. Bellomo, E., et al., *The metal face of protein tyrosine phosphatase 1B.* Coord Chem Rev, 2016. **327-328**: p. 70-83.
310. Hogstrand, C., et al., *Zinc transporters and cancer: a potential role for ZIP7 as a hub for tyrosine kinase activation.* Trends Mol Med, 2009. **15**(3): p. 101-11.
311. Ilouz, R., et al., *Inhibition of glycogen synthase kinase-3beta by bivalent zinc ions: insight into the insulin-mimetic action of zinc.* Biochem Biophys Res Commun, 2002. **295**(1): p. 102-6.
312. Popovics, P. and A.J. Stewart, *GPR39: a Zn(2+)-activated G protein-coupled receptor that regulates pancreatic, gastrointestinal and neuronal functions.* Cell Mol Life Sci, 2011. **68**(1): p. 85-95.
313. Geiser, J., et al., *A mouse model of acrodermatitis enteropathica: loss of intestine zinc transporter ZIP4 (Slc39a4) disrupts the stem cell niche and intestine integrity.* PLoS Genet, 2012. **8**(6): p. e1002766.
314. Wu, W., et al., *Src-dependent phosphorylation of the epidermal growth factor receptor on tyrosine 845 is required for zinc-induced Ras activation.* J Biol Chem, 2002. **277**(27): p. 24252-7.
315. Olechnowicz, J., et al., *Zinc status is associated with inflammation, oxidative stress, lipid, and glucose metabolism.* J Physiol Sci, 2018. **68**(1): p. 19-31.

316. Miyai, T., et al., *Zinc transporter SLC39A10/ZIP10 facilitates antiapoptotic signaling during early B-cell development.* Proc Natl Acad Sci U S A, 2014. **111**(32): p. 11780-5.
317. Supasai, S., et al., *Zinc deficiency affects the STAT1/3 signaling pathways in part through redox-mediated mechanisms.* Redox Biol, 2017. **11**: p. 469-481.
318. Taylor, K.M., et al., *Protein kinase CK2 triggers cytosolic zinc signaling pathways by phosphorylation of zinc channel ZIP7.* Sci Signal, 2012. **5**(210): p. ra11.
319. Buteau, J., *GLP-1 receptor signaling: effects on pancreatic beta-cell proliferation and survival.* Diabetes Metab, 2008. **34 Suppl 2**: p. S73-7.
320. Yamashita, S., et al., *Zinc transporter LIVI controls epithelial-mesenchymal transition in zebrafish gastrula organizer.* Nature, 2004. **429**(6989): p. 298-302.
321. Zhao, L., et al., *LIV-1 suppression inhibits HeLa cell invasion by targeting ERK1/2-Snail/Slug pathway.* Biochem Biophys Res Commun, 2007. **363**(1): p. 82-8.
322. Beharier, O., et al., *ZnT-1 protects HL-1 cells from simulated ischemia-reperfusion through activation of Ras-ERK signaling.* J Mol Med (Berl), 2012. **90**(2): p. 127-38.
323. Sindreu, C., R.D. Palmiter, and D.R. Storm, *Zinc transporter ZnT-3 regulates presynaptic Erk1/2 signaling and hippocampus-dependent memory.* Proc Natl Acad Sci U S A, 2011. **108**(8): p. 3366-70.
324. Fukada, T., et al., *The zinc transporter SLC39A13/ZIP13 is required for connective tissue development; its involvement in BMP/TGF-beta signaling pathways.* PLoS One, 2008. **3**(11): p. e3642.
325. Hojyo, S., et al., *The zinc transporter SLC39A14/ZIP14 controls G-protein coupled receptor-mediated signaling required for systemic growth.* PLoS One, 2011. **6**(3): p. e18059.
326. Zheng, D., et al., *Uptake epithelia behave in a cell-centric and not systems homeostatic manner in response to zinc depletion and supplementation.* Metallomics, 2014. **6**(1): p. 154-65.
327. Zheng, D., et al., *Dynamic transcriptomic profiles of zebrafish gills in response to zinc supplementation.* BMC Genomics, 2010. **11**: p. 553.
328. Zheng, D., et al., *Dynamic transcriptomic profiles of zebrafish gills in response to zinc depletion.* BMC Genomics, 2010. **11**: p. 548.

329. Kim, G., K.H. Shin, and E.K. Pae, *Zinc Up-Regulates Insulin Secretion from β Cell-Like Cells Derived from Stem Cells from Human Exfoliated Deciduous Tooth (SHED).* Int J Mol Sci, 2016. **17**(12): p. 2092.
330. Naya, F.J., C.M. Stellrecht, and M.J. Tsai, *Tissue-specific regulation of the insulin gene by a novel basic helix-loop-helix transcription factor.* Genes Dev, 1995. **9**(8): p. 1009-19.
331. Gu, C., et al., *Pancreatic beta cells require NeuroD to achieve and maintain functional maturity.* Cell Metab, 2010. **11**(4): p. 298-310.
332. Malecki, M.T., et al., *Mutations in NEUROD1 are associated with the development of type 2 diabetes mellitus.* Nat Genet, 1999. **23**(3): p. 323-8.
333. Rubio-Cabezas, O., et al., *Homozygous mutations in NEUROD1 are responsible for a novel syndrome of permanent neonatal diabetes and neurological abnormalities.* Diabetes, 2010. **59**(9): p. 2326-31.
334. Johnstone, K.A., et al., *Dysregulation of Hnf1b gene expression in cultured beta-cells in response to cytotoxic fatty acid.* JOP, 2011. **12**(1): p. 6-10.
335. Horikawa, Y., et al., *Mutation in hepatocyte nuclear factor-1 beta gene (TCF2) associated with MODY.* Nat Genet, 1997. **17**(4): p. 384-5.
336. Edghill, E.L., et al., *Mutations in hepatocyte nuclear factor-1beta and their related phenotypes.* J Med Genet, 2006. **43**(1): p. 84-90.
337. Wang, C., et al., *Scanning for MODY5 gene mutations in Chinese early onset or multiple affected diabetes pedigrees.* Acta Diabetol, 2004. **41**(4): p. 137-45.
338. Wang, C., et al., *Common variants of hepatocyte nuclear factor 1beta are associated with type 2 diabetes in a Chinese population.* Diabetes, 2009. **58**(4): p. 1023-7.
339. Bartoov-Shifman, R., et al., *Activation of the insulin gene promoter through a direct effect of hepatocyte nuclear factor 4 alpha.* J Biol Chem, 2002. **277**(29): p. 25914-9.
340. Jafar-Mohammadi, B., et al., *A role for coding functional variants in HNF4A in type 2 diabetes susceptibility.* Diabetologia, 2011. **54**(1): p. 111-9.
341. Lausen, J., et al., *Naturally occurring mutations in the human HNF4alpha gene impair the function of the transcription factor to a varying degree.* Nucleic Acids Res, 2000. **28**(2): p. 430-7.

342. Dukes, I.D., et al., *Defective pancreatic beta-cell glycolytic signaling in hepatocyte nuclear factor-1alpha-deficient mice.* J Biol Chem, 1998. **273**(38): p. 24457-64.

343. Tanahashi, T., et al., *Association study on chromosome 20q11.21-13.13 locus and its contribution to type 2 diabetes susceptibility in Japanese.* Hum Genet, 2006. **120**(4): p. 527-42.

344. Bernardo, G.M. and R.A. Keri, *FOXA1: a transcription factor with parallel functions in development and cancer.* Biosci Rep, 2012. **32**(2): p. 113-30.

345. Biddie, S.C., et al., *Transcription factor AP1 potentiates chromatin accessibility and glucocorticoid receptor binding.* Mol Cell, 2011. **43**(1): p. 145-55.

346. Swinstead, E.E., et al., *Steroid Receptors Reprogram FoxA1 Occupancy through Dynamic Chromatin Transitions.* Cell, 2016. **165**(3): p. 593-605.

347. Vatamaniuk, M.Z., et al., *Foxa1-deficient mice exhibit impaired insulin secretion due to uncoupled oxidative phosphorylation.* Diabetes, 2006. **55**(10): p. 2730-6.

348. Gao, N., et al., *Dynamic regulation of Pdx1 enhancers by Foxa1 and Foxa2 is essential for pancreas development.* Genes Dev, 2008. **22**(24): p. 3435-48.

349. Sund, N.J., et al., *Tissue-specific deletion of Foxa2 in pancreatic beta cells results in hyperinsulinemic hypoglycemia.* Genes Dev, 2001. **15**(13): p. 1706-15.

350. Doyle, M.J. and L. Sussel, *Nkx2.2 regulates beta-cell function in the mature islet.* Diabetes, 2007. **56**(8): p. 1999-2007.

351. Flanagan, S.E., et al., *Analysis of transcription factors key for mouse pancreatic development establishes NKX2-2 and MNX1 mutations as causes of neonatal diabetes in man.* Cell Metab, 2014. **19**(1): p. 146-54.

352. Mastracci, T.L., et al., *Nkx2.2 and Arx genetically interact to regulate pancreatic endocrine cell development and endocrine hormone expression.* Dev Biol, 2011. **359**(1): p. 1-11.

353. Swisa, A., et al., *PAX6 maintains β cell identity by repressing genes of alternative islet cell types.* J Clin Invest, 2017. **127**(1): p. 230-243.

354. Hart, A.W., et al., *The developmental regulator Pax6 is essential for maintenance of islet cell function in the adult mouse pancreas.* PLoS One, 2013. **8**(1): p. e54173.

355. Yasuda, T., et al., *PAX6 mutation as a genetic factor common to aniridia and glucose intolerance.* Diabetes, 2002. **51**(1): p. 224-30.

356. Ding, J., et al., *Pax6 haploinsufficiency causes abnormal metabolic homeostasis by down-regulating glucagon-like peptide 1 in mice.* Endocrinology, 2009. **150**(5): p. 2136-44.
357. Ahlqvist, E., et al., *A common variant upstream of the PAX6 gene influences islet function in man.* Diabetologia, 2012. **55**(1): p. 94-104.
358. Gálvez-Peralta, M., et al., *Tissue-Specific Induction of Mouse ZIP8 and ZIP14 Divalent Cation/Bicarbonate Symporters by, and Cytokine Response to, Inflammatory Signals.* Int J Toxicol, 2014. **33**(3): p. 246-258.
359. El Muayed, M., et al., *Acute cytokine-mediated downregulation of the zinc transporter ZnT8 alters pancreatic beta-cell function.* J Endocrinol, 2010. **206**(2): p. 159-69.
360. Docherty, H.M., et al., *Relative contribution of PDX-1, MafA and E47/beta2 to the regulation of the human insulin promoter.* Biochem J, 2005. **389**(Pt 3): p. 813-20.
361. Eskridge, E.M. and D. Shields, *Cell-free processing and segregation of insulin precursors.* J Biol Chem, 1983. **258**(19): p. 11487-91.
362. Rigler, R., et al., *Specific binding of proinsulin C-peptide to human cell membranes.* Proc Natl Acad Sci U S A, 1999. **96**(23): p. 13318-23.
363. Luppi, P., et al., *C-peptide is internalised in human endothelial and vascular smooth muscle cells via early endosomes.* Diabetologia, 2009. **52**(10): p. 2218-28.
364. Shafqat, J., et al., *Proinsulin C-peptide and its analogues induce intracellular Ca2+ increases in human renal tubular cells.* Cell Mol Life Sci, 2002. **59**(7): p. 1185-9.
365. Lindahl, E., et al., *Proinsulin C-peptide regulates ribosomal RNA expression.* J Biol Chem, 2010. **285**(5): p. 3462-9.
366. Fahumy, S.H., *An Overview of Proinsulin: Structure, Function, and Clinical Significance*. 2017, Rutgers: Molecular Anatomy Project.
367. Jiang, J. and S. Dutta. *What is Diabetes?* 2016 [cited 2018 08/05/2018].
368. Foster, M.C., et al., *Elemental composition of secretory granules in pancreatic islets of Langerhans.* Biophys J, 1993. **64**(2): p. 525-32.
369. Chan, S.J., et al., *A mutation in the B chain coding region is associated with impaired proinsulin conversion in a family with hyperproinsulinemia.* Proc Natl Acad Sci U S A, 1987. **84**(8): p. 2194-7.

370. Noormägi, A., et al., *Zn(II) ions co-secreted with insulin suppress inherent amyloidogenic properties of monomeric insulin.* Biochem J, 2010. **430**(3): p. 511-8.

371. Liu, F.Y., D.O. Kildsig, and A.K. Mitra, *Insulin aggregation in aqueous media and its effect on alpha-chymotrypsin-mediated proteolytic degradation.* Pharm Res, 1991. **8**(7): p. 925-9.

372. Brender, J.R., et al., *Role of zinc in human islet amyloid polypeptide aggregation.* J Am Chem Soc, 2010. **132**(26): p. 8973-83.

373. Ferrer, R., et al., *Effects of Zn2+ on glucose-induced electrical activity and insulin release from mouse pancreatic islets.* Am J Physiol, 1984. **246**(5 Pt 1): p. C520-7.

374. Kim, B.J., et al., *Zinc as a paracrine effector in pancreatic islet cell death.* Diabetes, 2000. **49**(3): p. 367-72.

375. Robertson, R.P., H. Zhou, and M. Slucca, *A role for zinc in pancreatic islet β-cell cross-talk with the α-cell during hypoglycaemia.* Diabetes Obes Metab, 2011. **13 Suppl 1**: p. 106-11.

376. Ishihara, H., et al., *Islet beta-cell secretion determines glucagon release from neighbouring alpha-cells.* Nat Cell Biol, 2003. **5**(4): p. 330-5.

377. Ravier, M.A. and G.A. Rutter, *Glucose or insulin, but not zinc ions, inhibit glucagon secretion from mouse pancreatic alpha-cells.* Diabetes, 2005. **54**(6): p. 1789-97.

378. Duckworth, W.C., R.G. Bennett, and F.G. Hamel, *Insulin degradation: progress and potential.* Endocr Rev, 1998. **19**(5): p. 608-24.

379. Caumo, A., I. Florea, and L. Luzi, *Effect of a variable hepatic insulin clearance on the postprandial insulin profile: insights from a model simulation study.* Acta Diabetol, 2007. **44**(1): p. 23-9.

380. Eaton, R.P., R.C. Allen, and D.S. Schade, *Hepatic removal of insulin in normal man: dose response to endogenous insulin secretion.* J Clin Endocrinol Metab, 1983. **56**(6): p. 1294-300.

381. Quarterman, J., C.F. Mills, and W.R. Humphries, *The reduced secretion of, and sensitivity to insulin in zinc-deficient rats.* Biochem Biophys Res Commun, 1966. **25**(3): p. 354-8.

382. Hendricks, D.G. and A.W. Mahoney, *Glucose tolerance in zinc-deficient rats.* J Nutr, 1972. **102**(8): p. 1079-84.

383. Vijayaraghavan, K., S. Iyyampillai, and S.P. Subramanian, *Antioxidant potential of zinc-flavonol complex studied in streptozotocin-diabetic rats.* J Diabetes, 2013. **5**(2): p. 149-56.
384. Faure, P., et al., *Comparison of the effects of zinc alone and zinc associated with selenium and vitamin E on insulin sensitivity and oxidative stress in high-fructose-fed rats.* J Trace Elem Med Biol, 2007. **21**(2): p. 113-9.
385. Jayawardena, R., et al., *Effects of zinc supplementation on diabetes mellitus: a systematic review and meta-analysis.* Diabetol Metab Syndr, 2012. **4**(1): p. 13.
386. Anderson, R.A., et al., *Potential antioxidant effects of zinc and chromium supplementation in people with type 2 diabetes mellitus.* J Am Coll Nutr, 2001. **20**(3): p. 212-8.
387. Goldberg, E.D., V.A. Eshchenko, and V.D. Bovt, *Diabetogenic activity of chelators in some mammalian species.* Endocrinologie, 1990. **28**(2): p. 51-5.
388. Goldberg, E.D., V.A. Eshchenko, and V.D. Bovt, *The diabetogenic and acidotropic effects of chelators.* Exp Pathol, 1991. **42**(1): p. 59-64.
389. Kechrid, Z., N. Bouzerna, and M.S. Zio, *Effect of low zinc diet on (65)Zn turnover in non-insulin dependent diabetic mice.* Diabetes Metab, 2001. **27**(5 Pt 1): p. 580-3.
390. Ruz, M., et al., *Zinc as a potential coadjuvant in therapy for type 2 diabetes.* Food Nutr Bull, 2013. **34**(2): p. 215-21.
391. Begin-Heick, N., et al., *Zinc supplementation attenuates insulin secretory activity in pancreatic islets of the ob/ob mouse.* Diabetes, 1985. **34**(2): p. 179-84.
392. Simon, S.F. and C.G. Taylor, *Dietary zinc supplementation attenuates hyperglycemia in db/db mice.* Exp Biol Med (Maywood), 2001. **226**(1): p. 43-51.
393. Cooper-Capetini, V., et al., *Zinc Supplementation Improves Glucose Homeostasis in High Fat-Fed Mice by Enhancing Pancreatic β-Cell Function.* Nutrients, 2017. **9**(10).
394. Wang, X., et al., *Effect of zinc supplementation on type 2 diabetes parameters and liver metallothionein expressions in Wistar rats.* J Physiol Biochem, 2012. **68**(4): p. 563-72.
395. Vardatsikos, G., N.R. Pandey, and A.K. Srivastava, *Insulino-mimetic and anti-diabetic effects of zinc.* J Inorg Biochem, 2013. **120**: p. 8-17.
396. Maret, W., *Zinc in Pancreatic Islet Biology, Insulin Sensitivity, and Diabetes.* Prev Nutr Food Sci, 2017. **22**(1): p. 1-8.

397. Sharonova, I.N., V.S. Vorobjev, and H.L. Haas, *Interaction between copper and zinc at GABA(A) receptors in acutely isolated cerebellar Purkinje cells of the rat.* Br J Pharmacol, 2000. **130**(4): p. 851-6.
398. Ran, F.A., et al., *Genome engineering using the CRISPR-Cas9 system.* Nat Protoc, 2013. **8**(11): p. 2281-2308.
399. Shen, B., et al., *Efficient genome modification by CRISPR-Cas9 nickase with minimal off-target effects.* Nat Methods, 2014. **11**(4): p. 399-402.
400. Hsu, P.D., E.S. Lander, and F. Zhang, *Development and applications of CRISPR-Cas9 for genome engineering.* Cell, 2014. **157**(6): p. 1262-78.
401. Gasteiger, E., et al., *ExPASy: The proteomics server for in-depth protein knowledge and analysis.* Nucleic Acids Res, 2003. **31**(13): p. 3784-8.
402. Sievers, F., et al., *Fast, scalable generation of high-quality protein multiple sequence alignments using Clustal Omega.* Mol Syst Biol, 2011. **7**: p. 539.
403. The UniProt Consortium, *UniProt: the universal protein knowledgebase.* Nucleic Acids Res, 2017. **45**(D1): p. D158-D169.
404. Lawson, R., W. Maret, and C. Hogstrand, *Expression of the ZIP/SLC39A transporters in β-cells: a systematic review and integration of multiple datasets.* BMC Genomics, 2017. **18**(1): p. 719.
405. Lawson, R., W. Maret, and C. Hogstrand, *Prolonged stimulation of insulin release from MIN6 cells causes zinc depletion and loss of β-cell markers.* Journal of Trace Elements in Medicine and Biology, 2018. **49**: p. 51-59.
406. Poudel, R.R., et al., *Role of zinc in insulin regulation and diabetes.* Journal of Social Health and Diabetes, 2017. **5**(2): p. 83-87.
407. Al-Timimi, D.J., et al., *Serum Zinc and Metabolic Health Status in Siblings of Patients with Type 2 Diabetes Mellitus.* Journal of Clinical and Diagnostic Research : JCDR, 2015. **9**(12): p. BC05-BC08.
408. Iqbal, S., et al., *Effect of glycation on human serum albumin-zinc interaction: a biophysical study.* J Biol Inorg Chem, 2018. **23**(3): p. 447-458.
409. Rondeau, P. and E. Bourdon, *The glycation of albumin: structural and functional impacts.* Biochimie, 2011. **93**(4): p. 645-58.
410. Kazi, T.G., et al., *Copper, chromium, manganese, iron, nickel, and zinc levels in biological samples of diabetes mellitus patients.* Biol Trace Elem Res, 2008. **122**(1): p. 1-18.

411. Al-Maroof, R.A. and S.S. Al-Sharbatti, *Serum zinc levels in diabetic patients and effect of zinc supplementation on glycemic control of type 2 diabetics.* Saudi Med J, 2006. **27**(3): p. 344-50.
412. Ruz, M., et al., *Does Zinc Really "Metal" with Diabetes? The Epidemiologic Evidence.* Curr Diab Rep, 2016. **16**(11): p. 111.
413. Saharia, G.K. and R.K. Goswami, *Evaluation of Serum Zinc Status and Glycated Hemoglobin of Type 2 Diabetes Mellitus Patients in a Tertiary Care Hospital of Assam.* Journal of Laboratory Physicians, 2013. **5**(1): p. 30-33.
414. Kukurba, K.R. and S.B. Montgomery, *RNA Sequencing and Analysis.* Cold Spring Harb Protoc, 2015. **2015**(11): p. 951-69.
415. Wang, Z., M. Gerstein, and M. Snyder, *RNA-Seq: a revolutionary tool for transcriptomics.* Nat Rev Genet, 2009. **10**(1): p. 57-63.
416. Norouzi, S., et al., *Zinc transporters and insulin resistance: therapeutic implications for type 2 diabetes and metabolic disease.* Journal of Biomedical Science, 2017. **24**: p. 87.
417. Robinson, M.D. and A. Oshlack, *A scaling normalization method for differential expression analysis of RNA-seq data.* Genome Biology, 2010. **11**(3): p. R25.
418. Pinero, J., et al., *DisGeNET: a comprehensive platform integrating information on human disease-associated genes and variants.* Nucleic Acids Res, 2017. **45**(D1): p. D833-d839.
419. Pirooznia, M., V. Nagarajan, and Y. Deng, *GeneVenn - A web application for comparing gene lists using Venn diagrams.* Bioinformation, 2007. **1**(10): p. 420-422.
420. Jeong, J. and D.J. Eide, *The SLC39 family of zinc transporters.* Mol Aspects Med, 2013. **34**(2-3): p. 612-9.
421. Huang, L. and S. Tepaamorndech, *The SLC30 family of zinc transporters - a review of current understanding of their biological and pathophysiological roles.* Mol Aspects Med, 2013. **34**(2-3): p. 548-60.
422. Hempel, S.L., et al., *Dihydrofluorescein diacetate is superior for detecting intracellular oxidants: comparison with 2',7'-dichlorodihydrofluorescein diacetate, 5(and 6)-carboxy-2',7'-dichlorodihydrofluorescein diacetate, and dihydrorhodamine 123.* Free Radical Biology and Medicine, 1999. **27**(1): p. 146-159.

423. LeBel, C.P., H. Ischiropoulos, and S.C. Bondy, *Evaluation of the probe 2',7'-dichlorofluorescin as an indicator of reactive oxygen species formation and oxidative stress.* Chem Res Toxicol, 1992. **5**(2): p. 227-31.
424. Slepchenko Kira, G., B.L. James Calvin, and V. Li Yang, *Inhibitory effect of zinc on glucose-stimulated zinc/insulin secretion in an insulin-secreting β-cell line.* Experimental Physiology, 2013. **98**(8): p. 1301-1311.
425. Wieczorek, G., A. Pospischil, and E. Perentes, *A comparative immunohistochemical study of pancreatic islets inlaboratory animals (rats, dogs, minipigs, nonhuman primates).* Experimental and Toxicologic Pathology, 1998. **50**(3): p. 151-172.
426. Hoyer, P.O. and A. Hyvarinen, *Independent component analysis applied to feature extraction from colour and stereo images.* Network, 2000. **11**(3): p. 191-210.
427. Nawy, T., *Contrasting PCA across datasets.* Nature Methods, 2018. **15**(8): p. 572-572.
428. Hyvarinen, A. and E. Oja, *Independent component analysis: algorithms and applications.* Neural Netw, 2000. **13**(4-5): p. 411-30.
429. Vallee, B.L., J.E. Coleman, and D.S. Auld, *Zinc fingers, zinc clusters, and zinc twists in DNA-binding protein domains.* Proceedings of the National Academy of Sciences of the United States of America, 1991. **88**(3): p. 999-1003.
430. Asahina, H., et al., *The XPA protein is a zinc metalloprotein with an ability to recognize various kinds of DNA damage.* Mutat Res, 1994. **315**(3): p. 229-37.
431. Morita, E.H., et al., *Implications of the zinc-finger motif found in the DNA-binding domain of the human XPA protein.* Genes Cells, 1996. **1**(5): p. 437-42.
432. Yoshihisa, T., C. Barlowe, and R. Schekman, *Requirement for a GTPase-activating protein in vesicle budding from the endoplasmic reticulum.* Science, 1993. **259**(5100): p. 1466-8.
433. Schaller, M.D., *Paxillin: a focal adhesion-associated adaptor protein.* Oncogene, 2001. **20**: p. 6459.
434. Tu, Y.H., et al., *An evolutionarily conserved gene family encodes proton-selective ion channels.* Science, 2018. **359**(6379): p. 1047-1050.
435. Chen, M.-Y., et al., *Serum uric acid levels are associated with obesity but not cardio-cerebrovascular events in Chinese inpatients with type 2 diabetes.* Scientific Reports, 2017. **7**: p. 40009.

436. Lu, J., et al., *Knockout of the urate oxidase gene provides a stable mouse model of hyperuricemia associated with metabolic disorders.* Kidney Int, 2018. **93**(1): p. 69-80.
437. Koedrith, P. and Y.R. Seo, *Advances in carcinogenic metal toxicity and potential molecular markers.* Int J Mol Sci, 2011. **12**(12): p. 9576-95.
438. Schwarz, K., et al., *Mutations affecting the secretory COPII coat component SEC23B cause congenital dyserythropoietic anemia type II.* Nat Genet, 2009. **41**(8): p. 936-40.
439. Kozhevnikova, O.S., et al., *Rat retinal transcriptome: effects of aging and AMD-like retinopathy.* Cell Cycle, 2013. **12**(11): p. 1745-61.
440. Kilic, M., et al., *Role of hypoxia inducible factor-1 alpha in modulation of apoptosis resistance.* Oncogene, 2007. **26**(14): p. 2027-38.
441. Pugh, C.W. and P.J. Ratcliffe, *Regulation of angiogenesis by hypoxia: role of the HIF system.* Nat Med, 2003. **9**(6): p. 677-84.
442. Semenza, G.L., *Regulation of mammalian O2 homeostasis by hypoxia-inducible factor 1.* Annu Rev Cell Dev Biol, 1999. **15**: p. 551-78.
443. Imtiyaz, H.Z. and M.C. Simon, *Hypoxia-inducible factors as essential regulators of inflammation.* Curr Top Microbiol Immunol, 2010. **345**: p. 105-20.
444. Chen, X., et al., *Vascular endothelial growth factor (VEGF) regulation by hypoxia inducible factor-1 alpha (HIF1A) starts and peaks during endometrial breakdown, not repair, in a mouse menstrual-like model.* Hum Reprod, 2015. **30**(9): p. 2160-70.
445. Jung, S.N., et al., *Reactive oxygen species stabilize hypoxia-inducible factor-1 alpha protein and stimulate transcriptional activity via AMP-activated protein kinase in DU145 human prostate cancer cells.* Carcinogenesis, 2008. **29**(4): p. 713-21.
446. Laughner, E., et al., *HER2 (neu) signaling increases the rate of hypoxia-inducible factor 1alpha (HIF-1alpha) synthesis: novel mechanism for HIF-1-mediated vascular endothelial growth factor expression.* Mol Cell Biol, 2001. **21**(12): p. 3995-4004.
447. Murphy, B.J., et al., *The metal-responsive transcription factor-1 contributes to HIF-1 activation during hypoxic stress.* Biochem Biophys Res Commun, 2005. **337**(3): p. 860-7.

448. Cheng, K., et al., *Hypoxia-inducible factor-1alpha regulates beta cell function in mouse and human islets.* J Clin Invest, 2010. **120**(6): p. 2171-83.
449. Carpene, E., G. Andreani, and G. Isani, *Metallothionein functions and structural characteristics.* J Trace Elem Med Biol, 2007. **21 Suppl 1**: p. 35-9.
450. Schmitt-Ulms, G., et al., *Evolutionary descent of prion genes from the ZIP family of metal ion transporters.* PLoS One, 2009. **4**(9): p. e7208.
451. Aydemir, T.B., et al., *Hepatic ZIP14-mediated Zinc Transport Contributes to Endosomal Insulin Receptor Trafficking and Glucose Metabolism.* J Biol Chem, 2016. **291**(46): p. 23939-23951.
452. Homma, K., et al., *SOD1 as a molecular switch for initiating the homeostatic ER stress response under zinc deficiency.* Mol Cell, 2013. **52**(1): p. 75-86.
453. Lin, W., et al., *Hepatic metal ion transporter ZIP8 regulates manganese homeostasis and manganese-dependent enzyme activity.* J Clin Invest, 2017. **127**(6): p. 2407-2417.
454. Tuschl, K., et al., *Mutations in SLC39A14 disrupt manganese homeostasis and cause childhood-onset parkinsonism-dystonia.* Nat Commun, 2016. **7**: p. 11601.
455. Bozym, R.A., et al., *Free zinc ions outside a narrow concentration range are toxic to a variety of cells in vitro.* Exp Biol Med (Maywood), 2010. **235**(6): p. 741-50.
456. Bettini, M.L. and G.J. Kersh, *Dual Specificity Phosphatase (DUSP) activity regulates ERK activation and positive selection of thymocytes (87.16).* The Journal of Immunology, 2007. **178**(1 Supplement): p. S130.
457. Nimmanon, T., et al., *Phosphorylation of zinc channel ZIP7 drives MAPK, PI3K and mTOR growth and proliferation signalling †Electronic supplementary information (ESI) available: Supplementary figures. See DOI: 10.1039/c6mt00286b Click here for additional data file.* Metallomics, 2017. **9**(5): p. 471-481.
458. Jarosz, M., et al., *Antioxidant and anti-inflammatory effects of zinc. Zinc-dependent NF-κB signaling.* Inflammopharmacology, 2017. **25**(1): p. 11-24.
459. Plum, L.M., L. Rink, and H. Haase, *The Essential Toxin: Impact of Zinc on Human Health.* International Journal of Environmental Research and Public Health, 2010. **7**(4): p. 1342-1365.
460. Slepchenko, K.G. and Y.V. Li, *Rising intracellular zinc by membrane depolarization and glucose in insulin-secreting clonal HIT-T15 beta cells.* Exp Diabetes Res, 2012. **2012**: p. 190309.

461. Gerich, J.E., *Is reduced first-phase insulin release the earliest detectable abnormality in individuals destined to develop type 2 diabetes?* Diabetes, 2002. **51 Suppl 1**: p. S117-21.
462. Cousins, R.J., et al., *A global view of the selectivity of zinc deprivation and excess on genes expressed in human THP-1 mononuclear cells.* Proc Natl Acad Sci U S A, 2003. **100**(12): p. 6952-7.
463. Daniel, H. and H. tom Dieck, *Nutrient-gene interactions: a single nutrient and hundreds of target genes.* Biol Chem, 2004. **385**(7): p. 571-83.
464. Birney, E., et al., *Identification and analysis of functional elements in 1% of the human genome by the ENCODE pilot project.* Nature, 2007. **447**(7146): p. 799-816.
465. Richard Boland, C., *Non-coding RNA: It's Not Junk.* Digestive Diseases and Sciences, 2017. **62**(5): p. 1107-1109.
466. Vallee, B.L. and D.S. Auld, *Active-site zinc ligands and activated H2O of zinc enzymes.* Proceedings of the National Academy of Sciences, 1990. **87**(1): p. 220.
467. Christianson, D.W., *Structural Biology of Zinc*, in *Advances in Protein Chemistry*, C.B. Anfinsen, et al., Editors. 1991, Academic Press. p. 281-355.
468. Coleman, J.E., *Zinc Proteins: Enzymes, Storage Proteins, Transcription Factors, and Replication Proteins.* Annual Review of Biochemistry, 1992. **61**(1): p. 897-946.
469. Ubersax, J.A. and J.E. Ferrell, Jr., *Mechanisms of specificity in protein phosphorylation.* Nat Rev Mol Cell Biol, 2007. **8**(7): p. 530-41.
470. Cheng, H.C., et al., *Regulation and function of protein kinases and phosphatases.* Enzyme Res, 2011. **2011**: p. 794089.
471. Kenner, K.A., et al., *Protein-tyrosine phosphatase 1B is a negative regulator of insulin- and insulin-like growth factor-I-stimulated signaling.* J Biol Chem, 1996. **271**(33): p. 19810-6.
472. Movafagh, S., S. Crook, and K. Vo, *Regulation of hypoxia-inducible factor-1a by reactive oxygen species: new developments in an old debate.* J Cell Biochem, 2015. **116**(5): p. 696-703.
473. Lee, S.Y., et al., *[Zinc induces normoxic accumulation of transcriptionally active hypoxia-inducible factor 1-alpha in mammary epithelial cells]*. Mol Biol (Mosk), 2017. **51**(1): p. 104-110.

474. Naldini, A., et al., *Hypoxia affects dendritic cell survival: role of the hypoxia-inducible factor-1alpha and lipopolysaccharide.* J Cell Physiol, 2012. **227**(2): p. 587-95.

475. Majmundar, A.J., W.J. Wong, and M.C. Simon, *Hypoxia-inducible factors and the response to hypoxic stress.* Mol Cell, 2010. **40**(2): p. 294-309.

476. Lv, X., et al., *The role of hypoxia-inducible factors in tumor angiogenesis and cell metabolism.* Genes & Diseases, 2017. **4**(1): p. 19-24.

477. Sakkiah, S., et al., *Insight the C-Site Pocket Conformational Changes Responsible for Sirtuin 2 Activity Using Molecular Dynamics Simulations.* PLOS ONE, 2013. **8**(3): p. e59278.

478. Wu, W., et al., *Zinc-induced PTEN protein degradation through the proteasome pathway in human airway epithelial cells.* J Biol Chem, 2003. **278**(30): p. 28258-63.

479. Niu, G., et al., *Signal transducer and activator of transcription 3 is required for hypoxia-inducible factor-1alpha RNA expression in both tumor cells and tumor-associated myeloid cells.* Mol Cancer Res, 2008. **6**(7): p. 1099-105.

480. Düvel, K., et al., *Activation of a Metabolic Gene Regulatory Network Downstream of mTOR Complex 1.* Molecular Cell, 2010. **39**(2): p. 171-183.

481. Flügel, D., et al., *Glycogen Synthase Kinase 3 Phosphorylates Hypoxia-Inducible Factor 1α and Mediates Its Destabilization in a VHL-Independent Manner.* Molecular and Cellular Biology, 2007. **27**(9): p. 3253-3265.

482. Cheng, K., et al., *Hypoxia-inducible factor-1α regulates β cell function in mouse and human islets.* The Journal of Clinical Investigation, 2010. **120**(6): p. 2171-2183.

483. Rosen, E.D. and O.A. MacDougald, *Adipocyte differentiation from the inside out.* Nature Reviews Molecular Cell Biology, 2006. **7**: p. 885.

484. Rosen, E.D., et al., *Targeted elimination of peroxisome proliferator-activated receptor gamma in beta cells leads to abnormalities in islet mass without compromising glucose homeostasis.* Mol Cell Biol, 2003. **23**(20): p. 7222-9.

485. Kim, H.-S., et al., *PPAR-γ Activation Increases Insulin Secretion through the Up-regulation of the Free Fatty Acid Receptor GPR40 in Pancreatic β-Cells.* PLoS ONE, 2013. **8**(1): p. e50128.

486. Hihi, A.K., L. Michalik, and W. Wahli, *PPARs: transcriptional effectors of fatty acids and their derivatives.* Cell Mol Life Sci, 2002. **59**(5): p. 790-8.

487. Lee, M.S., et al., *Structure of the retinoid X receptor alpha DNA binding domain: a helix required for homodimeric DNA binding.* Science, 1993. **260**(5111): p. 1117-21.

488. Meerarani, P., et al., *Zinc Modulates PPARγ Signaling and Activation of Porcine Endothelial Cells.* The Journal of Nutrition, 2003. **133**(10): p. 3058-3064.

489. Jhala, U.S., et al., *cAMP promotes pancreatic beta-cell survival via CREB-mediated induction of IRS2.* Genes Dev, 2003. **17**(13): p. 1575-80.

490. Van de Velde, S., M.F. Hogan, and M. Montminy, *mTOR links incretin signaling to HIF induction in pancreatic beta cells.* Proc Natl Acad Sci U S A, 2011. **108**(41): p. 16876-82.

491. Hussain, M.A., et al., *Increased pancreatic beta-cell proliferation mediated by CREB binding protein gene activation.* Mol Cell Biol, 2006. **26**(20): p. 7747-59.

492. Liu, J., et al., *Depletion of intracellular zinc down-regulates expression of Uch-L1 mRNA and protein, and CREB mRNA in cultured hippocampal neurons.* Nutr Neurosci, 2008. **11**(3): p. 96-102.

493. Kim, J.E. and J. Chen, *regulation of peroxisome proliferator-activated receptor-gamma activity by mammalian target of rapamycin and amino acids in adipogenesis.* Diabetes, 2004. **53**(11): p. 2748-56.

494. Jansson, D., et al., *Glucose controls CREB activity in islet cells via regulated phosphorylation of TORC2.* Proc Natl Acad Sci U S A, 2008. **105**(29): p. 10161-6.

495. Naqvi, S., K.J. Martin, and J.S. Arthur, *CREB phosphorylation at Ser133 regulates transcription via distinct mechanisms downstream of cAMP and MAPK signalling.* Biochem J, 2014. **458**(3): p. 469-79.

496. Katsura, S., et al., *Identification of Posttranslational Modifications in Peroxisome Proliferator-Activated Receptor gamma Using Mass Spectrometry.* PPAR Res, 2014. **2014**: p. 468925.

497. Vinkenborg, J.L., et al., *Genetically encoded FRET sensors to monitor intracellular Zn2+ homeostasis.* Nat Methods, 2009. **6**(10): p. 737-40.

498. Valasatava, Y., C. Andreini, and A. Rosato, *Hidden relationships between metalloproteins unveiled by structural comparison of their metal sites.* Scientific Reports, 2015. **5**: p. 9486.

499. Wang, H., et al., *Pdx1 level defines pancreatic gene expression pattern and cell lineage differentiation.* J Biol Chem, 2001. **276**(27): p. 25279-86.

500. Ohlsson, H., K. Karlsson, and T. Edlund, *IPF1, a homeodomain-containing transactivator of the insulin gene.* EMBO J, 1993. **12**(11): p. 4251-9.
501. Jonsson, J., et al., *Insulin-promoter-factor 1 is required for pancreas development in mice.* Nature, 1994. **371**(6498): p. 606-9.
502. Offield, M.F., et al., *PDX-1 is required for pancreatic outgrowth and differentiation of the rostral duodenum.* Development, 1996. **122**(3): p. 983-95.
503. Smith, S.B., et al., *Autoregulation and maturity onset diabetes of the young transcription factors control the human PAX4 promoter.* J Biol Chem, 2000. **275**(47): p. 36910-9.
504. Kent, W.J., et al., *The human genome browser at UCSC.* Genome Res, 2002. **12**(6): p. 996-1006.
505. Broos, S., et al., *ConTra v2: a tool to identify transcription factor binding sites across species, update 2011.* Nucleic Acids Res, 2011. **39**(Web Server issue): p. W74-8.
506. Wingender, E., et al., *TRANSFAC: a database on transcription factors and their DNA binding sites.* Nucleic Acids Res, 1996. **24**(1): p. 238-41.
507. Yuan, Z.L., et al., *Central role of the threonine residue within the p+1 loop of receptor tyrosine kinase in STAT3 constitutive phosphorylation in metastatic cancer cells.* Mol Cell Biol, 2004. **24**(21): p. 9390-400.
508. Chandrasekera, P.C. and J.J. Pippin, *Of rodents and men: species-specific glucose regulation and type 2 diabetes research.* ALTEX, 2014. **31**(2): p. 157-76.
509. Khoo, C., et al., *Research resource: the pdx1 cistrome of pancreatic islets.* Mol Endocrinol, 2012. **26**(3): p. 521-33.
510. Teo, A.K., et al., *PDX1 binds and represses hepatic genes to ensure robust pancreatic commitment in differentiating human embryonic stem cells.* Stem Cell Reports, 2015. **4**(4): p. 578-90.
511. Iype, T., et al., *Mechanism of insulin gene regulation by the pancreatic transcription factor Pdx-1: application of pre-mRNA analysis and chromatin immunoprecipitation to assess formation of functional transcriptional complexes.* J Biol Chem, 2005. **280**(17): p. 16798-807.
512. Thomas, P., et al., *Identification and characterization of membrane androgen receptors in the ZIP9 zinc transporter subfamily: II. Role of human ZIP9 in testosterone-induced prostate and breast cancer cell apoptosis.* Endocrinology, 2014. **155**(11): p. 4250-65.

513. Brun, T., et al., *The diabetes-linked transcription factor PAX4 promotes {beta}-cell proliferation and survival in rat and human islets.* J Cell Biol, 2004. **167**(6): p. 1123-35.

514. Lu, J., et al., *Pax4 paired domain mediates direct protein transduction into mammalian cells.* Endocrinology, 2007. **148**(11): p. 5558-65.

515. van der Meulen, T. and M.O. Huising, *Role of transcription factors in the transdifferentiation of pancreatic islet cells.* J Mol Endocrinol, 2015. **54**(2): p. R103-17.

516. Gao, N., et al., *Foxa1 and Foxa2 maintain the metabolic and secretory features of the mature beta-cell.* Mol Endocrinol, 2010. **24**(8): p. 1594-604.

517. Wang, H., et al., *MAFA controls genes implicated in insulin biosynthesis and secretion.* Diabetologia, 2007. **50**(2): p. 348-58.

518. Zhang, T., et al., *FoxO1 Plays an Important Role in Regulating beta-Cell Compensation for Insulin Resistance in Male Mice.* Endocrinology, 2016. **157**(3): p. 1055-70.

519. Beyersmann, D. and H. Haase, *Functions of zinc in signaling, proliferation and differentiation of mammalian cells.* Biometals, 2001. **14**(3-4): p. 331-41.

520. Azriel-Tamir, H., et al., *Extracellular zinc triggers ERK-dependent activation of Na+/H+ exchange in colonocytes mediated by the zinc-sensing receptor.* J Biol Chem, 2004. **279**(50): p. 51804-16.

521. Samet, J.M., et al., *Activation of MAPKs in human bronchial epithelial cells exposed to metals.* Am J Physiol, 1998. **275**(3 Pt 1): p. L551-8.

522. Mebratu, Y. and Y. Tesfaigzi, *How ERK1/2 activation controls cell proliferation and cell death: Is subcellular localization the answer?* Cell Cycle, 2009. **8**(8): p. 1168-75.

523. Nielsen, J.H., et al., *Regulation of beta-cell mass by hormones and growth factors.* Diabetes, 2001. **50 Suppl 1**: p. S25-9.

524. Yamamoto, K., et al., *Recombinant human betacellulin promotes the neogenesis of beta-cells and ameliorates glucose intolerance in mice with diabetes induced by selective alloxan perfusion.* Diabetes, 2000. **49**(12): p. 2021-7.

525. Garcia-Ocaña, A., et al., *Hepatocyte growth factor overexpression in the islet of transgenic mice increases beta cell proliferation, enhances islet mass, and induces mild hypoglycemia.* J Biol Chem, 2000. **275**(2): p. 1226-32.

526. Wang, M.Y., et al., *Overexpression of leptin receptors in pancreatic islets of Zucker diabetic fatty rats restores GLUT-2, glucokinase, and glucose-stimulated insulin secretion.* Proc Natl Acad Sci U S A, 1998. **95**(20): p. 11921-6.
527. De Groef, S., et al., *STAT3 modulates β-cell cycling in injured mouse pancreas and protects against DNA damage.* Cell Death Dis, 2016. **7**(6): p. e2272.
528. Lee, J.Y. and L. Hennighausen, *The transcription factor Stat3 is dispensable for pancreatic beta-cell development and function.* Biochem Biophys Res Commun, 2005. **334**(3): p. 764-8.
529. Haapaniemi, E., et al., *CRISPR–Cas9 genome editing induces a p53-mediated DNA damage response.* Nature Medicine, 2018.
530. Li, Y., et al., *beta-Cell Pdx1 expression is essential for the glucoregulatory, proliferative, and cytoprotective actions of glucagon-like peptide-1.* Diabetes, 2005. **54**(2): p. 482-91.
531. Sachdeva, M.M., et al., *Pdx1 (MODY4) regulates pancreatic beta cell susceptibility to ER stress.* Proc Natl Acad Sci U S A, 2009. **106**(45): p. 19090-5.
532. Nguyen, T.S., K. Kohno, and Y. Kimata, *Zinc depletion activates the endoplasmic reticulum-stress sensor Ire1 via pleiotropic mechanisms.* Biosci Biotechnol Biochem, 2013. **77**(6): p. 1337-9.
533. Taylor, K.M., et al., *Zinc transporter ZIP10 forms a heteromer with ZIP6 which regulates embryonic development and cell migration.* Biochem J, 2016. **473**(16): p. 2531-44.
534. Chowanadisai, W., B. Lönnerdal, and S.L. Kelleher, *Zip6 (LIV-1) regulates zinc uptake in neuroblastoma cells under resting but not depolarizing conditions.* Brain Res, 2008. **1199**: p. 10-9.
535. Matsui, C., et al., *Zinc and its transporter ZIP6 are key mediators of breast cancer cell survival under high glucose conditions.* FEBS Lett, 2017. **591**(20): p. 3348-3359.
536. Watts, J.C., et al., *Interactome analyses identify ties of PrP and its mammalian paralogs to oligomannosidic N-glycans and endoplasmic reticulum-derived chaperones.* PLoS Pathog, 2009. **5**(10): p. e1000608.
537. Dufner-Beattie, J., et al., *Mouse ZIP1 and ZIP3 genes together are essential for adaptation to dietary zinc deficiency during pregnancy.* Genesis, 2006. **44**(5): p. 239-51.

538. Kirschke, C.P. and L. Huang, *ZnT7, a novel mammalian zinc transporter, accumulates zinc in the Golgi apparatus.* J Biol Chem, 2003. **278**(6): p. 4096-102.
539. Taylor, K.M., et al., *Zinc transporter ZIP10 forms a heteromer with ZIP6 which regulates embryonic development and cell migration.* Biochem J, 2016.
540. Mussmann, R., et al., *Inhibition of GSK3 promotes replication and survival of pancreatic beta cells.* J Biol Chem, 2007. **282**(16): p. 12030-7.
541. Aydemir, T.B., et al., *Zinc transporter ZIP14 functions in hepatic zinc, iron and glucose homeostasis during the innate immune response (endotoxemia).* PLoS One, 2012. **7**(10): p. e48679.
542. Jeong, J., et al., *Promotion of vesicular zinc efflux by ZIP13 and its implications for spondylocheiro dysplastic Ehlers-Danlos syndrome.* Proc Natl Acad Sci U S A, 2012. **109**(51): p. E3530-8.
543. Hashimoto, A., et al., *Properties of Zip4 accumulation during zinc deficiency and its usefulness to evaluate zinc status: a study of the effects of zinc deficiency during lactation.* American Journal of Physiology-Regulatory, Integrative and Comparative Physiology, 2015. **310**(5): p. R459-R468.
544. Grzywacz, A., et al., *Metal responsive transcription factor 1 (MTF-1) regulates zinc dependent cellular processes at the molecular level.* Acta Biochim Pol, 2015. **62**(3): p. 491-8.
545. Wang, H., et al., *Hepatocyte nuclear factor 4alpha regulates the expression of pancreatic beta -cell genes implicated in glucose metabolism and nutrient-induced insulin secretion.* J Biol Chem, 2000. **275**(46): p. 35953-9.
546. Brink, C., K. Chowdhury, and P. Gruss, *Pax4 regulatory elements mediate beta cell specific expression in the pancreas.* Mech Dev, 2001. **100**(1): p. 37-43.
547. Vaxillaire, M. and P. Froguel, *Genetic basis of maturity-onset diabetes of the young.* Endocrinol Metab Clin North Am, 2006. **35**(2): p. 371-384.
548. Nakae, J., et al., *The forkhead transcription factor Foxo1 regulates adipocyte differentiation.* Dev Cell, 2003. **4**(1): p. 119-29.
549. Medema, R.H., et al., *AFX-like Forkhead transcription factors mediate cell-cycle regulation by Ras and PKB through p27kip1.* Nature, 2000. **404**(6779): p. 782-7.
550. Brunet, A., et al., *Akt promotes cell survival by phosphorylating and inhibiting a Forkhead transcription factor.* Cell, 1999. **96**(6): p. 857-68.
551. Hamasaki, A., et al., *Adult pancreatic islets require differential pax6 gene dosage.* Biochem Biophys Res Commun, 2007. **353**(1): p. 40-6.

552. Wen, J.H., et al., *Paired box 6 (PAX6) regulates glucose metabolism via proinsulin processing mediated by prohormone convertase 1/3 (PC1/3).* Diabetologia, 2009. **52**(3): p. 504-13.

553. Chamcheu, J.C., et al., *Delphinidin, a dietary antioxidant, induces human epidermal keratinocyte differentiation but not apoptosis: studies in submerged and three-dimensional epidermal equivalent models.* Exp Dermatol, 2013. **22**(5): p. 342-8.

554. Lo Furno, D., et al., *Decrease of apoptosis markers during adipogenic differentiation of mesenchymal stem cells from human adipose tissue.* Apoptosis, 2013. **18**(5): p. 578-88.

555. Kim, Y.J., et al., *Quercetin, a flavonoid, inhibits proliferation and increases osteogenic differentiation in human adipose stromal cells.* Biochem Pharmacol, 2006. **72**(10): p. 1268-78.

556. Sester, D.P., et al., *Bacterial/CpG DNA down-modulates colony stimulating factor-1 receptor surface expression on murine bone marrow-derived macrophages with concomitant growth arrest and factor-independent survival.* J Immunol, 1999. **163**(12): p. 6541-50.

557. Saile, B., et al., *Transforming growth factor beta and tumor necrosis factor alpha inhibit both apoptosis and proliferation of activated rat hepatic stellate cells.* Hepatology, 1999. **30**(1): p. 196-202.

558. Hermida, M.A., J. Dinesh Kumar, and N.R. Leslie, *GSK3 and its interactions with the PI3K/AKT/mTOR signalling network.* Advances in Biological Regulation, 2017. **65**: p. 5-15.

559. Meyuhas, O., *Physiological roles of ribosomal protein S6: one of its kind.* Int Rev Cell Mol Biol, 2008. **268**: p. 1-37.

560. Ruvinsky, I. and O. Meyuhas, *Ribosomal protein S6 phosphorylation: from protein synthesis to cell size.* Trends Biochem Sci, 2006. **31**(6): p. 342-8.

561. Pende, M., et al., *Hypoinsulinaemia, glucose intolerance and diminished beta-cell size in S6K1-deficient mice.* Nature, 2000. **408**(6815): p. 994-7.

562. Yokogami, K., et al., *Serine phosphorylation and maximal activation of STAT3 during CNTF signaling is mediated by the rapamycin target mTOR.* Curr Biol, 2000. **10**(1): p. 47-50.

563. Kim, J.H., M.S. Yoon, and J. Chen, *Signal transducer and activator of transcription 3 (STAT3) mediates amino acid inhibition of insulin signaling through serine 727 phosphorylation.* J Biol Chem, 2009. **284**(51): p. 35425-32.

564. Zhang, Y., et al., *ZIP4 regulates pancreatic cancer cell growth by activating IL-6/STAT3 pathway through zinc finger transcription factor CREB.* Clin Cancer Res, 2010. **16**(5): p. 1423-30.

565. Saarimäki-Vire, J., et al., *An Activating STAT3 Mutation Causes Neonatal Diabetes through Premature Induction of Pancreatic Differentiation.* Cell Rep, 2017. **19**(2): p. 281-294.

566. Shiao, M.-S., et al., *Adaptive Evolution of the Insulin Two-Gene System in Mouse.* Genetics, 2008. **178**(3): p. 1683-1691.

567. Zalewski, P.D., et al., *Video image analysis of labile zinc in viable pancreatic islet cells using a specific fluorescent probe for zinc.* J Histochem Cytochem, 1994. **42**(7): p. 877-84.

568. Qian, W.J., K.R. Gee, and R.T. Kennedy, *Imaging of Zn2+ release from pancreatic beta-cells at the level of single exocytotic events.* Anal Chem, 2003. **75**(14): p. 3468-75.

569. Stamateris, R.E., et al., *Glucose Induces Mouse β-Cell Proliferation via IRS2, MTOR, and Cyclin D2 but Not the Insulin Receptor*. Diabetes, 2016. **65**(4): p. 981-995.

570. Blandino-Rosano, M., et al., *Loss of mTORC1 signalling impairs β-cell homeostasis and insulin processing.* Nature Communications, 2017. **8**: p. 16014.

571. Mor, M., et al., *ZnT-1 enhances the activity and surface expression of T-type calcium channels through activation of Ras-ERK signaling.* Am J Physiol Cell Physiol, 2012. **303**(2): p. C192-203.

572. Colvin, R.A., et al., *Cytosolic zinc buffering and muffling: their role in intracellular zinc homeostasis.* Metallomics, 2010. **2**(5): p. 306-17.

573. Hogstrand, C., et al., *Cytosolic domains of zinc transporters as regulatory regions and potential signal transducers*. 2012.

574. Lawson, R., *Zinc Transporter 8 as a clinical target for treatment of Type 2 Diabetes*. 2015, King's College London: MRes Thesis.

575. Camarata, T., et al., *Pdlim7 (LMP4) regulation of Tbx5 specifies zebrafish heart atrio-ventricular boundary and valve formation.* Dev Biol, 2010. **337**(2): p. 233-45.

576. Camarata, T., et al., *Pdlim7 is required for maintenance of the mesenchymal/epidermal Fgf signaling feedback loop during zebrafish pectoral fin development.* BMC Developmental Biology, 2010. **10**(1): p. 104.
577. Bjorndahl, L. and U. Kvist, *Human sperm chromatin stabilization: a proposed model including zinc bridges.* Mol Hum Reprod, 2010. **16**(1): p. 23-9.
578. Buchner, D.A., et al., *Zinc finger protein 407 (ZFP407) regulates insulin-stimulated glucose uptake and glucose transporter 4 (Glut4) mRNA.* J Biol Chem, 2015. **290**(10): p. 6376-86.
579. Ravassard, P., et al., *A genetically engineered human pancreatic β cell line exhibiting glucose-inducible insulin secretion.* J Clin Invest, 2011. **121**(9): p. 3589-97.
580. Benner, C., et al., *The transcriptional landscape of mouse beta cells compared to human beta cells reveals notable species differences in long non-coding RNA and protein-coding gene expression.* BMC Genomics, 2014. **15**(1): p. 620.
581. Nakashima, K., et al., *MIN6 is not a pure beta cell line but a mixed cell line with other pancreatic endocrine hormones.* Endocr J, 2009. **56**(1): p. 45-53.
582. Skelin, M., M. Rupnik, and A. Cencic, *Pancreatic beta cell lines and their applications in diabetes mellitus research.* ALTEX, 2010. **27**(2): p. 105-13.
583. Cheng, K., et al., *High passage MIN6 cells have impaired insulin secretion with impaired glucose and lipid oxidation.* PLoS One, 2012. **7**(7): p. e40868.
584. Altschul, S.F., et al., *Basic local alignment search tool.* J Mol Biol, 1990. **215**(3): p. 403-10.
585. Masuoka, J. and P. Saltman, *Zinc(II) and copper(II) binding to serum albumin. A comparative study of dog, bovine, and human albumin.* J Biol Chem, 1994. **269**(41): p. 25557-61.

VIII. Appendices

Appendix 1. List of publications

R. Lawson, W. Maret, and C. Hogstrand, Prolonged stimulation of insulin release from MIN6 cells causes zinc depletion and loss of β-cell markers. Journal of Trace Elements in Medicine and Biology, 2018. 49: p. 51-59

R. Lawson, W. Maret, and C. Hogstrand, Expression of the ZIP/SLC39A transporters in β-cells: a systematic review and integration of multiple datasets. BMC Genomics, 2017. 18(1): p. 719.

Appendix 2. Oral presentations

Metal Group Summer Symposium Series, King's College London, 13th June 2018. **R Lawson**, W Maret, C Hogstrand. The pancreatic β-cell zinc response to chronic stimulation and extracellular zinc depletion.

MRC DTP Symposium, King's College London, 20th October 2017. **R Lawson**, W Maret, C Hogstrand. Expression of the ZIP/SLC39A transporters in β-cells: a systematic review and integration of multiple datasets.

Zinc-UK Conference, University of Belfast, Northern Ireland, 21-22nd November 2016. **R Lawson**, W Maret, C Hogstrand. Characterisation of the β-cell SLC39A transcriptome.

Appendix 3. Poster presentations

GMS/Zinc-Net Conference, Aachen, Germany, 28-30th September 2017. **R Lawson**, W Maret, C Hogstrand. A systematic review and reanalysis of transcriptomics datasets reveals ZIP proteins regulating zinc in pancreatic β-cells.

Diabetes and Nutritional Sciences Symposium, King's College London, 6th September 2017. **R Lawson**, W Maret, C Hogstrand. A systematic review and reanalysis of transcriptomics datasets reveals ZIP proteins regulating zinc in pancreatic β-cells.

International Society Zinc Biology Conference, Pyla, Cyprus, 18-22nd June 2017. **R Lawson**, W Maret, C Hogstrand. A systematic review and reanalysis of transcriptomics datasets reveals ZIP proteins regulating zinc in pancreatic β-cells.

KBI, MRC and BRC Symposium, King's College London, 13th January 2017. **R Lawson**, W Maret, C Hogstrand. ZIP Transporters in β-cell Function and Diabetes.

Diabetes and Nutritional Sciences Symposium, King's College London, 18th May 2016. **R Lawson**, W Maret, C Hogstrand. ZIP Transporters in β-cell Function and Dysfunction.

Appendix 4. Travel grants

King's Bioscience Institute travel grant (2017)

German Academic Exchange Service (DAAD) travel grant (2017)

COST/Zinc-UK travel grants (2016 & 2017)

Appendix 5. Metal ion compositions of growth media

Data shown: untreated growth media, growth media before addition of FBS, FBS before treatment with Chelex-100, FBS after treatment with Chelex-100, FBS after treatment with Chelex-100 following $CaCl_2$, $MgSO_4$ and KCl supplementation, and growth media containing supplemented FBS containing differing concentrations of $ZnCl_2$. Concentrations were determined through ICP-MS. All values are an average of 5 technical repeats and are expressed as µg/L. GF media = glucose-free media.

Preparation 1 (August 2016 – February 2017)

Sample	Ca 44 (ug/L)	Cu 65 (ug/L)	Fe 56 (ug/L)	K 39 (ug/L)	Mg 24 (ug/L)	Mn 55 (ug/L)	Na 23 (ug/L)	Ni 60 (ug/L)	Zn 66 (ug/L)
Growth media	1355.9	0.31	5.19	7699.9	940.3	0.07	117198	0.02	4.01
Growth media (no FBS)	1211.6	0.01	0.22	6638.6	878.2	0.01	118112	0.02	0.51
FBS	2387.2	1.60	35.32	11888.9	1093.9	0.46	107161	0.01	24.61
FBS (Chelex-100 treated)	118.8	1.40	33.02	10954.9	62.3	0.23	117140	0.01	4.35
FBS + $MgSO_4$ + $CaCl_2$ + KCl	286.7	1.35	34.29	11135.7	164.3	0.24	116476	0.01	4.61
Media [1uM Zn]	1045.8	0.19	4.94	5868.5	551.1	0.04	113565	0.02	1.08
Media [7.6uM Zn]	1077.3	0.21	5.33	6033.4	568.9	0.05	116987	0.02	7.59
Media [14uM Zn]	1120.6	0.20	5.13	6273.8	589.4	0.04	121101	0.02	13.94
Media [20uM Zn]	1140.5	0.20	5.25	6360.0	597.7	0.04	123241	0.02	20.43
Media [42uM Zn]	1179.5	0.21	5.36	6532.7	618.7	0.05	127174	0.02	42.45
Media [95uM Zn]	1252.6	0.24	6.79	6036.1	657.6	0.06	132697	0.03	95.50

Preparation 2 (March 2017)

Sample	Ca 44 (ug/L)	Cu 65 (ug/L)	Fe 56 (ug/L)	K 39 (ug/L)	Mg 24 (ug/L)	Mn 55 (ug/L)	Na 23 (ug/L)	Ni 60 (ug/L)	Zn 66 (ug/L)
FBS [untreated]	1050.4	1.04	19.78	4493.8	235.4	0.25	24647	0.01	16.24
FBS [Chelex-100 treated]	52.3	0.91	18.49	3764.1	8.7	0.13	26942	0.01	2.88
FBS + $MgSO_4$ + $CaCl_2$ + KCl	1967.1	1.40	33.4	15196.2	1227.1	0.19	115614	0.01	5.45
Media [1uM zinc (1)]	1167.6	0.22	4.93	6639.7	653.1	0.03	111534	0.00	1.61
Media [1uM zinc (2)]	1111.4	0.22	4.64	6290.6	621.0	0.03	104946	0.01	1.11
Media [7.6uM zinc (1)]	1139.2	0.21	4.76	6415.9	640.2	0.03	107473	0.01	7.63
Media [7.6uM zinc (2)]	1187.9	0.25	4.80	6654.1	663.2	0.03	111328	0.00	7.60
Media [42uM zinc (1)]	1195.3	0.24	4.95	6672.2	670.8	0.04	110767	0.01	42.19
Media [42uM zinc (2)]	1254.3	0.35	5.19	6940.2	700.5	0.04	114539	0.01	43.45
Media [95uM zinc]	1323.2	0.60	5.45	7172.6	738.0	0.05	118392	0.01	92.35
GF media [1uM zinc]	1314.1	0.30	5.55	7198.7	737.5	0.06	118625	0.01	1.36
GF media [7.6uM zinc]	1296.4	0.43	5.38	7086.5	726.4	0.07	116260	0.01	7.56
GF media [42uM zinc]	1304.1	0.34	5.34	7113.4	735.1	0.05	116572	0.01	42.55

Preparation 3 (April – May 2017)

Sample	Ca 44 (ug/L)	Cu 65 (ug/L)	Fe 56 (ug/L)	K 39 (ug/L)	Mg 24 (ug/L)	Mn 55 (ug/L)	Na 23 (ug/L)	Ni 60 (ug/L)	Zn 66 (ug/L)
Untreated growth media	1532.4	0.39	6.85	6936.4	798.9	0.15	138778	0.02	6.13
FBS (Chelex-100 treated)	26.9	6.76	24.11	6131.5	2.7	0.09	142280	0.03	4.08
FBS (Chelex-100 treated)	24.5	6.96	24.82	6161.1	2.3	0.07	142340	0.02	3.63
FBS + $MgSO_4$ + $CaCl_2$ + KCl	1481.0	6.08	22.25	20405.7	948.3	0.07	126528	0.01	3.47
FBS + $MgSO_4$ + $CaCl_2$ + KCl	1409.2	6.13	22.44	19421.3	890.7	0.11	123201	0.02	3.47
DMEM [1uM zinc (1)]	1215.3	0.88	3.54	7247.8	647.6	0.06	123005	0.04	1.65
DMEM [1uM zinc (2)]	1266.9	0.92	3.82	7523.3	681.3	0.06	128918	0.03	1.09
DMEM [1uM zinc (3)]	1301.9	0.91	3.49	7742.4	706.1	0.04	132308	0.01	1.54
DMEM [7.6uM zinc (1)]	1309.8	0.94	4.13	7766.2	719.2	0.10	133556	0.04	7.96
DMEM [7.6uM zinc (2)]	1367.6	0.96	4.02	8093.2	756.2	0.08	139832	0.01	7.61
DMEM [7.6uM zinc (3)]	1361.6	0.95	3.91	8075.3	756.3	0.05	139465	0.01	7.94
DMEM [7.6uM zinc (4)]	1359.6	0.97	3.86	8074.7	760.1	0.04	139847	0.02	7.20
DMEM [42uM zinc (1)]	1394.5	0.99	4.00	8352.6	786.0	0.12	143775	0.03	42.74
DMEM [42uM zinc (2)]	1395.0	0.98	4.00	8277.6	785.4	0.06	143154	0.02	42.34
DMEM [42uM zinc (3)]	1407.5	0.97	4.08	8314.5	799.3	0.06	145367	0.01	44.20

Preparation 4 (July – September 2017)

Sample	Ca 44 (ug/L)	Cu 65 (ug/L)	Fe 56 (ug/L)	K 39 (ug/L)	Mg 24 (ug/L)	Mn 55 (ug/L)	Na 23 (ug/L)	Ni 60 (ug/L)	Zn 66 (ug/L)
FBS [untreated]	2541.8	2.20	41.18	13067.2	1099.5	0.61	123005	0.00	29.31
FBS [Chelex-100 treated (1)]	22.2	2.05	40.24	8782.9	2.9	0.27	138920	0.00	2.81
FBS [Chelex-100 treated (2)]	32.8	2.03	40.05	8541.7	3.2	0.28	135150	0.00	4.44
DMEM [1uM zinc (1)]	1065.1	0.24	5.16	5603.0	547.9	0.06	121154	0.03	1.58
DMEM [1uM zinc (2)]	1067.5	0.26	5.02	5590.0	556.9	0.06	121011	0.03	1.69
DMEM [7.6uM zinc (1)]	1054.5	0.24	5.06	5472.7	552.8	0.06	119188	0.01	8.33
DMEM [7.6uM zinc (2)]	1074.7	0.23	4.80	5606.4	572.1	0.05	121237	0.00	8.12
DMEM [42uM zinc (1)]	1056.5	0.25	5.89	5453.3	558.9	0.06	118378	0.02	46.83

Preparation 5 (October 2017)

Sample	Ca 44 (ug/L)	Cu 65 (ug/L)	Fe 56 (ug/L)	K 39 (ug/L)	Mg 24 (ug/L)	Mn 55 (ug/L)	Na 23 (ug/L)	Ni 60 (ug/L)	Zn 66 (ug/L)
FBS [untreated]	2195.5	1.64	34.05	10570.1	1127.2	0.44	106136	0.03	23.95
FBS [Chelex-100 treated (1)]	44.9	1.25	34.12	8248.7	15.3	0.02	121257	0.00	3.07
FBS [Chelex-100 treated (2)]	34.2	1.30	36.58	8495.3	9.5	0.06	124356	0.16	3.20
DMEM [nothing added]	1156.9	0.07	0.21	4978.9	702.3	0.00	115458	0.01	0.20
Glucose-free DMEM [nothing added]	1240.2	0.08	0.05	5353.4	757.6	0.00	124209	0.02	0.43
RPMI [nothing added]	310.4	0.08	0.09	5656.6	406.7	0.00	115742	0.02	0.31
FBS + $MgSO_4$ + $CaCl_2$ + KCl	2106.3	1.20	35.22	15068.8	1076.5	0.03	129292	0.04	2.81
DMEM [1uM zinc (1)]	1358.4	0.19	5.62	6815.7	699.8	0.02	128565	0.07	0.60
DMEM [1uM zinc (2)]	1374.2	0.19	5.62	6865.5	713.3	0.01	130284	0.01	0.53
DMEM [8uM zinc (1)]	1386.4	0.20	5.63	6903.6	727.4	0.01	130447	0.04	8.06
DMEM [8uM zinc (2)]	1391.0	0.20	5.64	6874.1	725.7	0.02	129357	0.04	7.98
Glucose-free DMEM [1uM zinc]	1362.4	0.20	5.43	6771.4	723.8	0.01	127223	0.05	0.78
Glucose-free DMEM [8uM zinc]	1386.4	0.20	5.57	6823.1	732.0	0.01	128762	0.05	8.55
RPMI [1uM Zn]	489.2	0.14	3.86	6448.5	418.4	0.02	116164	0.04	0.47
RPMI [8uM Zn]	495.2	0.15	3.95	6483.2	422.9	0.02	117221	0.04	9.51

Appendix 6. Targeting of primers to mouse *Slc39a* isoforms. Predicted using Primer BLAST [506].

Transcript	RefSeq ID	Description
SLC39A1	NM_013901.2	Slc39a1
SLC39A2	NM_001039676.2	Slc39a2
SLC39A3	NM_134135.1	Slc39a3
SLC39A4	NM_028064.2	Slc39a4
SLC39A5	NM_028051.3	Slc39a5 transcript variant 1
	NM_028092.3	Slc39a5 transcript variant 2
	NM_001136237.1	Slc39a5 transcript variant 3
SLC39A6	NM_139143.3	Slc39a6
SLC39A7	NM_008202.2	Slc39a7 transcript variant 1
	NM_001077709.1	Slc39a7 transcript variant 2
SLC39A8	NM_001135150.1	Slc39a8 transcript variant 1
	NM_001135149.1	Slc39a8 transcript variant 2
	NM_026228.5	Slc39a8 transcript variant 3
SLC39A9	NM_026244.2	Slc39a9
SLC39A10	NM_172653.2	Slc39a10
SLC39A11	NM_001166503.1	Slc39a11 transcript variant 1
	NM_027216.5	Slc39a11 transcript variant 2
SLC39A12	NM_001012305.2	Slc39a12
SLC39A13	NM_001290765.1	Slc39a13 transcript variant 1
	NM_026721.3	Slc39a13 transcript variant 2
SLC39A14	NM_001135151.1	Slc39a14 transcript variant 1
	NM_001135152.1	Slc39a14 transcript variant 2
	NM_144808.4	Slc39a14 transcript variant 3

Appendix 7. Targeting of primers to human *SLC39A* isoforms. Predicted using Primer BLAST [506].

Transcript	Targeted		Not targeted	
	RefSeq ID	**Description**	**RefSeq ID**	**Description**
SLC39A1	NM_014437.4	SLC39A1 transcript variant 1	NM_001271957.1 NM_001271958.1 NM_001271959.1 NM_001271960.1 NM_001271961.1	SLC39A1 transcript variant 2 SLC39A1 transcript variant 3 SLC39A1 transcript variant 4 SLC39A1 transcript variant 5 SLC39A1 transcript variant 6
SLC39A2	NM_014579.3 NM_001256588.1	SLC39A2 transcript variant 1 SLC39A2 transcript variant 2		
SLC39A3	NM_144564.4	SLC39A3 transcript variant 1	NM_213568.1	SLC39A3 transcript variant 2
SLC39A4	NM_017767.2 NM_130849.3	SLC39A4 transcript variant 1 SLC39A4 transcript variant 2		
SLC39A5	NM_173596.2 NM_001135195.1	SLC39A5 transcript variant 1 SLC39A5 transcript variant 2		
SLC39A6	NM_012319.3 NM_001099406.1	SLC39A6 transcript variant 1 SLC39A6 transcript variant 2		
SLC39A7	NM_006979.2	SLC39A7 transcript variant 1	NM_001077516.1 NM_001288777.1	SLC39A7 transcript variant 2 SLC39A7 transcript variant 3
SLC39A8	NM_022154.5 NM_001135146.1 NM_001135147.1 NM_001135148.1	SLC39A8 transcript variant 1 SLC39A8 transcript variant 2 SLC39A8 transcript variant 3 SLC39A8 transcript variant 4		
SLC39A9	NM_018375.4	SLC39A9 transcript variant 1	NM_001252148.1	SLC39A9 transcript variant 2

	NM_001252150.1 NM_001252151.1 NM_001252152.1 NM_001330185.1	SLC39A9 transcript variant 3 SLC39A9 transcript variant 4 SLC39A9 transcript variant 5 SLC39A9 transcript variant 6		
SLC39A10	NM_001127257.1 NM_020342.2	SLC39A10 transcript variant 1 SLC39A10 transcript variant 2		
SLC39A11	NM_001159770.1 NM_139177.3 NM_001352691.1 NM_001352692.1 NM_001352693.1	SLC39A11 transcript variant 1 SLC39A11 transcript variant 2 SLC39A11 transcript variant 3 SLC39A11 transcript variant 4 SLC39A11 transcript variant 5		
SLC39A12	NM_001145195.1 NM_152725.3 NM_001282733.1	SLC39A12 transcript variant 1 SLC39A12 transcript variant 2 SLC39A12 transcript variant 3		
SLC39A13	NM_001128225.2 NM_152264.4 NM_001330245.1	SLC39A13 transcript variant 1 SLC39A13 transcript variant 2 SLC39A13 transcript variant 4		
SLC39A14	NM_001128431.3 NM_015359.5 NM_001135153.2 NM_001351655.1 NM_001351657.1 NM_001351658.1 NM_001351656.1 NM_001351659.1 NM_001351660.1	SLC39A12 transcript variant 1 SLC39A12 transcript variant 2 SLC39A12 transcript variant 3 SLC39A12 transcript variant 5 SLC39A12 transcript variant 6 SLC39A12 transcript variant 7 SLC39A12 transcript variant 8 SLC39A12 transcript variant 9 SLC39A12 transcript variant 10	NM_001135154.2	SLC39A12 transcript variant 4

Appendix 8. Agilent bioanalyzer samples analysis

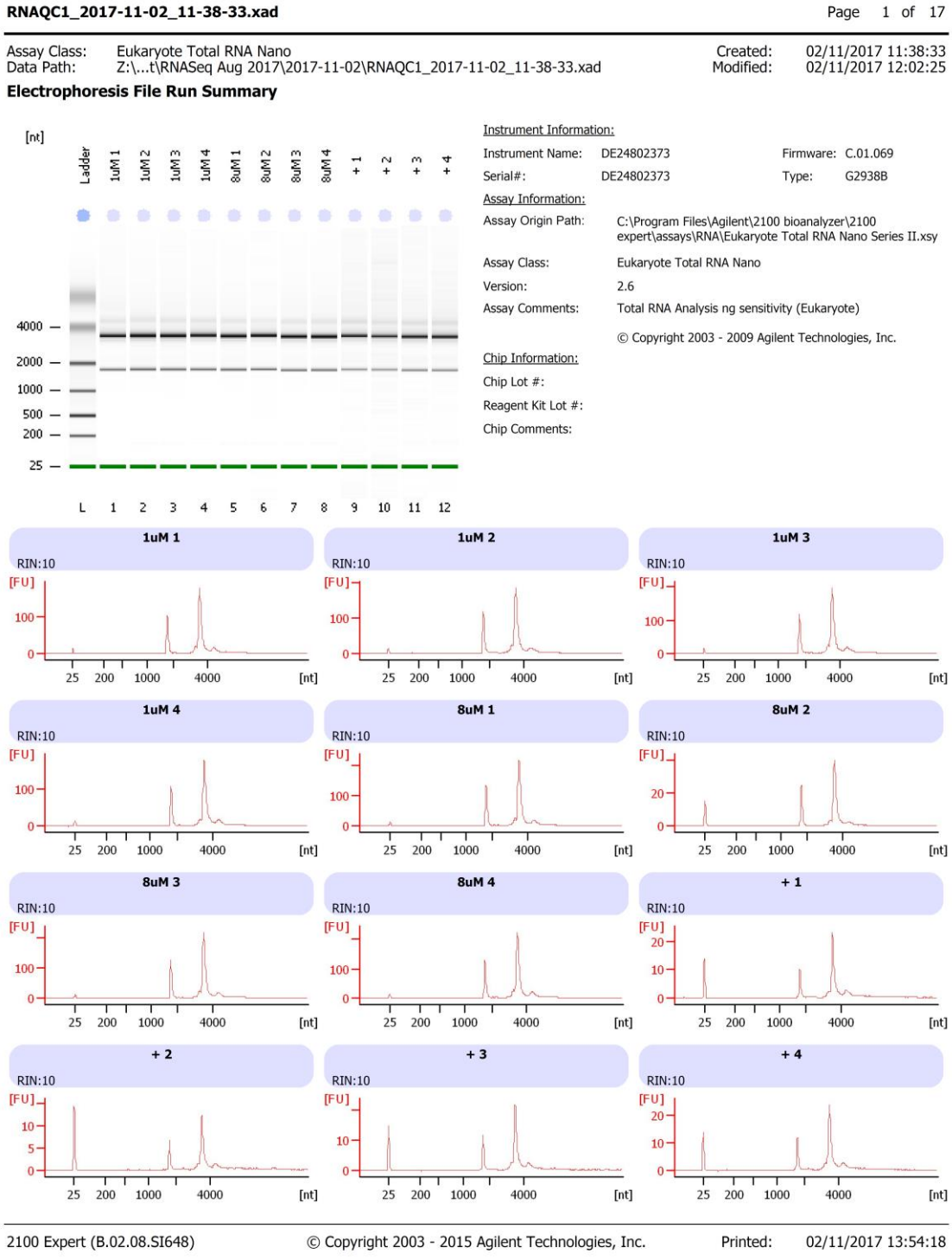

Assay Class: Eukaryote Total RNA Nano
Data Path: Z:\...t\RNASeq Aug 2017\2017-11-02\RNAQC2_2017-11-02_12-12-10.xad

Created: 02/11/2017 12:12:09
Modified: 02/11/2017 12:35:13

Electrophoresis File Run Summary

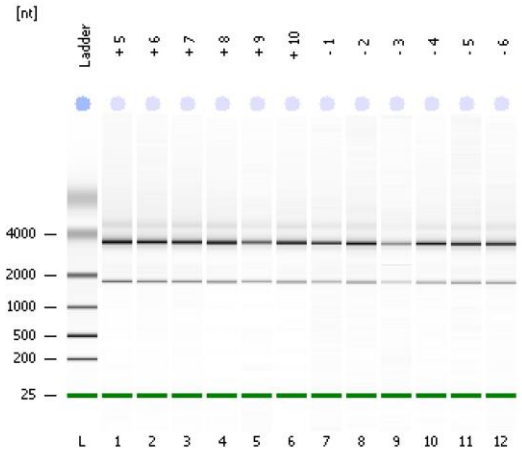

Instrument Information:

Instrument Name: DE24802373 Firmware: C.01.069
Serial#: DE24802373 Type: G2938B

Assay Information:

Assay Origin Path: C:\Program Files\Agilent\2100 bioanalyzer\2100 expert\assays\RNA\Eukaryote Total RNA Nano Series II.xsy
Assay Class: Eukaryote Total RNA Nano
Version: 2.6
Assay Comments: Total RNA Analysis ng sensitivity (Eukaryote)

Chip Information:

Chip Lot #:
Reagent Kit Lot #:
Chip Comments:

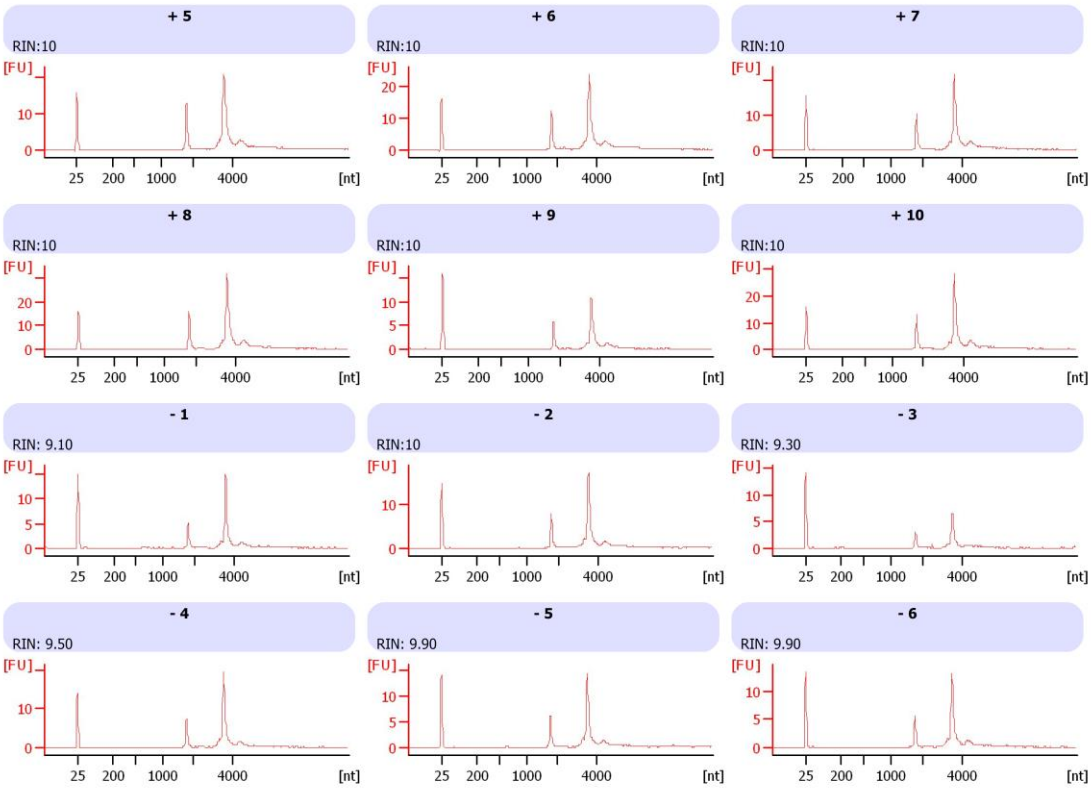

  Printed: 02/11/2017 13:54:50

Assay Class: Eukaryote Total RNA Nano
Data Path: Z:\...t\RNASeq Aug 2017\2017-11-02\RNAQC3_2017-11-02_12-47-37.xad

Created: 02/11/2017 12:47:36
Modified: 02/11/2017 13:00:29

Electrophoresis File Run Summary

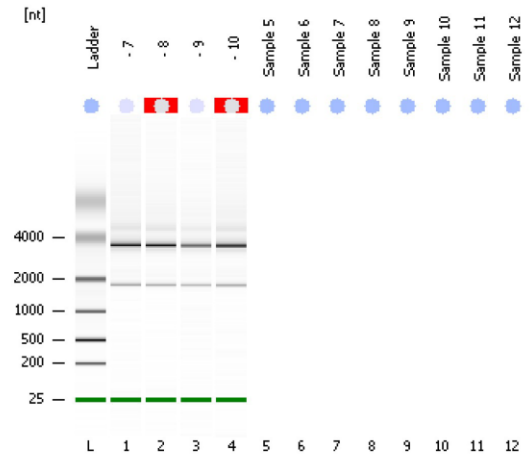

Instrument Information:

Instrument Name: DE24802373 Firmware: C.01.069
Serial#: DE24802373 Type: G2938B

Assay Information:

Assay Origin Path: C:\Program Files\Agilent\2100 bioanalyzer\2100 expert\assays\RNA\Eukaryote Total RNA Nano Series II.xsy
Assay Class: Eukaryote Total RNA Nano
Version: 2.6
Assay Comments: Total RNA Analysis ng sensitivity (Eukaryote)

Chip Information:

Chip Lot #:
Reagent Kit Lot #:
Chip Comments:

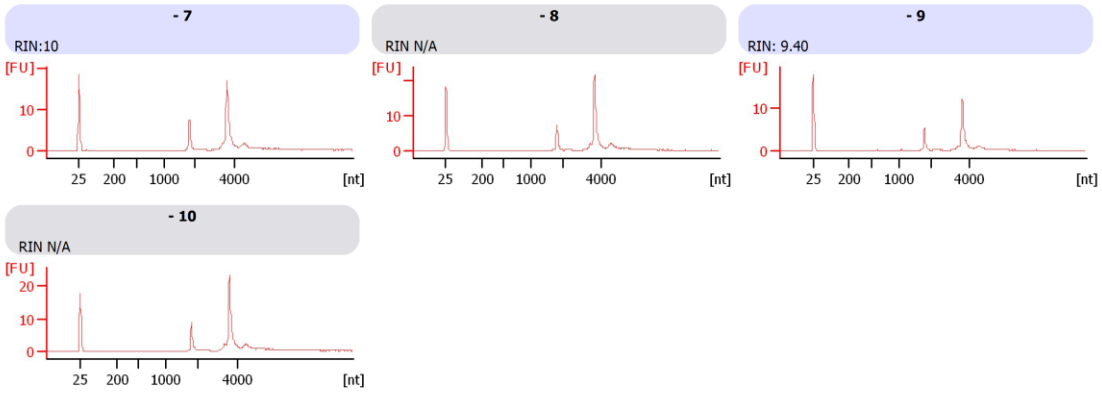

  Printed: 02/11/2017 13:53:37

Appendix 9. Quality control plot for RNA-seq data

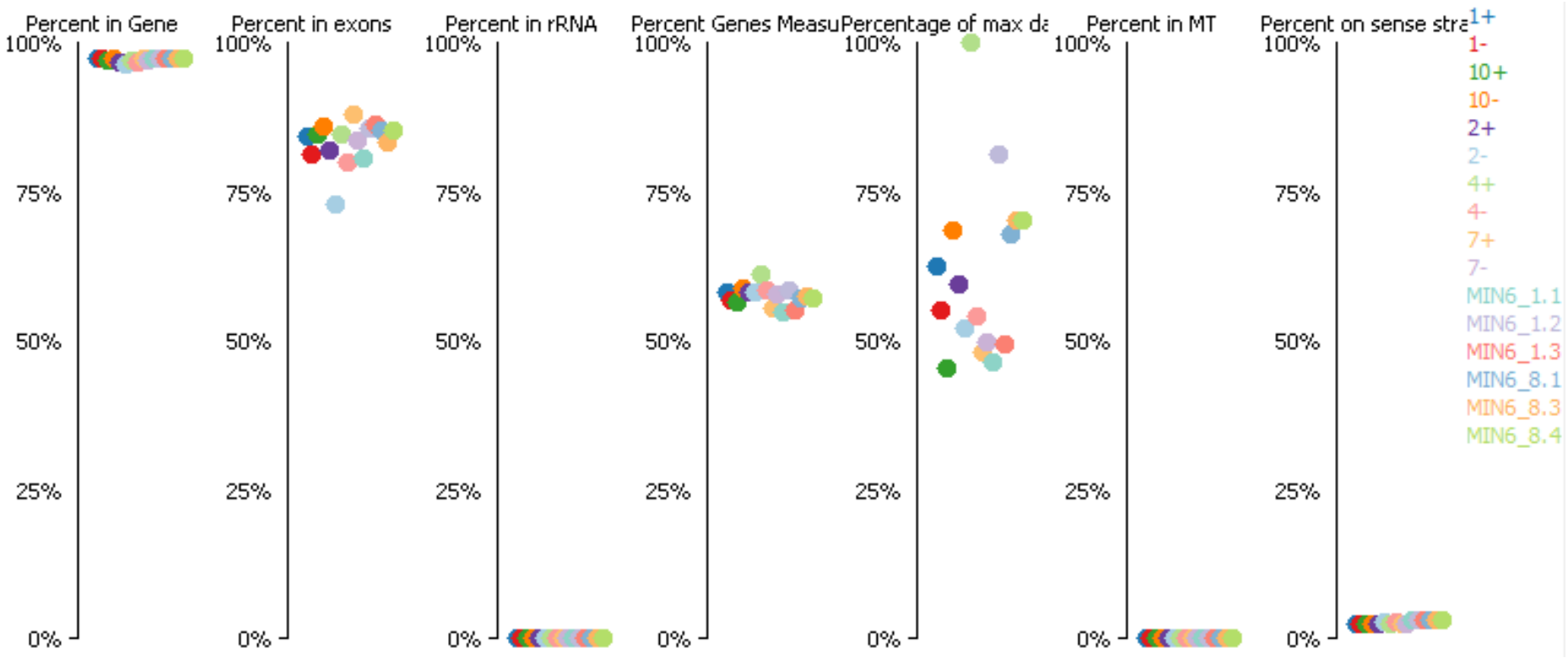

Appendix 10. Data store tree for RNA-seq samples

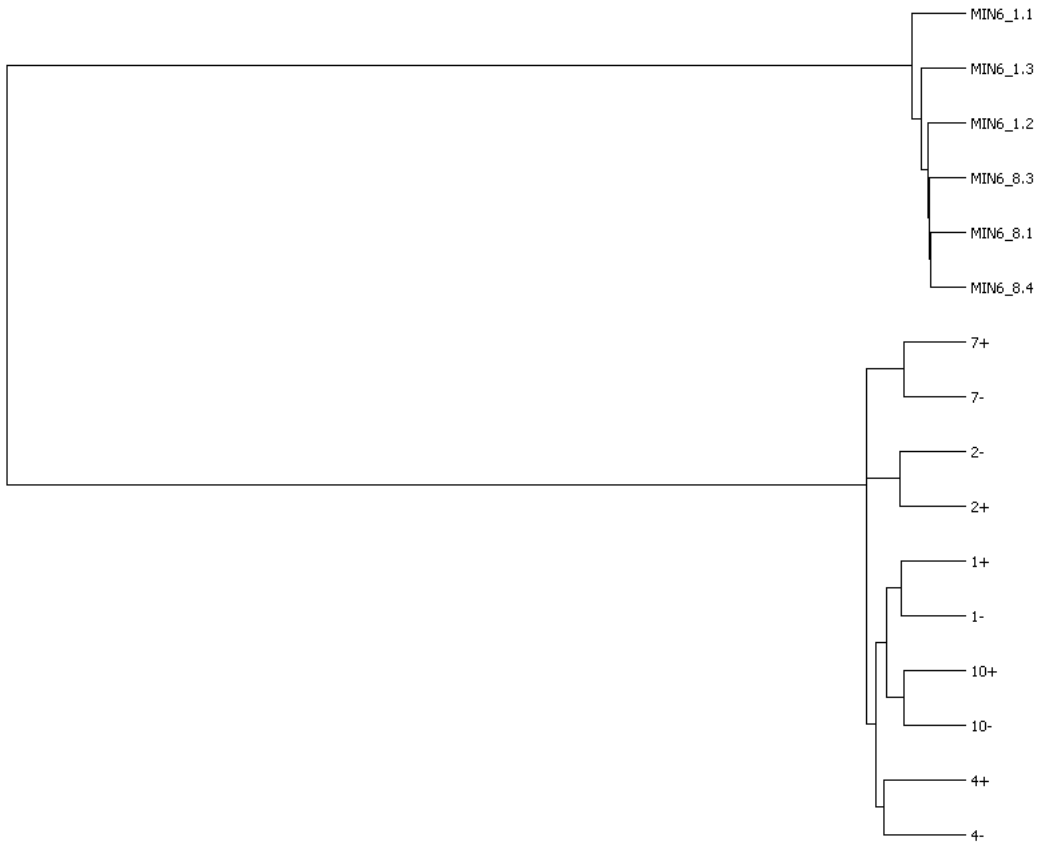

Appendix 11. Cumulative distribution plot for RNA-seq samples

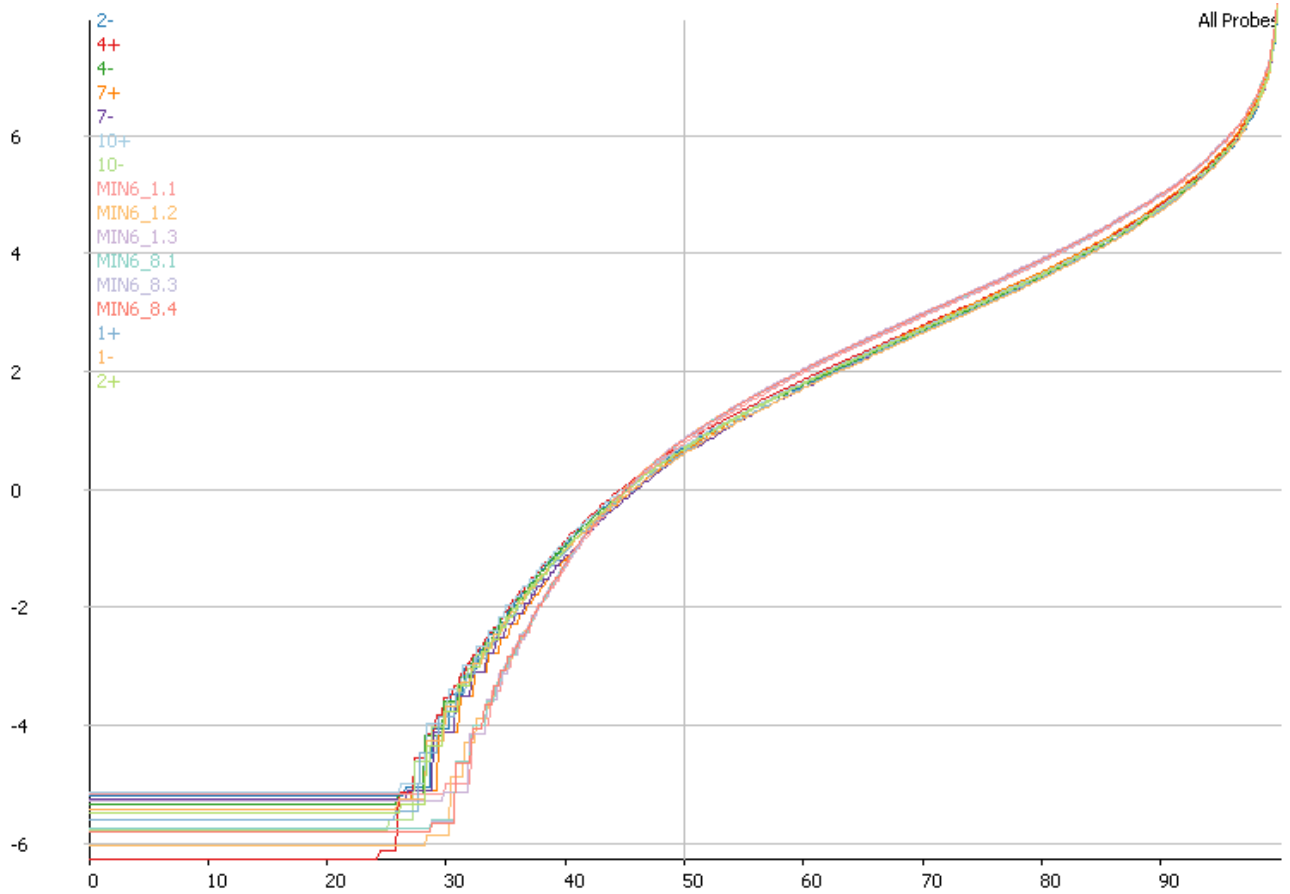

Appendix 12. Genes upregulated by zinc depletion in both MIN6 cells and islets (p <0.05)

Gene Symbol	p-value	q-value	Difference	Fold change
Gm36990	0.000167	0.70930157	1.526968	2.88179558
Casp9	0.000211	0.70930157	1.84394	3.58989095
Pls1	0.001551	0.70930157	0.53514	1.44908275
Gm19426	0.002214	0.70930157	1.67434	3.19173282
Fam186a	0.0023	0.70930157	1.37954	2.60185414
Gm6451	0.005478	0.70930157	1.31364	2.4856792
4933407K13Rik	0.005532	0.70930157	1.526954	2.88176748
Anks1b	0.010257	0.70930157	1.20996	2.3133122
Ppip5k2	0.01028	0.70930157	0.825689	1.7723808
Pctp	0.010302	0.70930157	1.37956	2.60189026
Gm16140	0.010752	0.70930157	0.42794	1.34531124
Mob3c	0.011446	0.70930157	1.696546	3.24123998
Avil	0.014266	0.70930157	1.284826	2.43652651
Abcd1	0.021673	0.70930157	1.599433	3.03024135
Tigd2	0.025656	0.70930157	1.062552	2.08862281
Hlf	0.027822	0.70930157	1.20998	2.31334393
B930095G15Rik	0.028085	0.70930157	1.062583	2.08866785
Gm15664	0.028085	0.70930157	1.06256	2.08863437
Gm28892	0.030101	0.70930157	0.5973	1.51288255
AC139319.1	0.032391	0.70930157	1.0649	2.09202493
BC005624	0.037613	0.70930157	1.20995	2.31329615
Itga2	0.040831	0.70930157	0.67708	1.59890036

Lcmt1	0.041302	0.70930157	1.062576	2.0886575
Gm9115	0.046622	0.70930157	1.062578	2.08866078
Gldc	0.047528	0.70930157	0.706361	1.63168363
Ecd	0.047914	0.70930157	0.808016	1.75080201
Cpb2	0.049531	0.70930157	1.115247	2.16632043
Snrk	0.049764	0.70930157	0.68367	1.60622053

Appendix 13. Genes downregulated by zinc depletion in both MIN6 cells and islets (p <0.05)

Gene Symbol	p-value	q-value	Difference	Fold change
Hcar2	0.001706	0.709301573	-1.15816	0.448084
Yipf6	0.00374	0.709301573	-1.1703	0.44433
Zfp92	0.004825	0.709301573	-1.62315	0.324625
Rassf10	0.005292	0.709301573	-0.67744	0.625274
4933417C20Rik	0.006045	0.709301573	-1.15636	0.448642
Gm44442	0.012097	0.709301573	-1.28158	0.411345
Acaa1a	0.012145	0.709301573	-0.62062	0.650391
Vta1	0.013988	0.709301573	-1.30379	0.405062
Ripply3	0.01402	0.709301573	-1.15639	0.448634
Papd4	0.014635	0.709301573	-0.98677	0.504606
H2-Q10	0.017707	0.709301573	-1.15637	0.44864
Kdm4b	0.018123	0.709301573	-1.82885	0.28149
Bicd1	0.020089	0.709301573	-1.42894	0.371404
Gm26637	0.021669	0.709301573	-0.9313	0.524386
Fbxo2	0.022091	0.709301573	-1.60615	0.328473
Gas2l2	0.022357	0.709301573	-1.13419	0.455592
Ift81	0.023246	0.709301573	-1.17029	0.444333
Cpne3	0.025662	0.709301573	-1.75355	0.29657
Idh3b	0.03045	0.709301573	-1.19209	0.437667
Tep1	0.030841	0.709301573	-1.18997	0.438311
Pole4	0.032652	0.709301573	-0.98678	0.504602
Gm45081	0.035358	0.709301573	-1.47336	0.360143
1700034H15Rik	0.036607	0.709301573	-0.59178	0.663524

Mrpl23	0.039678	0.709301573	-0.98678	0.504602
Cd82	0.039691	0.709301573	-1.1342	0.455589
Ncf1	0.041164	0.709301573	-0.62849	0.646854
Minpp1	0.04117	0.709301573	-0.4768	0.71857
A230057D06Rik	0.041298	0.709301573	-0.98678	0.504602
Rps12-ps3	0.042295	0.709301573	-0.83938	0.558884
B330016D10Rik	0.042429	0.709301573	-1.37863	0.384583
Dennd5a	0.045699	0.709301573	-0.99439	0.501949
Apoa5	0.046572	0.709301573	-1.13418	0.455594

Appendix 14. Survival of MIN6 cells in response to changes in extracellular zinc at 48 h

(A) MIN6 cell proliferation, calculated by BrdU incorporation. **(B)** MIN6 cell apoptosis, measured by Caspase 3/7 assays. **(C)** MIN6 cell oxidative stress, measured by dihydrofluorescin diacetate fluorescence. **(D-F)** Phosphorylation of RPS6 and ERK1/2. **(D)** Immunoblots for Ser235/236 RPS6, RPS6, p42/p44 ERK1/2 and ERK1/2. **(E-F)** Quantification of immunoblots for **(E)** Ser235/236 RPS6 vs RPS6 and **(F)** p42/p44 ERK1/2 vs ERK1/2. Immunoblot quantification was carried out using ImageJ software. All experiments were carried out following culture of MIN6 cells with 1µM, 8µM or 42µM zinc for 48 h. Results are relative to MIN6 cells in 8µM zinc (control). Data were analysed by 2-way ANOVA followed by Tukey's multiple comparison test. Error bars show ± SEM. N=3.

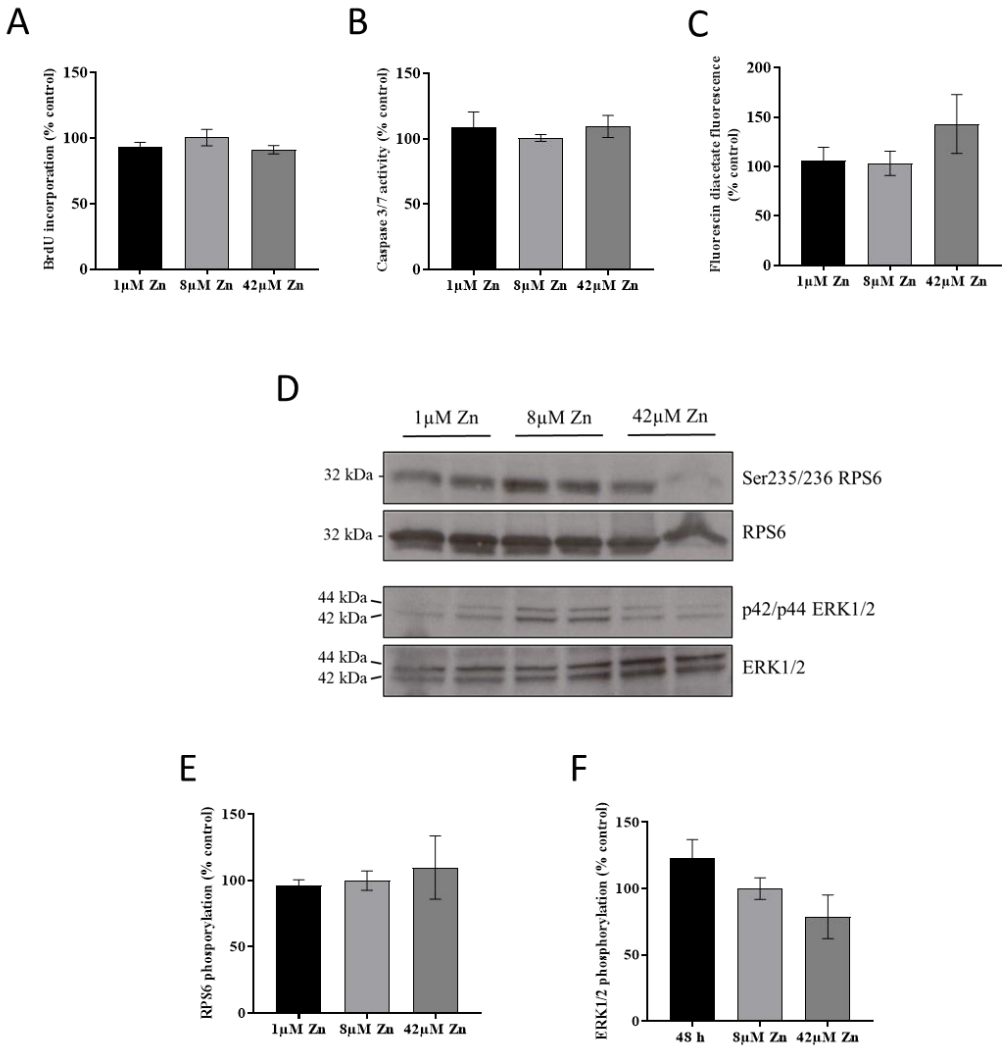

Appendix 15. MIN6 cell insulin gene expression and insulin secretion in response to changes in extracellular zinc at 24 and 48 h

(A-B) Abundance of *Ins1* and *Ins2* mRNA expression following culture with 1µM, 8µM or 42µM zinc for **(A)** 24 or **(B)** 48 h. Expression was assayed through qPCR and calculated as FD (Log2) relative to MIN6 cells cultured with 8µM zinc (control). **(C-D)** Insulin secretion from MIN6 cells in response to 3mM glucose (basal) or 40mM KCl (stimulated) following culture with 1µM, 8µM or 42µM zinc for **(C)** 24 or **(D)** 48 h. The amounts of secreted insulin were calculated through insulin secretion assays and normalised to total protein. Data were analysed by 2-way ANOVA followed by Tukey's multiple comparison test. Error bars show ± SEM. N=3.